Self-similar Heat Transfer in a Turbulent Particle-laden Free Flow

AMMCS 2023

INTERNATIONAL CONFERENCE

AUGUST 14–18

WATERLOO, ONTARIO, CANADA

BOOK OF ABSTRACTS

General Chairs

Marc Kilgour

Roderick Melnik

Sunny Wang

Interdisciplinary AMMCS Conference Series

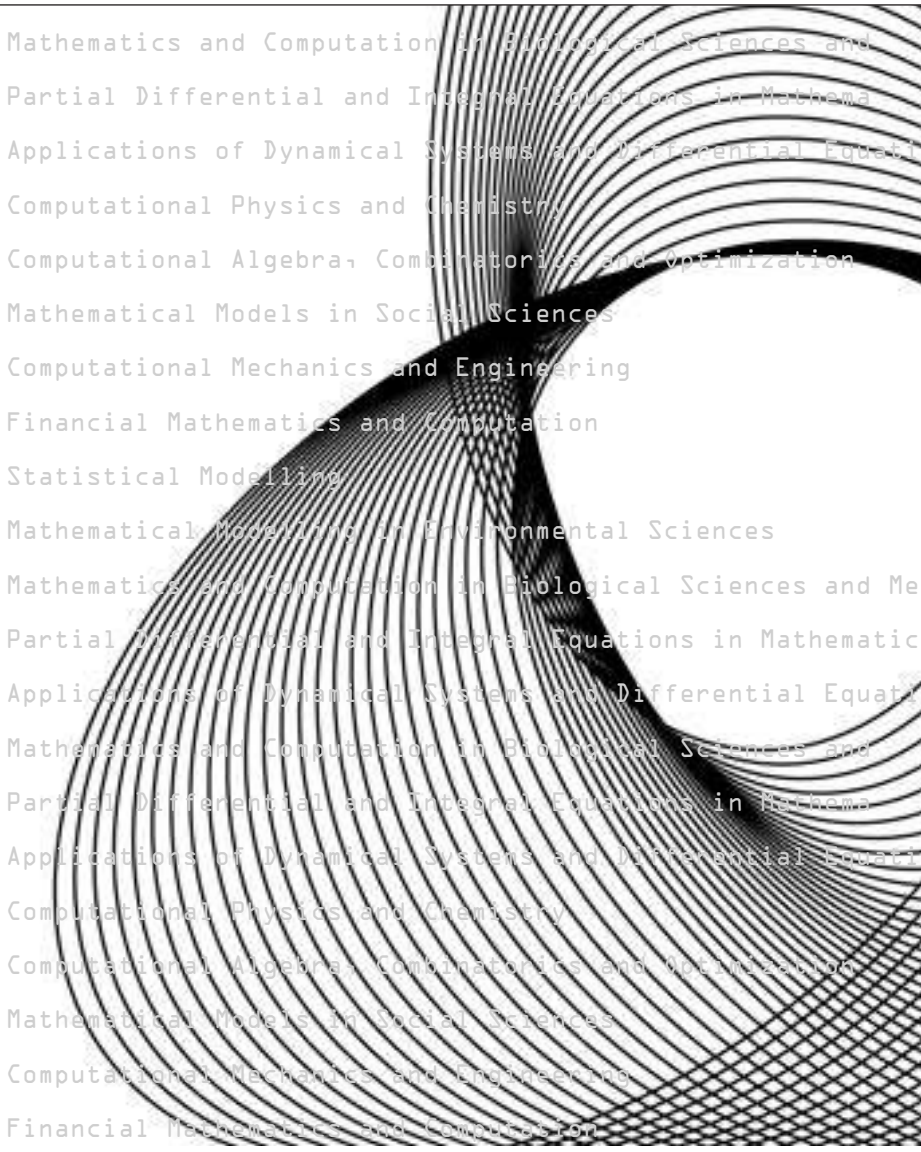

The AMMCS 2023 Conference

Book of Abstracts

Waterloo, Ontario, Canada

August 14–18, 2023

Disclaimer

This book contains abstracts of the AMMCS 2023 Conference. Authors are responsible for the contents and accuracy. Opinions expressed may not necessarily reflect the position of the AMMCS 2023 scientific and organizing committees.

Technical Designer: Roman N. Makarov

Compilation: Akepogu Venkateshwarlu

Publisher: AMMCS 2023

ISBN: 978-0-9918856-4-0

General Chairs

Marc Kilgour (Wilfrid Laurier University, Waterloo)

Roderick Melnik (Wilfrid Laurier University, Waterloo)

Sunny Wang (Wilfrid Laurier University, Waterloo)

Scientific Committee

Bjorn Birnir (University of California, Santa Barbara)

Alberto Bressan (Penn State University)

Carlos Garcia-Cevera (University of California, Santa Barbara)

Anatoli Ivanov (Penn State University)

Eduard Kirr (University of Illinois, Urbana-Champaign)

Shaofan Li (University of California, Berkeley)

Vakhtang Putkaradze (University of Alberta)

Enrico Scalas (University of Sussex)

Chi-Wang Shu (Brown University)

Konstantina Trivisa (University of Maryland)

Nicholas Zabaras (University of Warwick)

Peter Kloeden (University of Tuebingen)

Organizing Committee

Herb Kunze (Congress Program Chair, University of Guelph)

Roman Makarov (Congress Treasurer, WLU, Waterloo)

Hasan Shodiev (Local OC, Wilfrid Laurier University, Waterloo)

David Soave (Local OC, Wilfrid Laurier University, Waterloo)

Chester Weatherby (Student Prize Committee Chair, WLU, Waterloo)

Devan Becker (AMMCS Student Team Supervisor, WLU, Waterloo)

Jacques Belair (Global OC, Universite de Montreal)

Monica Cojocaru (Global OC, University of Guelph)

Dong Liang (Global OC, York University)

Scott MacLachlan (Global OC, Memorial University)

Zoran Miskovic (Global OC, University of Waterloo)

Nicolae Tarfulea (Global OC, Purdue University Northwest)

Technical Support Committee

Akshayveer A (Computer Support)

Arman AP (Web Coordinator)

Ruth MacNeil (Administrative Support)

Swadesh Pal (Digital Media Support)

Sangeeta Saha (Assistant to Student Team Supervisor)

Vishesh Verma (AMMCS Support)

Akepogu Venkateshwarlu (Electronic Publishing Support)

SIAM Representative

Roderick Melnik (Wilfrid Laurier University, Waterloo)

AMMCS 2023 Students Team

Ama Ansah

Nate Cullen

Mujahid Elmaki

Aya Khalaf

Agassi Lu

Daniel Mehta

Kenny Nguyen

Sydney Orlander

Dev Patel

Hina Shaheen

Gavan Singh

Howard Zhu

Sponsors


Interdisciplinary
AMMCS
Conference Series


WILFRID LAURIER UNIVERSITY
LAURIER
Inspiring Lives.


FIELDS


SHARCNET


Maplesoft


CRM


Société canadienne de
CFD
Society of Canada


AIMS


mprime


siam


PIMS

Contents

List of Sessions

List of Congress Plenary Lectures

Title	Speaker
The State of Representing and Solving Games	Tuomas Sandholm (Carnegie Mellon University)
Ex Ante Fairness and Worst Case Analysis	Hervé Moulin (University of Glascow)
Explainable AI via Semantic Information Pursuit	René Vidal (University of Pennsylvania)
Saddlepoint Approximations for Hawkes Jump-Diffusion Processes with an Application to Risk Management	Yacine Ait-Sahalia (Princeton University)
Skeletal models for two- and three-dimensional shape understanding	Kathryn Leonard (Occidental College, Los Angeles)
Combined multiscale modeling and experimental study of regulation mechanisms of shape and structure formation during tissue development	Mark Alber (University of California Riverside)
Theories of Deep Learning	Clayton Scott (University of Michigan, Ann Arbor)
Clustering and Classification in Networks	Peter Mucha (Dartmouth College)
Network geometry: from multiscale to ultra low dimensional representations of complex systems	M. Angeles Serrano (Universitat de Barcelona)
Fast and Powerful Minipatch Ensemble Learning for Discovery and Inference	Genevera Allen (Rice University)
Partial Differential Equations of Quantum Mechanics	Israel Michael Sigal (University of Toronto)
Mechanistic Modeling of Complex Social Systems	Hiroki Sayama (Binghamton University, State University of New York)
Supersingular isogeny graphs and orientations	Katherine Stange (University of Colorado, Boulder)

AMMCS Prize-Winning Lecture

Title	Speaker
The isometric immersions problem: from perspectives of PDE, geometry, and physics	Siran Li (Shanghai Jiao Tong & New York University)

AMMCS Special Sessions

CODE	TITLE
SS-AIIPMM	Artificial Intelligence, Inverse Problems, and Mathematical Modelling
SS-ASDEDS	Algebraic Structure of Discrete-Event Dynamical Systems, and Applications
SS-CCSMS	Coupled Complex Systems and Multiple Scales, Their Modelling, and Applications
SS-CNT	Computational Number Theory
SS-DF	Decisions and Fairness
SS-DSBEA	Dynamical Systems in Biological and Engineering Applications
SS-FDCW	Fluid dynamics in cold water
SS-MAAC	Modeling and analysis in analytical chemistry
SS-MACMQ	Mathematical Aspects of Condensed Matter and Quantum Theory
SS-MBM	Mathematics in Biology and Medicine
SS-MCSLS	Modeling complex systems in life sciences
SS-MF	Mathematical Finance
SS-MMNN	Mathematical Models for Nanoscience and Nanotechnology
SS-MNAPA	Modeling and Numerical Analysis for PDE Applications
SS-MNPE	Modelling NPI and PI in epidemics/pandemics
SS-MSD	Mathematics of Systems with Delay
SS-OCDGA	Optimal Control, Differential Games, and Applications
SS-QCQPQM	Quantum computation, and other quantum processes in quantum matter
SS-RANMSC	Recent Advances in Numerical Methods and Scientific Computing
SS-RATAWP	Recent Advances in the Theory and Applications of Wave Propagation
SS-RPCDSA	Recent progress in complex dynamical systems and applications
SS-SDMICN	Spatial data and modelling including the Canadian North
SS-SMPTTNP	Solution methods and preconditioning techniques for time-dependent and nonlinear problems
SS-TPCHES	Tipping Points in Coupled Human-Environment Systems
SS-TSMDA	Topics in Spatiotemporal Modelling and Data Analysis
SS-UAMLTDA	Utilizing AI and Machine Learning Techniques for Data Analytics

AMMCS Contributed Sessions

CODE	TITLE
CS-APMRE	Applied Problems and Methods in Research & Education
CS-BSM	Mathematics and Computation in Biological Sciences and Medicine
CS-CACO	Computational Algebra, Combinatorics, and Optimization
CS-CPC	Computational Physics and Chemistry
CS-DSDE	Applications of Dynamical Systems and Differential Equations
CS-ENV	Mathematical Modelling in Environmental Sciences and Models for Complex Media
CS-FINANCE	Financial Mathematics and Computation
CS-MECHE	Computational Mechanics and Engineering
CS-MODELING	Partial Differential and Integral Equations in Mathematical Modeling
CS-POST	AMMCS-2023 Poster Session

Lectures

Plenary Lectures

The State of Representing and Solving Games

Tuomas Sandholm, Carnegie Mellon University

Abstract: Game-theoretic solution concepts provide meticulous definitions of how rational parties should act. That has enabled humans to think rigorously about strategic interactions, leading to game theory revolutionizing many fields such as economics, political science, and biology. So far, game theory has mainly been used for reasoning by humans. The models have therefore been quite stylized and coarse: small enough for humans to solve in their heads or by paper and pen. The goal has been to draw insights from such models, which humans then judiciously apply to the drastically more complicated real world. The boundaries of game theory have thus been defined by the limits of humans. However, many - arguably most - important game classes lie beyond those boundaries. There is now another, more nascent, use of game theory that goes beyond human intelligence. The game is computationally solved in its full detail - or else in a large, faithful abstraction thereof - as opposed to solving a small, stylized version to obtain insights for humans. Novel approaches, game representations, and algorithms from the last 18 years have enabled game theory to advance significantly beyond its traditional boundaries. I will discuss that state of the art. The talk is based on my presentation at the December 2021 Nobel Symposium: 100 Years of Game Theory, and also includes brand new results.

Ex Ante Fairness and Worst Case Analysis

Hervé Moulin, University of Glascow

Abstract: Initiated by mathematicians in the 1940s, the formal analysis of fair division promptly attracted the interest of economists: what is a just allocation of scarce resources between agents with different needs and tastes?; political scientists: how to distribute fairly the collective decision power between the citizens?; and more recently computer scientists: which tests of fairness are computationally tractable when they involve a very large number of participants, e. g., on the internet?. A compelling message emerges from eight decades of mathematical and empirical research: mechanisms distributing valuable resources (be they commodities, decision power or computing resources) should always be evaluated from two complementary viewpoints on fairness: Ex Ante and Ex Post. If I can compare the way the mechanism treats me personally versus other participants, Ex Post fairness makes sure that I have no grounds to complain, no convincing objection questioning the legitimacy of the proposed solution. But ex ante, before the mechanism is implemented, I may have little or no prior knowledge of the other participants who will compete with me for these resources: what are the preferences guiding their choices, or is their behaviour dictated by other principles, is it strategically sophisticated or crudely myopic, or even adversarial to me? Then I must pay close attention to the worst case scenario where everything about them turns against me. A key parameter is how much protection the mechanism offers me in the gedankenexperiment of the worst case: my guarantee is my worst case welfare, the higher it is, the lower the risk that the other agents manhandle me, the safer it is to participate in - and abide by the outcome selected by - the mechanism. The seminal discussion of cake-cutting by the mathematicians Hugo Steinhaus and Harold Kuhn is about a canonical guarantee: how to divide a non atomic cake between agents with additive utilities in such a way that each participant can make sure to eat a share worth at least 1/n-th of the total cake to her (n is the number of participants). Later instances of guarantees underpin the fair division problem in the Arrow Debreu microeconomic model, cost and surplus sharing in the cooperative game model, and more recently the allocation of indivisible goods or bads. We discuss ex ante fairness first in the general collective decision problem variously interpreted as voting, bargaining or social choice. Guarantees there come from the veto rights allocated to individual as well as groups of agents: the proportional veto core gives more voice to minorities than the voting rules a la Condorcet or even Borda, in so doing it eliminates the "tyranny of the majority". The mathematical model of guarantees is more interesting but much harder to crack when we allow compromises by convex combinations of the final outcomes, interpreted as lotteries, time shares, or the

division of a fixed budget. Veto rights still generate guarantees but so does the random dictator rule: everyone gets a 1/n chance of selecting his/her best outcome. Vetoes and random dictatorship can be combined in many ways and are, in a precise sense, dual of one another. The veto guarantee is natural when we choose an expensive and long lasting infrastructure project or a person to hold a position for life; the random dictator approach makes more sense if we are dividing time between substitutable activities, or choosing a pair of roman consuls. The last part of the talk turns to the fair division of a single homogenous private commodity when preferences are not necessarily monotonic: say when coworkers share a workload or investors distribute shares in a project. In this simple model the versatile concept of ex ante guarantee suggests new ways to organize the division, and also opens challenging new mathematical questions.

Explainable AI via Semantic Information Pursuit

René Vidal, University of Pennsylvania

Abstract: There is a significant interest in developing ML algorithms whose final predictions can be explained in terms understandable to a human. Providing such an "explanation" of the reasoning process in domain-specific terms can be crucial for the adoption of ML algorithms in risk-sensitive domains such as healthcare. This has motivated a number of approaches that seek to provide explanations for existing ML algorithms in a post-hoc manner. However, many of these approaches have been widely criticized for a variety of reasons and no clear methodology exists in the field for developing ML algorithms whose predictions are readily understandable by humans. To address this challenge, we develop a method for constructing high performance ML algorithms which are "explainable by design". Namely, our method makes its prediction by asking a sequence of domain- and task-specific yes/no queries about the data (akin to the game "20 questions"), each having a clear interpretation to the end-user. We then minimize the expected number of queries needed for accurate prediction on any given input. This allows for human interpretable understanding of the prediction process by construction, as the questions which form the basis for the prediction are specified by the user as interpretable concepts about the data. Experiments on vision and NLP tasks demonstrate the efficacy of our approach and its superiority over post-hoc explanations. Joint work with Aditya Chattopadhyay, Stewart Slocum, Benjamin Haeffele and Donald Geman.

Saddlepoint Approximations for Hawkes Jump-Diffusion Processes with an Application to Risk Management

Yacine Ait-Sahalia, Princeton University

Abstract: We propose a statistical model based on Hawkes processes in which large financial losses can arise in close succession serially as well as cross-sectionally. We derive in closed-form saddlepoint approximations to the tails of profit and loss distributions, both marginal and joint, and use them to construct explicit risk measure formulae that account for the fact that a given bank's losses make it more likely that that bank will experience further losses, and that other banks will experience losses as well. These closed-form risk measures can be used for comparative statics, parameter calibration, and setting capital requirements and potential systemic risk charges. (joint work with Roger J.A. Laeven)

Skeletal models for two- and three-dimensional shape understanding

Kathryn Leonard, Occidental College, Los Angeles

Abstract: Shape understanding - looking at a shape and intuitively understanding which parts are, e.g., body, arms, legs, toes, and ears - is almost effortless for humans. Training a computer to understand shapes in a similar way, however, presents substantial challenges. This talk will describe a useful mathematical shape model, the Blum medial axis (BMA), and methodologies based on the BMA for automatically decomposing a shape into a hierarchy of parts and determining the similarity between those parts. In 2D, we compare our automated results to human perception data gathered from a massive user study, and also provide some useful applications. Unfortunately, the BMA is notoriously sensitive to noise, which is unavoidable in applications. To address this, we propose geometrically coherent approaches to denoising that provide approximation guarantees for the shape boundary. Finally, because the BMA also provides an interesting example of a Whitney stratified set, we will explore some of the resulting elegant mathematical constructions.

Combined multiscale modeling and experimental study of regulation mechanisms of shape and structure formation during tissue development

Mark Alber, University of California Riverside

Abstract: The regulation and maintenance of an organ's shape and structure is a major outstanding question in developmental biology. The Drosophila wing imaginal disc serves as a powerful system for elucidating design principles of the shape formation in epithelial morphogenesis. Yet, even simple epithelial systems such as the wing disc are extremely complex. A tissue's shape and structure emerge from the integration of many biochemical and biophysical interactions between proteins, subcellular components, and cell-cell and cell-ECM interactions. How cellular mechanical properties affect tissue size and patterning of cell identities on the apical surface of the wing disc pouch has been intensively investigated. However, less effort has focused on studying the mechanisms governing the shape of the wing disc in the cross-section. Both the significance and difficulty of such studies are due in part to the need to consider the composite nature of the material consisting of multiple cell layers and cell-ECM interactions as well as the elongated shape of columnar cells. Results obtained using iterative approach combining multiscale computational modelling and quantitative experimental approach will be used in this talk to discuss direct and indirect roles of subcellular mechanical forces, nuclear positioning, and extracellular matrix in shaping the major axis of the wing pouch during the larval stage in fruit flies, which serves as a prototypical system for investigating epithelial morphogenesis. The research findings demonstrate that subcellular mechanical forces can effectively generate the curved tissue profile, while extracellular matrix is necessary for preserving the bent shape even in the absence of subcellular mechanical forces once the shape is generated. The developed integrated multiscale modelling environment can be readily extended to generate and test hypothesized novel mechanisms of developmental dynamics of other systems, including organoids that consist of several cellular and extracellular matrix layers.

Theories of Deep Learning

Clayton Scott, University of Michigan, Ann Arbor

Abstract: Over the past decade, deep neural networks have brought about major advances in computer vision, natural language modeling, protein structure prediction, and several other applications. These neural networks succeed despite having far more model parameters than training data. Classical machine learning theory suggests that overparametrized models will overfit, and cannot explain deep networks' low generalization error. In this talk I will survey recent theoretical developments that seek to better explain the performance of deep learning models, and present new results on the generalization ability of quantized neural networks and interpolating predictors.

Clustering and Classification in Networks

Peter Mucha, Dartmouth College

Abstract: Real-world networks are neither completely random nor fully regular, frequently containing essential structural features whose identification can help better understand the nature and purpose of a network. One common task is to seek out clusters in the data, sometimes described as "community detection". In other settings, one aims to identify key network features in the data that might be used to classify whole networks, label nodes, or predict missing edges. But many of these tasks require selecting features or parameters that are not always obvious to experts in possible application domains. For example, the best use of modularity-based methods includes setting a parameter to control the resolution scale. In this talk, we demonstrate a variety of approaches for such tasks, with emphasis on best practices with readily available software packages.

Network geometry: from multiscale to ultra low dimensional representations of complex systems

M. Angeles Serrano, Universitat de Barcelona

Abstract: Recent advances in network science include the discovery that hyperbolic geometry captures the complex connectivity of real networks. Within this paradigm, we have been developing model-based methods for exploring their multiscale nature and their intrinsic dimensionality. More specifically, we produced a renormalization group technique that progressively coarse-grains and rescales networks, revealing a hierarchy of layers at different resolutions. We found that the multiscale shells of real networks, such as connectomes of the human brain, exhibit self-similarity across multiple scales. This symmetry is also evident in the growth of some real networks, suggesting that evolution can be modeled by a reverse renormalization process. In addition, geometric renormalization has practical applications, allowing us to produce scaled down and scaled up replicas of real networks. Our results were obtained by embedding real networks in two-dimensional hyperbolic space, but we have also developed a method to infer their intrinsic dimensionality since there is not fundamental reason to believe that it must be two. Our analysis has revealed ultra low dimensionality and unexpected regularities across different domains, such as extremely low dimensionality in tissue-specific biomolecular networks, close-to-three-dimensional brain connectomes, and slightly higher dimensionality in social networks and the Internet.

Fast and Powerful Minipatch Ensemble Learning for Discovery and Inference

Genevera Allen, Rice University

Abstract: Enormous quantities of data are collected in many industries and disciplines; this data holds the key to solving critical societal and scientific problems. Yet, fitting models to make discoveries from this huge data often poses both computational and statistical challenges. In this talk, we propose a new ensemble learning strategy primed for fast, distributed, and memory-efficient computation that also has many statistical advantages. Inspired by random forests, stability selection, and stochastic optimization, we propose to build ensembles based on tiny subsamples of both observations and features that we term minipatches. While minipatch learning can easily be applied to prediction tasks similarly to random forests, this talk focuses on using minipatch ensemble approaches in unconventional ways: making data-driven discoveries and for statistical inference. Specifically, we will discuss using this ensemble strategy for feature selection, clustering, and graph learning as well as for distribution-free and model-agnostic inference for both predictions and important features. Through huge real data examples from neuroscience, genomics and biomedicine, we illustrate the computational and statistical advantages of our minipatch ensemble learning approaches.

Semi-Plenary Lectures

Partial Differential Equations of Quantum Mechanics

Israel Michael Sigal, University of Toronto

Abstract: In this talk I will describe key partial differential equations of quantum mechanics and condensed matter physics. I will review briefly the origins of the equations, their properties and some of the recent results. I will also touch upon some open problems. No preliminary knowledge of quantum mechanics is required. All needed concepts will be introduced in the talk.

Mechanistic Modeling of Complex Social Systems

Hiroki Sayama, Binghamton University, State University of New York

Abstract: Discovering patterns in experimental and observational data is an essential step in any scientific endeavor and has been dramatically accelerated by recent advances in data science, machine learning, and AI. However, pattern discovery alone cannot complete the full cycle of scientific research. Mechanistic modeling complements pattern discovery and plays a critical role in generating deeper understanding of and insight into the hidden mechanisms that may have produced the observed patterns. While current trends of data science/ML/AI research and applications focus primarily on the pattern discovery side (e.g., classification, clustering, prediction), there is also a growing demand for knowledge, skills, capabilities, and tools for mechanistic modeling. This is because many of our complex societal problems arise with high uncertainty yet with very limited data available, and often require the exploration and testing of numerous hypothetical scenarios, not for prediction, but for preparation. In this talk, I will illustrate the importance of mechanistic modeling, especially when dealing with complex societal problems, using examples from our recent work on (1) pandemic response planning in early 2020 when COVID-19 hit our daily lives but no one knew much about the disease, and (2) socio-political opinion dynamics modeling to explore alternative pathways for society other than the currently dominant divide and polarization. I will also argue that there is an urgent need for education and training in mechanistic modeling, in which systems thinking and creativity play a key role.

Supersingular isogeny graphs and orientations

Katherine Stange, University of Colorado, Boulder

Abstract: A supersingular isogeny graph is a graph whose vertices are supersingular elliptic curves over $\overline{\mathbb{F}}_p$ (where p is typically a large prime in our context), and whose edges represent isogenies of degree ℓ (typically a small prime). Hard problems concerning pathfinding in supersingular isogeny graphs form a basis for post-quantum isogeny-based cryptography. In this talk, I will describe the structure of isogeny graphs of CM curves, and of oriented supersingular curves, and their relationship to the structure of supersingular isogeny graphs. In particular, the endomorphism ring of a supersingular elliptic curve is an order in a quaternion algebra. Embeddings of imaginary quadratic orders into this quaternion order are called *orientations*. Explicit knowledge of this endomorphism ring leads to well-known pathfinding algorithms. In joint work, we develop classical and quantum algorithms for path-finding under the assumption that *only one* endomorphism from this order is known (equivalently, one orientation). In related work, we demonstrate a bijection between the cycles in a fixed isogeny graph and the cycles in the union of all CM graphs which cover it. As a result, we count the cycles in the isogeny graph in terms of certain class numbers of imaginary quadratic orders.

AMMCS Prize-Winning Lecture

Kolmogorov–Wiener Prize for Young Researchers

The isometric immersions problem: from perspectives of PDE, geometry, and physics

Siran Li, Shanghai Jiao Tong & New York University

Abstract: We report our recent work on a classical problem in differential geometry: isometric immersions and/or embeddings of Riemannian and semi-Riemannian manifolds. The underlying PDE is the system of Gauss-Codazzi-Ricci equations. Existence of isometric immersions is studied under various curvature conditions, via elliptic and hyperbolic PDE techniques. Weak continuity of isometric immersions is investigated with the help of the theory of compensated compactness. Connections to other problems in mathematical physics, including fluid dynamics, harmonic maps, and Coloumb gauges, will be discussed. Our talk contains joint work with Gui-Qiang Chen, Reza Pakzad, Armin Schikorra, and Marshall Slemrod.

Session Presentations

Title
On effects of delay in SEIR systems with a quarantine stage modeling COVID-19 spread

A. Raza[1, 2]

[1]*Department of Mathematics, National College of Business Administration and Economics Lahore, Pakistan,*
[2]*Govt. Maulana Zafar Ali Khan Graduate College Wazirabad, Punjab Higher Education Department, Govt. of Punjab, Lahore, Pakistan. {alimustasamcheema@gmail.com}*

Delays in nonlinear infectious disease models reflect an important latency effect that an individual can become infectious before developing symptoms. Quarantine measures were an important tool in preventing the spread of the coronavirus infection, which motivated the development of the nonlinear susceptible-exposed-infected-quarantine-recovered (SEIQR) model. Delays naturally appear when describing the influence of both susceptible and exposed populations. First, a nonlinear delayed coronavirus pandemic model is introduced. We show that it is well posed, and a solution stays in the non-negative domain. Next, we find the equilibria and study their stability using the Routh Hurwitz criterion, Volterra Lyapunov functions, and the Lasalle invariance principle. As usual, the basic reproduction number has a crucial effect on the model: if the number is less than one, the spread of the disease has been controlled, while we get endemic for the reproduction number being greater than one. The effect of the quarantine component on the reproduction number is investigated. In the delayed analysis of the model, we proved that the disease's transmission dynamics depend on delay terms, which is also reflected in the basic reproduction number. Computer simulations illustrate this dependency on the delay in the system. The results were recently published in [1].

References

[1] A. Raza, A. Ahmadian, M. Rafiq, S. Salahshour and M. Ferrara, An analysis of a nonlinear susceptible-exposed-infected-quarantine-recovered pandemic model of a novel coronavirus with delay effect. Results in Physics, **21,** 1, pp. 01-07 (2021).

A continuum space is the infinitely great

Q. Li[1]

[1] *ShiJiaZhuang Traditional Chinese Medical Hospital, ShiJiaZhuang, ,China,liqingliyang@126.com*

Abstract An infinitely small quantity is defined as a one-dimensional quantity of finite length without the sizes of space, while an infinitely great quantity is reached by the superposition or accumulation of infinitely many finite quantities, by the way of the change in direction. The change in direction indicates that there is a jump from a finite quantity to infinitely many finite quantities (infinitely great). The form of the manifestation of the infinitely great is one quantitative continuum that cannot be operated by any algorithms and all parts of space we see is this one quantitative continuum. .Any value are this single quantitative continuum that indicates the infinitely great and compresses any quantities outside of it to nothing. As a result, the infinite exact value of a circumferential length (π) has been obtained here.

References

[1] Q. Li ,*A geomerty consisting of singularities containing only integers*. Research Square. DOI: 10.21203/rs.3.rs-219046/v1(2021).
[2] A.Wiles , *Modular elliptic curves and Fermat's Last Theorem*,Ann. Math. 141,3,pp. 443-552(1995).
[3] J. Kahn and V. Markovic, *Immersing almost geodesic surfaces in a closed hyperbolic three manifold*,Ann Math. 175,3,pp.1127-1190 (2012).
[4] C .Böhm and B. Wilking, *Manifolds with positive curvature operators are space forms*, Ann.Math.167, 3,pp.1079-1097 (2008).
[5] J. Cheeger and A. Naber, *Regularity of Einstein manifolds and the codimension 4 conjecture*, Ann. Math.182, 3,pp.1093-1165 (2015).

Droplet dynamics driven by electrowetting

Ke Xiao[1,2] and Chen-Xu Wu[1]

[1] *Xiamen University, China, cxwu@xmu.edu.cn*
[2] *Wenzhou Institute, University of Chinese Academy of Sciences, China*

Even though electrowetting-on-dielectric (EWOD) is a useful strategy in a wide array of biological and engineering processes with numerous droplet-manipulation applications, there is still a lack of complete theoretical interpretation on the dynamics of electrowetting. In this paper, we present an effective theoretical model and use Onsager variational principle to successfully derive general dynamic shape equations for electrowetting droplets in both overdamped and underdamped regimes. It is found that the spreading and retraction dynamics of a droplet on EWOD substrates can be fairly well captured by our model, which agrees with previous experimental results very well in the overdamped regime. We also confirm that the transient dynamics of EW can be characterized by a timescale independent of liquid viscosity, droplet size and applied voltage. Our model provides a complete fundamental explanation of EW-driven spreading dynamics, which is important for a wide range of applications, from self-cleaning to novel optical and digital microfluidic devices.

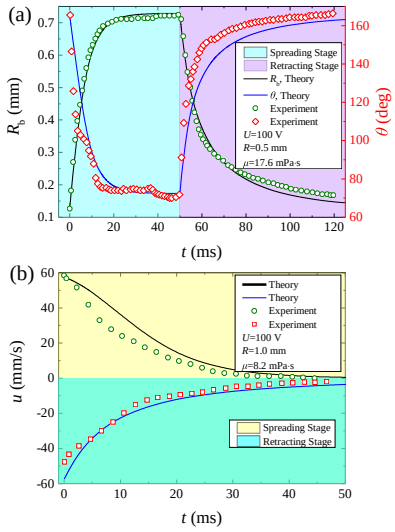

Figure 1: Comparison of theoretical time-dependent (a) base radius R_b and contact angle θ, and (b) contact line velocity u with those measured in Ref [1]. $\theta_Y = 165.4^\circ$ is used for calculation.

References

[1] Q. Vo and T. Tran, *Contact line friction of electrowet-ting actuated viscous droplets*, Phys. Rev. E **97**, 063101 (2018).
[2] K. Xiao and C.-X, Wu, *Droplet dynamics driven by electrowetting*, Phys. Rev. E **105**(6), 064609 (2022).
[3] K. Xiao, X. Chen and C.-X. Wu, *Electric field-triggered Cassie-Baxter-Wenzel wetting transition on textured surface*, Phys. Rev. Research **3**, 033277 (2021).
[4] K. Xiao and C.-X. Wu, *Curvature effect of electrowetting-induced droplet detachment*, J. Appl. Phys. **129**, 234701 (2021).

Analysis of blood flow through multiple stenoses in a narrow artery

S. Kumar[1], R. Sharma[2], A. Singh[3]

[1] *Dr. Bhimrao Ambedkar University, Agra, India skumar@dbrau.ac.in*
[2] *Dr. Bhimrao Ambedkar University, Agra, India, rashmi22sharma@gmail.com*
[3] *Dr. Bhimrao Ambedkar University, Agra, India, amendra1729@gmail.com*

A study of the effects of blood flow parameters in narrow arteries having multiple stenoses is discussed here. In this work, blood is considered as a non-Newtonian Kuang-Luo (K-L) fluid model, with no-slip conditions at the arterial wall. In fact, the main properties of K-L fluid mod- el are that the plasma viscosity and yield stress play a very important role. These parameters make this fluid remarkably similar to blood, however, when we change these parameters the flow characteristics change significantly. We have derived a numerical expression for the blood flow characteristics such as resistance to blood flow, blood flow rate, axial velocity, and skin friction. These numerical expressions have been solved by MATLAB 2021 software and dis- cussed graphically. Furthermore, these results have been compared with Newtonian fluid and observation made that resistance to blood flow and skin friction is decreased when blood is changed from non-Newtonian to Newtonian fluid.

References

[1] G. C. Shit, S. Maiti, J. C. Misra, *Pulsatile flow and heat transfer of blood in overlapping vibrating atherosclerotic artery: A numerical study*, Mathematics and Computers in Simulation, **166**, pp. 432-459 (2019).
[2] S. Kumar, S. Kumar, D. Kumar, *Comparative study of non-Newtonian physiological blood flow through the elastic stenotic artery with rigid body stenotic artery*, Series on Biomechanics, 34(4), pp. 26-41 (2020).

An Examination of Ranked-Choice Voting in the United States, 2004-2022

A. Graham-Squire[1], D. McCune[2]

[1] *High Point University, North Carolina, USA, agrahams@highpoint.edu*
[2] *William Jewell College, Missouri, USA, mccuned@william.jewell.edu*

From the perspective of social choice theory, ranked-choice voting (RCV) is known to have many flaws. RCV (also referred to as instant runoff voting, the Hare method, the plurality elimination rule, etc.) can fail to elect a Condorcet winner and is susceptible to monotonicity paradoxes and the spoiler effect, for example. The theoretical social choice literature has thoroughly investigated such flaws for many decades; the empirical literature has lagged behind the theoretical, presumably because historically not much vote data has been available. RCV has seen a recent surge in usage in the US and consequently much more vote data has become available, allowing for the investigation of empirical failure rates of RCV's various deficiencies. The deficiencies of RCV with which we are concerned are:

- RCV can fail to elect the Condorcet winner.
- RCV is susceptible to the spoiler effect.
- RCV is susceptible to downward and upward monotonicity paradoxes.
- RCV is susceptible to the truncation paradox, the most extreme version of which is the no-show paradox.
- RCV is susceptible to compromise strategic voting.
- The RCV winner can fail to secure a majority of the total votes cast.

We use a database of 182 American ranked-choice elections for political office from the years 2004-2022 to investigate empirically how frequently RCV's deficiencies manifest in practice. The deficiencies listed above can occur only in elections without a majority candidate, and thus our database consists only of such elections. Our general finding is that RCV's weaknesses are rarely observed in real-world elections, with the exception that ballot exhaustion frequently causes "majoritarian failures" where the RCV winner does not secure a majority of the total votes cast.

The VI International AMMCS
Interdisciplinary Conference
Waterloo, Ontario, Canada
DATE:

Fast solvers for centrosymmetric linear systems, applications to spectral methods

C. Greif[1], S. Nataj[2], M. Trummer[3]

[1]*Department of Computer Science, University of British Columbia, Vancouver, BC, Canada, greif@cs.ubc.ca*
[2]*Department of Mathematics, Simon Fraser University, Burnaby, BC, Canada, sarah_nataj@sfu.ca*
[3]*Department of Mathematics, Simon Fraser University, Burnaby, BC, Canada, trummer@sfu.ca*

A matrix is *centrosymmetric* if it is symmetric about its centre. This class includes a number of important types of matrices that arise in a variety of applications in computational science and engineering. In this talk we propose structure–preserving LU–type factorizations for centrosymmetric matrices and use them for the numerical solution of linear systems. For direct solvers we build on and extend existing algorithms and show that the factorizations along with equilibration and mixed precision arithmetic speed up the computation and increase the accuracy of the solution. For iterative solvers we develop novel incomplete factorizations and use them as preconditioners for Krylov subspace solvers. We apply these solvers to centrosymmetric linear systems arising from spectral methods for PDEs.

The VI International AMMCS
Interdisciplinary Conference
Waterloo, Ontario, Canada
DATE

Portfolio Time Consistency and Utility Weighted Discount Rates

O. Mbodji[1], T. Pirvu[2]

[1] *Independent Researcher*
[2] *McMaster University, Hamilton, Canada, tpirvu@math.mcmaster.ca*

Merton portfolio management problem is studied in this paper within a stochastic volatility model and non constant time discount rate framework. This problem is time inconsistent and the way out of this predicament is to consider the subgame perfect strategies. The later are characterized through a value function. A two stage approach is developed to find the value function: in a first step the utility weighted discount rate is introduced and characterized as the fixed point of a certain operator; in the second step, given the utility weighted discount rate, the value function is found through solving a parabolic linear equation. Numerical experiments explore the effect of the time discount rate on the subgame perfect and precommitment strategies.

The 0–1 Conjecture for polynoimals.

K.G. Hare[1]

[1] *University of Waterloo, Waterloo, Canada, kghare@uwaterloo.ca*

Let $c(x)$ is a monic integer polynomial with coefficients 0 or 1. Write $c(x) = s(x)b(x)$ where $s(x)$ and $b(x)$ monic polynomials with non-negative (not necessarily integer) coefficients. The 0–1 conjecture states that $s(x)$ and $b(x)$ are necessarily integer polynomials with coefficients 0 or 1. Given a candidate $s(x)$, this talk describes an algorithm to either find a $b(x)$ and $c(x)$ such that $b(x)$ has non-negative coefficients and $c(x)$ has coefficients 0 or 1, or (often) shows that such a $c(x)$ and $b(x)$ do not exist. Using this algorithm and significant computational effort, we provide support for the 0–1 conjecture.

Predator-prey dynamics influenced by fear, refuge and their velocities

Qamar Khan[1], Kawkab Al-Amri[1],

[1] *Department of Mathematics, College of Science, P.Box:36, Sultan Qaboos University, Al- Khod, OMAN. qjalil@squ.edu.om*
[1] *Department of Mathematics, College of Science, P.Box:36, Sultan Qaboos University, Al- Khod, OMAN. s52805@student.squ.edu.om*

In this article, we examined the dynamics of interactions between predators and prey in the refuge and outside the refuge, two distinct habitats. When the pressure of predation decreases, the prey emerges from its hiding place. Predators interact with prey outside their protected refuge and may even kill them. Depending on how many predators are there, the prey will shift to safe areas. It suggests that more prey will seek protection from predators in the refuge region and that the prey will choose to stay outside the refuge areas when the number of predators is reduced. By allowing predator density to influence prey velocity, we included predator and prey velocities as well as anti-predator behavior. Prey can reduce their velocities to avoid being attacked. We looked at anti-predator behavior and found that prey density rises with anti-predator behavior when either the predator or the prey velocity increases. We demonstrated that, under specific circumstances, the coexisting equilibrium will be globally stable and we discovered that there is saddle-node bifurcation at the coexisting equilibrium point.
Keywords: Predator-prey; Refuge; Fear; Velocities; Saddle node bifurcation.

The VI International AMMCS
Interdisciplinary Conference
Waterloo, Ontario, Canada
DATE

VIX Option pricing for non-parameter Heston stochastic local volatility model

J. Ma[1], J. Gong[2], W. Xu[3]

[1] *School of Mathematics, Shanghai University of Finance and Economics, Shanghai Key Laboratory of Financial Information Technology, Shanghai, 200433, China. email ma.junmei@mail.shufe.edu.cn*
[2] *School of Mathematics, Shanghai University of Finance and Economics, Shanghai Key Laboratory of Financial Information Technology, Shanghai, 200433, China. email: 18210690088@fudan.edu.cn*
[3] *Department of Mathematics, Toronto Metroplitan University, Toronto, Canada. email: wei.xu@torontomu.ca*

The Heston-Duprie model is a well-established stochastic local volatility model that offers a non-parametric representation. This model is known to closely match the implied volatility surface of options observed in the market. However, due to its non-parametric local component, Monte Carlo simulation is the only viable numerical method for derivative pricing under this model. This paper proposes a novel willow tree method to replace Monte Carlo simulation for pricing exotic options and VIX options under the Heston-Duprie model. We provide the convergence rate of this method and conduct several numerical experiments to demonstrate its accuracy and efficiency. Our proposed method offers an alternative numerical technique that can enhance the computational efficiency of pricing derivatives under the Heston-Duprie model.

The VI International AMMCS
Interdisciplinary Conference
Waterloo, Ontario, Canada
11th March, 2023

Deep learning method for the complex system of American options

C. Nwankwo[1], N. Umeorah[2], T. Ware[3], W. Dai[4]

[1] *University of Calgary, Canada, chinonso.nwankwo@ucalgary.ca*
[2] *Cardiff University, Cardiff, UK, umeorahn@cardiff.ac.uk*
[3] *University of Calgary, Canada, aware@ucalgary.ca*
[4] *Louisiana Tech University, Louisiana, USA, dai@latech.edu*

The solution of the American options free boundary PDE model comprises the free (or moving) boundary, value function and possibly, the Greeks. This options gives the holder of the option the right but not the obligation to exercise the options before the expiration. The objective of this talk is to solve the American options model with deep learning method which accounts for the value function, free boundary and the Greeks simultaneously and more precisely. To this end, we first fix the free boundary and implement following transformation [2] as described below

$$t^* = T - t, \quad x = \ln\left(\frac{S}{s_f(t^*)}\right), \quad V(S,t) = U(x,t^*). \tag{1}$$

$V(S,t)$ is the original option value and $U(x,t^*)$ is the transformed option value. In general, solving free boundary PDE models as a free boundary problem with deep learning is relatively new. For efficient implementation of the deep learning method to the transformed American options model, we further normalize as follows:

$$y = x/x_{max}, \quad \tau = t^*/T, \quad U(t^*,x) = P(\tau,y). \tag{2}$$

Hence, we present a normalized and non-linear fixed-free boundary PDE model with discontinuous co-efficient as shown in (3)

$$\frac{\partial P(\tau,y)}{T\partial\tau} - \frac{\sigma^2}{2x_{max}^2}\frac{\partial^2 P(\tau,y)}{\partial y^2} - \frac{1}{x_{max}}\left(r - \frac{\sigma^2}{2} + \frac{s_f'(\tau)}{Ts_f(\tau)}\right)\frac{\partial P(\tau,y)}{\partial y} + rP(\tau,y) = 0, \quad y > 0; \tag{3}$$

with $(\tau, y \in [\tau_{min}, 1], [0,1])$, $\tau_{min} > 0$, and $\tau_{min} \approx 0$. Furthermore, σ is the volatility, r is the interest rate and $s_f'(\tau)$ is the derivative of the free boundary which is singular at pay-off. With the above normalization, we can now efficiently implement our deep learning method. In this talk, we will discuss our proposed deep learning method [1] which is based on implicit dual solution framework consisting of a novel auxiliary function and free boundary equations. The auxiliary function enforces boundary conditions in approximate form due to the free boundary, includes deep neural network output, and satisfies the governing differential equation at the extremes. To approximate the free boundary, we take advantage of some linear relationship between the free boundary and the value function at the left boundary and establish equations that we called free boundary equations. This linear relationship represents the value matching condition in approximate form. Finally the validation of our implementation and its further extensions are concluded.

References

[1] C. Nwankwo, N. Umeorah and A. Ware, and W. Dai, *Deep learning and American options via free boundary framework*, arXiv preprint arXiv:2211.11803 (2022).

[2] L. Wu and Y. K. Kwok, *A front-fixing finite difference method for the valuation of American options*, Journal of Financial Engineering. **6**, 4, pp. 83-97 (1997)

Neural network method for solving parabolic two-temperature micro/nanoscale heat conduction in double-layered thin films exposed to ultrashort-pulsed lasers

Weizhong Dai[1]

[1] *Louisiana Tech University, Ruston, Louisiana, USA, dai@coes.latech.edu*

Ultrashort-pulsed lasers have been widely applied in biology, chemistry, medicine, physics, and optical technology due to their high efficiency, high power density, minimal collateral material damage, lower ablation thresholds, high precision production ability, and high precision control of heating times and locations in thermal processing of materials [1]. Simulation of the micro/nanoscale heat conduction induced by ultrashort-pulsed laser heating has been attracting great attention. Parabolic two-temperature energy transport model [2] is one of successful mathematical models for predicting phonon (lattice) temperature and electron temperature in metal at the micro/nanscale where energy is induced by ultrashort-pulsed laser heating. As we are moving towards the era of artificial intelligence, machine and deep learning techniques are becoming an important tool in engineering and science research.

In this talk, I will present some recently obtained research results in my group, which has been published in *International Journal of Heat and Mass Transfer* [3]. We have obtained an artificial neural network (ANN) method for solving the parabolic two-temperature heat conduction equations in double-layered thin films exposed to ultrashort-pulsed lasers. The ANN method is developed based on the PINN method, particularly the combination of the Adam optimization method and the L-BFGS iterative method for optimizing weights and biases. Note that the laser pulse duration is very short, only in the sub-picosecond/femtosecond domain and the non-equilibrium heating stage is usually in picoseconds. Thus, randomly sampling the learning points in the entire domain for the ANN method will not quickly capture the behavior during the pulse, which may cause the ANN solution to be inaccurate. To overcome this trouble, in this study we start at a small-time interval to obtain the ANN solution and then use the solution at the end of that small-time interval as the initial condition for the next small-time interval to obtain the next ANN solution. We continue this procedure from one small time interval to another small-time interval until the entire desired time interval is completed. Convergence of the ANN solution to the analytical solution is theoretically analyzed. Finally, the ANN method is used to predict the electron and lattice temperatures in a gold film padding on a chromium film when exposed to ultrashort-pulsed lasers, which is based on the parabolic two temperature heat conduction model.

References

[1] Y. Mao and M. Xu, *Lattice Boltzmann numerical analysis of heat transfer in nano-scale silicon films induced by ultra-fast laser heating*, Int. J. Therm. Sci. **89**, pp. 210-221 (2015).

[2] T.Q. Qiu and C.L. Tien, *Femtosecond laser heating of multi-layer metals-I. Analysis*, Int. J. Heat Mass Transf. **37**, pp. 2789-2797 (1994).

[3] A. Bora, W. Dai, J.P. Wilson, and J.C. Boyt, *Neural network method for solving parabolic two-temperature micro/nanoscale heat conduction in double-layered thin films exposed to ultrashort-pulsed lasers*, Int. J. Heat Mass Transf. **178**, 121616 (2021).

The VI International AMMCS
Interdisciplinary Conference
Waterloo, Ontario, Canada
DATE

New analysis of FEMs for miscible displacement in porous media

W. Sun[1]

Beijing Normal University, Zhuhai, P.R. China, maweiw@uic.edu.cn

The talk focuses on optimal error estimates of FEMs for problems involving multi-physics fields, which are often described by nonlinear and strongly coupled parabolic/elliptic systems A question to be concerned is the optimality of numerical approximations for each components involved in the physical system. For many popular models, existing analysis may not be optimal for certain component. A typical example given in this talk is the incompressible miscible flow in porous media which has been widely used in many engineering areas, such as reservoir simulations and surface contaminant transport and remediation. The analysis done in the last several decades shows that classical Galerkin FEMs provide the numerical concentration of the accuracy $O(h^{r+1}+h^s)$ in L^2-norm [1, 2, 3]. This analysis leads to the use of higher order finite element approximation to the pressure than that to the concentration in various numerical simulations to achieve the best rate of convergence. However, this error estimate is not optimal. In this talk, we introduce our recent work on new analysis of Galerkin-Galerkin methods to establish the optimal L^2 error estimate $O(h^{r+1}+h^{s+1})$ from which one can see that the best convergence rate can be achieved by taking the same order $(r=s)$ approximation to the concentration and pressure. Clearly Galerkin FEMs with $r=s$ are less expensive in computation and easier for implementation. Numerical results for both two and three-dimensional models are presented to confirm our theoretical analysis. Finally, we extend our analysis to Galerkin-mixed methods to obtain optimal error estimates for each components.

References

[1] J. Douglas, JR., R. Ewing and M.F. Wheeler, *A time-discretization procedure for a mixed finite element approximation of miscible displacement in porous media*, RAIRO Anal. Numer., **17** (1983), pp. 249–265.

[2] R.E. Ewing and M.F. Wheeler, *Galerkin methods for miscible displacement problems in porous media*, SIAM J. Numer. Anal., **17**(1980), pp. 351–365.

[3] B. Li and W. Sun, *Unconditional convergence and optimal error estimates of a Galerkin-mixed FEM for incompressible miscible flow in porous media*, SIAM J. Numer. Anal., **51**(2013), pp. 1959–1977.

Existence theory and Ulams stabilities for switched coupled system of implicit impulsive fractional order Langevin equations

R. Rizwan[1], Z. Zhen[1], A. Zada[2]

[1] *School of Mathematics, Renmin University of China, China, rizwan@ruc.edu.cn/rixwan4630@gmail.com*
[1] *School of Mathematics, Renmin University of China, China, zhengzy@ruc.edu.cn*
[2] *School of Mathematics, Renmin University of China, China, akbarzada@uop.edu.pk*

In this manuscript, switched coupled system of nonlinear implicit impulsive Langevin equations with two Hilfer fractional derivatives is considered. Using the techniques of nonlinear functional analysis, we establish appropriate conditions and results to discuss existence, uniqueness and Ulam's type stability results of our proposed model, with the help of Banach's fixed point theorem. An example is provided at the end to illustrate our results.

References

[1] I. A. Rus, Ulam stability of ordinary differential equations, Stud. Univ. Babes Bolyai Math., (54), 125—133, (2009).

[2] I. Podlubny, Fractional Differential Equations, Academic Press, San Diego, CA, 1999.

[3] Th. M. Rassias, On the stability of linear mappings in Banach spaces, Proc. Amer. Math., (72), 297—300, (1978).

[4] R. Rizwan, Existence theory and stability snalysis of fractional Langevin equation, Int. J. Nonlinear Sci. Numer. Simul., (20), , 7-8, 833—848, (2019).

[5] R. Rizwan, A. Zada, M. Ahmad, S. O. Shah, H. Waheed, Existence theory and stability alysis of switched coupled system of nonlinear implicit impulsive LEs with mixed derivatives, Math. Methods Appl. Sci., (44), 11, 8963—8985, (2021).

The VI International AMMCS
Interdisciplinary Conference
Waterloo, Ontario, Canada
DATE

Modelling transmission dynamics of Lassa fever transmission with environmental transmissions

C. E. Madubueze[1,2], J. M. Heffernan[1]

[1] *York University, Toronto, Canada,*
[2] *University of Agriculture Makurdi, Nigeria*

Lassa Fever (LF), caused by the Lassa virus, is an animal-borne disease endemic in some regions of Africa with a rodent called a natal multimammate rat as a natural reservior. It occurs more during the dry season when the bushes are dry and burned in preparation for the farming season, making the rodents move into human habitats for food to survive. The rodents excrete their faeces and contaminate the environment making environmental transmission vital in Lassa fever transmission dynamics. Therefore, studying the contaminated environment's impact on Lassa fever is essential. This study used a deterministic model to examine the situation of Lassa fever transmission incorporating environmental transmission. First, the model's stability is established regarding the model's basic reproduction number, R_0. Further, the model implements the sensitivity analysis to identify the parameters that fuel the Lassa fever spread using the Partial Rank Correlation Coefficient (PRCC) technique based on the Latin hypercube sampling (LHS).

Keywords: Natal Multimammate rat, Lassa fever, sensitivity analysis, contaminated environment.

A high-resolution, continental scale, and modular flood risk estimation framework

Chiranjib Chaudhuri[1] and Geosapiens R&D Team[1]

[1] *Geosapies Inc., Quebec, Canada*

The lack of up-to-date, easily available flood risk data has slowed down Canadian attempts to mitigate flood damage, notwithstanding the substantial historical losses associated with frequent and devastating flood episodes. To address this problem, we present a novel flood risk estimation framework. The pipeline is extremely modular and consists of an advanced geographical pre-processing system, a probabilistic deep learning based marginal regional regression model, an advanced hydraulic model, and a web-interface based SaaS platform for zonal risk estimation and visualization. The model is implemented on entire North America covering almost 14,000 network groups and 1.9 million catchments. There are 2 flavors of the model coarse-resolution (30m) and high-resolution (1m where HRDEM is available). The geographic pre-processing system include creation of topology of the river and catchment network, DEM conditioning, LU/LC processing, for the hydraulic model. It also pre-processes the location of the station, soil parameters, topographic variables, climate parameters for the input to the hydrologic model. The deep learning based probabilistic regional regression models relates an almost 130 catchment specific and upstream aggregated co-variates with the distribution of the annual maximum discharge of almost 16,000 stations. This model is further used to infer the distribution and in turn 15 quantiles/return periods (2-1500) of the discharge at all the ungauged locations. These discharge return periods are then used as input to the volumetric manning's equation based hydraulic model which estimates the corresponding flood maps for each catchment. The testing of the flood maps against observations and govt. studies indicated good performance.

The VI International AMMCS
Interdisciplinary Conference
Waterloo, Ontario, Canada
DATE

High-order state redistribution methods on cut cell grids

A. Giuliani[1], M. Berger[1]

[1] *Flatiron Institute, Simons Foundation, New York, USA*

In this talk, we present high-order state redistribution methods on embedded boundary grids. State redistribution relaxes the overly restrictive CFL condition that results from arbitrarily small cut cells when explicit time steppers are used. We show how to stabilize both finite volume and discontinuous Galerkin spatial discretizations and take time steps that are proportional to the size of Cartesian cells in the background grid. State redistribution works by post-processing the numerical solution after each stage or step of an explicit time stepping method. The advantage of this approach is that it does not require complex geometric manipulations. We solve a number of test problems with smooth and shocked solutions that demonstrate the encouraging potential of this technique for applications on embedded boundary grids.

Event-Driven Finance: Trading Biotech Events at Intermediate Timescales

Mike Lipkin[1]

[1] *NYU Tandon, Brooklyn, NY {mike.katama@gmail.com}*

The typical pricing models studied in academic settings are simple models with generally a single time scale. This has a consequence that the calculated volatility smiles are generic and actually never fit real events. One example of a financial event introducing an additional time scale is earnings. More complicated situations are drug announcements. The latter can involve multiple time scales, uncertain dates and asymmetric binary movement in the underlying. Paradoxically, one consequence of the nature of biotech events is that they nevertheless can be traded with ridiculously simple models. In this talk I will introduce and walk through a few illustrative examples of biotech events and how they might be monetized.

Optimal Bandwith Selection in Bio-FET Measurements

L.A. Melara[1], R. M. Evans[2], S. Cho[3],A. Balijepali[4], A.J. Kearsley[5]

[1] *Shippensburg University of Pennsylvania, USA, lamelara@ship.edu*
[2] *National Institute of Standards & Technology, Gaithersburg, Maryland, USA, ryan.evans@nist.gov*
[3] *National Institute of Standards & Technology, Gaithersburg, Maryland, USA, seulki.cho@nist.gov*
[4] *National Institute of Standards & Technology, Gaithersburg, Maryland, USA, arvind.balijepalli@nist.gov*
[5] *National Institute of Standards & Technology, Gaithersburg, Maryland, USA, anthony.kearsley@nist.gov*

The use of stochastic regression to separate signal from noise produced by Bio-FETs will be discussed in this talk. The noise realized by BioFETs interferes with quantitative and qualitative analysis, thus determining optimal bandwidth associated with experimental Bio-FET data measurements is an important task. Presented results suggest consistent across aspect rations and a choice of stochastic regression kernel function and yield what appear to be good results.

References

[1] Evans, Ryan M., Arvind Balijepalli, and Anthony J. Kearsley. *Transport Phenomena in Biological Field Effect Transistors.* SIAM Journal on Applied Mathematics **80**, 6, pp. 2586-2607 (2020).

[2] Evans, Ryan M., Arvind Balijepalli, and Anthony J. Kearsley. *Diffusion-limited reactions in nanoscale electronics.* Methods and Applications of Analysis **26**, 2, pp. 149-166 (2019).

The VI International AMMCS
Interdisciplinary Conference
Waterloo, Ontario, Canada

Shortcuts to Adiabaticity in Krylov Space

K. Takahashi[1,2], A. del Campo[2,3]

[1] *Mie University, Mie, Japan ktaka@phen.mie-u.ac.jp*
[2] *University of Luxembourg, Luxembourg, Luxembourg*
[3] *Donostia International Physics Center, San Sebastián, Spain adolfo.delcampo@uni.lu*

Shortcuts to adiabaticity provide fast protocols for quantum state preparation in which the use of auxiliary counterdiabatic controls circumvents the requirement of slow driving in adiabatic strategies. While their development is well established in simple systems, their engineering and implementation are challenging in many-body quantum systems with many degrees of freedom. We show that the equation for the counterdiabatic term, equivalently the adiabatic gauge potential, is solved by introducing a Krylov basis. The Krylov basis spans the minimal operator subspace in which the dynamics unfolds and provides an efficient way to construct the counterdiabatic term. We apply our strategy to paradigmatic single and many-particle models. The properties of the counterdiabatic term are reflected in the Lanczos coefficients obtained in the course of the construction of the Krylov basis by an algorithmic method. We examine how the expansion in the Krylov basis incorporates many-body interactions in the counterdiabatic term.

References

[1] Kazutaka Takahashi, Adolfo del Campo, *Shortcuts to Adiabaticity in Krylov Space*, arXiv:2302.05460.

Impact of feedforward and feedback controls on potassium homeostasis: A mathematical modeling analysis

Melissa M. Stadt[1], Jessica Leete[2], Sophia Devinyak[3], Anita T. Layton[1,4,5,6]

[1] *Department of Applied Mathematics, University of Waterloo, Waterloo, ON*
[2] *Computational Biology and Bioinformatics Program, Duke University, Durham, NC*
[3] *Department of Physics and Astronomy, University of Waterloo, Waterloo, ON*
[4] *Cheriton School of Computer Science, University of Waterloo, Waterloo, ON*
[5] *Department of Biology, University of Waterloo, Waterloo, ON*
[6] *Department of Pharmacy, University of Waterloo, Waterloo, ON*

Dysregulation of potassium is a common and dangerous side effect of many pathologies and medications. Potassium homeostasis is primarily mediated by (i) uptake of potassium into the cells via the sodium-potassium pump and (ii) renal regulation of urinary potassium excretion. Due to the importance of potassium in cellular function and the daily challenge of undergoing variations in potassium intake, mammals have evolved several regulatory mechanism to ensure proper balance of potassium levels in the extra- and intracellular fluids. These processes are complex and are not completely understood. In this project, we developed a compartmental model of extra- and intracellular potassium regulation including known feedforward and feedback mechanisms. To investigate the impact of individual regulatory mechanisms on potassium homeostasis, we conducted and analyzed simulations for a single meal and potassium loading or depletion over multiple days with and without different feedback and feedforward mechanisms. Additionally, we investigated a hypothesized muscle-kidney crosstalk signal. Model simulations revealed that a muscle-kidney crosstalk signal is necessary for physiological homeostatic recovery after a period of potassium loading or depletion. Using our mathematical model, we were able to unravel the multi-factorial mechanisms involved in potassium regulation by studying individual impacts of the feedforward and feedback mechanisms on potassium homeostasis.

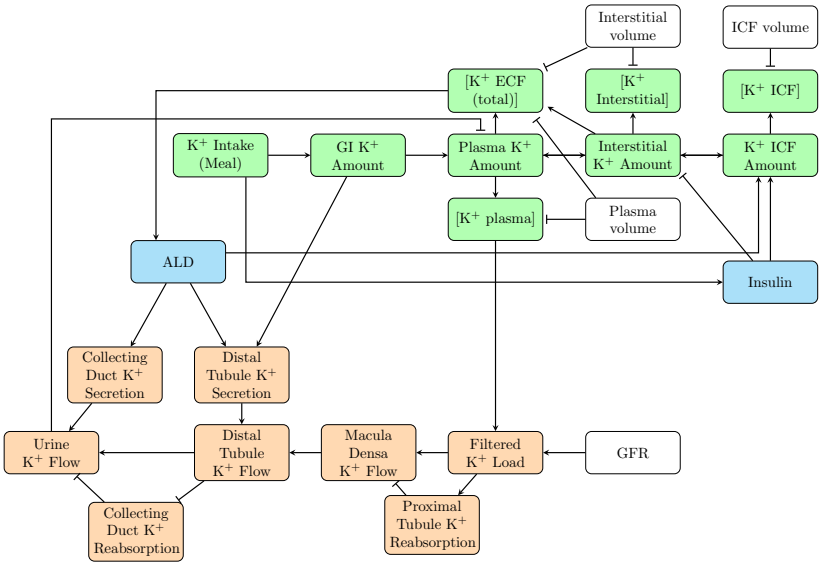

Figure 1: Flow chart depicting the compartments of our mathematical models of potassium regulation. Pointed arrows intdicate stimulation, blunted arrows indicate inhibition. GI: gastrointestinal, Interstitial: interstitial fluid, ICF: intracellular fluid, ECF: extracellular fluid

Unveiling out-of-time-order correlators from stochastic operator variance

Aurélia Chenu[1], Pablo Martinez-Azcona[1], Aritra Kundu[1], Adolfo del Campo[1,2]

[1] *Department of Physics and Materials Science, University of Luxembourg, L-1511 Luxembourg*
[2] *Donostia International Physics Center, E-20018 San Sebastián, Spain*

Quantum experiments are performed in noisy platforms. In NISQ devices [1], realistic setups can be described by open systems or noisy Hamiltonians. Starting from a generic noisy Hamiltonian, $H_t = \hat{H}_0 + \sqrt{2\gamma}\xi_t \hat{L}$, we go beyond the noise-averaged density matrix by introducing the concept of stochastic operator variance (SOV) of an observable $\hat{A}$, namely $\Delta\hat{A}_t^2 = \langle \hat{A}_t^2 \rangle - \langle \hat{A}_t \rangle^2$. The SOV [2] is an operator that characterizes the deviation of any operator $\hat{A}_t$ from the noise-averaged operator in a stochastic evolution governed by the Hamiltonian, as illustrated in Fig. 1. As such, it is relevant in the quantum simulation of open systems using NISQ devices, e.g., to engineer a given dissipative evolution.

Surprisingly, we find that the evolution of the noise-averaged variance, $\Delta\hat{A}_t^2 = e^{\mathscr{L}^\dagger t}[\hat{A}_0^2] - (e^{\mathscr{L}^\dagger t}[\hat{A}_0])^2$, relates to an out-of-time-order correlator (OTOC), which connects fluctuations of the system with scrambling. Indeed,

$$\frac{1}{N}\frac{\mathrm{dTr}(\Delta\hat{A}_t^2)}{\mathrm{d}t} = -\frac{2\gamma}{N}\mathrm{Tr}([\hat{L}, \langle \hat{A}_t \rangle]^2) \sim e^{\lambda t}. \tag{1}$$

where the exponential behavior holds only in systems with scrambling over the appropriate period. Importantly this connection may allow computing the Lyapunov exponent and experimentally access OTOCs without the need to invert the sign of the Hamiltonian. We illustrate the SOV-OTOC relation in a stochastic generalization of the Lipkin-Meshkov-Glick (sLMG) model undergoing energy dephasing, where the action of noise changes the stability region compared to the noiseless LMG [3]. Our results can be used to elucidate quantum chaos in noisy systems and benchmark NISQ devices.

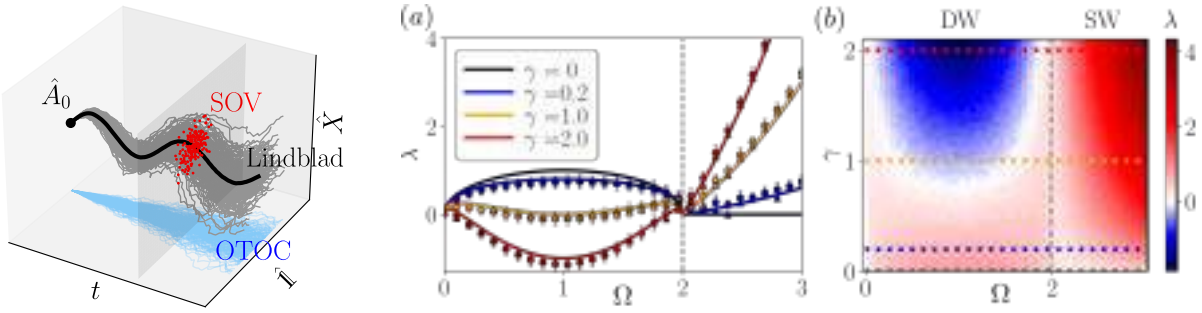

Figure 1: left: **The SOV-OTOC relation.** Illustration of the connection between the stochastic operator variance (SOV) and the out-of-time-order correlator (OTOC). right: Lyapunov exponent of the classical sLMG model at the saddle point (a) for different values of the noise strength γ and (b) over the phase diagram.

References

[1] K. Bharti, A. Cervera-Lierta, T. H. Kyaw, T. Haug, S. Alperin-Lea, A. Anand, M. Degroote, H. Heimonen, J. S. Kottmann, T. Menke, W.-K. Mok, S. Sim, L.- C. Kwek, and A. Aspuru-Guzik, Rev. Mod. Phys. **94**, 015004 (2022).
[2] P. Martinez-Azcona, A. Kundu, A. del Campo, and A. Chenu, ArXiv:2302.12845 (2023).
[3] H. J. Lipkin, N. Meshkov, and A. J. Glick, Nuclear Physics **62**, 188 (1965).

Dynamics of a Plant Virus Propagation Model with Vector Preference and Latent Periods

J.A. Collera[1], K.M. Gonzales[2]

[1] *University of the Philippines Baguio, Baguio City, Philippines, jacollera@up.edu.ph*
[2] *University of the Philippines Baguio, Baguio City, Philippines, kmgonzales2@up.edu.ph*

In this talk, we consider a plant virus propagation model with vector preference and latent periods in both the plant host and insect vector populations. We assume that the virus affects the behavior and movement of the insect vectors, and that there are time lags to become infectious that occur both within the plant host and insect vector after exposure to viruses. Hence, the resulting model is a system of delay differential equations with Beddington-DeAngelis type incidence rate and two discrete time delays to reflect, respectively, the insect vector preference and the latent periods. We first compute the basic reproduction number [1] of the system and provide existence conditions of the disease-free equilibrium and the endemic equilibrium in terms of this number. Our results show that only the disease-free equilibrium exists when the reproduction number is less than one, while the endemic equilibrium only exists when the reproduction number is greater than one. Using the time delays as main parameters, in the former case, the disease-free equilibrium is shown to be absolutely stable. That is, it is locally asymptotically stable for any positive values of the time delays. Meanwhile, in the latter case, we show that the endemic equilibrium can switch stability, possibly multiple times, when Hopf bifurcation occurs. We then illustrate these results in the two-parameter space using numerical continuation [2] to gain more insights on how the latent periods affect the dynamics of the system. We also examine the effects of one of the saturation-rate parameter which is not considered in previous works [3]. This saturation constant due to healthy plant hosts is inversely related to the reproduction number, and so the intuitive approach is to increase the value of this parameter in order to lower the reproduction number. Our analysis in the two-dimensional parameter space shows a better perspective on the dynamical behavior of the system when we vary the value of this saturation constant but the reproduction number remains larger than one.

References

[1] P. Van den Driessche and J. Watmough *Reproduction numbers and sub-threshold endemic equilibria for compartmental models of disease transmission*, Math. Biosci. **180**, 1-2, pp. 29-48 (2002).

[2] T.B. Luzyanina, J. Sieber, K. Engelborghs, G. Samaey and D. Roose, *Numerical bifurcation analysis of mathematical models with time delays with the package DDE-BIFTOOL*, Math. Biol. Bioinform. **12**, 2, pp. 496-520 (2017).

[3] M. Jackson and B.M. Chen-Charpentier, *Modeling plant virus propagation with delays*, J. Comput. Appl. Math. **309**, pp. 611-621 (2017).

Rotating waves of multi-strain virus with cross immunity

Bushra Majeed[1], Denis Fernandes da Silva[1], Jianhong Wu[1]

[1] *Laboratory for Industrial and Applied Mathematics, Department of Mathematics and Statistics,York University,Canada*

Genetic mutations play an important role in the evolution and spread of viruses. These genetic variations can lead to the emergence of new variants, thereby posing significant challenges in formulating effective preventive measures, therapies, and vaccines. Influenza is caused by a spectrum of respiratory infectious viruses that undergo constant mutations, resulting in different strains every year. Consequently, developing a new vaccine each year becomes an absolute necessity. Here we utilize a SIR-type indexed by strains in a discrete circular space to examine the temporally recurrent strain-specific prevalence patterns as a consequence of genetic drift, due to the evolution through point mutations in the viral genome. We use a finite-dimensional ring-shaped antigenic strain space and consider the existence of rotating waves of influenza strains using bifurcations with symmetry.

Large rank specializations of Shioda's curve and a conjecture of Erdös on powerful numbers

P.G. Walsh

University of Ottawa, Canada, gwalsh@uottawa.ca

Brown and Myers studied the family of curves $y^2 = x^3 - x + m^2$, and proved that any such curve with $|m| > 1$ has rank at least 2. We will discuss how this starting point has led to an ongoing investigation into a much larger class of curves with rank at least 2, along with the existence of curves in this family with remarkably large rank over the rationals. In the second part of the talk, we will describe a method to compute sets of four coprime powerful numbers in arithmetic progression using elliptic curves, settling a question of Erdös.

Correcting the Coherence of a Quantum State in a Noisy Environment

M. Byrd[1], L.-A. Wu[2,3,4]

[1] *Southern Illinois University, Carbondale, Illinois, USA mbyrd@siu.edu*
[2] *Department of Physics, University of the Basque Country UPV/EHU, 48080 Bilbao, Spain*
[3] *IKERBASQUE Basque Foundation for Science, 48013 Bilbao, Spain*
[4] *EHU Quantum Center, University of the Basque Country UPV/EHU, Leioa, Biscay 48940, Spain*

Quantum information processing uses quantum resources such as entanglement and coherence to achieve tasks that are difficult or impossible to perform using classical information processing [1]. Thus coherence and entanglement are considered quantum resources [2]. Errors from a noisy environment can degrade these resources. For quantum states, and quantum computing, there are quantum error correcting codes that are able to correct the quantum states by encoding quantum information and then detecting and correcting errors on the code. But how does one correct a quantum resource? To recover a quantum resource, one need not correct the state back to its original form. It is only necessary that the amount of the resource be the same before and after being affected by noise. This implies a different objective, one which allows different encoding, detection and recovery methods. In the case of coherence, this freedom will be discussed along with methods to correct the coherence of a quantum system to restore the amount of coherence. Examples of these methods will be also be given. These methods indicate that coherence can be retrieved without the need for full error correction. This saves computational resources such as quantum bits and quantum gates.

References

[1] Michael A. Nielsen and Isaac L. Chuang, *Quantum Computation and Quantum Information*, Cambridge University Press, NY, NY, USA.

[2] Eric Chitambar and Gilad Gour, *Rev. Mod. Phys.* **91**, 025001 (2019).

Developing optimal control of multicomponent contamination flows in porous media

Khan Enaet Hossain[1], Dong Liang[2], Hongmei Zhu[3]

[1] *Department of Mathematics and Statistics, York University, Toronto, On, Canada, enaet09@yorku.ca*
[2] *Department of Mathematics and Statistics, York University, Toronto, On, Canada, dliang@yorku.ca*
[3] *Department of Mathematics and Statistics, York University, Toronto, On, Canada, hmzhu@yorku.ca*

Compressible fluid flows in permeable media have broadly been experienced in numerous computational simulations in science and engineering regions, e.g., seawater interruption into coastal aquifers, groundwater pollution, environmental assurance, dangerous waste dumping, and oil recuperation within the supply. The reason for reenacting fluid flow in permeable media is to evaluate contamination transport, seawater interruption and control, contamination expectation, subsurface toxin transport and remediation, and in numerous other applications. It is imperative to completely recognize the overseeing physical behavior of stream and transport in permeable media to plan effective remediation procedures. In this work, we develop an optimization control of groundwater pollution subject to the nonlinear multi-component pollution flows in porous media. The optimization objective function is considered as the overall effects due to pollution at observation sites and the costs of emission reductions at the source piece's locations. The system of nonlinear flow and multicomponent transport PDEs are solved by the improved-upwind splitting finite difference method. Then the simulated results are used in the optimization problem which is solved by the differential evolution (DE) optimization algorithm. The main purpose of the pollution optimal control problem is to find optimal injection rates which minimize the difference between the simulated concentrations and allowable observed concentrations at observation sites and the overall abatement cost. Numerical experiments will be given to show the performance of the developed model and algorithm.

References

[1] L.J. Alvarez-Vazquez, A. Martinez, R. Munoz-Sola, C. Rodriguez, and M.E. Vazquez-Mendez, *Numerical optimization for the purification of polluted shallow waters*, J. Comput. Appl. (2006).

[2] D. Liang and Z. Zhou, *The conservative splitting domain decomposition method for multicomponent contamination flows in porous media*, J. Comput. Phys. **400**, pp. 108974 (2020).

[3] K. Vafai, *Handbook of porous media*, Crc Press, (2015).

[4] K. Price, R.M. Storn and J.A. Lampinen, *Differential evolution: a practical approach to global optimization*, SSBM (2006).

[5] Y. Yuan, D. Liang and H. Zhu, *Optimal control of groundwater pollution combined with source abatement costs and taxes*, J. Comput. Sci. **20**, pp. 17-29 (2017).

The VI International AMMCS
Interdisciplinary Conference
Waterloo, Ontario, Canada

Vanishing of twisted L-functions of elliptic curves over function fields

A. Comeau-Lapointe[1], C. David[2], M. N. Lalín[3], W. Li[4]

[1] *Concordia University, Montréal, Canada, antoine.comeau-lapointe@concordia.ca*
[2] *Concordia University, Montréal, Canada, chantal.david@concordia.ca*
[3] *Université de Montréal, Montréal, Canada, matilde.lalin@umontreal.ca*
[4] *Washington University St. Louis, St. Louis, USA, wanlin@wustl.edu*

Let E be an elliptic curve over the rationals, and let χ be a Dirichlet character of order ℓ for some odd prime ℓ. Heuristics based on the distribution of modular symbols and random matrix theory have led to conjectures predicting that the vanishing of the twisted L-functions $L(E,\chi,s)$ at $s=1$ is a very rare event (David-Fearnley-Kisilevsky [1, 2] and Mazur-Rubin [5, 6]). In particular, it is conjectured that there are only finitely many characters of order $\ell > 5$ such that $L(E,\chi,1)=0$ for a fixed curve E.

We investigate the case of elliptic curves over function fields. For Dirichlet L-functions over function fields, Li [4] and Donepudi-Li [3] have shown how to use the geometry to produce infinitely many characters of order $\ell \geq 2$ such that the Dirichlet L-function $L(\chi,s)$ vanishes at $s=1/2$, contradicting (the function field analogue of) Chowla's conjecture. We show that their work can be generalized to constant curves $E/\mathbb{F}_q(t)$, and we show that if there is one Dirichlet character χ of order ℓ such that $L(E,\chi,1)=0$, then there are infinitely many, leading to some specific examples contradicting (the function field analogue of) the number field conjectures on the vanishing of twisted L-functions. Such a dichotomy does not seem to exist for general curves over $\mathbb{F}_q(t)$, and we produce empirical evidence which suggests that the conjectures over number fields also hold over function fields for non-constant $E/\mathbb{F}_q(t)$.

References

[1] Chantal David, Jack Fearnley, and Hershy Kisilevsky. *On the vanishing of twisted L-functions of elliptic curves.* Experiment. Math., **13**, 2, pp. 185-198, (2004).

[2] Chantal David, Jack Fearnley, and Hershy Kisilevsky. *Vanishing of L-functions of elliptic curves over number fields.* Ranks of elliptic curves and random matrix theory, **341** London Math. Soc. Lecture Note Ser., pp 247-259. Cambridge Univ. Press, Cambridge, (2007).

[3] Ravi Donepudi and Wanlin Li. *Vanishing of Dirichlet L-functions at the central point over function fields.* Rocky Mountain J. Math., **51**, 5, pp. 1615-1628, (2021).

[4] Wanlin Li. *Vanishing of hyperelliptic L-functions at the central point.* J. Number Theory, **191**, pp. 85-103, (2018).

[5] Barry Mazur and Karl Rubin. *Diophantine stability.* Amer. J. Math., **140**, 3, pp. 571-616, (2018). With an appendix by Michael Larsen.

[6] Barry Mazur and Karl Rubin. *Arithmetic conjectures suggested by the statistical behavior of modular symbols.* Experimental Mathematics (2021).

Bounds on Codes from Fiber Products of Curves with Many Points

C. Brantner[1], P. Tan[1], M. West[1,2]

[1] *University of Wisconsin-Eau Claire, Eau Claire, USA,*
[2] *westmr@uwec.edu*

In an attempt to explore the possibilities of parameters produced through the construction in [1] and [3], the authors constructs codes from fiber products of curves that appear in [2]. The construction is as follows:

Given an equation $f(x,y) = 0$ defining a curve over the finite field $\mathbf{F}_q$, consider the curves $\mathscr{Y}_1$ and $\mathscr{Y}_2$ defined by $f(y_0,y_1) = 0$ and $f(y_2,y_0) = 0$ respectively. These curves both have projections onto the y_0 coordinate. We then take the fiber product of the curves above this projection $\mathscr{Y} = \mathscr{Y}_1 \times_{y_0} \mathscr{Y}_2$. Let $B \subseteq \mathscr{Y}(\mathbf{F}_q)$ be the set of points unramified over the projections onto the y_1- and y_2-coordinates. The data being encoded under this construction is polynomials in y_0, y_1, y_2 whose degrees are limited so that the evaluation map along B is injective and the degrees of y_1 and y_2 are limited so that polynomial interpolation can be used to restore them if a value is lost. The encoding is similar to that in the Reed-Muller code, this time limiting the evaluation points to those in B.

The purpose of this construction is that there are two axes along which restoration of a value can be done. If F is an encoded polynomial and $P \in B$ such that the value of $F(P)$ is lost or corrupted, then the sets

$$B_{i,P} = \{P' \in B \ : \ y_i(P) \neq y_i(P') \text{ and } y_j(P) = y_j(P') \ \forall j \neq i\} \tag{1}$$

for $i = 1,2$ can both act as recovery sets for the missing data. Thus if two pieces of data in the same recovery set are lost, they can be restored by their other recovery sets.

For these codes, often the dimension relative to their size is beyond the useful complexity, as of now. In an effort to further understand possible dimensions and rate, we explore more examples of these objects. In many cases the dimension and size parameters are slightly better for the new codes in comparison to the old ones when comparing across fixed base fields.

References

[1] M. Chara, S. Kottler, B. Malmskog, B. Thompson, M. West, *Minimum distance and parameter ranges of locally recoverable codes with availability from fiber products of curves.*, Des. Codes and Cryptogr., pp. 1-29 (2023).

[2] G. van der Geer, E.W. Howe, K.E. Lauter, C. Ritzenthaler *Tables of Curves with Many Points*, `http://www.manypoints.org`, (2009). Retrieved Apr. 2023.

[3] K. Haymaker, B. Malmskog, G.L. Matthews, *Locally recoverable codes with availability $t \geq 2$ from fiber products of curves*, Adv. Math. Commun., **12**(2), 317 (2018).

Simulation based exploration of the effect of ultrasound-induced mechanical stress on biofilm response to antibiotics

M. Ghasemi[1], S. Sivaloganathan[1]

[1] *University of Waterloo, Waterloo, Canada, {m23ghase,* ssivaloganathan*}@uwaterloo.ca*

Bacterial biofilms can lead to chronic infections, increase tolerance to antibiotics and disinfectants, resistance to phagocytosis, and other components of the body's immune system. Biofilm formation is implicated in the persistence of staphylococcal infections and chronic *Pseudomonas aeruginosa* lung infections in cystic fibrosis (CF) patients (which can result from biofilm-growing mucoid strains). Conventional treatments utilize aggressive antibiotic prophylaxis/therapy to prevent/eliminate biofilms, followed by chronic suppressive therapy. Recently, the use of enzymes to dissolve the biofilm matrix was investigated, in addition to quorum sensing inhibitors to increase biofilm susceptibility to antibiotics. In this study, we propose a novel strategy, utilizing ultrasound-induced inertial cavitation, to increase antibiotic efficacy. The wall shear stress at the biofilm interface is calculated, and viscoplastic constitutive equations are used to examine the biofilm response to the mechanical stress. Our simulations suggest that the maximum biofilm detachment occurs at high pressure/low frequency, and the mechanical disruption can affect the biochemical processes inside the biofilm resulting in vulnerability to antibiotics.

Generic Properties of Mean Field Games

A. Bressan[1] and K. T. Nguyen[2]

[1] *Department of Mathematics, Penn State University, axb62@psu.edu*
[2] *Department of Mathematics, North Carolina State University, khai@math.ncsu.edu*

We consider a class of first order Mean Field Games, where the state associated with each player evolves according to an ODE which is linear w.r.t. the control. Existence, uniqueness, and stability of solutions are studied from the point of view of generic theory. Within a suitable topological space of dynamics and cost functionals, it is proved that, for "nearly all" mean field games (in the Baire category sense) the best reply map is single valued for a.e. player. As a consequence, the mean field game admits a strong (not randomized) solution. Examples are given of open sets of games admitting a single solution, and other open sets admitting multiple solutions. Further examples show the existence of an open set of MFG having a unique solution which is asymptotically stable w.r.t. the best reply map, and another open set of MFG having a unique solution which is unstable. Finally, an example is given of a MFG with terminal constraints which does not have any solution, not even in the mild sense with randomized strategies.

References

[1] A. Bressan and K. T. Nguyen, Generic properties of mean field games, *Dynamic Games Appl.*, to appear.

Exponentially decaying solutions for models with delayed and advanced arguments: nonlinear effects in linear differential equations

L. Berezansky[1], E. Braverman[2], S. Pinelas[3]

[1] *Dept. of Math, Ben-Gurion University of the Negev, Israel, brznsky@bgu.ac.il*
[2] *Dept. of Math & Stats, University of Calgary, Calgary, AB, Canada, maelena@ucalgary.ca*
[3] *CINAMIL, Departamento de Ciencias Exatas e Engenharia, Academia Militar, Amadora, Portugal, sandra.pinelas@gmail.com*

We consider a scalar linear mixed differential equation with several terms, both delayed and advanced arguments and a bounded right-hand side

$$\dot{x}(t) + \sum_{k=1}^{m} b_k(t)x(h_k(t)) = f(t).$$

Assuming that the deviations of the argument are bounded, we present sufficient conditions when there exists a unique bounded solution on the positive half-line. Explicit tests for a bounded solution of a homogeneous equation to decay exponentially are obtained. Existence of exponentially decaying solutions for this class of differential equations is studied for the first time, and we illustrate sharpness of the results with examples. We show that the standard approach when convergence of all solutions is stated does not work for mixed equations; in addition to an exponentially decaying, there may be a growing solution. All the coefficients and the mixed arguments are assumed to be Lebesgue measurable functions, not necessarily continuous. Though the equation is linear, some properties, as well as the methods applied, are more typical for nonlinear models, for example, fixed-point theorems are used in the proofs. The results are to appear in [1].

References

[1] L. Berezansky, E. Braverman, and S. Pinelas, Exponentially decaying solutions for models with delayed and advanced arguments: nonlinear effects in linear differential equations, *Proc. AMS* **151** (2023), 4261–4277.

Parameter Estimation of Hodgkin-Huxley Model: A Comparative Study of Metaheuristics and Neural Network Approaches

P. Yue[1], M. Cojocaru[2], A. Willms[3]

[1] *University of Guelph, Guelph, Canada, yuep@uoguelph.ca*
[2] *University of Guelph, Guelph, Canada, mcojocar@uoguelph.ca*
[3] *University of Guelph, Guelph, Canada, awillms@uoguelph.ca*

The Hodgkin-Huxley (HH) model is a well-known mathematical model for the generation and propagation of action potentials in neurons. However, determining certain parameters of the model involves a tedious combination of experiments and data tuning, and there is often significant uncertainty in their values. Parameter estimation of the HH model has been an active research for several decades, and various optimization techniques have been used including metaheuristic algorithms. These methods have been successful in finding parameter values that fit experimental data well, but they can be computationally expensive and may require significant expertise to tune. More recently, Artificial Neural Networks (ANN) have been applied to parameter estimation of mathematical models, and it has the advantage of being able to handle noisy and incomplete data, which can often provide faster and more accurate results than traditional optimization methods. In this research, we propose an ANN-based approach for parameter estimation in the HH model, which employs a deep learning architecture that is trained on a large voltage-clamp type dataset with corresponding HH model parameters. We intend to demonstrate that the ANN can efficiently estimate the HH model parameters for a given set of data with minimal computation effort after completion of the training process. We focus primarily on the ANN method and aim to demonstrate its superiority over the metaheuristic approaches such as Genetic Algorithms, Differential Evolution and Simulated Annealing, in terms of computational efficiency and accuracy.

References

[1] L. Buhry, F. Grassia, A. Giremus, E. Grivel, S. Renaud and S. SaÃ¯ghi, *Automated Parameter Estimation of the Hodgkin-Huxley Model Using the Differential Evolution Algorithm: Application to Neuromimetic Analog Integrated Circuits*, Neural Computation **24**, 10, pp. 2599-2625 (2011).

[2] A. Willms, D. Baro, R. Harris-Warrick and J. Guckenheimer, *An improved parameter estimation method for Hodgkin-Huxley models*, Journal of Computational Neuroscience **6**, 2, pp. 145-68 (1999).

[3] T. T. Dufera, Y. C. Seboka, C. F. Portillo,, *Parameter Estimation for Dynamical Systems Using a Deep Neural Network*, Parameter Estimation for Dynamical Systems Using a Deep Neural Network, **2022**, 10, 2014510 (2022).

The Impact of Time Delays on Synchrony in a Neural Field Model

S.A. Campbell[1], Isam Al-Darabsah[2], Bootan Rahman[3], Wilten Nicola [4], Liang Chen [5]

[1] *University of Waterloo, Canada, sacampbell@uwaterloo.ca*
[2] *Jordan University of Science and Technology, Jordan, imaldarabsah@just.edu.jo*
[3] *University of Kurdistan Hewler, Iraq, bootan.rahman@ukh.edu.krd*
[4] *University of Calgary, Canada, wilten.nicola@ucalgary.ca*
[5] *University of Waterloo, Canada, l477chen@uwaterloo.ca*

We consider a neural field model which consists of a network of Wilson-Cowan nodes with homeostatic adjustment of the inhibitory coupling strength and time delayed, excitatory coupling:

$$\begin{aligned} \tau_E \frac{dE_i}{dt} &= -E_i + \phi\left(\sum_{j=1}^{N} W_{ij}^{EE} \int_0^\infty g(\tau) E_i(t-\tau) d\tau - W_i^{EI} I_i\right), \\ \tau_I \frac{dI_i}{dt} &= -I_i + \phi(W^{IE} E_i), \\ \tau_W \frac{dW_i^{EI}}{dt} &= I_i(E_i - p), \end{aligned} \tag{1}$$

Here E_i is the activity of the excitatory population, I_i is the activity of the inhibitory population, and W_i^{EI} is the homeostatically adjusted inhibitory to excitatory weight, in the i^{th} node. W_{IE} is the fixed excitatory to inhibitory weight, $W_{ij}^{EE} > 0$ are the (fixed) excitatory weights, $p > 0$ is the set-point for the excitatory weights and the $\tau_j > 0$ are the population time constants. The function $\phi(.)$ is the activation function which we take to be logistic. The function $g(.)$ is a delay distribution kernel which is positive and normalized to 1.

Without time delay, the system has been show to exhibit rich dynamics including mixed-mode oscillations and chaos. We show that small delays can be either synchronizing or desynchronizing, depending on the structure of the connectivity matrix. To study this further, we explore the Hopf bifurcations induced by the excitatory coupling, the connectivity structure and the delay. We show that these can lead to different patterns of phase-locked oscillations, either synchronized or desynchronized. Finally, we show how interaction between different Hopf bifurcations can lead to complex solutions, such as intermittent desynchronization. See Figure 1.

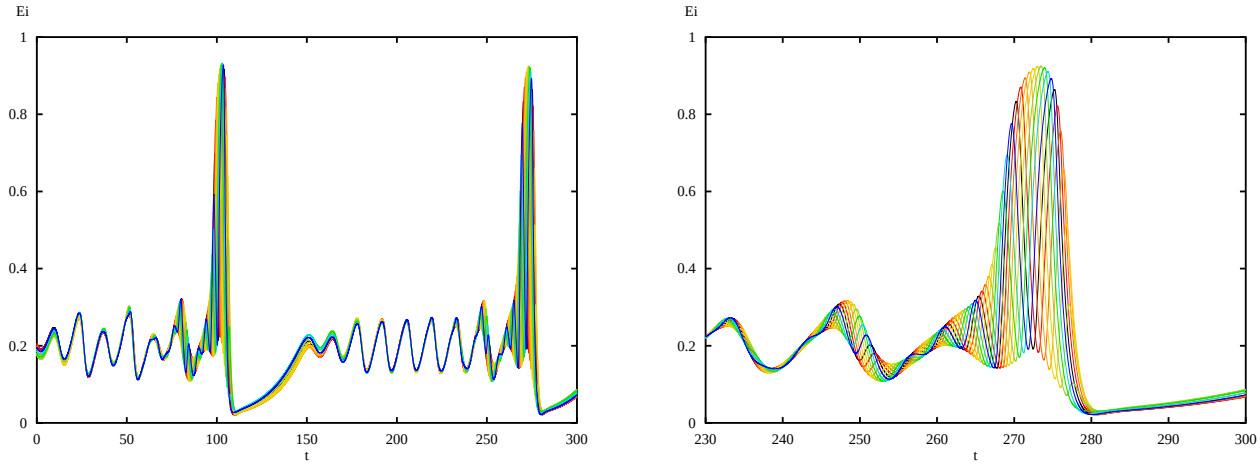

Figure 1: Solution exhibiting intermittent desynchronization. Colours correspond to excitatory activity in different nodes.

The VI International AMMCS
Interdisciplinary Conference
Waterloo, Ontario, Canada

Space-time HDG for advection-diffusion on deforming domains in the advection-dominated limit

Y. Wang[1], S. Rhebergen[2]

[1] *Department of Applied Mathematics, University of Waterloo, ON, Canada, yuan.wang@uwaterloo.ca*
[2] *Department of Applied Mathematics, University of Waterloo, ON, Canada, srheberg@uwaterloo.ca*

The time-dependent advection-diffusion equation on deforming domains is given by

$$\partial_t u + \overline{\mathbf{a}} \cdot \overline{\nabla} u - \nu \overline{\nabla}^2 u = f, \qquad \mathbf{x} := (x_1, ..., x_d) \in D(t),\ t \in (0, T], \tag{1}$$

where u is the quantity of interest, for example, a concentration or a temperature, $\overline{\mathbf{a}}$ is a d-dimensional flow field, which we assume is such that $\|\overline{\mathbf{a}}\|_{L^\infty(D)} = \mathscr{O}(1)$, ν a positive diffusion parameter, $\overline{\nabla} = (\partial_{x_1}, ..., \partial_{x_d})$, and $D(t) \subset R^d$ is a time-dependent domain in d-dimensions ($d = 2, 3$).

To facilitate the discretization of eq. (1), it is useful to introduce the space-time formulation of the advection-diffusion equation. This is done by introducing the space-time domain $\mathscr{E} := \{(t, \mathbf{x}) : \mathbf{x} \in D(t),\ 0 < t < T\} \subset R^{d+1}$, the space-time flow field $\mathbf{a} = (1, \overline{\mathbf{a}})$, and space-time gradient $\nabla = (\partial_t, \overline{\nabla})$. We can re-formulate eq. (1) then as:

$$\mathbf{a} \cdot \nabla u - \nu \overline{\nabla}^2 u = f, \qquad (t, \mathbf{x}) \in \mathscr{E}. \tag{2}$$

This equation resembles a "stationary" advection-diffusion problem in $(d+1)$-dimensions which we discretize, simultaneously in space and time, by a hybridizable discontinuous Galerkin (HDG) method [1].

We first introduced the space-time HDG method for eq. (2) in [1]. The well-posedness and error analysis of this discretization was presented in [[3] for sufficiently large diffusion parameter ν. In this talk I will present a new analysis that demonstrates that the space-time HDG method is also suitable for advection dominated ($\nu \ll 1$) flow problems.

References

[1] B. Cockburn, J. Gopalakrishnan, R. Lazarov, *Unified hybridization of discontinuous Galerkin, mixed, and continuous Galerkin methods for second order elliptic problems*, SIAM Journal on Numerical Analysis, **47**, 2, pp. 1319-1365 (2009).

[2] S. Rhebergen and B. Cockburn, *Space-time hybridizable discontinuous Galerkin method for the advection-diffusion equation on moving and deforming meshes*, in *The Courant-Friedrichs-Lewy (CFL) condition, 80 years after its discovery*, ed. C.A. de Moura and C.S. Kubrusly, pp. 45-63 (2013).

[3] K.L.A. Kirk, T. Horvath, A. Cesmelioglu and S. Rhebergen, *Analysis of a space-time hybridizable discontinuous Galerkin method for the advection-diffusion problem on time-dependent domains*, SIAM Journal on Numerical Analysis, **57**, 4, pp. 1677-1696 (2019).

Multiple solutions to the 2-dimensional Euler equations

A. Bressan

Department of Mathematics, Penn State University, axb62@psu.edu

For hyperbolic systems of conservation laws in one space dimension, a general existence-uniqueness theory is now available, for entropy weak solutions with bounded variation. In several space dimensions, however, it seems unlikely that a similar theory can be achieved.

For the 2-D Euler equations, various numerical simulations will be presented, for incompressible as well as compressible flow, indicating the existence of two distinct solutions for the same initial data. These appear to be "simplest possible" examples of Cauchy problems admitting multiple solutions. Typically, one of the solutions contains a single spiraling vortex, while the other solution contains two vortices.

Some theoretical work, aimed at validating the numerical results, will also be discussed.

References

[1] A. Bressan, Y. Jiang, and H. Liu, Numerical study of non-uniqueness for 2D compressible isentropic Euler equations, *J. Comp. Physics* **445** (2021) 110588.

[2] A. Bressan and R. Murray, On self-similar solutions to the incompressible Euler equations, *J. Differential Equations* **269** (2020), 5142–5203.

[3] A. Bressan and W. Shen, A posteriori error estimates for self-similar solutions to the Euler equations, *Discr. Cont. Dyn. Syst.* **41** (2021), 113–130.

A Lower Bound for the Area of the Fundamental Region of a Binary Form

J. Fang[1], A. Mosunov[2]

[1] *University of Waterloo, Waterloo, Canada, j7fang@uwaterloo.ca*
[2] *University of Waterloo, Waterloo, Canada, amosunov@uwaterloo.ca*

Let

$$F(x,y) = \prod_{k=1}^{n} (\delta_k x - \gamma_k y)$$

be a binary form of degree $n \geq 1$, with complex coefficients, written as a product of n linear forms in $\mathbb{C}[x,y]$. Let

$$h_F = \prod_{k=1}^{n} \sqrt{|\gamma_k|^2 + |\delta_k|^2}$$

denote the *height* of F and let A_F denote the area of the *fundamental region* $\mathscr{D}_F$ of F:

$$\mathscr{D}_F = \left\{(x,y) \in \mathbb{R}^2 : |F(x,y)| \leq 1\right\}.$$

We prove that $h_F^{2/n} A_F \geq \left(2^{1+(r/n)}\right)\pi$, where r is the number of roots of F on the real projective line $\mathbb{RP}^1$, counting multiplicity. In the case when $r = 0$ this inequality is sharp and can be attained by the form $F_{n,0}(x,y) = (x - iy)^n$. However, as F varies over all forms of degree n with $r > 0$ roots on $\mathbb{RP}^1$, we believe that it can be improved. We present a conjecture about the correct lower bound and provide computational evidence in support of this conjecture.

DSTree: A spatio-temporal indexing data structure for distributed networks

M. Hojati[1], S. Roberts[2], C. Robertson[2]

[1] *Department of Geography & Environmental Studies, Wilfrid Laurier University, Waterloo, Ontario, Canada, {mhojati}@wlu.ca*
[2] *Department of Geography & Environmental Studies, Wilfrid Laurier University, Waterloo, Ontario, Canada*

The widespread availability of tools to collect and share spatial data enables us to produce a large amount of geographic information on daily bases. This enormous production of spatial data requires scalable data management systems. Geospatial architectures have changed from clusters to cloud architectures and more parallel and distributed processing platforms to tackle these challenges. Peer-to-peer (P2P) systems as a backbone of the distributed systems have been established in several application areas such as web3, blockchains, and cryptocurrencies. Unlike centralized systems, data storage in P2P networks is distributed across network nodes, providing scalability and no single point of failure. However, managing and processing queries on these networks have always been challenging. In this work, we propose a spatio-temporal indexing data structure, DSTree (See Figure 1), that works on top of the distributed InterPlanetary File System network. DSTree does not require additional Distributed Hash Trees to perform multi-dimensional range queries. Inserting a piece of new geographic information can only cause an update of only a portion of the tree structure and does not impact the entire data graph. For example, for time-series data, such as storing sensor data, the DSTree performs better. Despite the advantages of our proposed framework, challenges remain. We conclude that more significant research effort from GIScience and related fields in developing decentralized applications is needed. One requirement is the need for the standardization of different geographic information when sharing data on the IPFS network.

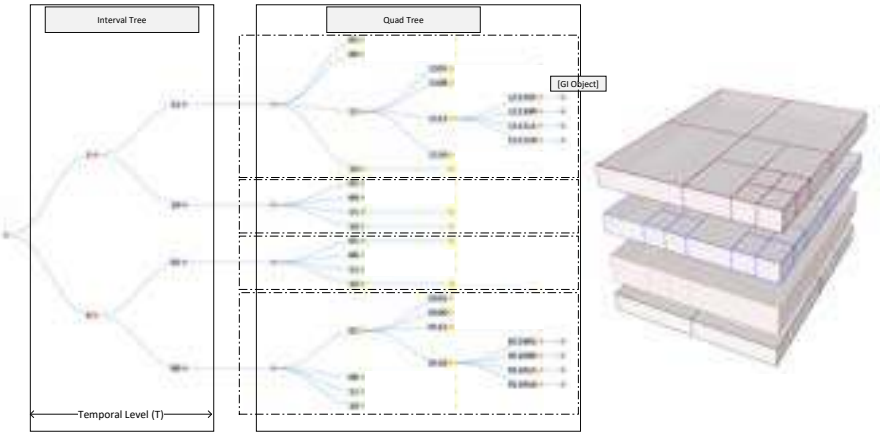

Figure 1: An example of DSTree Constructed from a set of sample points. Each DSTree has a temporal (Interval-tree) component and a spatial (quad-tree) component. The final graph will be a stack of quad-trees on top of each other.

Keywords: spatio-temporal indexing, temporal topology, query processing, *IPFS*, distributed systems, smart contracts, blockchain

Many-body State Preparation in a Jaynes-Cummings Lattice

P. Parajuli[1], K. Cai[1], A. Govindarajan[1] and L. Tian[1]

[1] *School of Natural Sciences, University of California, Merced, CA, USA {pparajuli, kcai5, agovindarajan, ltian}@ucmerced.edu*

Preparing quantum many-body states is a challenging task in engineered systems like quantum simulators and adiabatic quantum computers. Despite significant progress in developing various approaches such as adiabatic quantum evolution, quantum shortcut methods, quantum phase estimation, variational quantum eigensolvers, and open system approaches, generating the desired many-body states with high fidelity remains difficult. This is due to barriers such as the lack of prior knowledge of the energy spectrum and the rapid decrease of the energy gap with system size. Additionally, many-body states in strongly correlated systems are often highly entangled, making it impossible to create them using preprogrammed quantum logic gates.

Our objective is to examine various methods for generating many-body ground states in a Jaynes-Cummings (JC) lattice and compare their effectiveness. In JC lattices, strongly correlated polaritons can undergo quantum phase transitions between Mott-insulating and superfluid phases when the filling factor is an integer [1, 2, 3, 4, 5, 6]. However, to observe these transitions, it is necessary to inject polariton excitations into the JC lattice and prepare them in the appropriate ground states. JC lattices can be implemented in practical devices such as superconducting quantum devices and defects in optical cavities, making them ideal for testing different methods for many-body state preparation. We focus on two approaches: an optimized adiabatic method and a quantum optimal control method. The optimized adiabatic method [7] employs a Landau-Zener-like estimation to find the optimized ramping index during an adiabatic process. Meanwhile, the quantum optimal control method [8] uses the CRAB algorithm to optimize the time-dependent system parameters. Ultimately, we compare the results obtained from both approaches.

References

[1] M. J. Hartmann, F. G. S. L. Brandão, & M. B. Plenio, *Strongly interacting polaritons in coupled arrays of cavities*, Nat. Phys. **2**, pp. 849-855 (2006).

[2] A. D. Greentree, C. Tahan, J. H. Cole, & L. C. L. Hollenberg, *Quantum phase transitions of light*, Nat. Phys. **2**, pp. 856-861 (2006).

[3] D. G. Angelakis, M. F. Santos, & S. Bose, *Photon-blockade-induced Mott transitions and XY spin models in coupled cavity arrays*, Phys. Rev. A **76**, 031805(R) (2007).

[4] J. Koch & K. Le Hur, *Superfluid-Mott-insulator transition of light in the Jaynes-Cummings lattice*, Phys. Rev. A **80**, 023811 (2009).

[5] K. Seo & L. Tian, *Quantum phase transition in a multiconnected superconducting Jaynes-Cummings lattice*, Phys. Rev. B **91**, 195439 (2015).

[6] J. Xue, K. Seo, K., L. Tian, & T. Xiang, *Quantum phase transition in a multiconnected Jaynes-Cummings lattice*, Phys. Rev. B **96**, 174502 (2017).

[7] K. Cai, P. Parajuli, G.-L. Long, C.-W. Wong, and L. Tian, *Robust Preparation of Many-body Ground States in Jaynes-Cummings Lattices*, Npj Quantum Information **7**, 96 (2021).

[8] P. Parajuli and L. Tian, *Quantum Optimal Control for Preparing Many-body States in a Jaynes-Cummings Lattice*, in preparation.

The VI International AMMCS
Interdisciplinary Conference
Waterloo, Ontario, Canada
August 14-18, 2023

Event-Triggered Stabilization for Linear Time-Delay Systems

Kexue Zhang

Queen's University, Kingston, ON, Canada, kexue.zhang@queensu.ca

Event-triggered control provides an effective way to update the control signals at a sequence of discrete-time moments determined by a certain execution rule, often referred to as an event. The main advantage is to improve the efficiency of control implementations while still guaranteeing the desired performance levels of closed-loop systems. There are two main challenges in this study. First, the control algorithms for delay-free systems cannot be applied to time-delay systems directly. Another challenge, which is also the main difficulty of this research, is to exclude the Zeno behavior from the proposed event-triggered control algorithms.

This talk focuses on event-triggered control for the stabilization of linear time-delay systems. Based on two new Halanay-type inequalities, the global asymptotic stability of the event-triggered control system can be guaranteed, and a lower bound of the inter-event times, the intervals between successive control updates, can be derived to ensure the practical implementation of the proposed event-triggering condition. Two examples are given to demonstrate the suggested control method.

Emulating some exotic topological quantum effects with ultracold atoms

Z. D. Wang[1-2]

[1] *The University of Hong Kong, Hong Kong SAR, China, zwang@hku.hk*
[2] *HK Institute of Quantum Science & Technology at The University of Hong Kong, Hong Kong SAR, China*

Emulation of exotic quantum systems using ultracold atoms has been attracting considerable attention. As is known, magneto-optical (MO) effects are generated when the lights pass through certain kinds of magnetic medium, but the effects may be quite weak for experimental detection sometimes. In this talk, we will address an arresting theoretical scheme for emulating the famous MO Faraday effect in ultracold atomic gases. We will elaborate that an artificial MO Faraday effect is readily signalled by the spin imbalance of atoms, with the setup of laser fields offering a high controllability for quantum manipulation. In addition, with the underlying polarization state being extracted in the synthetic dimension, the artificial MO effect can emerge under an entirely different mechanism from the conventional picture, and the MO rotation is particularly related to the bulk topology in synthetic dimensions, providing an unambiguous evidence for the desired topological MO effect. At last, we will also discuss a possible experimental scheme for simulating the violation of Fermion doubling phenomenon emergent in non-Hermitian topological semimetals based on cold atomic systems.

The work was done in collaboration with Z. Zheng, W.B. Rui, and C. J. Wang. Z. D. Wang has been supported by the the CRF (Grant No. C6009-20G) and GRF (Grant No. 17300220) of Hong Kong, and the NSFC/RGC JRS Grant No. N_HKU774/21. The support from Guangdong-Hong Kong Joint Laboratory of Quantum Matter is also acknowledged.

References

[1] Z. Zheng and Z. D. Wang, Quantum emulation of topological magneto-optical effects using ultracold atoms, npj Quantum Information, Vol. 8, 1, 15, 1-6 (2022).
[2] W. B. Rui, Z. Zheng, C. Wang, and Z. D. Wang, Non-Hermitian spatial symmetries and their stabilized normal and exceptional topological semimetals, **Phys. Rev. Lett. 128**, 226401 (2022).

The VI International AMMCS
Interdisciplinary Conference
Waterloo, Ontario, Canada
14/04/2023

Space-Time Spectral Methods for Partial Differential Equations

S.H. Lui[1], C.P.W. Liyanage[2],

[1] *University of Manitoba, Canada, Shaun.Lui@umanitoba.ca*
[2] *University of Manitoba, Canada, wilegocp@myumanitoba.ca*

This presentation has two main objectives. The first part will focus on the area of space-time spectral methods for solving stream function formulation of Navier-Stokes and Magnetohydrodynamics equations numerically for high Reynolds numbers using the nonlinear preconditioning method RASPEN [2]. In the second part, we focus on solving PDEs in irregular domains using space-time spectral collocation methods. Space-time spectral methods provide the basis for our research in achieving the two objectives thereof. When a solution for a PDE is analytic, the rate of convergence of the numerical solution is exponential; that is, the error decays exponentially. In time-dependent PDEs, low-order finite difference schemes and spectral schemes are traditionally being used for the time and spatial derivatives, respectively. However, applying spectral schemes in both space and time has been thought of recently [4]. These methods have spectral convergence in both spatial and temporal domains.

We implemented the Navier-Stokes equation for the well-known regularized driven cavity flow using the RASPEN method for high Reynolds numbers and secondary vortices were observed [6]. Further, we are planning to present Hopf-bifurcation results for Navier-Stokes and MHD at high Reynolds numbers. To observe Hopf-Bifurcation, we start with a steady flow and try to find the critical *Re* at which bifurcation appears. Beyond some critical *Re*, a steady solution loses stability and we get a time-periodic solution. That means fluid flow will oscillate and energy is no longer constant with time.

One major drawback of spectral methods is their inability to handle irregularly shaped domains, which is why these methods have only been used sparingly in many engineering problems. However, there have been attempts to use spectral methods in irregular domains. S. Orszag presented some new techniques that permit the efficient application of spectral methods for solving problems in (nearly) arbitrary geometries [5]. Also, the papers [1] and [3] proposed extensions of the spectral method to enable it to solve PDEs on complex geometries. We propose a numerical method to approximate the solution of PDEs in irregular domains using space-time spectral collocation methods. The main idea of here is to embed the irregular domain in a regular one and apply the Fourier continuation method [1]. We have implemented the 2D Poisson equation, Heat equation, steady and unsteady Stokes equations, and Navier-Stokes equations defined in irregular domains. Spectral error convergence was observed in each instance and the results are presented.

References

[1] O. Bruno, M. Lyon, *High-order unconditionally stable FC-AD solvers for general smooth domains II. Elliptic, parabolic and hyperbolic PDEs; theoretical considerations*, Journal of Computational Physics 229 (2010), pp. 3358-3381.

[2] V. Dolean, M. Gander, W. Kheriji, F. Kwok, and R. Masson, *Nonlinear Preconditioning: How to use a Nonlinear Schwarz Method to Precondition Newton's Method*, SIAM J. SCI. COMPUT (2016), vol. 38, No. 6, pp. A3357-A3380.

[3] S. Lui, *Spectral Domain embedding for Elliptic PDEs in Complex Geometry*, J. Comput. and Appl. Math. 225 (2009), pp541-557.

[4] S. Lui, *Legendre spectral collocation in space and time for PDEs*, Numer. Math., 136 (2017), pp. 75-99.

[5] S. Orszag, *Spectral methods for problems in complex geometries*, J. Comput. Phys., 37 (1980), pp. 70-92.

[6] W.L.C. Piyasndara, *Space-time spectral collocation methods for the magnetohydrodynamics equations*, http://hdl.handle.net/1993/35927, 2021.

Analytical Solutions to Delay Fractional Differential Equations by Using Sumudu Iterative Method

M.O. Aibinu[1], S. Moyo[2]

[1] *Durban University of Technology, South Africa, moaibinu@yahoo.com / mathewa@dut.ac.za*
[2] *Stellenbosch University, South Africa, smoy@sun.ac.za*
[3] *ational Institute for Theoretical and Computational Sciences (NITheCS), South Africa*

Fractional Differential Equations (FDEs) play an important role in the modeling of evolution of a system due to their ability to model complex phenomena. Moreover, a large class of dynamical systems are associated with delays as their natural components. The vitality and suitability of a mathematical model in describing several phenomena can be improved by introducing a delay into it. It is unfortunate that most differential equations with delay often defy analytical methods for finding their solutions. This study considers the use of Sumudu iterative methods for obtaining the solutions of delayed FDEs. The study presents a technique that blends Sumudu transform method with a new iterative method. The technique solves the equations directly and produces reliable results. The graphs of the solutions that this technique produces show that they are in good agreement with the exact solutions.

References

[1] D.S. Bodkhe and S.K. Panchal, *On Sumudu Transform of fractional derivatives and its applications to fractional differential equations*, Asian Journal of Mathematics and Computer Research **11** (1), pp. 69-77 (2016).

[2] A.T. Moltot and A.T. Deresse, *Approximate analytical solution to nonlinear delay differential equations by using Sumudu iterative method*, Advances in Mathematical Physics, **2022**, Article ID 2466367, (2022). https://doi.org/10.1155/2022/2466367

[3] M. O. Aibinu, S.C. Thakur and S. Moyo, *Solving delay differential equations via Sumudu Transform*, Int. J. Nonlinear Anal. Appl., **13** (2), pp. 563-575 (2022).

Orienteering with One Endomorphism

S. Arpin[1], M. Chen[2], K. E. Lauter[3], R. Scheidler[4], K. E. Stange[5], H. T. N. Tran[6]

[1] *Universiteit Leiden, Leiden, The Netherlands, SArpinMath@gmail.com*
[2] *University of Birmingham, Birmingham, UK, m.chen.1@bham.ac.uk*
[3] *META AI, Seattle, USA, klauter@fb.com*
[4] *University of Calgary, Calgary, Canada, rscheidl@ucalgary.ca*
[5] *University of Colorado, Boulder, USA, kstange@math.colorado.edu*
[6] *Concordia University of Edmonton, Edmonton, Canada, hatran1104@gmail.com*

In supersingular isogeny-based cryptography, the path-finding problem reduces to the endomorphism ring problem. Can path-finding be reduced to knowing just one endomorphism? It is known that a small endomorphism enables polynomial-time path-finding and endomorphism ring computation (Love-Boneh [1]). An endomorphism gives an explicit orientation of a supersingular elliptic curve. In this paper, we use the volcano structure of the oriented supersingular isogeny graph to take ascending/descending/horizontal steps on the graph and deduce path-finding algorithms to an initial curve. Each altitude of the volcano corresponds to a unique quadratic order, called the primitive order. We introduce a new hard problem of computing the primitive order given an arbitrary endomorphism on the curve, and we also provide a sub-exponential quantum algorithm for solving it. In concurrent work (Wesolowski [2]), it was shown that the endomorphism ring problem in the presence of one endomorphism with known primitive order reduces to a vectorization problem, implying path-finding algorithms. Our path-finding algorithms are more general in the sense that we don't assume the knowledge of the primitive order associated with the endomorphism. This is joint work with Sarah Arpin, Kristin E. Lauter, Renate Scheidler, Katherine E. Stange and Ha T. N. Tran.

References

[1] J. Love and D. Boneh, *Supersingular Curves With Small Non-integer Endomorphisms*, in *ANTS XIV, Proceedings of the Fourteenth Algorithmic Number Theory Symposium*, volume 4 of *Open Book Ser.*, Math Sci. Publ., Berkeley, CA, pp 7-22 (2020)

[2] B. Wesolowski, *Orientations and the supersingular endomorphism ring problem*, in *Advances in Cryptology—EUROCRYPT 2022*, volume 13277 of *Lectures Notes in Comput. Sci.,* Springer, Cham, pp 345-371 (2022)

The impact of endoplasmic reticulum morphology on IRE1 protein clustering

L. Kischuck and A. Brown

Department of Physics, Toronto Metropolitan University, Toronto, Canada, aidan.brown@torontomu.ca

The endoplasmic reticulum (ER) is a cell-spanning organelle composed of a single connected network of sheets and tubes. As an important location for protein synthesis and folding, the ER membrane and lumen harbour many unfolded proteins. The presence of excess unfolded proteins in the ER can lead to protein aggregation and otherwise disrupt cell activities. The unfolded protein response (UPR) directs the cellular response to high levels of unfolded proteins in the ER, acting to return the ER to a healthy homeostatic level of unfolded proteins. Unfolded proteins in the ER activate the transmembrane signaling protein IRE1, which subsequently forms dimers, oligomers, and clusters with signaling activity that ultimately modifies gene expression to initiate the UPR. Experiments have shown that IRE1 clusters have complex shapes, including wrapping around ER tubes, and dynamics consistent with coarsening behaviour. However, the influence of ER tube and network geometry on IRE1 cluster dynamics is largely unexplored. We quantitatively modeled IRE1 protein cluster dynamics on a tubular surface as a lattice gas, simulated using a kinetic Monte Carlo algorithm. We show that ER tube geometry — tube diameter — controls whether clusters can undergo a transition from an approximately round conformation to a conformation that 'wraps' around the tube. These wrapped clusters can grow without further energy-penalizing increases in interface length. Narrower tubes enable cluster wrapping at smaller cluster sizes. Our simulations show that wrapped clusters on narrow tubes grow more rapidly, evaporate more slowly, and are stable at lower protein concentrations compared to equal-sized round clusters on wider tubes. Our results suggest that cluster wrapping, facilitated by narrower tubes, could be an important factor in the growth and stability of IRE1 clusters, impacting the persistence of the UPR. This work may tie into cell and human health, as UPR signaling persistence and dysfunction is associated with pathologies such as cancer and neurodegeneration.

Mapping Regional Change in Snow Water Equivalent using Deep UNET- Siamese Convolutional Neural Networks

Karim Malik[1], Colin Robertson[2]

[1] *University of Toronto, Toronto, Canada, karim.malik@utoronto.ca*
[2] *Geospatial Technology Solutions, Victoria, Canada, Colin.Robertson@gsts.ca*

Snow Water Equivalent (SWE), the amount of water that would be yielded if a given snow-pack melted, is a useful surrogate for understanding the impacts of climate change on the Winter season's length in cold regions. Previous studies have been conducted using time series of historical temperatures to highlight the impact of warming temperatures on the duration of the Winter Season and Outdoor Skating in Canada [1]. However, given that SWE and Snow Extent are a function of both diurnal temperature change and deposition/accumulation processes, integrating temperatures analysis with spatially explicit pattern comparison methods would likely provide a wealth of information on the impact of global warming on the Earth System across space and time.

In this study, the GlobSnow SWE Maps over the cold regions of Canada and parts of the Arctic were used to train a UNET-Siamese convolutional neural network model. The model was developed using training data (4000 SWE Maps) from 1980 – 2001. The training and validation splits were 75% and 25%, respectively. We used the binary cross-entropy loss function instead of the widely recommended contrastive loss function as this yielded the best results. To assess the generalizability of the model, independent validation data were drawn between 2002 – 2013 SWE Maps to test the model's performance. Our model predicted similarity between a pair of SWE Maps that were drawn randomly from 2002 – 2013 with a similarity confidence score as high as 77% for SWE Maps that were not perceptually distinguishable. As shown in earlier studies, computer vision metrics hold the potential to detect subtle changes in SWE Maps [2]. For SWE Map pairs that could be easily distinguished perceptually to be dissimilar, the model's confidence score ranged between 0 – 25%.

To illuminate the potential impact of climate change and global warming on the dynamics of Snow cover and the duration of the Winter season, we compared SWE Maps in the months in which Snow cover in Canada is expected to be at the optimum level – January, February, March, and April. We then built similarity confidence plots from 2002 – 2013 to represent temporal variability in the patterns of SWE Maps similarity between successive days and months. The model similarity confidence plots depict high variability in daily and monthly SWE. Daily SWE similarity showed an increasing trend for the months of January and February; contrarily, SWE similarity portrayed a declining trend for March and April. While the daily variability in SWE turns out to be less predictable, we discovered low similarity confidence scores (0 – 15%) for monthly SWE Maps compared between 2010 – 2013. This suggests a potential shift in climate regime (e.g., arrival and retreat of snow) and warming trends due to climate change events.

Keywords: Spatial pattern comparison, UNet-Siamese network, convolutional neural networks, snow water equivalent, climate change

References

[1] K. Malik, R. McLeman, C. Robertson, and H. Lawrence, "Reconstruction of past backyard skating seasons in the Original Six NHL cities from citizen science data," *Can. Geogr.*, vol. 64, no. 4, pp. 564–575, 2020, doi: 10.1111/cag.12640.

[2] K. Malik and C. Robertson, "Exploring the Use of Computer Vision Metrics for Spatial Pattern Comparison," *Geogr. Anal.*, pp. 1–25, 2019, doi: 10.1111/gean.12228.

Heterogeneity in Disease-Free Social Influence Affects Disease Dynamics

C. Tovissodé[1], B. Baumgaertner[2]

[1] *Institute for Modeling Collaboration and Innovation, University of Idaho, Moscow, USA, ctovissode@uidaho.edu*
[2] *Department of Politics and Philosophy, University of Idaho, Moscow, USA, bbaum@uidaho.edu*

Research coupling social influence-based opinion dynamics with disease dynamics has recently emerged to understand feedback loops between the distribution of opinions on costly prophylactic behaviors and disease evolution. In this regard, Tyson et al. [1] have examined how the distribution of opinions at disease introduction and the relative rates of opinion and disease dynamics affect the severity of an epidemic using an SIR-Opinion model where the susceptible population is structured into four opinion groups with different prophylactic behaviors and thus different susceptibilities to disease. In this model, interactions between individuals from different opinion groups lead to opinion-changing processes with rates governed by social influences (persuasive powers) which vary with disease incidence. The SIR-Opinion model assumes that demographic changes (births and natural death) are negligible in the target time period, and social influence is homogeneous in the absence of disease.

In this paper we consider a model where the susceptible population is structured into three opinion classes (S_{-1} for the most prophylactic class, S_1 for the least prophylactic class, and S_0 for an intermediate group with moderate prophylactic behaviors) and demographic changes are allowed. We notice that in such a model, the assumption of homogeneous social influence in disease-free conditions is inconsistent with the expectation that most of a population does not adhere to costly prophylactic behaviors in the total absence of disease.

Considering the epidemiology of a COVID-19 like disease and prophylactic behaviours such as hand washing, face-mask wearing, and social distancing, we introduce the first compartmental model allowing for heterogeneous social influence in the absence of disease in addition to demographic rates, differentiated infectious states (asymptomatic/symptomatic), testing effort and the related incomplete disease prevalence information available to individuals. In this setting, we investigate how heterogeneity in social influence under disease-free conditions determines not only the distribution of opinions at disease introduction, but also the course of an epidemic (e.g. waves, peak sizes, reproductive number). This provides some insights on how measuring differences between the persuasive powers of holders of various prophylactic behavior-related opinions might help assess the severity of an epidemic after a potential outbreak.

References

[1] R.C. Tyson, S.D. Hamilton, A.S. Lo, B.O. Baumgaertner and S.M. Krone, *The timing and nature of behavioural responses affect the course of an epidemic*, Bulletin of mathematical biology **82**, 1, pp. 1-28 (2020).

The VI International AMMCS
Interdisciplinary Conference
Waterloo, Ontario, Canada

A posteriori Error Estimates for Numerical Solutions to Hyperbolic Conservation Laws

A. Bressan[1], M.T. Chiri[2], W. Shen[3]

[1] *Penn State University, University Park, US, axb62@psu.edu*
[2] *Queen's University, Kingston, Canada, maria.chiri@queensu.ca*
[3] *Penn State University, University Park, US, wxs27@psu.edu*

Consider the Cauchy problem for a strictly hyperbolic system of conservation laws in one space dimension

$$u_t + f(u)_x \;=\; 0, \qquad u(0,x) \;=\; \bar{u}(x).$$

Assuming small total variation, it is well known that there exists a unique entropy-weak solution, depending continuously on the initial data. A priori estimates on the $\mathbf{L}^1$ distance between an approximate solution and the exact solution have been obtained in connection with (i) front tracking approximations, (ii) the Glimm scheme, and (iii) vanishing viscosity approximations. However, no a priori estimate is yet known for approximate solutions obtained by fully discrete schemes, such as the Lax-Friedrichs or the Godunov scheme. Therefore we focus on *a posteriori* error estimates. The result we show is the following.
Let u^{approx} be an approximate solution produced by a conservative scheme which dissipates entropy, and assume that

(i) the total variation of $u^{approx}(t,\cdot)$ is uniformly bounded,

(ii) outside a finite number of narrow strips in the domain $[0,T]\times\mathbb{R}$, the local oscillation of u^{approx} remains small.

Then the $\mathbf{L}^1$ distance

$$\|u^{approx}(T,\cdot) - u^{exact}(T,\cdot)\|_{\mathbf{L}^1(\mathbb{R})}.$$

is small. Our estimates do not require any regularity of the exact solution. We provide an error bound which can be applied to a wide class of approximation schemes.

References

[1] A. Bressan, M.T. Chiri and W. Shen, A posteriori Error estimates for numerical solutions to hyperbolic conservation laws. *Arch. Rat. Mech. Anal.* , **241** (2021), 357–402

Controlling the spread of invasive biological species

A. Bressan[1], M.T. Chiri[2], N. Salehi[3]

[1] *Penn State University, University Park, US, axb62@psu.edu*
[2] *Queen's University, Kingston, Canada, maria.chiri@queensu.ca*
[3] *Saint Mary's College, Notre Dame, US, nsalehi@saintmarys.edu*

We consider a controlled reaction-diffusion equation, motivated by a pest eradication problem, and derive a simpler model, describing the controlled evolution of a contaminated set.
The controlled spreading of a population, in a simplest form, can be described by a semilinear parabolic equation

$$u_t \;=\; f(u)+\Delta u - g(u,\alpha),$$

where $u = u(t,x)$ denotes the population density at time t, at a location $x \in \mathbb{R}^2$, the function f represents the reproduction rate, while $\alpha = \alpha(t,x)$ is a distributed control. One may think of $\alpha(t,x)$ as the quantity of pesticides sprayed at time t at location x, while $g(u,\alpha)$ describes the amount of population eliminated by this strategy.
We first analyze the optimal control of 1-dimensional traveling wave profiles. Using Stokes' formula, explicit solutions are obtained, which in some cases require measure-valued optimal controls. Then we introduce a family of optimization problems for a moving set and show how these can be derived from the original parabolic problems, by taking a sharp interface limit. In connection with moving sets, we show some results on controllability, existence of optimal strategies, and necessary conditions.

References

[1] A. Bressan, M. T. Chiri, and N. Salehi, On the optimal control of propagation fronts, *Math. Models Methods Appl. Sci.*, **32** (2022), 1109–1140.

[2] A. Bressan, M. T. Chiri, and N. Salehi, Optimal control of moving sets. *J. Differential Equations*, **361**, (2023), 97–137.

Portfolio optimization in the family of 4/2 stochastic volatility models

Y. Cheng[1], M. Escobar-Anel[2]

[1] *Western University, Canada, yche259@uwo.ca*
[2] *Western University, Canada, marcos.escobar@uwo.ca*

The state-of-the-art 4/2 stochastic volatility model was recently proposed in [1] and has gained great attention ever since. This model is a superposition of a Heston (1/2) component and a 3/2 component, bringing the best of the two nested models.

$$dX(t) = \mu X(t)dt + \left(a\sqrt{v(t)} + \frac{b}{\sqrt{v(t)}}\right) X(t)dW(t), \quad (1)$$

$$dv(t) = \kappa(\theta - v(t))dt + \sigma\sqrt{v(t)}dB(t), \quad (2)$$

$$\langle dB(t), dW(t)\rangle = \rho dt \quad (3)$$

This talk gives an overview of recent progress in the application of the model (see [2], [4], [3]), as well as a multivariate generalization (see [5]), to portfolio optimization, in particular within expected utility theory.

The work includes the study of CRRA and HARA utilities, the presence of consumption, as well as considerations about complete/incomplete markets and ambiguity-aversion. All is complemented with the analysis of wealth-equivalent losses to gain insight into popular embedded suboptimal strategies.

References

[1] M. Grasselli *The 4/2 stochastic volatility model: a unified approach for the Heston and the 3/2 model*. Mathematical Finance, 27(4), pp. 1013-1034 (2017).

[2] Y. Cheng, and M. Escobar-Anel, *Optimal investment strategy in the family of 4/2 stochastic volatility models*. Quantitative Finance, 21(10), pp. 1723-1751 (2021).

[3] Y. Cheng, and M. Escobar-Anel, *Optimal consumption and robust portfolio choice for the 3/2 and 4/2 stochastic volatility models*. International Journal of Theoretical and Applied Finance. Under Review. (2023)

[4] Y. Cheng, and M. Escobar-Anel, *Robust portfolio choice under the 4/2 stochastic volatility model.* IMA Journal of Management Mathematics 34.1, pp. 221-256 (2023).

[5] Y. Cheng, and M. Escobar-Anel, *A multivariate 4/2 stochastic covariance model: properties and applications to portfolio decisions*. Quantitative Finance 23.3: pp. 497-519 (2023).

Advanced discretization schemes for phase-field fracture

B. Bourdin[1], F. Marazzato[2]

[1] *Department of Mathematics & Statistics, McMaster University, Canada, bourdin@mcmaster.ca*
[2] *Department of Mathematics, Louisiana State University, USA,, marazzato@lsu.edu*

Variational phase-field models of fracture [1, 2] have established themselves as a powerful and efficient computational approach in fracture mechanics. They are based on a regularization of Francfort and Marigo variational energy [3], where the crack geometry and discontinuous displacements are represented by smooth functions The most common implementations are based on finite element discretization via continuous finite elements, and a staggered minimization scheme.

In this talk, we present a new discretization scheme where displacements are discretized using discontinuous Lagrange elements and the phase field variable by Crouzeix-Raviart elements [4]. We compare this scheme to the classical continuous Galerkin scheme and highlight how it leads to a better approximation of the fracture energy.

References

[1] B. Bourdin, G. A. Francfort and J.-J.Marigo, *Numerical experiments in revisited brittle fracture*. J. Mech. Phys. Solids, **48** (1), pp.797–826 (2000).

[2] B. Bourdin, G. A. Francfort and J.-J.Marigo, *The variational approach to fracture*, J. Elasticity, **91** (1-3), pp. 1–148, (2008).

[3] G. A. Francfort and J.-J. Marigo, *Revisiting brittle fracture as an energy minimization problem*, J. Mech. Phys. Solids., **46** (8), pp. 1319–1342, 1998.

[4] F. Marazzato and B. Bourdin, *A DG/CR discretization for the variational phase-field approach to fracture*, Comp. Mech, (2023)

The VI International AMMCS
Interdisciplinary Conference
Waterloo, Ontario, Canada
August, 2023

Towards Exact DGGS representation using Hierarchical Goldberg Polyhedron base solids

S. A. Roberts[1]

[1] *Department of Geography and Environmental Studies, Wilfrid Laurier University, Waterloo, Canada, sroberts@wlu.ca*

In the last few years Digital Global Grid Systems (DGGS) have emerged as an alternative new approach to storing and analysing spatial data. Benefits of this technology include, consistent toplogical neighbourhoods for spatial dependence calculations, inherent data uncertainty modelling via the grid resolutions, and the ability to model hierarchical spatial structure among other features. Existing implementations of this approach generally comprise a hierarchical tiling of regular polygons (often hexagons) projected to common coordinate sytems.

In this paper we propose an alternative basis for DGGS wherein starting from a truncated icosahedron base solid, modified recursive chamfering operations create a hierarchy of Goldberg polyhedra GP{2n,2n} (or $c \ldots ctI$ in Conway notation) of increasing spatial resolution via decreasing polygonal face size. In the paper we describe the geometric operations and provide some diagnostic evaluations of the properties of the hexagon faces created. These include analysis of variations in hexagonal face areas and regularity in the hexagonal faces via a Full Procrustes distance measure of each hexagonal face against one of the 20 basis faces generated at the centre of the original truncated icosahedron faces and propagated as regular hexagons in each succeeding generation of GP.

Further, we propose that in addition to storing floating point coordinate points to aid in visulization, we also store the coordinate information exactly via an algebraic representation stored in a spatial database. This process starts with the algebraic (exact) coordinates being created in the computer algebra software then converted into latex and then stored as BLOBs in a Sqlite database structure. We demonstrate some preliminary results for this with the base truncated icosahedron.

Multiscale modeling of biofilm communities with flux balance analysis

T. Zhang[1], I. Klapper[2]

[1] *Montana State University tianyu.zhang@montana.edu*
[2] *Temple University klapper@temple.edu*

The microbial community structure and its surrounding environment are often intimately connected. Most environments outside of the lab are physically and chemically heterogeneous. On one hand, spatial variations introduce physics such as diffusive and advective transport of nutrients and byproducts. On the other hand, microbial metabolic activity can affect the environment. Hence it is important to link metabolism at the cellular level to physics and chemistry at the community level.

To introduce metabolism to community-scale population dynamics, many models rely on large numbers of reaction kinetics parameters that are either unmeasured or unmeasurable, also making detailed metabolic information mostly unusable. The bioengineering community has addressed this difficulty by implementing kinetics-free formulations at the cellular level, known as flux balance analysis. To combine the two scales, we propose to replace classical kinetics functions in community scale models with cell-level metabolic models, and predict metabolism and its interaction with the environment. Furthermore, our methodology permits assimilation of many types of measurement data. We will discuss the background and motivation, model development, and some numerical simulation results. Some modeling equations and simulation results are given in equations (1) - (3) and fig. 1.

$$S^{(j)}\mathbf{v}^{(j)} = \mathbf{0}, \quad j = 1,2,\ldots,N \tag{1}$$

$$\frac{\partial}{\partial t}X_j + \nabla\cdot(\mathbf{u}X_j) = Y(h_j(\mathbf{v}^{(j)}) - d_j)X_j, \quad j = 1,2,\ldots,N \tag{2}$$

$$D_k\nabla^2 C_k = -\sum_{j=1}^{N} e_{jk}X_j, \quad k = 1,2,\ldots,M \tag{3}$$

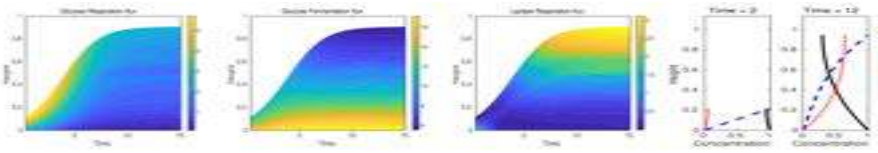

Figure 1: Simulated flux magnitude and metabolite concentration in growing biofilm.

Risk heterogeneity, in-groups, and epidemic waves

B. Baumgaertner[1], C. Tovissode[2]

[1] *University of Idaho, Idaho, USA bbaum@uidaho.edu*
[2] *University of Idaho, Idaho, USA ctovissode@uidaho.edu*

There is a growing interest in the joint modeling of the dynamics of disease and health-related beliefs and attitudes. For example, we know that risk tolerance varies in populations, including non-pharmaceutical responses such as mask-wearing and other prophylactic behaviors. However, the decision to, e.g., wear a mask is not a mere combination of risk tolerance and perceived prevalence of a disease; mask wearing is also informed by the aggregate behaviors of others. In-group norms can influence how people interpret the behavior in relation to disease prevalence. There are few, if any, models that explore the dynamics of a system in which behavior contributes to and is a function of both perceived disease prevalence and a social domain. Consequently, we do not yet understand how feedback loops between risk heterogeneity and in-group behaviour are contributing factors to patterns in disease dynamics, such as epidemic waves.

To study potential impacts of risk heterogeneity and in-group behaviour on disease dynamics, we explore a behaviour-disease model. Our model of study can be described in two parts. The first part is a standard Susceptible-Exposed-Infectious-Recovered (SEIR) compartmental model, but with the infectious class broken into three: the asymptomatic, the sympotmatic, and the detected. The detected class serves as the primary source of disease-related information on which different susceptible populations, S_i, will decide to be prophylactic. I.e., disease prevalence, P, and relative change in new positive cases, Q, make up an information aggregate, η_i:

$$\eta_i = a_{pi}P + u_{pi}P^2 + v_iPQ + u_{qi}Q^2 + a_{qi}Q \tag{1}$$

where a_{pi}, a_{qi}, u_{pi}, u_{qi}, and v_i are weights of linear, quadratic, and interaction components of P and Q for S_i.

The second part governs the dynamics of prophylactic behavior. Here the susceptibles are broken into two populations with different standards of evidence based on their sensitivities to P and Q (e.g. small vs large a_{pi}). The evolution (increase or decrease) of the proportion of mask-wearers m_i in each S_i is also a function of the proportion already engaging in prophylactic behavior. This is achieved using a modified Richards growth equation. Accordingly, the proportion m of prophylactic individuals in susceptible group i evolves in time (t) through the differential equation:

$$\frac{\partial m_i}{\partial t} = \left[m_i \frac{1 - m_i^{\alpha_i}}{\alpha_i} \right] \frac{\partial \eta_i}{\partial t} \tag{2}$$

where α_i expresses the dependence of m_i on the aggregate behavior of other in-group individuals.

Using simulation experiments we find that risk heterogeneity has a complicated impact on disease dynamics. In particular, the level of protection that prophylactic behaviour provides has an unexpected impact: at a medium level of 50% we see decreased disease severity but otherwise a single wave; at a high level of 95% we see the emergence of multiple epidemic waves, but only if the delay of information to η is neither too short nor too long. Our results provide insights into the conditions under which we might expect secondary waves of infections and the importance of knowing how effective a prophylactic behaviour is (or should be).

Modeling of Charging Dynamics in Electrochemical Systems with a Graphene Electrode

M. Yavarian[1]

[1] *University of Waterloo, Waterloo, ON, N2L 3G1, Canada*

A classical electrochemistry problem related to the polarization of a graphene electrode immersed in an aqueous solution and subjected to a small external ac voltage is revisited. The Poisson-Nernst-Planck equations with proper boundary conditions are linearized and normalized, leading to an analytical formula for the impedance of the electrochemical system containing a graphene-metal electrode pair. Electrochemical impedance spectroscopy is utilized to compare the impedance behavior of the graphene-metal electrode pair with the standard metal-metal electrode pair for a range of ion concentrations in the electrolyte. Also studied is the electrochemical capacitive spectroscopy to provide a detailed analysis related to the effects of the quantum capacitance of graphene on the total capacitive properties of the system.

Spatially distributed modelling of ice thickness and phenology on Northern Lakes

G. Attiah[1], H. Kheyrollah Pour[1], K. A. Scott[2]

[1] *Wilfrid Laurier University, Waterloo, Canada, gattiah@wlu.ca; hpour@wlu.ca*
[2] *University of Waterloo, Waterloo, Canada, ka3scott@uwaterloo.ca*

Spatially distributed modelling of lake ice thickness involves simulating the ice cover as a continuous surface, which accounts for variations in physical and environmental factors across the lake basin. This is important for predicting the impact of climate change on freshwater resources and ensuring ice safety during winter travel for northern communities. The increasing warming in climate is detrimental to lake ice since air temperature impacts ice phenology and ice cover duration on lakes. Ménard et al. (2002) assert that a one-degree increase or decrease in air temperature leads to a 6-day almost linear change in ice cover duration. Therefore, monitoring these changes and the factors influencing their evolution for safety and planning is essential. However, relying on a single data source to monitor lake ice proves challenging due to the difficulty in continuous in-situ monitoring and gaps in remote sensing data (Beckers et al., 2017). Furthermore, methods adopted to monitor lakes, such as one-dimensional thermodynamic lake ice models, rely on weather station input data, which are sparse, especially at high latitudes. This study adopts a multimethod monitoring approach to address these limitations by using remote sensing data coupled with a spatially distributed 1-D thermodynamic lake ice model to study the trends and spatial distribution of lake ice thickness and phenology.

Ice thickness was modelled for predominantly small to medium lakes in the Northwest Territories. A retrieval algorithm was adapted and applied to Landsat satellite series to generate a lake surface temperature dataset (North Slave LST). Input model variables, such as wind speed (m s-1), mean air temperature (°C), relative humidity (%), snow depth (m) and cloud cover (0-1), were compiled from 1984 to the present using reanalysis gridded data from European Centre for Medium-Range Weather Forecasts Reanalysis v5 ECMWF (ERA5) in addition to generated North Slave LST. The model was run on each 30 m pixel to estimate ice thickness and phenology. Model outputs include daily lake ice thickness for each pixel over the lake and the yearly freeze-up and break-up dates. The model was validated using collected in-situ field data by Ground-penetrating Radar and manually drilling and measuring ice thickness on various locations of several lakes, as well as time series of ice thickness measured by an automated Snow and Ice Mass Balance Apparatus (SIMBA). Outputs derived from the model effectively estimated lake ice thickness and highlighted the spatial variation of ice thickness and its extent over the lake. Preliminary results from the model on selected lakes showed a root mean square deviation of ice thickness from 3 cm to 7 cm compared to measured data.

Further analysis of model results shows decreasing trends in ice cover duration (-0.28 day/year to -0.35 day/year) and ice thickness (-0.12 cm/year to -0.14 cm/year) on lakes surrounding Yellowknife from 1984 to the present. Additionally, later freeze-up (0.08 day/year to 0.22 day/year) and earlier break-up (-0.16 day/year to -0.21 day/year) was observed. Information on lake ice thickness and phenology are provided to neighbouring communities, researchers, and stakeholders, helping reduce uncertainties on lake ice.

References

[1] J.F. Beckers, J.A. Casey and C. Haas, *Retrievals of lake ice thickness from great slave lake and great bear lake using cryoSat-2*, IEEE Trans. Geosci. Remote Sens. 55, pp. 3708-3720 (2017).
[2] P. Ménard, C.R. Duguay, G.M. Flato, W.R. Rouse, *Simulation of ice phenology on Great Slave Lake, Northwest Territories, Canada*, Hydrol. Process. 16, pp. 3691–3706 (2002). https://doi.org/10.1002/hyp.1230

On the effects of suitably designed space microstructures in the propagation of waves in time modulated composites

O. Mattei[1], V. Gulizzi[2]

[1] *San Francisco State University, USA, mattei@sfsu.edu*
[2] *University of Palermo, Italy, vincenzo.gulizzi@unipa.it*

The amplitude of a pulse that propagates in a homogeneous material whose properties are instantaneously changed periodically in time will undergo an exponential increase, due to the interference between the reflected and transmitted pulses generated at each sudden switch. Here we resolve the issue by designing suitable reciprocal PT-symmetric space-time microstructures both in the one-dimensional and two-dimensional case, so that the interference between the scattered waves is such that the overall amplitude of the wave will be constant in time in each constituent material. Remarkably, for the geometries here proposed, a pulse will propagate with constant amplitude regardless of the impedance between the constituent materials, and for some, regardless of the wave speed mismatch. Given that the energy associated with the wave will increase exponentially in time, this creates the possibility to exploit the stable propagation of the pulse to accumulate energy for harvesting.

References

[1] O. Mattei. V. Gulizzi, *On the effects of suitably designed space microstructures in the propagation of waves in time modulated composites*, Appl. Phys. Lett, 122, 061701 (2023).

[2] O. Mattei, G.W. Milton, *Field patterns: A new type of wave with infinitely degenerate band structure*. Europhys. Lett. 120(5), 54003 (2017).

[3] O. Mattei, G.W. Milton, *Field patterns without blowup*. New J. Phys. 19, 093022(2017).

[4] G.W. Milton, O. Mattei, *Field patterns: A new mathematical object*. Proc. R. Soc. A 20160819 (2017).

Adhesion in Polymer Membranes

Keith Promislow[1], Sulin Wang[2], Zhengqian Tan3

[1] *Michigan State University, kpromisl@math.msu.edu*
[2] *Hunan University, China, 1036975733@qq.com*

Many processes in material science involve entropic contributions from packing – the constraints imposed by volume occupied by other material. Diblock polymers offer a rich environment to study the packing of soft materials as gradient flows of a system energy. Ideas from Γ−convergence provide powerful tools to extract simplified models in certain singular limits. We present examples of packing dichotomies in which limiting problems may be more complex. We start with an alternate random phase reduction of self-consistent mean field models that leads to density functional energies with stronger nonlocality. We identify regimes in which the energies reduce to a functionalized Cahn-Hilliard energy and examine a strong segregation limit. For the latter, computational results motivate a sharp interface reduced energy for interfaces that balances a classical Canham-Helfrich formulation against a longer-range adhesion term that induces self-stacking behavior observed in various cellular organelles.

References

[1] A. Christlieb, K. Promislow, Z. Tan, S. Wang, B. Wetton, S. Wise, Benchmark Computation of Morphological Complexity in the Functionalized Cahn-Hilliard Gradient Flow, Arxiv, https://arxiv.org/abs/2006.04784

An Algorithm to Generate Random Factored Smooth Integers

Eric Bach[1], Jonathan Sorenson[2]

[1] *University of Wisconsin-Madison, USA, bach@cs.wisc.edu*
[2] *Butler University, Indianapolis IN, USA, jsorenso@butler.edu*

We say an integer n is *y-smooth* if every prime divisor of n is $\leq y$. Let $\Psi(x,y)$ count the number of y-smooth integers $\leq x$.

We present a new algorithm that will generate an integer $n \leq x$ uniformly at random, with known prime factorization, such that n is y-smooth. In particular, the algorithm accepts a real input r, with $0 \leq r < 1$, such that asymptotically, n is at position $r\Psi(x,y)(1+o(1))$ in the list of y-smooth integers ordered lexicographically by prime factorization.

The running time of our algorithm depends on algorithmic choices for prime testing [5], search [4], and estimating $\Psi(x,y)$ for various x,y pairs [6, 3]. For a particular choice of such algorithms, we show that under the assumption of the Extended Riemann Hypothesis, our algorithm produces the desired output with probability $1-o(1)$ with a running time of

$$O\left(\frac{(\log x)^3}{\log\log x}\right) \tag{1}$$

arithmetic operations on average.

The central organizing structure of our algorithm is Buchstab's identity,

$$\Psi(x,y) = 1 + \sum_{p \leq y} \Psi(x/p, p), \tag{2}$$

which decomposes $\Psi(x,y)$ by its largest prime divisor [7, §5.3]. After reviewing this identity, we present a recursive algorithm that enumerates all y-smooth integers $\leq x$ in lexicographic order based on their prime factorizations. We then show how to prune this algorithm to obtain our main result.

References

[1] E. Bach. How to generate factored random numbers. *SIAM Journal on Computing*, 2:179–193, 1988.

[2] Eric Bach and Jonathan Sorenson. An algorithm to generate random factored smooth integers, 2020. Available on arxiv.org at https://arxiv.org/abs/2006.07445.

[3] Eric Bach and Jonathan P. Sorenson. Approximately counting semismooth integers. In *Proceedings of the 38th International symposium on symbolic and algebraic computation*, ISSAC '13, pages 23–30, New York, NY, USA, 2013. ACM.

[4] R. P. Brent. *Algorithms for Minimization Without Derivatives*. Dover, 2013. Originally published by Prentice-Hall 1973.

[5] R. Crandall and C. Pomerance. *Prime Numbers, a Computational Perspective*. Springer, 2001.

[6] A. Hildebrand and G. Tenenbaum. Integers without large prime factors. *Journal de Théorie des Nombres de Bordeaux*, 5:411–484, 1993.

[7] Gérald. Tenenbaum. *Introduction to Analytic and Probabilistic Number Theory*, volume 46 of *Cambridge Studies in Advanced Mathematics*. Cambridge University Press, english edition, 1995.

The VI International AMMCS
Interdisciplinary Conference
Waterloo, Ontario, Canada

Gravitational Models with State-Dependent Delay: Gravitating Binaries

E.I. Verriest[1]

[1] *Georgia Institute of Technology, Atlanta, GA, USA, erik.verriest@ece.gatech.edu*

In [1] we proposed an approximation to Einstein's field equations in the case of low velocities and weak gravitational fields. Essentially, we still assume a notion of simultaneity, and a flat space. This approximation was based on a finite propagation speed of the (Newtonian) gravitational force, which leads to the modification of Newton's equation by a state-dependent delay. The positions and velocities of the gravitational masses constitute the state variables. A mass distribution due to a unit point mass in motion, prescribed by a trajectory, $\vec{r}_p(t)$ is described by a three-dimensional Dirac-delta mass density $\rho(\vec{r'},t') = \delta(\vec{r'} - \vec{r}_p(t'))$. The resulting gravitational potential at the fixed point and time, $(\vec{r},t)$, in such a post-Newtonian (pN) theory is then

$$\phi(\vec{r},t) = G\int_{\mathbb{R}^3} \frac{\delta(\vec{r'} - \vec{r}_p(t_b))}{|\vec{r} - \vec{r'}|}\,\mathrm{d}V(\vec{r'}) \tag{1}$$

where $t_b = t - \tau(\vec{r'})$ is the *backward or retarded time* satisfying $c\tau(\vec{r'}) = |\vec{r} - \vec{r'}|$.
In this paper we present a new proof, which is somewhat more streamlined than the one in [1] for:
Theorem 1
The gravitational potential at the observation point, $\vec{r}$, at time, t, due to a unit point mass at $\vec{r}_p$ in motion is given by

$$\phi(\vec{r},t) \quad = \quad \frac{Gc}{\left| c|\vec{r} - \vec{r}_p(t_b)| - (\vec{r} - \vec{r}_p(t_b))^\top \dot{\vec{r}}_p(t_b) \right|}.$$

The proof is analogous to the derivation of the Liénard-Wiechert potentials in electrodynamics, which is based on a reduction of a three-dimensional Dirac impulse to a one-dimensional one. (See [2]). We deduce the:
Theorem 2
The pN-gravitational force exerted by a unit mass in motion on a unit-mass test particle at $\vec{r}$ is directed towards the predicted position based on a uniform motion *given by the delayed information (i.e., delayed position and velocity) and given by*

$$\nabla_r \phi(\vec{r},t) = -\frac{G(\vec{r} - \widehat{\vec{r}}_p(t))^\top}{|\vec{r} - \vec{r}_p(t_b)||\mathbf{1}^\top_{\vec{r} - \vec{r}_p(t_b)}(\vec{r} - \widehat{\vec{r}}_p(t))|^2}. \tag{2}$$

where delay, τ, and backward time, t_b, are related by $c\tau(t_b) = |\vec{r} - \vec{r}_p(t_b)|$, and the predicted position for time t $\widehat{\vec{r}}_p(t) = \vec{r}(t_b) + \tau(t_b)\dot{\vec{r}}(t_b)$.

We then apply this result to predict the kinematics of gravitating binaries, to find that Newton's results for the orbital speeeds hold if the masses are replaced by the relativistic ones

$$m_{rel} = \frac{m}{\sqrt{1 - \frac{v^2_{orb}}{c^2}}}.$$

References

[1] E.I. Verriest, *Post-Newtonian Gravitation*, in *Mathematical and Computational Approaches in Modern Science and Engineering*, Bélair, J., Frigaard, I.A., Kunze, H., Makarov, R., Melnik, R., Spiteri, R.J. (Eds.), pp. 153-164, Springer-Verlag (2016).
[2] G. Smith, *Classical Electromagnetic Radiation*. Cambridge University Press (1997).

The VI International AMMCS
Interdisciplinary Conference
Waterloo, Ontario, Canada

An Optimization-based Approach to Image Fusion using Structural Similarity

F. Hirbodvash[1], M. Ebrahimi[2]

[1]*Ontario Tech University, Oshawa, Ontario, Canada, Fatemeh.Hirbodvash@ontariotechu.ca,*
[2]*Ontario Tech University, Oshawa, Ontario, Canada, Mehran.Ebrahimi@ontariotechu.ca*

Multiple imaging sensors are being used in surveillance, medical imaging, and machine vision. To effectively combine the information from multiple imaging sensors, image fusion techniques have emerged to produce an improved single image.
We propose that the widely used Euclidean distance in the fusion process, which is considered a poor measure of visual quality [1, 2, 3, 4], can be replaced with the structural similarity index measure (*SSIM*), which is known to be one of the most effective measures of visual proximity.

Since image fusion integrates complementary information from multiple images to produce a higher-quality image of the scene compared to any of the individual images alone, the *SSIM*-Mean would be a suitable choice for fusion. We formulate image fusion as an optimization problem and propose a general mathematical framework for image fusion using *SSIM*-Mean.

Problem: Given $\{\mathbf{y}_1, \mathbf{y}_2, \ldots, \mathbf{y}_n\}$ a set of n images in vector format of size $\mathtt{n} \times 1$, $\{\mathbf{p}_1, \mathbf{p}_2, \ldots, \mathbf{p}_n\}$, a set of associated weights, $\{\mathscr{H}_1, \mathscr{H}_2, \ldots, \mathscr{H}_n\}$ a set of degradation operators of size $\mathtt{n} \times \mathtt{m}$, $g(\mathbf{x})$ a regularization term, and λ its corresponding regularization parameter, find $\mathbf{x}$ of size $\mathtt{m} \times 1$ that maximizes

$$\sum_{i=1}^{n} \mathbf{p}_i \, SSIM(\mathscr{H}_i \mathbf{x}, \mathbf{y}_i) + \lambda g(\mathbf{x}). \tag{1}$$

This problem will be solved numerically using gradient-based approaches.

The greatest advantage of the proposed formulation compared to Brunet's work in [5] is that it is flexible by allowing various types of degradation operators $\mathscr{H}_i$ and regularization terms $g(\mathbf{x})$. We apply the proposed method for both denoising and resolution enhancement of a set of given degraded images, where *SSIM*-Mean is used as data fidelity. The results will be evaluated both qualitatively and quantitatively.

References

[1] Z.Wang and A. C. Bovik, *A universal image quality index IEEE Signal Processing Letters*, vol. 9, no. 3, pp. 81-84, March (2002).

[2] Z.Wang, A. C. Bovik, H. R. Sheikh and E. P. Simoncelli, *Image quality assessment: from error visibility to structural similarity*, in *IEEE Transactions on Image Processing*, vol. 13, no. 4, pp. 600-612, April (2004).

[3] D. Otero, D. La Torre, O. Michailovich, E.R. Vrscay, *Optimization of Structural Similarity in Mathematical Imaging* in *Optimization and Engineering* 22 (2021).

[4] D. Otero, D. La Torre, O. Michailovich, E.R. Vrscay, *An Efficient Algorithm for Computing the Derivative of Mean Structural Similarity Index Measure* in Image Analysis and Recognition. ICIAR 2019. Lecture Notes in Computer Science, vol 11662, (2019)

[5] D.Brunet. A Study of the Structural Similarity Image Quality Measure with Applications to Image Processing. PhD Thesis, UWSpace. (2012)

Mathematical Modeling of Wound Angiogenesis: Understanding the Dynamics of Cellular Interactions and Signaling Pathways

E. Agyingi[1], L. Wakabayashi[2], T. Wiandt[3], S. Maggelakis[4]

[1] *Rochester Institute of Technology, Rochester, New York, United State (eoasma@rit.edu)*
[2] *Rochester Institute of Technology, Rochester, New York, United State (lkw7139@rit.edu)*
[3] *Rochester Institute of Technology, Rochester, New York, United State (tiwsma@rit.edu)*
[4] *Rochester Institute of Technology, Rochester, New York, United State (sxmsma@rit.edu)*

Wound angiogenesis refers to the process of new blood vessel formation that occurs in response to tissue injury or damage. This process is a critical component of the body's natural healing response, as it helps to supply the injured tissue with oxygen and nutrients, and remove waste products. During wound angiogenesis, specialized cells called endothelial cells proliferate and migrate to the site of the injury, where they form new blood vessels. Angiogenesis is a complex process that is regulated by a variety of factors, including growth factors, cytokines, and extracellular matrix components. Disruptions in this process can lead to delayed or impaired wound healing, as well as the formation of abnormal blood vessels. In this paper, we simulate angiogenesis in cutaneous wound by using a variant of the Eden model for cluster aggregation to recreate a healing process where capillary blocks are laid behind moving capillary sprouts within the wound region. The regeneration process is orchestrated by planting seeds along the wound edge and allowing them to grow as sprouts into the wound space. Capillary blocks are formed when the tips of two sprouts converge. We present simulations illustrating different healing strategies, including bacterial infection for several wound geometries.

References

[1] M. Tonnesen, X. Feng and R. Clark. *Angiogenesis in wound healing*. J Investig Dermatol Symp Proc.**5**(1):40-6 (2000). doi: 10.1046/j.1087-0024.2000.00014.x. PMID: 11147674.

[2] E. Agyingi, L. Wakabayashi,T. Wiandt and S. Maggelakis, *Eden Model Simulation of Re-Epithelialization and Angiogenesis of an Epidermal Wound*. Processes, *6*, 207 (2018). https://doi.org/10.3390/pr6110207

[3] E. Agyingi, S. Maggelakis and D. Ross, *The effect of bacteria on epidermal wound healing,* Math. Model. Nat. Phenom., 5(3): 28-39 (2010) DOI: https://doi.org/10.1051/mmnp/20105303

Application of Symbolic Differential Operator Discovery in Biological Sciences

L. Podina[1,*], B. Eastman[2,*], M. Kohandel[3]

[1] *University of Waterloo, Canada, lpodina@uwaterloo.ca*
[2] *OpenAI, USA*
[3] *University of Waterloo, Canada, kohandel@uwaterloo.ca*
[*] *equal contribution*

This work focuses on the application of symbolic discovery of differential operators in situations where experimental data is sparse, specifically in biology. The small data regime in machine learning can be made more manageable by incorporating prior knowledge about the underlying dynamics. Physics Informed Neural Networks (PINNs) [1] have been extremely successful in reconstructing entire ODE or PDE solutions using only a single point or a few measurements of the initial condition. The Universal PINN approach (UPINN) further enhances the power of PINNs by adding a neural network that learns the representation of unknown hidden terms in the differential equation or the entire equation. The algorithm outputs a surrogate solution to the differential equation and a black-box representation of the hidden terms. These hidden term neural networks can then be converted into symbolic equations using symbolic regression techniques like AI Feynman [2]. The algorithms are provided with noisy measurements of the initial condition and synthetic experimental data obtained at later times. The UPINN demonstrates strong performance in identifying drug action in chemotherapeutics, Lotka-Volterra predator-prey interactions, and interactions within a model of cell apoptosis, even when provided with limited measurements of noisy data.

References

[1] M. Raissi, P. Perdikaris, G.E. Karniadakis, *Physics-informed neural networks: A deep learning framework for solving forward and inverse problems involving nonlinear partial differential equations*, Journal of Computational Physics, Volume 378, 2019, Pages 686-707, ISSN 0021-9991, https://doi.org/10.1016/j.jcp.2018.10.045.

[2] S. Udrescu and M. Tegmark, *AI Feynman: A physics-inspired method for symbolic regression*. Sci. Adv. 6, eaay2631 (2020). DOI:10.1126/sciadv.aay2631

The VI International AMMCS
Interdisciplinary Conference
Waterloo, Ontario, Canada

Macroscopic Dynamics of a Neural Network with Synaptic Delay

L. Chen[1], S. A. Campbell[1]

[1] *Department of Applied Mathematics and Centre for Theoretical Neuroscience, University of Waterloo, Canada, {l477chen,sacampbell}@uwaterloo.ca*

This paper investigates the impact of time delays on the macroscopic dynamics of large-scale neural networks through exact mean-field reductions.

The brain can be seen as a network with a large number of synaptically coupled neurons. Whether the brain can perform its function depends on the network's emerging macroscopic dynamics. Time delays plaguing communication between neurons are an essential factor that cannot be ignored. They are comparable to the characteristic time scales of the system in most situations and have a significant influence on collective dynamics, such as oscillation and synchronization. The analysis of the large-scale neural network has either relied on heuristic models motivated by biophysical data, e.g., the Wilson-Cowan model, or involved substantial computational costs. Exact mean-field reductions recently developed by statistical physics, known as the Ott-Antonsen and Watanabe-Strogatz approaches, allow one to obtain low-dimensional dynamical systems for population-averaged variables by bridging the microscopic properties of individual neurons and macroscopic dynamics of the neural network.

This paper follows the theoretical framework of the Ott-Antonsen reduction and employs the Lorentzian ansatz to arrive at a mean-field model for the network of quadratic integrate-and-fire (QIF) neurons with the standard synaptic expression. We also incorporate fixed, homogeneous delays and heterogeneous delays with a distribution function. The correspondence is exact in the thermodynamic limit.

Bifurcation analysis allows us to identify the regions in the parameter space where the network exhibits macroscopic dynamics, including the transition between states where the individual neurons exhibit asynchronous tonic firing and synchronous bursting. More importantly, our mean-field system reveals significantly different bifurcation structures than the system using the simplified synaptic model, including a novel mechanism for the emergence of population bursting behaviours not previously observed in the excitatory network of QIF neurons. Our results will provide insights into the model-based inference of neurological mechanisms and the impact of time delays on the macroscopic dynamics that underpin brain function and dysfunction from the perspective of theoretical neuroscience.

Convolution Quadrature solutions of 3D scattering problems in the time domain

Catalin Turc[1], Peter Petropoulos[1],

[1] *New Jersey Institute of Technology (NJIT), 23 DR Martin Luther King Jr Blvd Ste B, Newark, NJ 07102, USA. cct21@njit.edu*
[1] *New Jersey Institute of Technology (NJIT), 23 DR Martin Luther King Jr Blvd Ste B, Newark, NJ 07102, USA. peter.p.petropoulos@njit.edu*

We investigate high-order Convolution Quadratures methods for the solution of the wave equation in unbounded domains in three dimensions that rely on high-order discretizations of the BIE solution of the ensemble of associated Laplace domain modified Helmholtz problems. Two classes of CQ discretizations are employed, one based on linear multistep methods and the other based on Runge-Kutta methods and two classes of Nystrom discretizations are considered for the discretization of the BIE formulations for modified Helmholtz scattering problems—one based on Alpert quadratures and another based on QBX. A variety of accuracy tests are presented that showcase the high-order in time convergence (up to and including fifth order) that the Nystrom CQ discretizations are capable of delivering.

Keywords: Wave equation, Convolution Quadratures, Boundary Integral Equations.

The New Regulatory Capital Regime and It's Impact on Trading Businesses in Banking

Karl Wouterloot[1],

[1] *Scotiabank, 44 King St W., Toronto, M5H 1H1, Canada, karl.wouterloot@scotiabank.com*

The Basel Revisions and the Fundamental Review of the Trading Book are taking effect in Canada this year. The new regulations will result in large impacts on the regulatory capital requirements of Canadian banks. The increased focus these regulations have on standardized approaches presents new challenges for practitioners in finance and risk management departments large banks, along with their business lines. This talk will include an overview of Basel Revisions and the Fundamental Review of the Trading Book with a focus on trading products. Also, some of the practical implications that these regulations have on banks will be presented.

The VI International AMMCS
Interdisciplinary Conference
Waterloo, Ontario, Canada

Efficient Pricing and Hedging of High-Dimensional American Options using Deep Recurrent Neural Networks

A. S. Na[1], J. W.L. Wan[2]

[1] *David R. Cheriton School of Computer Science, University of Waterloo, Waterloo, Canada, andrew.na@uwaterloo.ca*
[2] *David R. Cheriton School of Computer Science, University of Waterloo, Waterloo, Canada, justin.wan@uwaterloo.ca*

We propose a deep Recurrent neural network (RNN) framework for computing prices and deltas of American options in high dimensions. Our proposed framework uses two deep RNNs, where one network learns the continuation price and the other learns the delta for each timestep. Our proposed framework yields prices and deltas for the entire spacetime, not only at a given point (e.g. $t = 0$). The computational cost of the proposed approach is linear in N, which improves on the quadratic time seen for feedforward networks that price American options. The computational memory cost of our method is constant in N, which is an improvement over the linear memory costs seen in feedforward networks. Our numerical simulations demonstrate these contributions, and show that the proposed deep RNN framework is computationally more efficient than traditional feedforward neural network frameworks in time and memory.

The VI International AMMCS
Interdisciplinary Conference
Waterloo, Ontario, Canada

L^2 theory for compressible Euler equations

Geng Chen[1]

[1] *University of Kansas, gengchen@ku.edu*

Compressible Euler equations are a typical system of hyperbolic conservation laws,whose solution forms shock waves in general. It is well known that global BV solutions of system of hyperbolic conservation laws exist, when one considers small BV initial data. As a major breakthrough for system of hyperbolic conservation laws in 1990's, by Bressan and etc, solutions have been proved to be unique among BV solutions verifying either the so-called Tame Oscillation Condition, or the Bounded Variation Condition on space-like curves.

In this talk, I will discuss the recent works with Krupa and Vasseur. In these works, for systems with two unknowns and the non-isentropic Euler equations with three unknowns, we established an L^2 stability theory using the method of relative entropy. As an application, we proved all BV solutions must statisfy the Bounded Variation Condition, hence showed the uniqueness of BV solution without any additional condition.

If time is permitted, I will briefly introduce the recent progress on the vanishing viscosity limit from Navier-Stokes equations to the BV solution of compressible Euler equations. This is a collaboration work with Kang and Vasseur.

Shocks interaction for the Burgers-Hilbert Equation

A. Bressan[1], S. T. Galtung[2] , K. Grunert[3], and K.T. Nguyen[4]

[1] *Penn State University, State College, USA, bressan@math.psu.edu*
[2] *NTNU Norwegian University of Science and Technology, Trondheim, Norway, sondre.galtung@ntnu.no*
[3] *NTNU Norwegian University of Science and Technology, Trondheim, Norway, katrin.grunert@ntnu.no*
[4] *North Carolina State University, Raleigh, USA, khai@math.ncsu.edu*

In 2009 J. Biello and J. Hunter derived a balance law modeling nonlinear waves with constant frequency, obtained from Burgers' equation by adding the Hilbert transform as a source term [1]. For a general initial data $\bar{u} \in \mathbf{L}^2(\mathbb{R})$, the global existence of entropy weak solutions was proved in [2], together with a partial uniqueness result. Moreover, piecewise continuous solutions with a single shock and the shock formation have been recently studied in [3, 5]. This talk will describe a further type of local generic singularities for solutions, namely, points where two shocks interact [4]. The solution is obtained as the sum of a function with H^2 regularity away from the shocks plus a corrector term having an asymptotic behavior like $|x| \ln ln |x|$ close to each shock. A key step in the analysis is the construction of piecewise smooth solutions with a single shock for a general class of initial data

References

[1] J. Biello and J. K. Hunter, Nonlinear Hamiltonian waves with constant frequency and surface waves on vorticity discontinuities, *Comm. Pure Appl. Math.* **63**, pp. 303-336 (2009).

[2] A. Bressan and K.T. Nguyen, *Global Existence of Weak Solutions for the Burgers-Hilbert Equation*, SIAM J. Math. Anal. **46** , 4, 2884-2904 (2014).

[3] A. Bressan and T. Zhang, *Piecewise smooth solutions to the Burgers-Hilbert equation*, Commun. Math. Sci. **15** , 1, pp. 165-184 (2017).

[4] A. Bressan , S. T. Galtung , K. Grunert, and K.T. Nguyen, *Shock interactions for the Burgers-Hilbert Equation*, Communications in Partial Differential Equations. **47**, 9, pp. 1795-1844 (2022).

[5] R. Yang, *Shock formation of the Burgers-Hilbert equation*, SIAM J. Math. Anal. **53** , 5, pp. 5756-5802 (2021).

The VI International AMMCS
Interdisciplinary Conference
Waterloo, Ontario, Canada

Fibonacci Primes, Primes of the form $2^n - k$ and Beyond

Jon Grantham[1], Andrew Granville[2]

[1] *Center for Computing Sciences, Institute for Defense Analyses, Bowie, MD, USA.*
[2] *Department de Mathématqiues et de statistiqué, Université de Montréal, Canada.*

We speculate on the distribution of primes in exponentially growing, linear recurrence sequences $(u_n)_{n\geq 0}$ in the integers. By tweaking a heuristic which is successfully used to predict the number of prime values of polynomials, we guess that either there are only finitely many primes u_n, or else there exists a constant $c_u > 0$ (which we can give good approximations to) such that there are $\sim c_u \log N$ primes u_n with $n \leq N$, as $N \to \infty$. We compare our conjecture to the limited amount of data that we can compile.

The VI International AMMCS
Interdisciplinary Conference
Waterloo, Ontario, Canada

Fairer Shootouts in Soccer: The *m*-*n* Rule

S. Brams[1], M. Ismail[2], M. Kilgour[3]

[1]*New York University, New York, NY, USA (steven.brams@nyu.edu)*
[2]*King's College London, England, UK (mehmet.ismail@kcl.ac.uk)*
[3]*Wilfrid Laurier University, Waterloo, Canada (mkilgour@wlu.ca*)

Winning the coin toss at the end of a tied soccer game gives a team the right to choose whether to kick either first or second on all five rounds of penalty kicks, when each team is allowed one kick per round. There is considerable evidence that the right to make this choice, which is usually to kick first, gives a team a significant advantage. To make the outcome of a tied game fairer, we suggest a rule that handicaps the team that kicks first (*A*), requiring it to succeed on one more penalty kick than the team that kicks second (*B*). We call this the *m* - *n* rule and, more specifically, propose (*m*, *n*) = (5, 4): For *A* to win, it must successfully kick 5 goals before the end of the round in which *B* kicks its 4th; for *B* to win, it must succeed on 4 penalty kicks before *A* succeeds on 5. If both teams reach (5, 4) on the same round—when they both kick successfully at (4, 3)—then the game is decided by round-by-round "sudden death," whereby the winner is the first team to score in a subsequent round when the other team does not. We show that this rule is fair in tending to equalize the ability of each team to win a tied game in a penalty shootout. We also discuss a related rule that precludes the teams from reaching (5, 4) at the same time, obviating the need for sudden death and extra rounds.

The VI International AMMCS
Interdisciplinary Conference
Waterloo, Ontario, Canada

Surfaces with maximal Picard number

A. Auel[1], A. Logan[2],[3], J. Voight[1]

[1] *Dartmouth College, Hanover, New Hampshire, USA,* {asher.auel@dartmouth.edu, john.voight@gmail.com}

[2] *Tutte Institute for Mathematics and Computation, Ottawa, Canada* [3] *School of Mathematics and Statistics, Carleton University, Ottawa, Canada,* adam.m.logan@gmail.com

A variety V has *maximal Picard rank* if the rank of its Néron-Severi group is equal to the dimension of $\mathrm{H}^{1,1}(V)$. This property is interesting in part because the Galois representation on the transcendental lattice $\mathrm{H}^2(V)/\mathrm{H}^{1,1}(V)$ should be related to a modular form of a well-understood type, rather than a mysterious automorphic form.

The K3 surfaces of this type that are defined over $\mathbb{Q}$ were fully described by Elkies and Schütt. Shioda constructed many elliptic surfaces with this property, and Persson and others have described some that are of general type. In this talk we will describe a new construction of such surfaces and discuss the modularity properties of existing and new examples and the correspondences that they suggest.

Stability and Qualitative Analysis of a Switched SQEAIR-Based Epidemic Model

Z. Abbasi[1], X. Liu[2]

[1] *University of Waterloo, Waterloo, Canada, zoya.abbasi@uwaterloo.ca*
[2] *University of Waterloo, Waterloo, Canada, xinzhi.liu @uwaterloo.ca*

This study presents a switched SQEIAR-based epidemic model that considers the variability of the contact rate, which is the average number of contacts between individuals in a population per unit of time, during an outbreak in the real world. Specifically, the period of infection is divided into multiple subsystems or modes, each representing a phase of the disease based on its severity. The severity of the disease is determined by the contact rate, which can be high, medium, or low, depending on the level of contact in society. The basic reproduction number (R_0), which indicates the ability of a disease to spread in a susceptible population, is calculated for the proposed model. If R_0 is greater than one, the disease is likely to spread in society, and the subsystem is considered unstable. Conversely, if R_0 is less than one, the disease is eradicated and the subsystem is stable. The equilibria of the proposed model are calculated, and their stabilities are analyzed. Furthermore, the qualitative analysis of the model is conducted through two theorems, including the invariance property of the solutions and their positivity. To control the spread of the disease, a mode-dependent average dwell time (MDADT) strategy is proposed, which determines the amount of time the system remains in each subsystem based on the contact rate of the disease. The goal is to spend less time in unstable subsystems and more time in stable ones, resulting in globally uniformly exponential stability (GUES) of the entire switched system. This approach is supported by a Lyapunov function, and sufficient conditions are derived in terms of linear matrix inequalities (LMIs) to ensure stability. Finally, the effectiveness of the proposed strategy is validated with a numerical example, which enables policymakers to optimize budget allocation. Additionally, this method eliminates the need for constant quarantine and government interventions.

The VI International AMMCS
Interdisciplinary Conference
Waterloo, Ontario, Canada

Simulating spin qubit control in realistic semiconductor quantum dot devices

B. Khromets[1], Z. Merino[2], J. Baugh[3]

[1] *Institute for Quantum Computing, University of Waterloo, Waterloo, Canada, bohdan.khromets@uwaterloo.ca*
[2] *Institute for Quantum Computing, University of Waterloo, Waterloo, Canada, zmerino@uwaterloo.ca*
[3] *Institute for Quantum Computing, University of Waterloo, Waterloo, Canada, baugh@uwaterloo.ca*

Electron spin qubits in gate-defined semiconductor quantum dots (QDs) are a promising platform for scalable universal quantum processors. In a proposal for a scalable processor based on gated Si/SiO_2 QDs [1], we combine a global magnetic field for electron spin resonance (ESR), $\vec{B}_{\mathrm{ESR}}$, with the voltage-controlled electronic g-factors $g_i(\vec{V})$ and exchange couplings $J_{ij}(\vec{V})$ to realize locally addressable quantum operations. The complex, nonlinear dependency of the QD spin and charge states on the device geometries and voltage configurations motivates research towards high-fidelity qubit control in realistic device models. In this talk, we describe the simulation of gate-defined QD arrays based on the construction of effective spin and charge models, as well as an efficient algorithm for voltage and ESR pulse design that yields high-fidelity quantum logic operations.

An open-source Python software we developed, QuDiPy [2], takes as input the electrostatic potentials of realistic QD devices modeled in the nextnano++ [3] finite element simulation tool. We modify the Linear Combination of Harmonic Orbitals – Configuration Interaction (LCHO-CI) algorithm [4] to efficiently calculate many-electron spectra for a large ensemble of voltage configurations. Constructing effective Heisenberg and Hubbard Hamiltonians based on these spectra enables simulating the evolution of spin states and predicting charge stability diagrams.

In addition, we propose a novel unitary pulse design method to handle the nonlinear voltage control of the spin interaction parameters and the effects of cross-talk in QD arrays. We prove that if all the nonzero effective parameters are proportional to the same normalized, dimensionless shape function $S(t)$:

$$\frac{g_i(t)-g_0}{\langle g_i(t)-g_0\rangle}=\frac{J_{ij}(t)-J_0}{\langle J_{ij}(t)-J_0\rangle}=\frac{B_{\mathrm{ESR}}(t)}{\langle B_{\mathrm{ESR}}(t)\rangle}=S(t),\quad \forall i,j, \tag{1}$$

the gate voltage pulses $\vec{V}(t)$ can be determined uniquely for *any* chosen shape $S(t)$ with only one numerical integration of a system of ODEs of type $\mathrm{d}\vec{V}/\mathrm{d}S=\vec{F}(\vec{V},S)$. In particular, this method enables a global ESR field to address qubits individually, even under a very restricted range of local g-factor control in silicon ($\Delta g/g\sim 10^{-5}-10^{-4}$). We also leverage the time-orderedness of the spin Hamiltonian guaranteed by this approach to construct nontrivial quantum gates, e.g. the Control-Z (control-phase) gate realized by simultaneous modulation of g-factors and exchange couplings. Finally, we demonstrate the simulated control of a 4-qubit array by implementing a Variational Quantum Eigensolver for the ground state of the hydrogen molecule using the Unitary Coupled Cluster algorithm. We expect these results to facilitate the experimental design and control of silicon quantum processors.

References

[1] B. Buonacorsi, Z. Cai, E. Ramirez et al. *Network architecture for a topological quantum computer in silicon*, Quantum Sci. Technol. **4**, p. 025003 (2019).

[2] GitHub Repository: *https://github.com/mainCSG/QuDiPy.*

[3] S. Birner, T. Zibold, T. Andlauer et al. *nextnano: general purpose 3-D simulations*, IEEE Trans. Electron Dev. **54**, pp.2137-2142 (2007).

[4] B. Buonacorsi, M. Korkusinski, B. Khromets and J. Baugh *Optimizing lateral quantum dot geometries for reduced exchange noise,* arXiv:2012.10512 (2020).

The Discrete Convolution and Convolution Equations for Fractional Cosine-Sine Series

Q. Feng, R. B. Wang

Yanan University, Yanan, Shaanxi, China, yadxfq@yau.edu.cn

The convolution plays an important role in various fields, such as solving integral and differential equations and design of filters in signal processing. Different convolutions are as much important as many properties and applications they will be able to exhibit. Therefore, it is worthwhile and interesting to investigate convolution and associated theorems continually for its high potential in exhibiting new properties and concrete applications.

During the past years, the discrete Fourier cosine convolution $(x \underset{F_{cDT}}{*} y)(n)$ [1] and the discrete Fourier sine convolution $(x \underset{F_{sDT}}{*} y)(n)$ [2] of two series $x(n)$ and $y(n)$ on $\mathbb{N}_0$ were defined as follows

$$\begin{aligned}(x \underset{F_{cDT}}{*} y)(n) &= \sum_{m=1}^{\infty} x(m)[y(n+m)+y(|n-m|)]+x(0)y(n),\ n\geq 0\\ (x \underset{F_{sDT}}{*} y)(n) &= \sum_{m=1}^{\infty} x(m)[y(|n-m|)-y(n+m)],\ n\geq 0\end{aligned} \tag{1}$$

respectively. And the following two convolution theorems fulfills

$$\begin{aligned}F_{cDT}\{(\underset{F_{cDT}}{*})(n)\}(w) &= 2F_{cDT}\{x(n)\}(w)F_{cDT}\{y(n)\}(w)\\ F_{sDT}\{(x*y)(n)\}(w) &= 2F_{sDT}\{x(n)\}(w)F_{cDT}\{y(n)\}(w)\end{aligned} \tag{2}$$

respectively, where F_{cDT} and F_{sDT} denotes the Fourier cosine series and he Fourier sine series

$$\begin{aligned}F_{cDT}x(n)(\omega) &= \tfrac{x(0)}{2}+\sum_{n=1}^{\infty} x(n)\cos(n\omega),\ \omega\in[0,\pi]\\ F_{sDT}x(n)(\omega) &= \sum_{n=0}^{\infty} x(n)\sin(n\omega),\ \omega\in[0,\pi]\end{aligned} \tag{3}$$

In recent years, the convolution equation has important applications in various fields such as engineering mechanics and digital signal processing [3], how to obtain solution of the convolution equation is one of the meaningful issues of equation theory. However, the signal analysis capability of the Fourier transform is limited by the time-frequency domain. Therefore, it is imperative to find a more flexible tool than the Fourier transform.

In this paper, we extend the Fourier sine series and the Fourier cosine series to the fractional domain. The fractional sine series (FRSS) and the fractional cosine series (FRCS) is defined. Several kinds of discrete convolution operations for FRSS and FRCS are presented, and the corresponding discrete convolution theorems are derived. The relationship of these discrete convolution operations is further discussed. In addition, two types of discrete convolution equations are studied based on the proposed convolution theorems, and the explicit solutions for these discrete convolution equations are obtained.

References

[1] N. X. Thao, V. K. Tuan and N. A. Dai, *Discrete-time Fourier cosine convolution*, Integral Transform Spec. Funct., **29**, 11, pp. 866-874 (2018).

[2] N. X. Thao, V. K. Tuan and N. A. Dai, *A discrete convolution involving Fourier sine and cosine series and its applications*, Integral Transform Spec. Funct., **31**, 3, pp. 243-252 (2020).

[3] D. O. E. Silva and R. Quilodran, *Smoothness of solutions of a convolution equation of restricted-type on the sphere*, Forum. Math. Sigma., **9**, 12, pp. 1-40 (2021).

Understanding Phage-Antibiotic Treatment of Biofilms in Mathematical Framework

Blessing O. Emerenini

Rochester Institute of Technology, New York, USA, science@rit.edu

Biofilm formation within host can be extremely problematic if left untreated. Certain lung diseases such as cystic fibrosis can cause biofilms formation in the lungs. With antibiotic-resistant bacteria, the use of phage therapy has been introduced as an alternative or an additive to the use of antibiotics in order to combat biofilm growth. The aim of using phage treatment is to reduce biofilm growth or completely eradicate biofilm from the host. There are several factors that still need to be understood during this process, e.g the role of burst size, dosage and application time. This presentation will introduce the use of mathematical models and data assimilation to determine several factors that could lead to controlling biofilm growth or eradicate it using phage-antibiotic combined therapy.

Agent-based models of interacting microbial populations: model calibration

A. Ahmadi[1], A. Yip[1], B. Ingalls[1]

[1] *University of Waterloo, Waterloo, Canada, bingalls@uwaterloo.ca*

Microbial populations play a wide array of roles in systems of interest, impacting health, agriculture, manufacturing, waste water treatment, and environmental remediation. The activity of these populations is driven by ecological interactions among the many microbial species that make up microbiome populations. Current efforts toward manipulation of these communities span the range from direct interactions with environmental populations (top-down) to characterization of simple communities in idealized laboratory settings (bottom-up) [1].

Our group is developing frameworks for predictive modelling of bacterial populations interacting in monolayer, captured with time-lapse fluorescence microscopy. We are currently focused on communities consisting of two populations interacting via antagonism, cross-protection, or horizontal gene transfer. Our modelling pipeline begins with image processing [2], allowing us to collect spatio-temporal data on cell position, length, growth rate, and genetic state.

We implement agent-based models of these systems using the CellModeller platform [3]. Calibration of agent-based models is generally challenging. Both the underlying system and the simulations are stochastic. Consequently, rather than assess model quality by simulation of specific experimental runs, best-fit parameterizations can be determined by accurately capturing spatio-temporal patterns in system behaviour. We surveyed relevant patterns, or summary statistics [4], prior to selecting those that best represent our systems of interest. We infer model parameter values by Approximate Bayesian Computation [5], which provides insight into uncertainty of the inference. Finally, we validate model calibration against training data that was not used for training.

References

[1] Lawson, Christopher E., et al. "Common principles and best practices for engineering microbiomes." Nature Reviews Microbiology 17.12 (2019): 725-741.

[2] Jeckel, Hannah, and Knut Drescher. "Advances and opportunities in image analysis of bacterial cells and communities." FEMS Microbiology Reviews 45.4 (2021): fuaa062.

[3] Rudge, Timothy J., et al. "Computational modeling of synthetic microbial biofilms." ACS synthetic biology 1.8 (2012): 345-352.

[4] Yip, Aaron, et al. "Calibrating spatiotemporal models of microbial communities to microscopy data: A review." PLOS Computational Biology 18.10 (2022): e1010533.

[5] Liepe, Juliane, et al. "A framework for parameter estimation and model selection from experimental data in systems biology using approximate Bayesian computation." Nature protocols 9.2 (2014): 439-456.

The VI International AMMCS
Interdisciplinary Conference
Waterloo, Ontario, Canada

The pipeline externalities game

C. Trudeau[1], E.C. Rosenthal[2]

[1] *University of Windsor, Canada, trudeauc@uwindsor.ca*

[2] *Temple University, Philadelphia, USA, edward.rosenthal@temple.edu*

We consider a set of agents who are located along a pipeline with a single source. These agents consume discrete units of flow, where their utility from successive units exhibits diminishing marginal returns. Additionally, flows along each edge in the pipeline create negative externalities, which are non-decreasing as a function of flow. The agents cooperate toward obtaining group welfare maximization. In this environment we first provide an algorithm that yields the sequence of flows to maximize net surplus for the agent set. Next, we develop cooperative games to determine how best to share the damages from the flows. Using optimistic and pessimistic formulations for the characteristic function, we study, respectively, the anti-core and core of the cooperative game and show that the core of the pessimistic game is nonempty. We develop a marginal damage as well as an average damage allocation method, and show that they are elements of the core. In addition, we provide a partial characterization of the core and also propose a procedure to compensate agents who are left out of the optimal solution but nevertheless have blocking power in the pipeline.

Example

Suppose that we have 3 agents, with agent 1 closest to the source, followed by agent 2, with agent 3 furthest from the source. All agents are interested in at most one unit of good, to be delivered from the source. The value of that unit is 18 for agent 1, 56 for agent 2 and 12 for agent 3. Flows create damages locally. We suppose here that the first unit of flow does not create damage, but additional units do. The second unit of flow on the edge to agent 1 creates a damage of 6. The third unit creates a damage of 30. On the edge from agent 1 to agent 2, the second unit creates 6 of damage.

We can check that the optimal utilization of the pipeline is to send 2 units of flow to the node of agent 1, and one to the node of agent 2, thus allowing 1 unit of consumption for agents 1 and 2. This creates a net benefit of 18+56-6=68.

The paper first proposes a greedy algorithm to determine the optimal flows. We then study how to share that net benefit among the agents. The marginal damage allocation method simply uses the algorithm: at each stage it determines an agent that receives an additional unit of flow. We then assign to that agent the marginal net benefit of that unit. Here, it assigns 12 to agent 1, 56 to agent 2 and 0 to agent 3. The average damage allocation method assigns to each unit of flow the average damage on the edges it goes through. Here it implies that agents 1 and 2 equally split the damage of 6 on the edge to the node of agent 1, for an allocation of 15 to agent 1, 53 to agent 2, and 0 to agent 3.

We define proper coalitional games from the pipeline externalities game and show that these allocations are in the core of these games. We then describe core allocations that allow to compensate agents that are crowded out of consumption, like agent 3 in our example. One such way is to take the Shapley value of the so-called optimistic coalitional game, in which each coalition supposes that outside agents are not consuming, but most be compensated for the externalities they suffer.

A preliminary draft is available at: `https://www.dropbox.com/s/5sx6l3qo3dgwkau/pipeline_externality_paper_v4.pdf?dl=0`

The VI International AMMCS
Interdisciplinary Conference
Waterloo, Ontario, Canada
April 21, 2023

Annealing a Genetic Algorithm for Constrained Optimization

F. Mendivil[1], R. Shonkwiler[2]

[1] *Acadia University, Wolfville, Nova Scotia, Canada, franklin.mendivil@acadiau.ca*
[2] *Georgia Tech, Atlanta, Ga, shenk@math.gatech.edu*

Genetic algorithms (GAs) are a class of optimization algorithms that take inspiration from biological evolution. They are a form of directed random search, using a population of potential solutions in this search and updating this population by applying both a mutation and a recombination operation. Like many global optimization algorithms, GAs suffer from the problem of *niching*, or getting stuck in sub-optimal states. However, the randomness used in a GA will guarantee that eventually the population will wander away and will (under reasonable assumptions) visit the optimal states with probability one.

Mathematically, since the next population is only based on the current population, a GA is an instance of a Markov Chain with state space the set of all possible populations. As such it (usually) has an invariant distribution and the random walk induced by the GA will be recurrent.

In this talk, we will discuss the application of GAs to constrained optimization problems. A natural way of implementing a GA for a constrained problem is to initialize the population with some randomly generated feasible states and then structure the mutation and recombination operations to ensure that only feasible states are generated. However, this is usually completely impractical as often it is difficult to even generate one feasible state. An alternative is to use a penalty function to steer the algorithm away from infeasible states.

In this talk we discuss using a dynamic penalty which we view as a type of "annealing" (in analogy with Simulated Annealing). We give two very general and different ways of doing this and prove that in the limit the random process will only be supported on the set of optimal populations.

Title: Recent results on the stability of solitons and kinks

F. Pusateri[1]

[1] *University of Toronto, Canada, {fabiop}@math.toronto.edu*

Abstract: We will some recent results on nonlinear evolution equations with potentials, and applications to the stability of solitons and kinks, as well as to the phenomenon of "radiation damping". Our approach to this class of problems is based on the use of the distorted Fourier transform and the development of multilinear harmonic analysis in this setting. This talk is based on joint works with P. Germain (Imperial), A. Soffer (Rutgers), T. Leger (Princeton), Gong Chen (Georgia Tech), Zhiyuan Zhang (NYU) and Adilbek Kairzhan (U of Toronto); see list of references.

References

[1] Chen, G. and Pusateri, F. *The 1d nonlinear Schrödinger equation with a weighted L^1 potential*. *arXiv:1912.10949*. 45 pages. To appear in **Analysis & PDE**.

[2] Germain, P. and Pusateri, F. *Quadratic Klein-Gordon equations with a potential in one dimension*. **Forum Math. Pi** 10 (2022), Paper No. e17, 172 pages.

[3] Germain, P., Pusateri, F. and Zhang, Z. *On 1d quadratic Klein-Gordon equations with a potential and symmetries*. **Arch. Ration. Mech. Anal.** 247, Article number 17 (2023), 39 pages.

[4] Pusateri, F. and Soffer, A. *Bilinear estimates in the presence of a large potential and a critical NLS in 3d*. *arXiv:2003.00312*. 94 pages. To appear in **Memoirs of the AMS**.

[5] Léger, T. and Pusateri, F. *Internal mode-induced growth in 3d nonlinear Klein-Gordon equations*. 22 pages. *arXiv:2203.05694*. To appear in **Rend. Lincei Mat. Appl.**

[6] Léger, T. and Pusateri, F. *Internal modes and radiation damping for quadratic Klein-Gordon in 3D*. 125 pages. *arXiv:2112.13163*.

[7] Chen, G. and Pusateri, F. *On the 1d cubic NLS with a non-generic potential*. 54 pages. *arXiv:2205.01487*.

[8] Kairzhan, A. and Pusateri, F. *Asymptotic stability near the soliton for quartic Klein-Gordon in 1D*. 35 pages. *arXiv:2206.15008*.

Stochastic perturbations of El Nino Southern Oscillations (ENSO) : a Wiener chaos approach

Y. Aydogdu[1], P. Baxendale[2], N. S. Namachchivaya[3]

[1] *Department of Applied Mathematics, University of Waterloo, Waterloo, Canada yaydogdu@uwaterloo.ca*
[2] *Department of Mathematics, University of Southern California, Los Angeles, USA baxendal@usc.edu,*
3 *Department of Applied Mathematics, University of Waterloo, Waterloo, Canada nsnamachchivaya@uwaterloo.ca*

The phenomena of El Nino Southern Oscillations (ENSO) is modeled by coupled atmosphere-ocean mechanism together with sea surface temperature (SST) budget at the equatorial Pacific and has a significant impact on the global climate. We consider a modeling framework that was originally developed by Majda and co-workers in [1, 2], which is physically consistent and amenable to detailed analysis. The coupled model is mainly governed by the equatorial atmospheric and oceanic Kelvin and Rossby waves and it is shown that stochastic forcing gives rise to the model anomalies and unpredictable behavior. The purpose of our work is to investigate the influence of randomness on the model dynamics, construct the appropriate model components with stochastic noise and calculate the statistical properties. We also provide analytical and numerical solutions of the model to prove the convergence of the numerical scheme developed in our work.

We use Wiener-Chaos Expansion (WCE) to study stochastic ENSO models. The WCE method is based on reducing stochastic partial differential equations (SPDEs) into an infinite hierarchy of deterministic PDEs called propagators-Fourier modes [3] and represents the stochastic solution as a spectral decomposition of deterministic components with respect to a set of random Hermite bases. We solve the WCE propagators, which are forced by a set of complete orthonormal bases, by applying numerical integration and finite-difference methods. We compare WCE-based results with Monte Carlo simulations of SPDEs.

Our results depict that the mean and variance of the solutions obtained from the WCE method provide remarkably accurate results with a reasonable convergence rate and error range. We first test the WCE-based method on the ocean model with white noise and show that 10-Fourier modes are able to approach the theoretical variance values. We also show that the OU process with a specific noise strength and dissipation over a one-time period can be recovered with less than 50-Fourier modes for the ENSO model. To illustrate the particular weight of variance, we also generate the ensembles of solutions by using different stochastic bases.

References

[1] Thual, S., Majda, A. J., Chen, N., & Stechmann, S. N. (2016). Simple stochastic model for El Nino with westerly wind bursts. Proceedings of the National Academy of Sciences, 113(37), 10245-10250.

[2] Chen, N., Majda, A. J., & Thual, S. (2018). Observations and mechanisms of a simple stochastic dynamical model capturing El Nino diversity. Journal of Climate, 31(1), 449-471.

[3] Lototsky, S., & Rozovskii, B. (2006). Stochastic differential equations: a Wiener chaos approach. From stochastic calculus to mathematical finance: the Shiryaev festschrift, 433-506.

Dynamic event-triggered stability of delayed stochastic systems

P. L. Yu[1], F. Q. Deng[2], X. Z. Liu[3]

[1] *South China University of Technology, Guangzhou, China, yupeilin_0828@163.com*
[2] *South China University of Technology, Guangzhou, China, aufqdeng@scut.edu.cn*
[3] *University of Waterloo, Waterloo, Canada, xzliu@uwaterloo.ca*

The event-triggered of linear systems has been studied by many scholars, but the event-triggered stability of stochastic systems is not particularly well investigated, mainly because of the difficulty in dealing with stochastic systems to eliminate Zeno phenomena, which cannot be replicated for linear systems. Due to the existence of random effects, the state of the system is difficult to predict and control, and the behavior of the system changes over time, even when the test is conducted under the same initial conditions. This presented significant challenges, particularly in determining sampling/execution times and evaluating closed-loop performance, which led us to develop powerful and complex approaches to analyze and design random event-triggered controls. The corresponding closed-loop stability analysis remains challenging and will certainly be substantially different from the analysis in Refs. [1, 2, 3] due to differences in execution/sampling mechanisms. This article addresses the dynamic event-triggered stability for delayed stochastic systems, which including some input-to-state stability characteristics. To avert Zeno behavior in each sample path, our event-triggered mechanisms force a pause time after each successful execution, which will lead to intermittent detection of system status, thus greatly saving communication resources. One utilizes the Hanalay-type inequality to obtain the less conservative stability criterion. In addition, a collaborative design method of event-triggered mechanism and linear controller is proposed. Ultimately, an paraphrastic example is shown to indicate the availability of the mentioned collaborative design process.

References

[1] X. Mao, W. Liu, L. Hu, Q. Luo, J. Lu, *Stabilization of hybrid stochastic differential equations by feedback control based on discrete-time state observations*, Syst. Control Lett. **73**, pp. 88-95 (2014).

[2] L. Wu, Y. Gao, J. Liu, H. Li, *Event-triggered slidingmode control of stochastic systems via output feedback*, Automatica. **82**, pp. 79-92 (2017).

[3] Y. Wang, W. Zhang, H. Zhang, *Dynamic event-based control of nonlinear stochastic systems*, IEEE Trans. Autom.Control. pp. **62**, 12, pp. 6544-6551 (2017).

Neural network-based hybrid impulsive control of vehicle platoons

Z. L. Liang[1], X. Z. Liu[2]

[1] *University of Waterloo, Waterloo, Canada, z22liang@uwaterloo.ca*
[2] *University of Waterloo, Waterloo, Canada, xinzhi.liu@uwaterloo.ca*

Automated highway systems (AHS) and intelligent vehicle highway systems have been extensively studied in recent years in an effort to reduce traffic congestion, traffic accidents, and environmental pollution through vehicle platoon movements. Specifically, the fundamental objective of vehicle platoon control is to ensure the stability of the desired lane configuration with respect to the platoon leader, so that adjacent vehicles can maximize highway capacity by maintaining close tracking distances. According to Refs. [1], the dynamics of each vehicle can be described by

$$\dot{p}_i = v_i, \quad \dot{v}_i = a_i, \quad \dot{a}_i = f_i(v_i, a_i) + g_i(v_i)b_i, \quad \forall i \tag{1}$$

In the meantime, in order to compensate for unknown intrinsic dynamics $f_i(v_i, a_i)$ of the system, we employ the radial basis function neutral networks (RBF NNs), which is a trending strategy for dynamic approximation satisfying

$$f_i(v_i, a_i) = W_i^T \varphi_i(v_i, a_i) + \varepsilon_i \tag{2}$$

where W_i stands for the desired weight matrix, $\varphi(.)$ is the Gaussian basis function vector, and ε_i is a bounded approximation error. Moreover, it differs from most existing works, such as Refs. [2, 3] utilizing fully continuous control schemes, we developed our tracking control protocol by using an impulsive mechanism that is capable of generating abrupt changes in system states at some predefined time instants. Through this approach, we can efficiently reduce control costs, overcome transmission limitations, and enhance data security. Therefore, based on the above setup, this paper proposes a distributed hybrid impulsive control scheme to achieve the string stability of vehicle platoons; in particular, we apply the Lyapunov-Razumikhin technique along with relative state information transmission and the design of an overall topological structure, such that the tracking mismatch of the desired spacing, velocity and acceleration can be maintained in a compact error bound. Finally, the effectiveness and performance of our proposed control protocol are validated using numerical simulation examples.

References

[1] A. Ghasemi, R. Kazemi, and S. Azadi, *Stable Decentralized Control of a Platoon of Vehicles With Heterogeneous Information Feedback*", IEEE transactions on vehicular technology 62, 9, pp. 4299-4308 (2013).

[2] L. Tan, C. Li, X. Wang, and T. Huang, *Neural network-based adaptive synchronization for second-order nonlinear multiagent systems with unknown disturbance*, Chaos, 32 (3): 033112 (2022).

[3] T. Xiong, Z. Pu, J. Yi, and X. Tao, *Fixed-time observer based adaptive neural network time-varying formation tracking control for multi-agent systems via minimal learning parameter approach*, IET Control Theory & Applications, 14, 9, pp. 1147-1157 (2020).

ODE and FDE Models for Cancer Radiotherapy with a Death-Rate Term

N. Wilson[1], C.S. Drapaca[2], H. Enderling[3], J.J. Caudell[3], K.P. Wilkie[1,*]

[1] *Toronto Metropolitan University, Toronto, Canada, kpwilkie@torontomu.ca*
[2] *Pennsylvania State University, University Park, USA*
[3] *H. Lee Moffitt Cancer Center and Research Institute, Tampa, USA*

The desire to more accurately model and predict cancer patient response to treatment has lead to more and more complex mathematical models, such as those replacing ordinary differential equations with fractional differential equations. The Caputo fractional derivative incorporates an initial condition and a singular kernel[1], making it suitable for real-world applications, including tumour growth modelling. The definition of the Caputo fractional derivative is

$$D^{\mu} f(t) = \frac{1}{\Gamma(1-\mu)} \int_0^t \frac{1}{(t-\xi)^{\mu}} \frac{df}{d\xi} d\xi. \tag{1}$$

In this talk, I will discuss the advantages and disadvantages of replacing an ordinary derivative (OD) with a fractional derivative (FD) when modelling cancer radiotherapy. We compare three ODE models of tumour growth and the corresponding three FDE models for exponential, 2, logistic, 3, and exponential-linear, 4, growth. The order of the fractional derivative satisfies $\mu \in (0,1]$ with $\mu = 1$ corresponding to the ordinary derivative.

$$D^{\mu} v = av, \tag{2}$$

$$D^{\mu} v = av\left(1 - \tfrac{v}{K}\right), \tag{3}$$

$$D^{\mu} v = \lambda_0 v \left(1 + \left(\tfrac{\lambda_0}{\lambda_1} v\right)^{\psi}\right)^{-\frac{1}{\psi}}. \tag{4}$$

Due to the nature of fractional derivatives, we must replace the typical impulsive model for radiotherapy treatment with a continuous death rate term. Using hyperbolic tangent to continuously approximate the Heaviside function, we can simulate radiation induced cell death over a defined treatment window time interval. The continuity of this death rate term preserves the history dependence of the fractional derivative. It also improves computation time for both ODE and FDE models, providing a speed-up that would benefit large scale computations such as parameter fitting with stochastic algorithms or virtual clinical trials.

Our work shows that for the clinical data application we explored, the fractional derivative provided no additional benefit to the model. In fact, fractional orders below 1 showed unphysiological regrowth following treatments. Model comparisons through information criterion confirm the fractional order was not well exploited for this application. The best model for our clinical dataset was found to be the simplest one, the ODE model for exponential growth.

References

[1] M. Caputo, *Linear models of dissipation whose Q is almost frequency independent-II*, Geophys J Int **13**, 5, pp. 529-539 (1967). https://doi.org/10.1111/j.1365-246X.1967.tb02303.x.

[2] N. Wilson, C.S. Drapaca, H. Enderling, J.J. Caudell, and K.P. Wilkie, *Modelling Radiation Cancer Treatment with a Death-Rate Term in Ordinary and Fractional Differential Equations*, Bull Math Biol, to appear, (2023).

The VI International AMMCS
Interdisciplinary Conference
Waterloo, Ontario, Canada

Ideal solutions in the Prouhet–Tarry–Escott problem

Don Coppersmith[1], Michael J. Mossinghoff[2], Danny Scheinerman[3], Jeffrey M. VanderKam[4]

[1] *Center for Communications Research, dcopper@idaccr.org*
[2] *Center for Communications Research, m.mossinghoff@idaccr.org*
[3] *Center for Communications Research, danny.scheinerman@gmail.com*
[4] *Center for Communications Research, vanderkm@idaccr.org*

For given positive integers m and n with $m < n$, the *Prouhet–Tarry–Escott problem* asks if there exist two disjoint multisets of integers of size n having identical kth moments for $1 \leq k \leq m$; in the *ideal* case one requires $m = n - 1$, which is maximal. We describe some searches for ideal solutions to the Prouhet–Tarry–Escott problem, especially solutions possessing a particular symmetry, both over $\mathbb{Z}$ and over the ring of integers of several imaginary quadratic number fields. Over $\mathbb{Z}$, we significantly extend searches for symmetric ideal solutions at sizes 9, 10, 11, and 12, and we conduct extensive searches for the first time at larger sizes up to 16. For the quadratic number field case, we find new ideal solutions of sizes 10 and 12 in the Gaussian integers, of size 9 in $\mathbb{Z}[i\sqrt{2}]$, and of sizes 9 and 12 in the Eisenstein integers.

Optimal Experimental Design for Systems and Synthetic Biology

N. Braniff[1], N. Treloar[2], C. Barnes[2], B. Ingalls[1]

[1] *University of Waterloo, Waterloo, Canada, bingalls@uwaterloo.ca*
[2] *University College London, London, UK*

Calibration of mathematical models in systems and synthetic biology is typically carried out as an inverse problem: observations of system behaviour are compared against model simulations in an attempt to infer the values of model parameters. Accurate parameterization is required to ensure confidence in model predictions for use in investigation of existing phenomena and in model-based design of constructed or modified systems.

The collection of experimental data to support model calibration (e.g. precise measurements of dynamic behaviour) often consumes considerable resources. Consequently, it is worthwhile to pay careful attention to the design of these experiments. The theory of optimal experimental design (OED) provides theoretical tools for identifying experiments and data collection procedures that will most efficiently contribute to a given model calibration objective.

When working with linear, static, systems there is a well-established literature on optimal experimental design, dating back to the work of Fisher in the 1920s [1]. However, when working with nonlinear, dynamic models, the theory is much less robust, with specific tools having been developed for particular model types and application domains. Here we present our recent work on the development of OED tools for use in the area of systems and synthetic biology – for calibration of dynamic models of biomolecular networks.

In particular, we introduce the opportunities for model-based OED in molecular biology [2] and present a case study on investigating the effect of growth rate on physiological parameters in bacteria [3]. We then present a novel reinforcement-learning based approach to OED, illustrated by application to the task of characterizing growth characteristics of a culture in chemostat conditions [4], and close by introducing a novel software tool (NLoed) for easy access to efficient OED techniques [5]. The package's capabilities are illustrated by application to an optically controlled gene regulatory network in an engineered *E. coli* strain.

References

[1] Yates, Frank. "Sir Ronald Fisher and the design of experiments." Biometrics 20.2 (1964): 307-321.

[2] Braniff, Nathan, and Brian Ingalls. "New opportunities for optimal design of dynamic experiments in systems and synthetic biology." Current Opinion in Systems Biology 9 (2018): 42-48.

[3] Braniff, Nathan, Matthew Scott, and Brian Ingalls. "Component characterization in a growth-dependent physiological context: optimal experimental design." Processes 7.1 (2019): 52.

[4] Treloar, Neythen J., et al. "Deep reinforcement learning for optimal experimental design in biology." PLOS Computational Biology 18.11 (2022): e1010695.

[5] Braniff, Nathan, et al. "NLoed: A Python package for nonlinear optimal experimental design in systems biology." ACS Synthetic Biology 11.12 (2022): 3921-3928.

Slave River Delta Ice Cover and Water Classification Using Machine Learning Techniques

I. Moalemi[1], HK. Pour[2], KA. Scott[3]

[1] *Remote Sensing of Environmental Change (ReSEC) Research Group, Wilfrid Laurier University, Waterloo, Canada, imoalemi@wlu.ca*
[2] *Remote Sensing of Environmental Change (ReSEC) Research Group, Wilfrid Laurier University, Waterloo, Canada, hpour@wlu.ca*
[3] *University of Waterloo, Waterloo, Canada, ka3scott@uwaterloo.ca*

The Great Slave Lake (GSL) experiences seasonal variation in long-term temperature trends and ice phenology, which are influenced by changes in Slave River inflow due to the factors such as climate change, upstream water management, and water extraction (see Refs. [1, 2]). The Slave River flows through Lake Athabasca and the Slave River Delta (SRD) before reaching GSL, bringing a rise in temperature that triggers the ice break-up process in the lake (see Refs. [3, 1]). Therefore, monitoring the SRD break-up processes and trend can serve as indicator of the overall break-up trend in GSL.

This research aims to develop a tool for mapping the SRD ice break-up processes, using machine learning (ML) techniques. Among ML methods, Random Forest (RF) has shown strong potential in lake ice mapping (see Refs. [4]). To achieve this goal, a combination of satellite images with optical sensors at high spatial resolution, including Landsat-5, Landsat-8, Sentinel-2a, and Sentinel-2b, are used. The RF model was trained using manually selected training pixels to classify ice, open water, and cloud within the SRD. In addition to Landsat and Sentinel-2 bands, two indexes, including the Water and Ice Classification Index (WICI) and a texture-based variable, the local average gradient of the red band, have been added to improve the model's performance (see Refs. [5]). Testing with independent scenes shows accuracies of 90% and 97% for the Sentinel2 and Landsat models, respectively.

Break-up dates are identified based on the proportion of the ice versus water pixels in images with less than 20% cloud coverage. The break-up start period is defined by minimum and maximum thresholds of 60% and 90% on ice fraction, which is a trade-off between maximizing the available images and not including images captured after the break-up period. The results show a statistically significant trend from 1984 to 2020 with a magnitude of 0.7 using the Mann-Kendall test and Sen's Slope estimator. These findings can inform policymakers and resource managers in making decisions that support the needs of northern communities in Canada.

References

[1] P. Menard, C. R. Duguay, G. M. Flato, and W. R. Rouse, *Simulation of ice phenology on Great Slave Lake, Northwest Territories, Canada*, in *Hydrological Processes* **16**, 18, pp. 3691-3706 (2002).

[2] T. D. Prowse, F. M. Conly, M. Church, and M.C. English, *A Review of Hydroecological Results of the Northern River Basins Study, Canada. Part 1. Peace AND Slave Rivers*, in *River Research and Applications* **18**, 5, pp. 429-446 (2002).

[3] L. Bengtsson, *Spatial variability of lake ice covers*, in Geografiska Annaler: Series A, Physical Geography **68**, 1-2, pp. 113-121 (1986).

[4] Y. Wu, C. R. Duguay, and L. Xu, *Assessment of machine learning classifiers for global lake ice cover mapping from MODIS TOA reflectance data*, in *Remote Sensing of Environment* **253**, pp. 112206 (2021).

[5] K. Barbieux, A. Charitsi, and B. Merminod, *Icy lakes extraction and water-ice classification using Landsat 8 OLI multispectral data*, in *International journal of remote sensing* **39**, 11, pp. 3646-3678 (2018).

The VI International AMMCS
Interdisciplinary Conference
Waterloo, Ontario, Canada

Fractional-order sliding-mode-based adaptive robust predictive control of saturated input network connected systems with singular control gain

L. Khoshnevisan[1], X. Liu[2]

[1] *Department of Applied Mathematics, University of Waterloo, Waterloo, ON, Canada, lkhoshnevisan@uwaterloo.ca*

[2] *Department of Applied Mathematics, University of Waterloo, Waterloo, ON, Canada, xzliu@uwaterloo.ca*

Abstract: Nonlinear networked connected systems, like multi-agent systems, intelligent transportation systems, and communication systems, mostly suffer from time delay, due to the transferred data either in system states or in input signals, which may cause ineffective control and instability. On the other hand, based on the system specifications, the control gain may consist of the delayed state, which results in singularity in control procedures. Moreover, practical systems are inevitably exposed to external disturbances. On the other hand, in real applications there are hardware constraints, such as throttling saturations in intelligent transportation systems, or software limitations, such as packet drop probability in networks, which leads the control procedures to be designed specifically to satisfy the system restrictions.

To this end, a general format of nonlinear system description is assumed as below:

$$\begin{aligned} &\dot{X}_1(t) = N_1 - g(X_1(t), X_1(t-\tau), t)u(t-\tau) + d_1(t)\,, \\ &\dot{X}_2(t) = AX_1(t) + N_2 + d_2(t)\,, \\ &X_1(t) = \varphi_1(t), \forall t \in [-\tau, 0]\,, \\ &X_2(t) = \varphi_2(t), \forall t \in [-\tau, 0], \end{aligned} \tag{1}$$

where $X_1(t) \in \mathbb{R}^{n\times 1}$ and $X_2(t) \in \mathbb{R}^{m\times 1}$ are system states, $g(X_1(t), X_1(t-\tau), t) \in \mathbb{R}^{n\times l}$ represents a nonlinear matrix function, $u \in \mathbb{R}^{l\times 1}$ is the input signal vector in which l is the number of input signals, τ is a known constant time delay, $N_1 \in \mathbb{R}^{n\times 1}$ and $N_2 \in \mathbb{R}^{m\times 1}$ are constant vectors, $A \in \mathbb{R}^{m\times n}$ is a constant matrix, $d_1(t)$ and $d_2(t)$ are disturbances with the appropriate dimensions, $\varphi_1(t) \in C([-\tau, 0], R^n)$ and $\varphi_2(t) \in C([-\tau, 0], R^m)$ are vector-valued initial-condition functions.

Therefore, it is imperative to propose a robust procedure to tackle the impacts of external disturbances and input delay as well as to be implementable in constrained systems with singular control gain. To this end, an adaptive robust procedure is proposed based on fractional order predictive sliding mode method through which,

1) The stability of the nonlinear system with both input- and state-delay is ensured via Lyapunov theorem.
2) The control objectives are achieved despite there exists singularity in the control gain.
3) Input delay is compensated.
4) The input signal saturation is achieved by a systematically designed procedure, but not by limiting the control parameters.
5) The procedure is robust against external disturbances.

The prevalent procedures generally ignore input delay and rely on parameter design to address system limitations, which leads to a highly restricted feasibility of the method. Furthermore, singular control gains are usually ignored by simplifying approximations, which results in inappropriate control methods. However, this study takes a different approach. It first develops a predictor to mitigate the effects of input delay and then proposes a compensated system to address input signal limitations and singular control gain. Furthermore, the designed method incorporates a fractional-order sliding mode approach to ensure robustness, with adaptive laws designed to alleviate chattering phenomenon, as an unavoidable aspect of sliding mode procedures. Finally, simulation results of an application are presented to illustrate the effectiveness of the theoretical advancements.

Keywords: Adaptive fractional-order control, Input delay compensation, Nonlinear delayed systems, Saturated input, Singular control gain, Sliding mode procedure.

The VI International AMMCS
Interdisciplinary Conference
Waterloo, Ontario, Canada

Limiting absorption principle and virtual levels of operators in Banach spaces

N. Boussaïd[1], A. Comech[2]

[1] *Université Franche-Comte, Besançon, France, nabile.boussaid@univ-fcomte.fr*
[2] *Texas A&M University, College Station, USA, comech@tamu.edu*

Virtual levels, also known as threshold resonances, admit several heuristic characterizations:

(1) there are corresponding "virtual states" from L^2 or a space "slightly weaker" than L^2;

(2) there is no limiting absorption principle (LAP) in their vicinity (e.g., no weights such that the "sandwiched" resolvent is uniformly bounded);

(3) an arbitrarily small perturbation can produce an eigenvalue bifurcating from z_0.

We generalize the classical approach by Jensen–Kato [1] and Jensen–Nenciu [2] to the case of general Banach spaces and provide applications to Schrödinger operators with nonselfadjoint potentials and in any dimension. We describe a construction which allows us to derive optimal LAP estimates on the resolvent near a point of the spectrum which is not a virtual level. In particular, the construction applies to the Laplacian in dimension 2 (where the estimates were not known even in the selfadjoint case).

In our framework [3, 4], $A \in \mathscr{C}(\mathbf{X})$ is a closed operator in the Banach space $\mathbf{X}$. We pick Banach spaces $\mathbf{E}$ and $\mathbf{F}$ with continuous embeddings $\mathbf{E} \overset{\varepsilon}{\hookrightarrow} \mathbf{X} \overset{\varphi}{\hookrightarrow} \mathbf{F}$ (not necessarily dense). We assume that A is closable in $\mathbf{F}$.

Definition. Let $\Omega \subset \rho(A)$ be a subset of the resolvent set of $A \in \mathscr{C}(\mathbf{X})$. We say that a point $z_0 \in \sigma_{\text{ess}}(A) \cap \partial\Omega$ is a *point of the essential spectrum of rank* $r \in \mathbb{N}_0$ *relative to* $(\Omega, \mathbf{E}, \mathbf{F})$ if it is the smallest nonnegative integer for which there is an operator $b \in \mathscr{B}_{00}(\mathbf{F}, \mathbf{E})$ of rank r such that $\Omega \cap \mathbb{D}_\delta(z_0) \subset \rho(A+B)$, where $B = \varepsilon \circ b \circ \varphi \in \mathscr{B}_{00}(\mathbf{X})$ and $\delta > 0$, and such that there exists the following limit in the weak operator topology of $\mathscr{B}(\mathbf{E}, \mathbf{F})$:

$$(A+B-z_0 I_{\mathbf{X}})^{-1}_{\Omega,\mathbf{E},\mathbf{F}} := \operatorname*{w\text{-}lim}_{z \to z_0,\, z \in \Omega \cap \mathbb{D}_\delta(z_0)} \varphi \circ (A+B-zI_{\mathbf{X}})^{-1} \circ \varepsilon : \mathbf{E} \to \mathbf{F}. \tag{1}$$

If $r = 0$, so that in (1) one can take $B = 0$, we say that the resolvent of A *satisfies LAP at* z_0 *relative to* $(\Omega, \mathbf{E}, \mathbf{F})$. If $r \geq 1$, then we say that z_0 is a *virtual level of rank* r relative to $(\Omega, \mathbf{E}, \mathbf{F})$.

If $\Psi \in \operatorname{Range}\big((A+B-z_0 I_{\mathbf{X}})^{-1}_{\Omega,\mathbf{E},\mathbf{F}}\big)$ (where $B = \varepsilon \circ b \circ \varphi$, $b \in \mathscr{B}_{00}(\mathbf{F}, \mathbf{E})$ is such that the limit (1) exists), $\Psi \neq 0$, and $(A - z_0 I_{\mathbf{F}})\Psi = 0$, then Ψ is called a *virtual state* of A relative to $(\Omega, \mathbf{E}, \mathbf{F})$ corresponding to z_0.

In the application to Schrödinger operators, we prove, in particular, that for $V : L^2(\mathbb{R}^2, \mathbb{C}) \to L^2(\mathbb{R}^2, \mathbb{C})$ which is Δ-compact, there is the following dichotomy:

- Either there is nonzero $\Psi \in L^\infty(\mathbb{R}^2, \mathbb{C})$ such that $(-\Delta + V)\Psi = 0$ ("$z_0 = 0$ is a virtual level");
- Or for any $s > 1$ the mappings $(-\Delta + V - zI)^{-1} : L^1(\mathbb{R}^2, \mathbb{C}) \to L^2_{-s}(\mathbb{R}^2, \mathbb{C})$ and $L^2_s(\mathbb{R}^2, \mathbb{C}) \to L^\infty(\mathbb{R}^2, \mathbb{C})$ are bounded uniformly for $|z| < \delta$, $z \notin [0, +\infty)$, with some $\delta > 0$ ("resolvent satisfies LAP at $z_0 = 0$").

References

[1] A. Jensen and T. Kato, *Spectral properties of Schrödinger operators and time-decay of the wave functions*, Duke Math. J. **46** (1979), pp. 583–611.

[2] A. Jensen and G. Nenciu, *A unified approach to resolvent expansions at thresholds*, Rev. Math. Phys. **13** (2001), pp. 717–754.

[3] Nabile Boussaïd, Andrew Comech, *Virtual levels and virtual states of linear operators in Banach spaces. Applications to Schrödinger operators*, arXiv:2101.11979 (2021). http://arxiv.org/abs/2101.11979

[4] Nabile Boussaïd, Andrew Comech, *Limiting absorption principle and virtual levels of operators in Banach spaces*, Ann. Math. Quebec **46** (2022), pp. 161–180. http://arxiv.org/abs/2109.07108

The Mutation Spectrum May Promote Cancer Development in Most Cancer Types

M. Z. Tuffaha[1], D. Castellano[2], R. N. Gutenkunst[2], L. Wahl[1]

[1] *Western University, London, Ontario, Canada, mtuffaha@uwo.ca, lwahl@uwo.ca*
[2] *University of Arizona, Tucson, Arizona, USA, dcastellano@arizona.edu, rgutenk@arizona.edu*

Mutational processes in human cancer differ across cancer types. Understanding these processes can yield insight into the development of malignancy, and thus there is increasing interest in genome sequencing of cancer cells and detailed analyses of cancer mutations. It is well-known in asexual populations that increased mutation rates can be advantageous by giving more access to beneficial mutations. We have recently demonstrated that having the "right" mutation spectrum can also improve access to beneficial mutations, while having the “wrong” mutation spectrum counters this effect. Since cancer cells reproduce asexually, we test this idea in cancer by finding the Cancer Driver Mutation Spectrum (CDMS), and comparing it to mutation spectra in different cancer types. We find that spectra in hyper-mutator cancer types (skin and colon) are moderately positively correlated with the CDMS, while spectra of most other non-hyper-mutator cancer types are almost perfectly correlated with it. This indicates that non-hyper-mutator cancers may be favoured to develop due to their spectrum, while the elevated mutation rates alone for skin and colon cancers give a sufficient influx of cancer-driving mutations.

The VI International AMMCS
Interdisciplinary Conference
Waterloo, Ontario, Canada

Proportional Consistency in Apportionment Methods

M.A. Jones[1], D. McCune[2], J. Wilson[3]

[1] *American Mathematical Society, Providence, RI, maj@ams.org*
[2] *William Jewell College, Liberty, MO, mccuned@william.jewell.edu*
[3] *The New School, New York City, NY, wilsonj@newschool.edu*

This talk explores a little-studied property of apportionment methods that captures how allocations scale as the house size scales: specifically, if for a fixed population distribution, a house size and allocation can be scaled down within the set of integers, then the apportionment should be correspondingly scaled down. We analyze this property, which Balinski and Young [1] identify, along with weak proportionality, as among the fundamental requirements for "reasonable" apportionment methods. We argue that this property is better understood as a consistency requirement since quota-based apportionments that are less proportional meet this requirement while others that are more proportional do not. We also show that the family of quotatone methods based on stationary divisors (including the Quota Method [1]), do not meet this requirement.

References

[1] M.L. Balinski and P. Young, *Fair Representation: Meeting the Ideal of One Man, One Vote*, Brookings Institute, Washington D.C. (2001).

Magnesium transport in the kidneys: effect of sodium transport inhibition

P. Dutta[1], A. T. Layton[1,2,3,4]

[1] *Department of Applied Mathematics, University of Waterloo, Waterloo, Ontario, Canada*
[2] *Cheriton School of Computer Science, University of Waterloo, Waterloo, Ontario, Canada*
[3] *Department of Biology, University of Waterloo, Waterloo, Ontario, Canada*
[4] *School of Pharmacy, University of Waterloo, Waterloo, Ontario, Canada*

Magnesium (Mg^{2+}) plays an important role in several physiological functions and its deficiency has been associated with neurological and heart disorders, hypertension, and type 2 diabetes. The kidneys play a central role in maintaining serum Mg^{2+} within a narrow range (0.70–1.10 mmol/L). To understand the mechanisms involved in Mg^{2+} reabsorption in the kidney, we integrated Mg^{2+} transport to our previously developed epithelial cell-based computational model of solute transport along male and female rat nephron [1] (Fig. 1). Mg^{2+} transport along the nephron is strongly coupled to active sodium (Na^+) transport. Different antihypertensive diuretics inhibit Na^+ transporters that facilitate Mg^{2+} reabsorption along the thick ascending limb (TAL) and distal convoluted tubule (DCT). In this study, we investigated the effect of acute inhibition of three such Na^+ transporters on Mg^{2+} excretion: (1) Na-K-2Cl cotransporter (NKCC2) (bounded by the green box in Fig. 1(A)) which is inhibited by loop diuretics, (2) Na-Cl cotransporter (NCC) (bounded by the blue box in Fig. 1(A)) which is inhibited by thiazide diuretics, and (3) epithelial Na channel (ENaC) (bounded by the pink box in Fig. 1(A)) which is inhibited by K-sparing diuretics. Our model simulations show that acute inhibition of NKCC2 and NCC cause significant increase in Mg^{2+} excretion, whereas ENaC inhibition decreases Mg^{2+} excretion compared to the baseline values (Fig. 1(B)). Also, female rats have higher increase in Mg^{2+} excretion with NKCC2 inhibition compared to male rats (~10% higher), whereas for the other cases, the increase is similar.

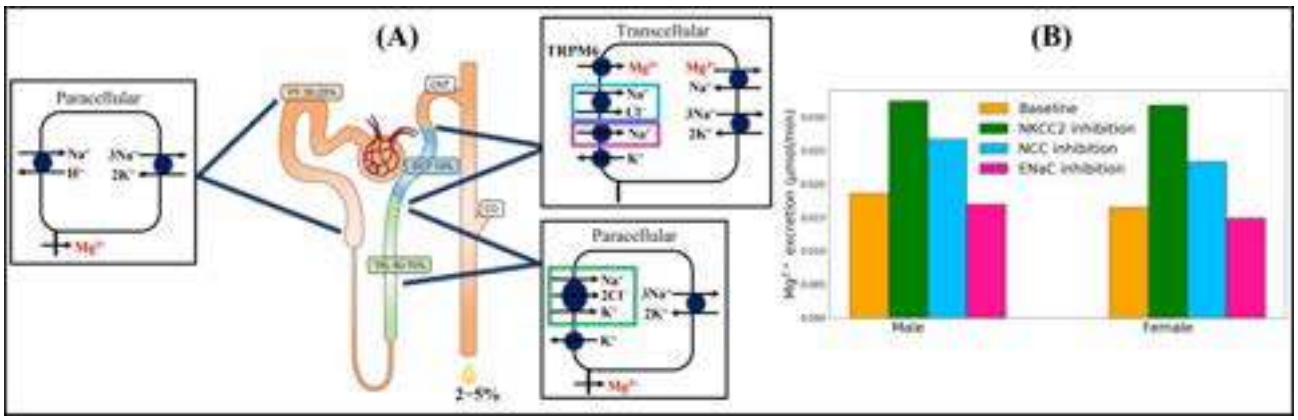

Figure 1: (A) Schematic diagram of Mg^{2+} transport along a nephron and (B) Mg^{2+} excretion in the baseline case and on NKCC2, NCC, and ENaC inhibition in male and female rats. Nephron image adopted from [2].

References

[1] R. Hu, A.A. McDonough, and A.T. Layton, *Sex differences in solute transport along the nephrons: effects of Na+ transport* inhibition, Am. J. Physiol. Renal Physiol. **319**, 3, pp. F487-F505 (2020).
[2] J.H. De Baaij, J.G. Hoenderop, and R.J. Bindels, *Magnesium in man: implications for health and disease*. Physiol. Rev. **95**, 1, pp. 1-46 (2015).

Observer and Command Filter-Based Prescribed Performance Control for a Class of Nonlinear System with Mismatched Disturbances

Min Wang[1], Xinzhi Liu[2], Jinsheng Sun[3]

[1] *Nanjing University of Science and Technology, Jiangsu, China, wangm0811@njust.edu.cn*
[2] *University of Waterloo, Waterloo, Canada, xzliu@uwaterloo.ca*
[3] *Nanjing University of Science and Technology, Jiangsu, China, jssun67@163.com*

In this paper, a command filter-based prescribed performance controller is designed for a class of nonlinear systems subject to mismatched disturbances.

A general strict-feedback nonlinear system can be represented by a family of equations of the form

$$\begin{cases} \dot{x}_i(t) = x_{i+1}(t) + f_i(\bar{x}_i) + d_i(t),\ i = 1,2,\ldots,n-1, \\ \dot{x}_n(t) = u(t) + f_n(\bar{x}_n) + d_n(t), \\ y(t) = x_1(t), \end{cases} \tag{1}$$

where $x(t) = [x_1(t),\ldots,x_n(t)]^{\mathrm{T}} \in \mathbb{R}^n$ denotes system state, $u(t)$ denotes control input and $y(t)$ denotes system output, f_i, $i = 1,\cdots,n$ are continuous nonlinear functions, $d_i(t)$, $i = 1,\cdots,n$ are mismatched external disturbances.

In the design of intermediate control signal, disturbance estimations are introduced to compensate the effects caused by external disturbances.

The disturbance $d_i(t)$ can be expressed by the following exogenous system

$$\begin{aligned} \dot{\omega}_i(t) &= B_i\omega_i(t) \\ d_i(t) &= E_i\omega_i(t) \end{aligned} \tag{2}$$

where $\omega_i \in \mathbb{R}^m$ is the state vector of exogenous system, $B_i \in \mathbb{R}^{m\times m}$ and $E_i \in \mathbb{R}^{1\times m}$ are the known matrices.

The so-called "explosion of complexity" problem in traditional backstepping procedure is solved by command filter technique. To enhance the control performance further, a prescribed performance function (PPF) characterizing transient and steady-state performance is used for the tracking error transformation. The proposed controller can ensure that the output tracking error converges to a predefined arbitrarily small residual set, and all the signals of the closed-loop system can be bounded. Theoretical results are validated and illustrated via simulation example.

On mean field games and master equations through the lens of conservation laws

P. Jameson Graber[1], A. Mészáros[2]

[1] *Baylor University, Waco, Texas Jameson_Graber@baylor.edu*

[2] *Durham University, Durham, United Kingdom alpar.r.meszaros@durham.ac.uk*

It is now well-understood that the Master Equation in mean field game theory is a non-standard nonlinear transport equation on the space of probability measures, whose “characteristics" are a forward/backward system of Hamilton-Jacobi/Fokker-Planck equations. It turns out that, when the coupling occurs only in the terminal cost for the game, one can write instead solve the mean field game through a transport equation that has a more standard structure.

We can study classical solutions to such equations by taking “monotone" data, in the sense derived from the classical study of balance laws. It turns out this condition corresponds neither to Lasry-Lions nor to displacement monotonicity.

In addition, in the case where this balance law becomes conservative, it turns out a dimension reduction occurs that allows us to view it as a classical (finite-dimensional) conservation law. Then we can study entropy solutions, and in particular we can see whether and in what sense these solutions correspond to Nash equilibria. In some cases it they can be shown to select among multiple equilibria in a natural way. In other cases, due to well-understood phenomena in the theory of conservation laws, entropy solutions do not always give us equilibria, even when such equilibria exist!

Figure 1: The AMMCS Conference is organized in cooperation with SIAM and AIMS.

References

[1] P. Graber and A. Mészáros, *On mean field games and master equations through the lens of conservation laws*, https://arxiv.org/abs/2208.10360

The VI International AMMCS
Interdisciplinary Conference
Waterloo, Ontario, Canada

The Combination Method for Multidimensional Black-Scholes Partial Differential Equations

R. Wu[1], C. Christara[2]

[1] *University of Toronto, Toronto, Ontario, Canada, rwu@cs.toronto.edu*
[2] *University of Toronto, Toronto, Ontario, Canada, ccc@cs.toronto.edu*

A fundamental challenge in the numerical solution of multidimensional partial differential equations (PDEs) is the exponential increase of the number of unknowns as the number of dimensions increases; on an isotropic grid with d dimensions and n unknowns in each dimension, the number of unknowns is $\mathcal{O}(n^d)$. This exponential increase is known as the curse of dimensionality, which creates difficulties in obtaining accurate solutions for even moderate-dimension problems. In the context of computational finance, multidimensional PDEs arise from the pricing of multiasset options or options with multiple risk factors considered, as each option/risk factor leads to a spatial variable. We use a sparse grid combination method to alleviate the curse of dimensionality and present computationally efficient results for multidimensional pricing problems for European and American options in the Black-Scholes model.

Vreman Stabilization for Nonlinear Greenshield's Model

M. Neda[1], J. Reyes[2]

[1] *University of Nevada Las Vegas, Las Vegas, USA Monika.Neda@unlv.edu*
[2] *Virginia Tech, Blacksburg, USA*

This report investigates a stabilization method for the first order hyperbolic differential equations of traffic flow. The Lighthill-Whitham-Richards (LWR) model utilizes the continuity equation to model the behavior of traffic [1]. We use the LWR model in conjunction with the Greenshield's model, resulting in (1),

$$\frac{\partial \rho}{\partial t} + \left(v_f - \frac{2v_f}{\rho_m}\rho \right) \frac{\partial \rho}{\partial x} = 0, \tag{1}$$

Where $\rho(x,t)$ represents the density, v_f is the free flow speed, and ρ_m is the maximum jam density. It is known that the usual unstabilizaed finite element method contains spurious oscillations for non-smooth solutions. To stabilize the finite element method the authors consider adding a Vreman filter based stabilization term in space used in [2]. Numerical analysis of the stabilized finite element algorithms and computations describing a traffic settings are studied herein.

References

[1] P. Kachroo, *Pedestrian Dynamics: Mathematical Theory and Evacuation Control*, Boca Raton: CRC Press, (2009).

[2] A. Dunca and M. Neda, *On the Vreman filter based stabilization for the advection equation*, Applied Mathematics and Computation **269**, pp. 379-388, (2015).

MODELING DELAY PROPAGATION WITHIN A NETWORK OF THE OUTBOUND FLIGHTS AT A HUB AIRPORT

A. Seifi[1], K. Ponnambalam[2], L. Autlman-Hall[3]

[1] *Amirkabir University of Technology, Tehran, Iran, aseifi@aut.ac.ir*
[2] *Dept. of Systems Design Engineering, University of Waterloo, Waterloo, Canada, ponnu@uwaterloo.ca*
[3] *Dept. of Systems Design Engineering, University of Waterloo, Waterloo, Canada, laultman@uwaterloo.ca*

The unprecedented growth of demand in aviation industry has caused over-capacity flight scheduling by most commercial airlines leading to congestion and scarcity of resources in many airports. A major drawback of such developments is increasing flight delays, especially when a major disruption occurs. The execution of the airline operation is often deviated from the original schedule due to some unexpected disruptions, such as aircraft breakdowns and severe weather conditions. Any delay related to resources of upstream flights will further impact its connected downstream flights. In this situation, a recovery plan is needed to get the irregular operation back to normal. During the last decade, considerable attention has been given to producing proactive schedule recovery plans to limit the impact of flight delays in the network.

Because of the interdependencies of different resources such as aircrafts, crews, and passengers, the delay of an earlier flight can propagate across multiple downstream flights. Analysis of delay propagation is a complex task and is not fully understood, especially if the scarcity of airport resources is also considered. Recently, researchers have paid more attention on how both airline and airport-related capacity limitations influence delay propagation across a network. This research is motivated by exploring the interdependencies between flight scheduling and airport operations to make better resource allocation. In this on-going research, we are trying to develop a simple approach to quantifying delay propagation caused by prioritizing and rescheduling the flights in a hub airport. A congested airport may propagate delays to its connecting airports through the delayed flights. However, we do not consider delays caused by congestions at other airports downstream in the network and only trace the propagated delays caused by flight schedule displacements. Studies like [1] focused on predicting delay as a result of recovery decisions made by an airline. However, we intend to evaluate the downline impact of an airport operational decisions to reschedule the flights based on priority setting and its constrained resources. The study in [2] assumes that the reference airline has some influence on flight prioritization when deciding on flights' departure times at a hub airport. The study in [3] investigated the relationship between planned schedules and delay propagation on sequential flights. They created a propagation tree representing the set of all downstream flights that could potentially be delayed as a result of the root delay. However, impacts through cabin crew and passengers as well as recovery options are excluded in their study. Propagation tree is a useful tool for tracking the delay originated from a single flight through the network. The TREE modelling approach in [4] considers both limited airport capacity and flight connections as mechanisms for delay propagation.

References

[1] Abdelghany, K., Shah, S., Raina, S., Abdelghany, A. A model for projecting flight delays during irregular operation conditions. Journal of Air Transport Management 10, (2004), 385–394.
[2] B.F. Santos, M.E.C. Wormer, T. A.O. Achola, R. Curran, "Airline delay management problem with airport capacity constraints and priority decisions", Journal of Air Transport Management 63 (2017) 34-44.
[3] AhmadBeygi, S., Cohn, A., Guan, Y. and Belobaba, P., "Analysis of the potential for delay propagation in passenger airline networks. Journal of Air Transport Management", Vol. 14, (2008), 221-236.
[4] B. Campanelli, P. Fleurquin, A. Arranz , I. Etxebarria, C. Ciruelos, V. M. Eguíluz, J. Ramasco, "Comparing the modeling of delay propagation in the US and European air traffic networks", Journal of Air Transport Management 56 (2016) 12-18.

New insights into estimating the time since deposition of bloodstained evidence

Theresa Stotesbury[1]

[1] *Ontario Tech University, Oshawa, Canada, Theresa.stotesbury@ontariotechu.ca*

The identification and quantification of (bio)molecules and their metabolism, formation, degradation and persistence are important features of forensic evidence; and are particularly useful in time series estimation approaches to date evidence. For example, estimating the time since deposition (TSD) of a bloodstain can provide important medicolegal information for crime scene investigation (e.g., answering the question, "When did the bloodshed occur?"). Most TSD research to-date focuses on investigating either hemoglobin or genetic material degradation over time, and a clear analytical strategy for forensic casework is not yet established. We propose a holistic approach to developing TSD models, as forensic scenarios inherently lend themselves to variability in factors surrounding the crime (e.g., environment, target substrate, initial blood properties). Support for this idea comes from our meta-analysis [1], where we determined that from 25 research studies that contained usable summary statistics there was an overall strong effect size across studies (Fisher's Zr = 1.5, r =0.91), and generally we found that the type of biomolecule (e.g., hemoglobin, DNA) analyzed has equal effect sizes for TSD estimation. We did find that significant differences exist between the analytical technique used, porosity of the substrate and environment. In this talk I will describe new and collaborative approaches housed in analytical chemistry and other analytical sciences that we are taking to develop more robust TSD methods useful for crime scene investigation. Pending time, beyond the meta-analysis, I will present novel approaches in mass spectrometry, XPS and/or fluorimetry for TSD estimation. The goal of future work is to develop robust and likely combined approaches that can one day be used in crime scene investigation.

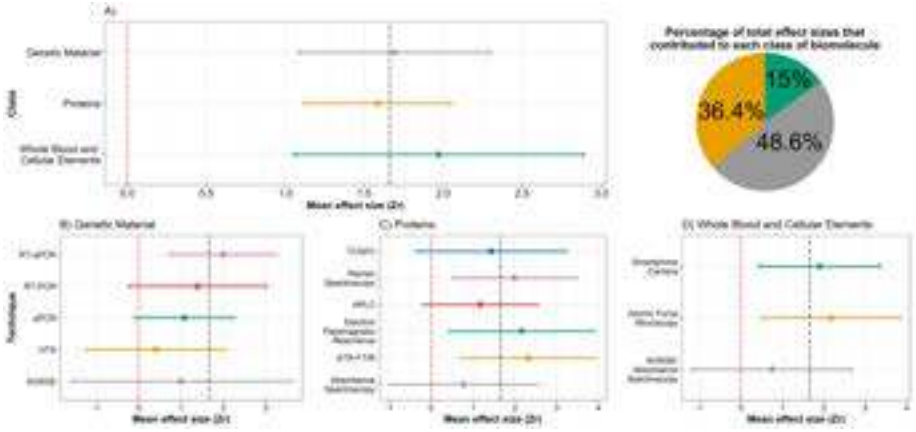

Figure 1: Forest plots of bloodstain TSD effect sizes for class of defined biomolecules and the analytical techniques used to analyze them. The pie chart divides the 25 studies retained for the meta-analysis according to number of summary statistics that contributed to each class of biomolecule. Diamonds indicate the mean effect size of that biomolecule or technique, horizontal lines represent the 95% confidence interval, red dashed line represent an effect size of 0, and grey dashed line and the overall mean effect size [1].

References

[1] C. Elliott, A. Shafer, and T. Stotesbury, *The crux of time: A meta-analysis of ex-vivo whole blood degradation*, Front. Anal. Sci. **2**, pp. 1-13 (2022).

[2] K. Yeh, S. Castel, N. Stock, T. Stotesbury and W. Burr, *subMALDI: an open framework R package for processing irregularly-spaced mass spectrometry data*, J. Open Source Softw. **6**, 65, pp. 2694.

A new approach to Scattering: On the Asymptotic states of Nonlinear Dispersive and Hyperbolic equations with General Data

Avy Soffer[1],

[1] *Rutgers University, 191 Ryders Ln, New Brunswick, NJ 08901, USA, soffer@math.rutgers.edu*

I will present a new approach to finding the asymptotic states of Nonlinear Wave Equations with general initial data. In particular we find for a large class of equations that all asymptotic states are linear combinations of free wave, localized part(solitons, breathers..) and a possibility of self-similar solutions as well in some cases. These results hold for initial data for which the H1Sobolev norm (the energy norm) is uniformly bounded in time. This answers the question of Asymptotic Completeness to a large class of equations, including for the first time, equations with time dependent potentials. These are joint works with Baoping Liu (Peking Univ) and Xiaoxu Wu(Rutgers).

Computational modelling of heat transport in kinked nanowires

Alexander N. Robillard[1], Graham W. Gibson[1], Ralf Meyer[2]

[1]*Laurentian University, Sudbury, Ontario {an_robillard,gw_gibson}@laurentian.ca*
[2]*Laurentian University, Sudbury, Ontario rmeyer@cs.laurentian.ca*

Thermal transport in nanosystems is difficult to understand: simple diffusive models do not capture the nuances of vibrations in systems that are on a fundamentally small scale. Scattering mechanisms must be considered when the transit lengths of vibrational quanta, phonons, are large compared to characteristic system sizes. In this work, we seek to compare classical solutions of the heat equation with the result of an up-and-coming method for phononic thermal transport: the Lattice Boltzmann Method [1]. This generalized method uses a discretized lattice to model the Boltzmann Transport Equation and takes into account flow and scattering of arbitrary carriers. In the case of thermal transport, phonons are used as carriers to model heat. We apply these two calculation methods to models of nanosystems in order to examine both surface and size effects.

Serpentine nanowires (nanowires with 90-degree bends) are an interesting field of study, due to their significant thermal transport suppression and unique phenomena such as phonon-blocking and corner cutting [2, 3]. This work examines kinked nanowires, where a bend is applied at the center of the wire, obstructing phonon transit. We compare the results of classical solutions of the heat equation and the Lattice Boltzmann method, and use these to study the difference between heat transfer in classical systems and nanosystems.

References

[1] Nabovati, A. et al.: *On the lattice Boltzmann method for phonon transport.* Journal of Computational Physics. 230, 15, 5864â5876 (2011). https://doi.org/10.1016/j.jcp.2011.03.061.

[2] Park, W. et al.: *Phonon Conduction in Silicon Nanobeam Labyrinths*. Sci Rep. 7, 1, 6233 (2017). https://doi.org/10.1038/s41598-017-06479-3.

[3] Anufriev, R. et al.: *Probing ballistic thermal conduction in segmented silicon nanowires.* Nanoscale. 11, 28, 13407â13414 (2019). https://doi.org/10.1039/C9NR03863A.

The VI International AMMCS
Interdisciplinary Conference
Waterloo, Ontario, Canada

Stability-Type Properties for Cascade Impulsive Systems with Input Disturbance

M. S. Alwan

University of Saskatchewan, Saskatoon, Canada, m.alwan@math.usask.ca

This work is concerned with a class of nonlinear interconnected systems undergoing input disturbance and impulsive effects. The disturbance is time-varying with bounded amplitude and impulses are viewed as jump disturbances to the system.

Some sufficient conditions are given for *input to state stability* (ISS), a stability notion that deals with the impact of the input disturbance to the exponential (or asymptotic) stability of the equilibrium solution of the unforced system. To achieve ISS, the system is decomposed into two cascaded impulsive subsystems, namely the derived subsystem with the input disturbance and driven subsystem with input being the state of the derived subsystem. Then, the ISS for each impulsive subsystem is developed. We observed that the cascade of two ISS impulsive subsystems is ISS and, as a special case, the cascade of exponentially stable unforced impulsive subsystem and ISS impulsive driven subsystems is exponentially stable.

The above ISS result is carried further to establish the *integral-output to state stability* (iOSS) for the cascade of an *integral-input to integral-output stable* impulsive subsystem that is stabilized by an H_∞ controller and an ISS impulsive subsystem. iOSS is a characterization of ISS where the available output of the derived subsystem is cascaded to the driven system.

The Lyapunov method is used to achieve ISS and iOSS where each subsystem admits an ISS-Lyapunov function. Then, the full system is ISS or iOSS with a Lyapunov function being the composite of the aforementioned ISS functions.

Numerical examples and simulations are presented to clarify the findings of this work.

The VI International AMMCS
Interdisciplinary Conference
Waterloo, Ontario, Canada

A modified error in constitutive equations formulation for elastodynamics inverse problems in the elastography field

O. Babaniyi[1], W. Aquino[2]

[1] *Rochester Institute of Technology, Rochester, USA, obsma@rit.edu*[2] *Duke University, Durham, USA, wilkins.aquino@duke.edu*

Shear wave elastography is a technique used to estimate the mechanical properties of tissue from measurements of its deformation [3]. These mechanical properties can be used to noninvasively diagnose and help with the treatment of various diseases like cancer, and liver fibrosis. To compute the mechanical properties, one needs to solve an inverse problem governed by a differential equation model [2]. I present a modified error in constitutive equations (MECE) formulation to solve the elastodynamics inverse problem. This formulation is a variant of the least squares method that has been widely used in the inverse problems field. Some advantages of the MECE formulation include the fact that it is robust in dealing with noisy or missing measurements, and it does not require boundary conditions in the forward model [1]. I explain some of these mathematical properties and show some computational experiments with simulated and measured data.

References

[1] Wilkins Aquino and Marc Bonnet. Analysis of the error in constitutive equation approach for time-harmonic elasticity imaging. *SIAM Journal on Applied Mathematics*, 79(3):822–849, 2019.

[2] Paul E Barbone and Assad A Oberai. A review of the mathematical and computational foundations of biomechanical imaging. In D. Suvranu, G. Farshid, and M. Mohammad, editors, *Computational Modeling in Biomechanics*, pages 375–408. Springer, 2010.

[3] Armen P Sarvazyan, Oleg V Rudenko, Scott D Swanson, J Brian Fowlkes, and Stanislav Y Emelianov. Shear wave elasticity imaging: a new ultrasonic technology of medical diagnostics. *Ultrasound in medicine & biology*, 24(9):1419–1435, 1998.

Calculation of carriers mobility in single-layer supported Phosphorene using the energy loss method

Milad Moshayedi[1]

[1] *Department of Applied Mathematics, University of Waterloo, Waterloo, Ontario, Canada N2L 3G1, mmoshaye@uwaterloo.ca*

In this study the energy loss method (ELM) within the self-consistent transport theory is used to investigate the mobility of carriers in a single-layer of doped Phosphorene that is supported with a substrate. It is assumed that the main limiting process for the mobility of carriers is the Coulomb interaction between them and charged impurities that are randomly distributed in the substrate. These charged impurities are distributed in a two-dimensional (2D) plane inside the supporting material, and a hard-disk model for the charged impurities is used to investigate impurity structures with large packing fractions. To obtain the dc mobility of carriers in Phosphorene using the ELM, the polarization function of doped Phosphorene is obtained from the Lindhard function of a 2D electron gas in the zero-temperature limit, and an appropriate transformation is applied to take the anisotropic effects of Phosphorene into account. It is shown that the dependence of Phosphorene's mobility on its charge carrier density is strongly affected by the Phosphorene-dielectric gap and the precise position of the 2D distribution of charged impurities. The anisotropy in the mobilities in the zigzag and armchair directions is also strongly affected by the structure of the randomly distributed charged impurities and the carrier concentration. The investigation also takes into account the impact of different structures of charged impurities such as 2D and 3D uniform distributions on the mobility of carriers. Finally, the results obtained from the ELM are compared with those obtained from the Boltzmann transport theory, which requires a non-linear integral equation to be solved to find the zero-temperature momentum relaxation times. It is shown that the two sets of results are in excellent agreement.

Spectral Expansions for Credit Risk Modelling with Occupation Times

H. Kato[1], G. Campolieti[2], R.N. Makarov[3]

[1] *Wilfrid Laurier University, Waterloo, Canada, kato4650@mylaurier.ca*
[2] *Wilfrid Laurier University, Waterloo, Canada, gcampolieti@wlu.ca*
[3] *Wilfrid Laurier University, Waterloo, Canada, rmakarov@wlu.ca*

We study new structural credit risk models that provide flexible alternatives to the well-known Black–Cox model. The defaults within our models are characterized in accordance with Chapter 7 (a liquidation process) and Chapter 11 (a reorganization process) of the U.S. Bankruptcy Code. There are three possible regimes: the firm value is above a reorganization barrier (normal state), below a liquidation barrier (default state), in between the two barriers (danger state). Firms have lower default rates in the normal state while having higher default rates in the danger state. Firms are forced to liquidate as soon as they enter the default state. The risk-neutral default probabilities hence involve joint probability distributions of the underlying firm value with imposed killing at the liquidation barrier and its occupation time with respect to the reorganization barrier. Occupation times are powerful tools in credit risk modelling as they correctly measure the cumulative time spent in each regime.

An analytical method is used to find the no-arbitrage value of credit derivatives. The joint probability distributions are expressed as spectral series expansions which allow us to write pricing formulas explicitly as infinite series that converge rapidly. The spectral methodology works for solvable diffusion, such as the geometric Brownian motion (GBM) and the state-dependent volatility diffusion based on the squared Bessel process. We also calibrate our models to market credit default swap (CDS) spreads. Our calibration results show that the computations are done in efficient manner and the fit is near-perfect.

References

[1] G. Campolieti, H. Kato, and R.N. Makarov, *Spectral Expansions for Credit Risk Modelling with Occupation Times*. Risks, 10(12), 228 (2022).

Probability distributions in proteomics data analysis: current status and next steps

N. Mdziniso[1], S. Schulze[2]

[1] *Rochester Institute of Technology, USA, {ncmsma}@g.rit.edu*
[2] *Rochester Institute of Technology, USA, sxssbi1@rit.edu*

One of the goals of tandem mass spectrometry experiments is to identify the presence of peptides or proteins in a complex biology sample. Applications of proteomics studies include the detection of biomarker proteins for the early detection of cancer. In practice, peptide-level and protein level identification experiments do not always yield perfect results. For the purpose of interpreting experimental results and designing follow-up experiments, biologists benefit from the availability of statistical scores to measure the accuracy of these experiments. As a result, many methods have been developed in literature to compute statistical scores associated with peptide-level and protein-level identification experiments. This work presents a review of recently developed parametric and non-parametric probability methods used to analyze data for peptides and proteins from tandem mass spectrometry. We highlight limitations for some of these methods and explore possible extensions for future research.

References

[1] L. K*ä*ll, J.D. Storey, M.J. MacCoss, and W.S. Noble., *Posterior Error Probabilities and False Discovery Rates: Two Sides of the Same Coin*, J. Proteome Res. **7**, 1, pp. 40-44 (2008).

[2] S. Datta, and ,B. Mertens *Statistical Analysis of Proteomics, Metabolomics, and Lipidomics Data Using Mass Spectrometry*, 1st ed., Springer International Publishing Switzerland, pp. 65-80 (2017).

The VI International AMMCS
Interdisciplinary Conference
Waterloo, Ontario, Canada

On Constructing Finite Automata by Relational Programming

A. Egri-Nagy[1], C.L. Nehaniv[2]

[1] *Akita International University, Japan, egri-nagy@aiu.ac.jp*
[2] *University of Waterloo, Canada, cnehaniv@uwaterloo.ca*

We have powerful tools for the algebraic analysis of finite state automata (FSA) and their associated transformation semigroups [1, 2]. However, constructing an automaton meeting the requirements for a given computational problem may cause some difficulty. We can consider FSA as a low-level programming language, similar to Turing-machines, where one can write programs for this mathematical definition of a computer. Unfortunately, FSA are even further away from high-level programming languages, since a Turing-machine has at least its tape as a dedicated memory device, while the FSA need to implement memory structure in their state sets. Thus, FSA can be truly horrible as a programming paradigm to solve arbitrary problems requiring finite memory. On the other hand, they can have more exotic and efficient memory handling tailored for a given task.

We define a computational task as a list of input-output pairs. The goal here is to have a faithful finite state automaton representation realizing the behaviour specified by the set of word-symbol pairs. We require that the synthesized FSA are able to reproduce the same output symbols as specified by the pairs in the course of processing any given input word. This is similar to machine learning, but the process is exact and not statistical. One envisioned application is to create FSA to play a perfect strategy in a game.

In this paper we describe how to use relational (logic) programming [4, 3] to solve the FSA construction problem and compare that to other algorithms.

References

[1] J. D. Mitchell et al. *Semigroups - GAP package, Version 5.2.1*, Mar 2023.

[2] Attila Egri-Nagy, Chrystopher L. Nehaniv, and James D. Mitchell. SGPDEC – *software package for Hierarchical Composition and Decomposition of Permutation Groups and Transformation Semigroups, Version 0.9.4*, 2022. `https://gap-packages.github.io/sgpdec/`.

[3] William Byrd. *Relational Programming in miniKanren: Techniques, Applications, and Implementations*. PhD thesis, Indiana University, 2009.

[4] Daniel P. Friedman, William E. Byrd, and Oleg Kiselyov. *The Reasoned Schemer*. The MIT Press, July 2005.

The VI International AMMCS
Interdisciplinary Conference
Waterloo, Ontario, Canada

Compact Notation for Finite Transformations

A. Egri-Nagy[1], C. L. Nehaniv[2]

[1] *Akita International University, Japan egri-nagy@aiu.ac.jp*
[2] *University of Waterloo, Canada, cnehaniv@uwaterloo.ca*

We describe a new notation for finite transformations. This compact notation extends the orbit-cycle notation for permutations and builds upon existing transformation notations. It gives insight into the structure of transformations and reduces the length of expressions without increasing the number of types of symbols.

In this paper, we review previously proposed notations, define our compact notation by a grammar and give a canonical form.

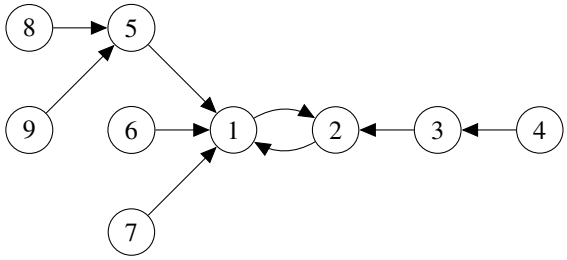

Figure 1: Digraph for an example transformation with a 'conveyor belt' trajectory `[4,3,2]` and a branching tree `[[8,9|5],6,7|1]` collapsing into a transposition `(1,2)`. In compact notation this is denoted `([[8,9|5],6,7|1],[4,3,2])`

References

[1] Gonca Ayik, Hayrullah Ayik, and John M. Howie. On factorisations and generators in transformation semigroups. *Semigroup Forum*, 70:225–237, 2005.

[2] Olexandr Ganyushkin and Volodymyr Mazorchuk. *Classical Transformation Semigroups*. Algebra and Applications. Springer Verlag, 2009.

[3] John M. Howie. Review of "*Symmetric Inverse Semigroups* (Mathematical Surveys and Monographs 46) by Stephen Lipscomb: 166 pp., US$49.00, ISBN 0 8218 0627 0 (American Mathematical Society, 1996)". *Bulletin of the London Mathematical Society*, 29(6), 1997.

[4] S. Lipscomb. *Symmetric Inverse Semigroups*, volume 46 of *Mathematical Surverys and Monographs*. American Mathematical Society, 1996.

[5] Boaz Tsaban. Decompositions of graphs of functions and fast iterations of lookup tables. *Discrete Appl. Math.*, 155(3):386–393, February 2007.

The VI International AMMCS
Interdisciplinary Conference
Waterloo, Ontario, Canada

A new BART prior for flexible modeling of areal spatial data

S.K. Deshpande[1]

[1] *University of Wisconsin–Madison, Madison, USA, sameer.deshpande@wisc.edu*

We describe an extension of the Bayesian Additive Regression Trees (BART) model to model spatial data that has been aggregated into small regions (e.g. census tracts, neighborhoods, etc.). Default implementations of BART would represent these areas using several binary indicators, one for each region. Regression trees built with these indicators partition the regions using a "remove one a time strategy." Unfortunately, the vast majority of partitions of the levels cannot be built with this strategy, severely limiting BART's ability to "borrow strength" across areas. We overcome this limitation with a new class of regression tree and a new decision rule prior that can assign multiple levels to both the left and right child of a decision node. Our decision rule prior that partitions the areas into spatially contiguous regions by deleting edges from random spanning trees of a suitably defined network. We implemented our new regression tree priors in the flexBART package, which, compared to existing implementations, often yields improved out- of-sample predictive performance without much additional computational burden. We demonstrate the efficacy of flexBART using an example about the spatiotemporal modeling of crime.

Dynamic behaviors of a stochastic genetic regulatory networks with switching parameters and impulsive effects

Y. Song[1], X. Liu[2], W. Xu[3]

[1] *Northwestern Polytechnical University, Xi'an, China, yisong@mail.nwpu.edu.cn*
[2] *University of Waterloo, Waterloo, Canada, xinzhi.liu@uwaterloo.ca*
[3] *Northwestern Polytechnical University, Xi'an, China, weixunpu@nwpu.edu.cn*

Gene regulation plays a crucial role in cell metabolism, signal transduction, and disease in biological growth and reproduction. In this process, genes are mutually regulated by each other[1, 2]. Genetic regulatory networks is a powerful tool to reveal the internal mechanisms. Considering the non-ignorability of the random perturbations[3], temporal variation of environmental parameters[4] and impulsive effects caused by subsystem switching[5], the dynamical behavior of stochastic switched genetic regulatory networks (1) with impulsive effects is modeled:

$$\begin{cases} dX = (G_{\sigma(t)} f_{\sigma(t)}(X) - K_{\sigma(t)} X)dt + h_{\sigma(t)}(X)dW(t), & t \neq t_k, \\ \Delta X(t) = P_{\sigma(t)} X, & t = t_k. \end{cases} \tag{1}$$

Here, $X(t) = [x_1(t), x_2(t), \cdots x_n(t)]$, $x_i(t)$ is the concentration of the protein transcribed by the ith gene. The switching rule $\sigma(t)$ is a piecewise constant function about time. $G_{\sigma(t)} = diag\{g_{1\sigma(t)}, g_{2\sigma(t)}, \cdots, g_{n\sigma(t)}\}$ is production rate. $K_{\sigma(t)} = diag\{k_{1\sigma(t)}, k_{2\sigma(t)}, \cdots, k_{n\sigma(t)}\}$ represents degradation rate. $f_{\sigma(t)}(X) = diag\{f_{1\sigma(t)}, f_{2\sigma(t)}, \cdots, f_{n\sigma(t)}\}$ and $f_{i\sigma(t)}$ is shifted Hill function,$h_{\sigma(t)}(X)$ is the noise intensity matrix. $W(t)$ denotes a n-dimensional independent standard Brownian motions. $\Delta X(t) = P_{\sigma(t)} X = X(t^+) - X(t^-)$ is the impulse.

Then, based on the Itô formula and inequality techniques, several new sufficient conditions are established to ensure the stochastic stability in the mean square. Finally, numerical examples and computer simulations are provided to confirm the validity of the theoretical results.

References

[1] Q. Zhou, et al., *A gene regulatory network in mouse embryonic stem cells*, PNAS., **104**, 42, pp. 16438-16443 (2007).

[2] M. Bansal and V. Belcastro, et al., *How to infer gene networks from expression profiles*, Mol. Syst. Biol., **3**, 1, pp. 78 (2007).

[3] M. Elowitz and A. Levine, et al., *Stochastic gene expression in a single cell*, Science **297**, 5584, pp. 1183-1186 (2002).

[4] C. Richard and H. Jong, et al., *Piecewise-linear models of genetic regulatory networks: equilibria and their stability*, J. Math. Biol.,**52**, 1, pp. 27-56 (2006).

[5] K. Pavlov and A. Dimitry, et al., *Genetic determinants of aggression and impulsivity in humans*, J. Appl. Genet., **53**, pp. 61-82 (2012).

Modelling the Effect of Sex Steroid Hormones on the Resolution of Absence Seizures

M. Ahmed[1], S. A. Campbell[2]

[1] *University of Waterloo, Waterloo, Canada, m243ahme@uwaterloo.ca*
[2] *University of Waterloo, Waterloo, Canada, sacampbell@uwaterloo.ca*

Childhood absence epilepsy (CAE) is an idiopathic generalized epilepsy disorder which affects children between the ages of 4-12 years. It is characterized by sudden brief periods of impaired consciousness occurring several times a day. One of the most confounding features of CAE is its ability to spontaneously resolve in adolescence in roughly 80% of cases, while in others it can progress into more severe types of epilepsy. There remains an inadequate understanding of some of the factors involved in remission that can inform early intervention practices. According to some functional connectivity studies, there exist pre-treatment connectivity differences between patients who ultimately experience remission and those who do not, namely increased frontal cortical connections at the time of diagnosis. There is also substantial evidence on the effect of sex steroids on human (and animal) brain rhythmic discharges, particularly the effect of progesterone metabolite allopregnanolone on the action of gamma-Aminobutyric acid (GABA), an inhibitory neurotransmitter. We have developed a computational model of the thalamocortical network to study the role of allopregnanolone on network behaviour in the eventual resolution of CAE. The results from this research can possibly better inform therapeutic decisions relating to early interventions tailored to intrinsic network connectivity arrangements, which can be evaluated prior to the start of treatment and at the time of diagnosis.

References

[1] A. Knox, T. Glauser, J. Tenney, W. W. Lytton, and K. Holland, *Modeling pathogenesis and treatment response in childhood absence epilepsy*, Epilepsia. **59**, 1, pp. 135-145 (2018).

[2] A. Destexhe, *Spike-and-wave oscillations based on the properties of GABAb receptors*, Journal of Neuroscience. **18**, 21, pp. 9099-9111 (1998).

[3] M. D. Majewska, N. L. Harrison, R. D. Schwartz, J. L. Barker, and S. M. Paul, *Steroid hormone metabolites are barbiturate-like modulators of the GABA receptor*, Science. **232**, 4753, pp. 1004-1007 (1986).

[4] O, Yalcin, *Genes and molecular mechanisms involved in the epileptogenesis of idiopathic absence epilepsies*, Seizure. **21**, 2, pp. 79-86 (2012).

The VI International AMMCS
Interdisciplinary Conference
Waterloo, Ontario, Canada
August 14-18, 2023

Event-Triggered Impulsive Stabilization for Nonlinear Systems

Kexue Zhang

Queen's University, Kingston, ON, Canada, kexue.zhang@queensu.ca

Impulsive control is a control paradigm that uses impulses that are state abrupt changes over negligible time periods to control dynamic systems. Most of the existing results on impulsive control problems focus on time-triggered control strategies. More specifically, the moments when the impulses happen, normally called impulse times, are pre-scheduled which makes time-triggered control strategies simple to implement. To improve impulsive control efficiency, event-triggered impulsive control has been successfully developed recently, the idea of which is to determine the impulse times or the instants of updating the control signals by a certain event that occurs only when the system dynamics violates a well-designed triggering condition.

This talk focuses on the impulsive stabilization of nonlinear systems. We propose two types of event-triggering algorithms to update the impulsive control signals with actuation delays. The first algorithm is based on continuous event detection, while the second type makes decisions about updating the impulsive control inputs according to periodic event detection. Sufficient conditions are derived to ensure asymptotic stability of the impulsive control systems with the designed event-triggering algorithms. Lower bounds of the time period between two consecutive events are also obtained so that the closed-loop impulsive systems are free of Zeno behavior.

Noise-induced Synchrony Near a Hopf Bifurcation with Asymmetric Noise and Uneven Coupling

Gurpreet Jagdev, Na Yu

Toronto Metropolitan University, Toronto, Canada, gjagdev@torontomu.ca

The study of emergent dynamics in complex neuronal networks has been a topic of great interest in neuroscience. Two fundamental components, coupling and noise, have been identified as key factors that contribute to the emergence of these dynamics. While the roles of equal coupling and symmetric noise have been extensively studied, the mechanisms behind unequal coupling strength and asymmetric noise, and their respective effects on neural dynamics, are still not well understood, despite their apparent relevance.

Moreover, this study aims to investigate the simultaneous interplay of these two components in the simplest network motif: two bi-directionally coupled excitable neuronal oscillators, each subject to its own intrinsic noise. Our results indicate that the synchronization of neuronal oscillators can be maximized through noise-induced synchrony when one oscillator (source) with weak intrinsic noise is strongly coupled to another oscillator (receiver) with strong intrinsic noise.

Importantly, we also found that the level of asymmetry in respective coupling and noise applied to the two neural oscillators has a profound influence on the level of synchrony. In other words, the degree of asymmetry between the two components affects the synchronization of the oscillators, and thus the emergence of complex dynamics in the network. We further extended these findings to a three-coupled neural oscillator in a feed-forward schematic.

These results shed new light on the intricate interplay between coupling and noise in neural networks and offer insights into the emergence of complex dynamics that arise as a result of this interaction. By optimizing the levels of coupling and noise, we may be able to induce and optimize network synchrony, which has implications for the treatment of neurological disorders such as epilepsy and essential tremors. Overall, this study contributes to a more comprehensive understanding of the mechanisms behind emergent dynamics in complex neuronal networks.

Turnpike phenomena in optimal control

R. Guglielmi[1] and Z. Li[1]

[1] *University of Waterloo, Canada, rguglielmi@uwaterloo.ca*

We provide a characterization of the exponential turnpike property for infinite dimensional generalized linear-quadratic optimal control problems in terms of structural properties of the control system, such as exponential stabilizability and detectability. The proof relies on the analysis of the exponential convergence of solutions to the differential Riccati equations to the algebraic counterpart, and on a necessary condition for exponential stabilizability in terms of a closed range test.

References

[1] L. Grüne and R. Guglielmi, *Turnpike properties and strict dissipativity for discrete time linear quadratic optimal control problems*, SIAM J. Control Optim., 2018, 56(2): 1282-1302.

[2] L. Grüne and R. Guglielmi, *On the relation between turnpike properties and dissipativity for continuous time linear quadratic optimal control problems*, Mathematical Control and Related Fields, 2021, 11(1): 169-188. doi: 10.3934/mcrf.2020032.

[3] R. Guglielmi and Z. Li, *Turnpike property for generalized linear-quadratic problems*, submitted.

The VI International AMMCS
Interdisciplinary Conference
Waterloo, Ontario, Canada

Real-time pest management

R. Guglielmi[1]

[1] *University of Waterloo, Canada, rguglielmi@uwaterloo.ca*

We develop a model-based real-time optimal control scheme for pest management by means of the Sterile Insect Technique (SIT). The proposed framework allows to tune the release of sterile insects according to the actual presence of pest, and takes into account the constraints on availability of resources in the deployment of the control strategy.

Transmission and establishment of monkeypox in the primary and secondary host

Y. Tan[1,3], H. Zhu[2,3]

[1] *Laboratory of Mathematical Parallel Systems (LAMPS), York University, Canada, lbxty@yorku.ca*
[2] *Canadian Centre for Diseases Modeling (CCDM), York University, Canada, huaiping@yorku.ca*
[3] *Department of Mathematics and Statistics, York University, Canada*

Monkeypox virus, which is typically limited to Africa, began spreading globally, including Europe and North America in Mid-May 2022. The sustained transmission in Africa and widespread outbreaks globally highlight the importance of risk evaluation, using a one health approach to understand how the virus spread and how to stop it [1, 2, 3, 4]. Monkeypox virus can infect a wide range of mammal species, including rope squirrels, tree squirrels, Gambian pouched rats, and dormice. African rope squirrel is considered as a particularly plausible primary host in Africa. For other areas where African rope squirrels are less abundant, or absent, other species including incidentally infected wild hosts or captive animals, contribute to viral persistence. In this talk, I will first present an ODE model for the spread of monkeypox in the primary and secondary host. I will explain how different factors affect the spillover of monkeypox virus from the primary host to the secondary host. Then, I will use a SDE model to illustrate the environmental stochasticity in the transmission of monkeypox. I will then compare the results under random perturbations with those of the deterministic model. In the end I will discuss how our results can inform the implementation of control measures, especially as the virus adapts to new hosts in new regions.

References

[1] P. Yuan, Y. Tan, L. Yang, E. Aruffo, N. H. Ogden, J. Bélair, et al., *Assessing transmission risks and control strategy for monkeypox as an emerging zoonosis in a metropolitan area*, Front. Public Health **10**, (2022).

[2] P. Yuan, Y. Tan, L. Yang, E. Aruffo, N. H. Ogden, J. Bélair, et al., *Modeling vaccination and control strategies for outbreaks of monkeypox at gatherings*, J. Med. Virol. **95**, 1, (2023).

[3] I. Lauko, G. Pinter, and R. TeWinkel, *Equilibrium analysis for an epidemic model with a reservoir for infection*, Lett. Biomath. **5**, 1, pp. 255-274 (2018).

[4] S. Usman and I. I. Adamu, *Modeling the transmission dynamics of the monkeypox virus infection with treatment and vaccination interventions*, J. appl. math. phys. **5**, 12, (2017).

The VI International AMMCS
Interdisciplinary Conference
Waterloo, Ontario, Canada

Bifurcations in Nonlinear Schrödinger Equations with Multi–Well Potentials: Insights from the Infinite Eigenvalue Case

E. Kirr[1], P. G. Kevrekidis[2], H. Uecker[3]

[1] *University of Illinois at Urbana-Champaign, US, ekirr@illinois.edu*
[2] *University of Massachusetts at Amherst, US, kevrekid@math.umass.edu*
[3] *University of Oldenburg, Germany, hannes.uecker@uol.de*

We will present a new mathematical technique aimed at discovering all coherent structures supported by a given nonlinear wave equation. It relies on global bifurcation analysis which shows that, inside the Fredholm domain, the coherent structures organize themselves in in manifolds which either form closed surfaces or must reach the boundary of this domain. We will show how one can find all the limit points at the Fredholm boundary for the particular case of Nonlinear Schrödinger/Gross-Pitaevskii Equation and use these limit points to find all coherent structures (bound states) and their bifurcation points.

The VI International AMMCS
Interdisciplinary Conference
Waterloo, Ontario, Canada

Predicting Ranked Choice Voting Winners on Sampled Votes

A. Kahng[1], M. Iceland[2]

[1] *University of Rochester, Rochester, USA, anson.kahng@rochester.edu*
[2] *University of Rochester, Rochester, USA, miceland@u.rochester.edu*

Ranked choice voting (RCV), also known as instant runoff voting (IRV), is a social choice function used to determine the winner of an election in which n voters report partial or complete rankings over m candidates. RCV proceeds in rounds by repeatedly eliminating the candidate with the fewest first-place votes, whereupon supporters of that candidate shift their support to their next-most preferred candidate in their ranking. The first candidate to win majority support wins the election. We investigate how to predict the RCV winner of an election given a uniformly random sample (without replacement) drawn from the complete input profile. In our empirical analysis, we draw inspiration from recent work on the "map of elections" [1, 2] in order to test our predictive methods on elections generated by a wide range of statistical cultures.

We propose and empirically test whether we can use other common (deterministic) voting rules to predict the RCV winner given a uniformly random sample of votes from the input profile. We observe that, for small sample sizes over a large range of real-world and simulated data, rules like the Borda rule and the Copeland rule more accurately predict the RCV winner than RCV itself. Notably, the results vary depending on where in the map of elections the input profiles are located, which suggests that one could obtain more accurate predictions on elections by first estimating where the complete profile is located in the map of elections and then applying the most accurate voting rule for that specific location.

As an extension to our approach for predicting the RCV winner by using other deterministic voting rules, we also examine how well common voting rules (Borda, Copeland, the harmonic scoring rule, plurality, and RCV) predict each others' winners for a wide range of elections generated by statistical cultures in the map of elections, extending work previously started by [3] (although they study social welfare functions, which return rankings, and we study social choice functions, which return single winners). Results vary by specific statistical culture, but, in general, Borda, Copeland, and the harmonic scoring rule are strong predictors of themselves for almost all noise models and sample sizes, but plurality and RCV are often not the best self-predictors.

Lastly, inspired by a similar question asked in the context of positional scoring rules and social welfare functions [3], we begin an inquiry into the theoretical question of the worst-case accuracy of RCV predicting itself on a sample. We provide a construction showing that, even given access to a sample of size $n-1$, the probability that the RCV winner on this sample coincides with the RCV winner on the entire profile is at most $(m-1)/m^2 < 1/m$.

References

[1] S. Szufa, P. Faliszewski, P. Skowron, A. Slinko, and N. Talmon. *Drawing a map of elections in the space of statistical cultures*, in *Proceedings of the 19th International Conference on Autonomous Agents and Multiagent Systems* (AAMAS-20), pp. 1341-1349 (2020).

[2] N. Boehmer, R. Bredereck, P. Faliszewksi, R. Niedermeier, and S. Szufa. *Putting a compass on the map of elections*, in *Proceedings of the 30th International Joint Conference on Artificial Intelligence* (IJCAI-21), pp. 59-65 (2021).

[3] E. Micha and N. Shah. *Can we predict the election outcome from sampled votes?*, in *Proceedings of the 34th AAAI Conference on Artificial Intelligence* (AAAI-20), pp. 2176-2173 (2020).

Multiplex network modeling for the impact of the opinion and behavior of mask-wearing on the spreading and control of COVID-19

S. Gholizadeh[1], H. Zhu[2]

[1] *York University, Toronto, Canada, sanazgh@yorku.ca*
[2] *York University, Toronto, Canada, huaiping@yorku.ca*

Initial control measures for Covid 19 that are still in use in most affected countries are non-pharmaceutical interventions (NPIs), which have been efficient in controlling virus spread [1]. The efficacy of policy measures for curbing transmission relies on the extent to which they are known, understood, accepted, and adopted in time [2]. On the scale of adherence, social distancing, following isolation in lock-down and mask-wearing behavior can be roughly defined as being 'adherent' or 'not-adherent' [3]. Bearing in mind the disruptive effects of most NPIs, and due to their high societal and economic cost and consequences, the implementation of effective public information campaigns and mask requirements can present large benefits with fewer efforts than other NPIs [4]. Mask-wearing is simple to use and its availability made more governments around the world put policies with recommendations or mandates to wear masks in public during the pandemic. Hence, we study people's attitudes toward mask-wearing protection measures. We propose a network model to find out how and to what extent the level of people's behavior and opinion toward protection measures will affect the spread and transmission of a disease spreading, such as the SEAIRS epidemiological model of COVID-19. We have demonstrated how two simultaneous spreading processes such as disease spreading and behavior-changing propagation mutually impact each other within the same population group by utilizing a multiplex network. Fear of increasing confirmed cases and intent for behavior conformity are two behavioral indices we ascribed to individuals. We could quantify the behavior changing of individuals due to the first act of matching attitudes and the influence pressure of other connections with the threshold model and secondly due to the fear of the increased number of confirmed infected cases by the logistic function. These two behavior effects may occur via media news, virtual networks, and communication between friends. Then by using Micro Markov Chain modeling, we show all the system's possibilities and transition probabilities. Our results show the emergence of periodic solutions that indicate a reciprocal relationship between disease spread and behavior changes. The existence of periodic solutions provide a reasonable explanation of Covid-19 peak waves. We observed that when people wear masks due to peer pressure or the fear of confirmed cases, it helps reduce the spread of Covid-19. However, when individuals perceive a decrease in the number of cases or lower usage of masks among their connections, they may stop wearing masks, leading to an increase in the number of infected confirmed cases. We have shown that repetitive occurrence is associated with these behavioral changing probabilities.

References

[1] Aruffo E, Yuan P, Tan Y, Gatov E, Gournis E, Collier S, Ogden N, Bélair J, Zhu H. *Community structured model for vaccine strategies to control COVID19 spread: a mathematical study*. Plos one. 2022 Oct 27;17(10):e0258648.
[2] Denford S, Morton KS, Lambert H, Zhang J, Smith LE, Rubin GJ, Cai S, Zhang T, Robin C, Lasseter G, Hickman M. *Understanding patterns of adherence to COVID-19 mitigation measures: a qualitative interview study*. Journal of Public Health. 2021 Sep;43(3):508-16.
[3] Williams SN, Armitage CJ, Tampe T, Dienes K. *Public Perceptions of Non-Adherence to COVID-19 Measures by Self and Others in the United Kingdom*." medRxiv, 2020.11. 17.20233486.
[4] Mendez-Brito A, El Bcheraoui C, Pozo-Martin F. *Systematic review of empirical studies comparing the effectiveness of non-pharmaceutical interventions against COVID-19*. Journal of Infection. 2021 Sep 1;83(3):281-93.

The VI International AMMCS
Interdisciplinary Conference
Waterloo, Ontario, Canada

Optimal Control of Nonsmooth Dynamical Systems via Direct Methods

P. Stechlinski[1]

[1] *University of Maine, Orono, USA, peter.stechlinski@maine.edu*

Nonsmoothness can arise in dynamical systems frameworks because of the physical problem being modeled, the need for nonsmooth control, or mathematical techniques that introduce nonsmoothness to aid in simulation/optimization methods. Such nonsmoothness necessitates the development of specialized tools and theory, since conventional methods typically require smoothness assumptions to hold. After reviewing the landscape of nonsmooth/discontinuous/hybrid dynamical systems frameworks, we turn our attention to nonlinear complementarity systems (NCSs), a class of highly nonlinear and nonsmooth systems which finds use in mechanical systems, electrical systems, process engineering, and economics. A computationally-relevant sensitivity theory is established for NCSs that is suitable for solving optimal control problems using a direct approach, i.e., parametrically discretizing the control and applying gradient-based sequential methods to update the parameters. Using lexicographic directional differentiation, a new tool in nonsmooth analysis, generalized derivative information is obtained that characterizes the sensitivity of an objective function with respect to parameters in the NCS system. We highlight similar results for other nonsmooth frameworks, including ODEs and differential-algebraic equations, and how this theory can be specialized to linear complementarity systems and optimization-constrained ODEs.

Recent advances in generating convex relaxations for parametric dynamical systems

K.A. Khan[1]

[1] *McMaster University, Hamilton, Canada, kamilkhan@mcmaster.ca*

Several engineering applications require deterministic global optimization of dynamical systems that are modeled as parametric systems of ordinary differential equations (ODEs):

$$\dot{\mathbf{x}} = \mathbf{f}(t, \mathbf{p}, \mathbf{x}), \qquad \mathbf{x}(0, \mathbf{p}) = \mathbf{x}_0(\mathbf{p})$$

A corresponding global dynamic optimization problem is then:

$$J^* = \min_{\mathbf{p} \in P} J(\mathbf{p}), \tag{1}$$

where $J(\mathbf{p}) \equiv g(\mathbf{p}, \mathbf{x}(t_f, \mathbf{p}))$ involves the final value of the ODE solution trajectory.

Typical methods for deterministic global optimization proceed by generating upper and lower bounds on the unknown globally optimal value J^*, and then progressively refining these bounds. In this setting, lower bounds are typically obtained by minimizing convex relaxations of the original system using local nonlinear programming (NLP) solvers. Developing useful convex relaxations is therefore critical in global optimization, as is furnishing subgradients of these relaxations for use by a subgradient-based NLP solver.

This presentation discusses our recent work in developing convex relaxations for the global dynamic optimization problem (1). We developed a new versatile method [1] for constructing these convex relaxations as the solution of an auxiliary ODE system that employs convex and concave relaxations of the original right-hand side function $\mathbf{f}$. Though subgradients of nonsmooth parametric ODEs are traditionally difficult to furnish, we developed and implemented a new subgradient evaluation approach based on adjoint sensitivity analysis [3] and new results in nonsmooth analysis. As an alternative to this approach, we developed a tractable underestimation approach based on derivative-free sampling [2], for computing weaker yet computationally inexpensive lower bounds without any access to gradients or subgradients. Numerical examples are presented for illustration, and implications are discussed.

References

[1] Y. Song and K.A. Khan, *Optimization-based convex relaxations for nonconvex parametric systems of ordinary differential equations*, Math. Program. **196**, pp. 521-565 (2022).

[2] Y. Song, H. Cao, C. Mehta, and K.A. Khan, *Bounding convex relaxations of process models from below by tractable black-box sampling*, Comput. Chem. Eng. **153**, article 107413 (2021).

[3] Y. Zhang and K.A. Khan, *Implementing adjoint subgradient evaluation for use in global dynamic optimization*, in *Proceedings of FOCAPO-CPC 2023*, San Antonio, USA, in press (2023).

The VI International AMMCS
Interdisciplinary Conference
Waterloo, Ontario, Canada
August 2023

Study of high-order time-stepping schemes with non-smooth initial conditions

D. Wang[1], C. Christara[2], K. Serkh[3]

[1] *University of Toronto, Toronto, Canada, dwang@cs.toronto.edu*
[2] *University of Toronto, Toronto, Canada, ccc@cs.toronto.edu*
[3] *University of Toronto, Toronto, Canada, kserkh@math.toronto.edu*

Nonsmooth payoff functions are common in financial contracts and pose problems in obtaining high-order solutions of the contract prices. In this work, we consider convection-diffusion equations with initial conditions involving various types of non-smoothness. We apply a fourth-order finite difference space discretization method and BDF4 time stepping, and study the solution behaviour. From the Fourier transform of the discrete initial conditions directly sampled from the exact Dirac delta, Heaviside and ramp functions, we observe that the low-order error terms of the discretized initial conditions in the Fourier domain can be canceled out by simple initial condition correction schemes that we propose. We also prove that by performing BDF4 time stepping with a third-order Runge-Kutta (RK3) starting scheme for the first three time steps, the low-order errors generated by RK3 for nonsmooth data in the high frequency domain get damped away, while there are no low-order errors in the low frequency domain. With our new initial condition discretization, and the proposed time stepping scheme, we theoretically prove and numerically verify that stable fourth-order convergence is obtained. Numerical examples of European-style digital and call options are also given to demonstrate the fourth-order convergence of our methods.

Does the Rule Matter? A Comparison of Preference Elicitation Methods and Voting Rules Based on Data from an Austrian Regional Parliamentary Election in 2019

A. Darmann[1], C. Klamler[3]

[1] *University of Graz, Austria, andreas.darmann@uni-graz.at*
[2] *University of Graz, Austria, christian.klamler@uni-graz.at*

Based on data collected in connection with the 2019 parliamentary election in the Austrian region of Styria we analyze (the hypothetical use of) different voting rules. Following previous empirical studies in the literature, such as [4], [1] and [3], we provide empirical evidence that the choice of the voting rule has in fact an impact on the outcome of the election, at least in certain parts of the social ranking. In that respect, the paper also follows our analysis of the 2015 parliamentary elections (see [2]).

Our data shows that among the voters there exists a certain desire for voting rules using more fine-grained preference information. In the survey, 75% of the voters stated that providing more detailed preference information is (rather) easy. In that context, we investigate the degree of consistency in the voters' declaration of preferences, something of relevance when different voting rules, that require different levels of information, are used. Our analysis shows to which extent the apparent simplicity of different preference elicitation methods actually can be confirmed when voters do state their preferences.

Finally, we check for the discrepancy between elicited preferences and reported votes in the case of Plurality Rule. In that respect we analyze to which extent strategic voting has occurred in the election and what the specific reasons for such a behavior might have been.

References

[1] A. Baujard, H. Igersheim and I. Lebon, *Some Regrettable Grading Scale Effects Under Different Versions of Evaluative Voting*, Social Choice and Welfare, **56**, pp. 803-834 (2021).

[2] A. Darmann, J. Grundner and C. Klamler, *Election Outcomes Under Different Ways to Announce Preferences: An Analysis of the 2015 Parliament Election in the Austrian Federal State of Styria*, Public Choice, **173**, 1, pp. 201-2016 (2017).

[3] U. Evci and M. Kaminski, *Shot in the Foot: Unintended Political Consequences of Electoral Engineering in the Turkish Parliamentary Elections in 2018*, Turkish Studies, **22**, 3, pp. 481-494 (2022).

[4] D. McCune and L. McCune, *Does the Choice of Preferential Voting Method Matter? An Empirical Study Using Ranked Choice Elections in the United States*, Representation, DOI: 10.1080/00344893.2022.2133003 (2022).

Mathematical Models of Novel Ocular Drug Delivery Systems

L. Carichino[1]

[1] *School of Mathematical Sciences, Rochester Institute of Technology, Rochester, USA, lcsma1@rit.edu*

Age-related macular degeneration and glaucoma are the first two common cause of blindness world- wide, affecting more than 4.7 million Americans age 40 or older. The only treatments available for such ocular diseases are drug therapies administered via topical eye drops or intraocular injections, that have several disadvantages [1-3]. In this talk I will present mathematical models for two of the recently proposed ocular drug delivery systems: gene therapy treatments [4] and drug delivery by contact lenses [2]. We develop a mathematical model of human ocular pharmacokinetics in three ocular compartments (aqueous, vitreous and retina) to study and compare the target protein levels in the eye for gene therapy treatment vs intraocular injection treatment, leveraging publicly disclosed information from a current gene therapy trial [5]. Then, as a first step in modeling contact lenses as a drug delivery system, we use a mathematical model to estimate the drug release diffusion coefficient for different contact lenses using previously published experimental results.

References

[1] Patel A. et al., *Ocular drug delivery systems: an overview*, World. J. Pharmacol. 2(2): 47 (2013).
[2] Bengani L. et al, *Contact lenses as a platform for ocular drug delivery*, Expert. Opin. Drug. Del. 10(11):1483–1496 (2013).
[3] Spooner KL. et al, *The burden of neovascular age-related macular degeneration: a patient's perspective*, Clin. Ophthalmol. (Auckland, NZ) 12:2483 (2018).
[4] Al-Khersan H. et al, *Innovative therapies for neovascular age-related macular degeneration*, Expert. Opin. Pharmacother. 20(15): 1879–1891 (2019).
[5] Carichino L. et al., *Gene therapy bio-factory: Mathematical modeling of the human eye pharmacokinetics,* Applied Mathematical Analysis and Computation - 1st SGMC, Statesboro, USA, April 2–3, 2021(Virtual), Springer Proceedings in Mathematics & Statistics, in press.

The VI International AMMCS
Interdisciplinary Conference
Waterloo, Ontario, Canada

A Biologically-Detailed, Multi-Scale Simulation of Retinal Physiology

B. Abuelnasr[1], A. R. Stinchcombe[1]

[1] *University of Toronto, Toronto, Canada, {belal.abuelnasr@mail.utoronto.ca, stinch@math.toronto.edu}*

We present a detailed physiological model of the retina that includes the biochemistry and electrophysiology of phototransduction, neuronal electrical coupling, and the spherical geometry of the eye. The model is a parabolic-elliptic system of partial differential equations based on the mathematical framework of the bi-domain equations. While there has been some modeling work based on the bi-domain equations on the retina, this model is the first model that includes the spherical geometry of the eye and this level of biological detail.

We generalize the bi-domain framework to a multi-domain one to account for multiple cell-types. We discretize in space with non-uniform finite differences and step through time with a custom, adaptive time-stepper that employs a backward differentiation formula and an inexact Newton method. A refinement study confirms the accuracy and efficiency of our numerical method. Numerical simulations using the model compare favorably with experimental findings, such as desensitization to light stimuli and calcium buffering in photoreceptors. Other numerical simulations suggest an interplay between photoreceptor gap junctions and inner segment, but not outer segment, calcium concentration. We highlight two special applications: analysis of retinal calcium imaging experiments and patient-specific design of electroretinograms.

A Hamiltonian Dysthe equation for deep-water gravity waves with constant vorticity

P. Guyenne[1], A. Kairzhan[2], C. Sulem[3]

[1] *University of Delaware, Newark, USA (guyenne@udel.edu)*
[2] *University of Toronto, Canada (kairzhan@math.toronto.edu)*
[3] *University of Toronto, Canada (sulem@math.utoronto.ca)*

In this talk I present a study of the water wave problem in a two-dimensional domain of infinite depth in the presence of nonzero constant vorticity. A goal is to describe the effects of uniform shear flow on the modulation of weakly nonlinear quasi-monochromatic surface gravity waves. Starting from the Hamiltonian formulation of this problem and using techniques from Hamiltonian transformation theory, we derive a Hamiltonian Dysthe equation for the time evolution of the wave envelope. Consistent with previous studies, we observe that the uniform shear flow tends to enhance or weaken the modulational instability of Stokes waves depending on its direction and strength. Our method also provides a non-perturbative procedure to reconstruct the surface elevation from the wave envelope, based on the Birkhoff normal form transformation to eliminate all non-resonant triads. This model is tested against direct numerical simulations of the full Euler equations and against a related Dysthe equation derived by Curtis et al. [1] in the context of constant vorticity. Very good agreement is found for a range of values of the vorticity.

References

[1] C.W. Curtis, J.D. Carter, H. Kalisch, Particle paths in nonlinear Schrödinger models in the presence of linear shear currents, *J. Fluid Mech.* **855** (2018), 322–350.

A Parallel Spectral Solver for the Incompressible Navier-Stokes Equations in Simple Toroidal Coordinates

M.C. Haslam[1] and V. Siewnarine[2]

[1]*Department of Mathematics and Statistics, York University, Toronto, Canada, mchaslam@yorku.ca*
[2]*Department of Mathematics and Statistics, York University, Toronto, Canada, vsiewnar@yorku.ca*

Pressure Poisson Equation reformulations of the Navier-Stokes equations have been used extensively in the design of accurate and efficient solvers; see, for example [1, 2]. Using this approach, the incompressibility constraint $\nabla \cdot \mathbf{u} = 0$ is replaced by a Poisson equation for the pressure p; the accompanying Neumann boundary conditions ensure that incompressibility is maintained throughout the solution domain. The particular formulation used in our solvers, due to Johnston and Liu [2], reads

$$\mathbf{u}_t + (\mathbf{u}\cdot\nabla)\mathbf{u} = -\nabla p + \frac{1}{\mathrm{Re}}\nabla^2\mathbf{u} \qquad \text{in} \qquad \Omega\times(0,T], \tag{1}$$

$$\nabla^2 p = -\nabla\cdot(\mathbf{u}\cdot\nabla\mathbf{u}) \qquad \text{in} \qquad \Omega\times(0,T], \tag{2}$$

with boundary conditions

$$\mathbf{u} = \mathbf{f} \qquad \text{and} \qquad \frac{\partial p}{\partial \mathbf{n}} = -\frac{1}{\mathrm{Re}}\mathbf{n}\cdot(\nabla\times\nabla\times\mathbf{u}) \qquad \text{on} \qquad \partial\Omega\times[0,T]. \tag{3}$$

While approaches based on projection methods may result in numerical boundary layers [3], approaches based on a Pressure Poisson Equation reformulation of the problem avoids this issue altogether. Our solvers are specialized to the simple toroidal coordinate system defined by the coordinate transformation

$$\begin{aligned} x(r,\theta,\phi) &= (R_0 + r\cos\theta)\cos\phi \\ y(r,\theta,\phi) &= (R_0 + r\cos\theta)\sin\phi \\ z(r,\theta,\phi) &= r\sin\theta \end{aligned} \tag{4}$$

where r is the polar radius, θ is the polar angle, R_0 is the toroidal radius and ϕ is the toroidal angle. Our algorithm is based on the high-order representation of the unknown quantities in terms of Fourier and Chebyshev series. At higher Reynolds numbers, the field quantities are treated explicitly, and the time stepping accomplished using a fourth order RK4 time stepping, which is known to be convectively stable. In this talk we will discuss details of the parallel numerical implementation using OpenMP, and in particular we will examine the overall performance of the code using different Poisson solvers we have developed based on direct methods, as well as an iterative solver based on a V-cycle multigrid method.

References

[1] W. D. Henshaw, *A fourth-order accurate method for the incompressible Navier-Stokes equations on overlapping grids*. Journal of Computational Physics, **113**(6): 13-25, 1994.

[2] H. Johnston and J.-G. Liu, *Accurate, stable and efficient Navier-Stokes solvers based on explicit treatment of the pressure term*. Journal of Computational Physics, **199**(1): 221-259, 2004.

[3] E. Weinan and J.-G. Liu, *Projection method I: convergence and numerical boundary layers*. SIAM Journal on Numerical Analysis, **32**(4): 1017-1057, 1995.

Viscous Flow Between Oscillating Concentric Torii

M.C. Haslam[1] and V. Siewnarine[2]

[1]*Department of Mathematics and Statistics, York University, Toronto, Canada, mchaslam@yorku.ca*
[2]*Department of Mathematics and Statistics, York University, Toronto, Canada, vsiewnar@yorku.ca*

We have recently developed solvers for the incompressible Naview-Stokes problem based on a Pressure Poisson Equation reformulation. The particular formulation used as a basis for our solvers due to Johnston and Liu [2] reads

$$\mathbf{u}_t + (\mathbf{u}\cdot\nabla)\mathbf{u} = -\nabla p + \frac{1}{\mathrm{Re}}\nabla^2\mathbf{u} \qquad \text{in} \qquad \Omega\times(0,T], \tag{1}$$

$$\nabla^2 p = -\nabla\cdot(\mathbf{u}\cdot\nabla\mathbf{u}) \qquad \text{in} \qquad \Omega\times(0,T], \tag{2}$$

with boundary conditions

$$\mathbf{u} = \mathbf{f} \qquad \text{and} \qquad \frac{\partial p}{\partial \mathbf{n}} = -\frac{1}{\mathrm{Re}}\mathbf{n}\cdot(\nabla\times\nabla\times\mathbf{u}) \qquad \text{on} \qquad \partial\Omega\times[0,T]. \tag{3}$$

Our solvers are specialized to the simple toroidal coordinate system defined by the coordinate transformation

$$\begin{aligned} x(r,\theta,\phi) &= (R_0 + r\cos\theta)\cos\phi \\ y(r,\theta,\phi) &= (R_0 + r\cos\theta)\sin\phi \\ z(r,\theta,\phi) &= r\sin\theta \end{aligned} \tag{4}$$

where r is the polar radius, θ is the polar angle, R_0 is the toroidal radius and ϕ is the toroidal angle; a corresponding velocity field is $\mathbf{u} = (u_r, u_\theta, u_\phi)$. Our algorithm is based on the high-order representation of the velocity and pressure fields in terms of Fourier and Chebyshev series. At higher Reynolds numbers, the field quantities are treated explicitly, and the time stepping accomplished using a fourth order RK4 time stepping, which is known to be convectively stable. In this talk we will discuss results from an interesting physical problem we have examined, corresponding to the flow inside an oscillating toroidal shell. In this case, the velocity boundary conditions have the form

$$\mathbf{u}(r,\theta,\phi,t) = \begin{cases} (0,0,(R_0 + r_a\cos\theta)\sin(\omega t)) & r = r_a \\ (0,0,(R_0 + r_b\cos\theta)\sin(\omega t)) & r = r_b \end{cases}, \tag{5}$$

where r_a and r_b are the radii of the inner and outer shells respectively. Such a configuration was recently suggested as a mechanical damping system, prompting our study.

References

[1] W. D. Henshaw, *A fourth-order accurate method for the incompressible Navier-Stokes equations on overlapping grids*. Journal of Computational Physics, **113**(6): 13-25, 1994.

[2] H. Johnston and J.-G. Liu, *Accurate, stable and efficient Navier-Stokes solvers based on explicit treatment of the pressure term*. Journal of Computational Physics, **199**(1): 221-259, 2004.

The VI International AMMCS
Interdisciplinary Conference
Waterloo, Ontario, Canada

Green's $\mathscr{J}$-classes and Subduction Classes in Finite Transformation Semigroups

A. Egri-Nagy[1], C. L. Nehaniv[2]

[1] *Akita International University, Japan, egri-nagy@aiu.ac.jp*
[2] *University of Waterloo, Canada, cnehaniv@uwaterloo.ca*

Subduction is preorder relation defined on the set of images induced by a transformation semigroup. It can be viewed as the generalization of set-theoretic inclusion, since a set can be transformed under the action of the semigroup in order to contain another set. The holonomy decomposition algorithm [2,4,9,10] is a wreath product decomposition theorem for finite transformation semigroups and it depends on the subduction preorder. Therefore, subduction is worth studying in itself.

Green's preorders give ample information about the semigroup's internal structure [1,6,7], while subduction captures details of the semigroup action. Therefore, the natural question arises: *What is the connection between the Green's relations and the subduction relation?* More generally, by aiming to describe the connection between a semigroup action and the internal structure of semigroup itself we may get information on what transformation representations are possible for an abstract semigroup.

Here, we establish the connection between Green's $\mathscr{J}$-classes and the subduction equivalence classes defined on the image sets of an action of a semigroup. The construction of the skeleton order (on subduction equivalence classes) is shown to depend on transformation semigroups and surjective morphisms, and to factor through the $\leq_{\mathscr{L}}$-order and $\leq_{\mathscr{J}}$-order on the semigroup and through the inclusion order on image sets. For right regular representations, the correspondence between the $\mathscr{J}$-class order and the skeleton is one of isomorphism.

The mathematical analysis is illustrated by the computational examples produced by the packages [3,8] for the GAP computer algebra system [5].

References

[1] A.H. Clifford and G.B. Preston. *The Algebraic Theory of Semigroups, Vol. 1*. Number 7 in Mathematical Surveys. American Mathematical Society, 2nd edition, 1967.

[2] Pál Dömösi and Chrystopher L. Nehaniv. *Algebraic Theory of Finite Automata Networks: An Introduction*, volume 11 of *SIAM Series on Discrete Mathematics and Applications*. Society for Industrial and Applied Mathematics, 2005.

[3] Attila Egri-Nagy, Chrystopher L. Nehaniv, and James D. Mitchell. SGPDEC – *software package for Hierarchical Composition and Decomposition of Permutation Groups and Transformation Semigroups, Version 0.9.4*, 2022. `https://gap-packages.github.io/sgpdec/`.

[4] Samuel Eilenberg. *Automata, Languages and Machines*, volume B. Academic Press, 1976.

[5] The GAP Group. *GAP – Groups, Algorithms, and Programming, Version 4.12.2*, 2022.

[6] John M. Howie. *Fundamentals of Semigroup Theory*, volume 12 of *London Mathematical Society Monographs New Series*. Oxford University Press, 1995.

[7] Gerard Lallement. *Semigroups and Combinatorial Applications*. Pure and Applied Mathematics. Wiley, New York, 1976.

[8] J. D. Mitchell et al. *Semigroups - GAP package, Version 5.2.1*, Mar 2023.

[9] H. Paul Zeiger. Cascade synthesis of finite state machines. *Information and Control*, 10(4):419–433, 1967. Erratum: **11**(4): 471 (1967).

[10] H. Paul Zeiger. Cascade Decomposition Using Covers. In Michael A. Arbib, editor, *Algebraic Theory of Machines, Languages, and Semigroups*, chapter 4, pages 55–80. Academic Press, 1968.

The VI International AMMCS
Interdisciplinary Conference
Waterloo, Ontario, Canada

Markoff mod p Graphs and Maximal Divisors

J. Eddy[1], E. Fuchs[2], M. Litman[3], D. Martin[4]

[1] *University of California, Davis, USA, jeddy@ucdavis.edu*
[2] *University of California, Davis, USA, efuchs@math.ucdavis.edu*
[3] *University of California, Davis, USA, mclitman@ucdavis.edu*
[4] *University of California, Davis, USA, daemartin@ucdavis.edu*

The Markoff graph is formed by taking one vertex for each nonzero integer solution to $x^2+y^2+z^2=3xyz$ and connecting two vertices with an edge when one triple can be obtained from the other by a Vieta involution: $(x,y,z)\mapsto(yz-x,y,z)$, $(x,y,z)\mapsto(x,xz-y,z)$, or $(x,y,z)\mapsto(x,y,xy-z)$. As Markoff showed in 1879 [1], the Markoff graph is simply a 3-regular tree. Complications arise, however, when triples from $\mathbb{Z}^3$ are replaced by triples from $(\mathbb{Z}/p\mathbb{Z})^3$ that solve $x^2+y^2+z^2\equiv 3xyz \bmod p$ for some prime p. The resulting graph is generally far from simple. In fact, there is currently no known, efficient way to find a path from one vertex to another, nor is it known whether such a path always exists. (Though Silverman has just given a path-finding algorithm with subexponential complexity under some heuristic assumptions [2].) It was first conjectured by Baragar in 1991 that Markoff mod p graphs are indeed path connected [3], but only the last 8 years has seen significant progress toward a proof. Specifically, Bourgain, Gamburd, and Sarnak showed that the set of primes for which the Markoff graph is connected has density 1 among all primes [4], and a subsequent result of Chen's implies that the set of exceptional primes is in fact finite [5].

In this talk, we show that the Markoff mod p graph is connected if $p > 2.564\cdot 10^{394}$. The novel theory behind this lower bound is that of maximal divisors. We call a divisor of $n\in\mathbb{N}$ maximal with respect to some $x\in\mathbb{R}$ if it neither exceeds x nor properly divides another divisor of n not exceeding x. We give explicit upper bounds on the number of maximal divisors (depending on the relative sizes of n and x) along with data that suggests a conjectural refinement of our bound, and we discuss how maximal divisors find use in analyzing certain inclusion-exclusion summations like those appearing in Bourgain, Gamburd, and Sarnak's work on Markoff mod p graphs.

References

[1] A. Markoff, *Sur les formes quadratiques binaires indéfinies*, Math. Ann. **15**, pp. 381–409 (1879).
[2] J. Silverman, *A Heuristic Subexponential Algorithm to Find Paths in Markoff Graphs Over Finite Fields* , arXiv:2211.08511 (2022).
[3] A. Baragar, *The Markoff equation and equations of Hurwitz*, PhD Thesis, Brown University (1991).
[4] J. Bourgain, A. Gamburd, and P. Sarnak, *Markoff Surfaces and Strong Approximation: 1*, arXiv:1607.01530 (2016).
[5] W. Chen, *Nonabelian level structures, Nielsen equivalence, and Markoff triples*, To appear in Ann. Math. (2022).

Data-driven modelling of two-dimensional chaotic fluid flows

J. Alam[1], S. Mugdho[2]

[1] *Memorial University of Newfoundland, Canada, alamj@mun.ca*
[2] *Memorial University of Newfoundland, Canada, ssmugdho@mun.ca*

The solution of the Navier-Stokes equations at high Reynolds number is generally chaotic, random, dissipative, and characterized by a wide range of length and time scales. Recently, data-driven methods have gained increasing popularity for the analysis of Navier-Stokes turbulent flows. This is a critically important new direction because the question concerning global-in-time existence of smooth solutions remain open as one of the milliennium problems of the Clay Mathematics Institute. In this paper, we propose a data-driven methodology to perform a computational search for the observability and reconstruction of 2D Navier-Stokes flows. First, we study the proper orthogonal decomposition (POD) method for observing some a priori bounds of the spatial solution modes on a finite time interval $[0,T]$:

$$\int_0^T ||\boldsymbol{u}(\boldsymbol{x},t')||_{L^q(\Omega)}^{\frac{4q}{3(q-2)}} dt' \leq \mathscr{E}_0^{\frac{2q}{3(q-2)}},$$

where $\mathscr{E}_0 := \frac{1}{2}||\boldsymbol{u}(\boldsymbol{x},0)||_{L^2(\Omega)}$, $3 \leq q \leq 6$, and $\boldsymbol{u}(\boldsymbol{x},t)$ is a local solution of the Navier-Stokes equation. Next, we study the dynamic mode decomposition (DMD) technique to reconstruct the observed solution and predict the future state in order to analyse the global-in-time regularity of classical solutions. In particular, we present the DMD analysis of moving shocks in 1D Burgers equation and chaotic dynamics in 2D Navier-Stokes equations in the presence of cylinder- and airfoil-like solid objects. We show that if the dynamics is observed by maximizing the energy on a low-dimensional space, the dynamic modes of the flow captures the global in time regularity of the solution. The results indicate that the smooth solution is uniquely determined by a finite set of successive observations, where the necessary number of observations depends on the chaotic nature of the dynamics. Thus, the data-driven DMD analysis of 3D Navier-Stokes flows at very high Reynolds number may reconstruct the global-in-time smooth solution if the observations capture the maximum growth of the energy.

Mathematical modelling of the adaptive immune response: B-lymphocytes and SARS-CoV-2 neutralizing antibodies

S. Farhang-Sardroodi[1,2,3], X. Deng[4], S. Gazeau[4], S. Portet[1], J. Arino[1], K. L. Liao[1], M. Craig[4]

[1] *Department of Mathematics, University of Manitoba, Winnipeg, Canada, {Suzan.Farhangsardroodi@umanitoba.ca}*
[2] *Centre for Disease Modelling (CDM), York University, Toronto, Ontario, Canada*
[3] *Modelling Infection and Immunity Lab, York University, Toronto, Ontario, Canada*
[4] *Sainte-Justine University Hospital Research Centre and UniversitÃ© de MontrÃ©al, Montreal, Quebec, Canada {morgan.craig@umontreal.ca}*

Mechanistic modelling approaches have become integral to systems biology to describe known physiology and fill in the gaps in our understanding of which complex interactions drive host-pathogen responses. They, therefore, provide valuable insights for public health planning and infectious disease control.

In this mini-symposium, I will present our work on developing a mathematical model to study humoral (antibody-mediated) immunity. B cells and their antibodies are critical to protecting against COVID-19 over time [1]. However, it is increasingly evident that waning antibodies after natural infection or vaccination translate to reduced defence against repeated SARS-CoV-2 infections. To understand the dynamics of antibody production from B cells, we constructed a computational biology model describing B cells and IgG-neutralizing antibodies coupled with host-pathogen interactions. This model provides better insight into the kinetic processes and mechanisms driving the humoral response against SARS-CoV-2. Our model delineates the initiation of B cell responses through their differentiation to germinal center cells, long-lived plasma cells, and memory cells. It sheds light on how antibodies are produced in primary and secondary reactions.

References

[1] Akkaya, M., Kwak, K., & Pierce, S. K., *B cell memory: building two walls of protection against pathogens*, Nature Reviews Immunology, **20**, 4, pp. 229-238 (2020).

Analysis of the Semigroup Related to the Petri Net of a Traffic Roundabout

M. Zheplinska[1], C. L. Nehaniv[1]

[1] *University of Waterloo, Waterloo, Canada, {mzheplin,cnehaniv}@uwaterloo.ca*

The Petri nets have proven their effectiveness in modeling discrete dynamic systems whose state evolves over configuration space in discrete time steps [4]. In this paper, we construct a Petri net that models the flow of cars on a roundabout with n entrances, which is symmetrical about its places, and analyse the semigroup related to the constructed Petri net. An example of the "roundabout" Petri nets with 3 and 4 entrances can be seen in Figure 1. The paper focuses on investigating the complexity of the model in Krohn-Rhodes terms using the holonomy decomposition of the "roundabout" transformation semigroup and the general properties of such Petri nets for different n [2, 1]. The Petri net is built and converted into a corresponding transformation semigroup with the

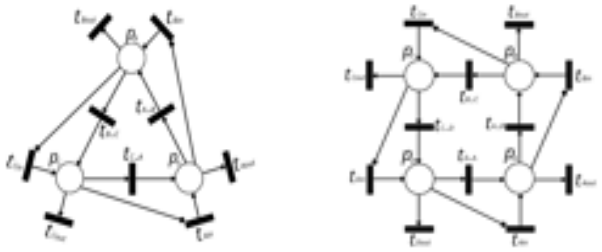

Figure 1: The Petri net of a roundabout with 3 entrances (left) and 4 entrances (right). Circles denote places that can be occupied by single vehicles. Transitions, represented by rectangles and arrows connect places and allow a vehicle 1) to leave roundabout or 2) to enter the roundabout (though this is inhibited by the presence of a vehicle to the left of the entrance place) and also 3) to move forward clockwise into a place unless it is occupied by another vehicle.

GAP computer algebra system [3], particularly the *pn2a* package [5]. We examine the resulting semigroup using holonomy decomposition with the *SgpDec* package [6], which represents the hierarchical structure of the building blocks of the semigroup. We study the natural subsystems of the configuration space and the permutator groups acting on them, some of which are non-abelian or non-solvable.

Exploring the "roundabout" Petri net using holonomy decomposition has given us a deeper understanding of the processes taking place on the traffic roundabout. We obtain interesting patterns of changes in the number and location of vehicles on the traffic roundabout, which are described by permutator groups.

References

[1] A. Egri-Nagy and C. L. Nehaniv, Algebraic properties of automata associated to Petri nets and applications to computation in biological systems. *Biosystems*, 94(1-2):135-144, 2008.

[2] H. Paul Zeiger. Cascade synthesis of finite state machines. *Information and Control*, 10(4):419–433, 1967. Erratum: **11**(4): 471 (1967).

[3] The GAP Group. GAP - Groups, Algorithms, and Programming. `http://www.gap-system.org` .

[4] James Lyle Peterson. *Petri Net Theory and the Modeling of Systems*. Prentice-Hall, Englewood Cliffs, NJ, 1981.

[5] A. Egri-Nagy, C.L. Nehaniv. PN2A: Petri Net Analysis GAP Package. `https://github.com/egri-nagy/pn2a` .

[6] A. Egri-Nagy, J. D. Mitchell, C. L. Nehaniv, (2015). SgpDec: Cascade (de)compositions of finite transformation semigroups and permutation groups. In: Hong, H., Yap, C. (eds) Mathematical Software – ICMS 2014. Lecture Notes in Computer Science, vol 8592, pp 75-82, Springer, Berlin, Heidelberg. `https://github.com/gap-packages/sgpdec` .

The VI International AMMCS
Interdisciplinary Conference
Waterloo, Ontario, Canada

The study of the transformation semigroup of the Abelian and directed non-Abelian sandpiles

H. Derets[1], C. L. Nehaniv[2]

[1] *University of Waterloo, Waterloo, Canada, h2derets@uwaterloo.ca*
[2] *University of Waterloo, Waterloo, Canada, chrystopher.nehaniv@uwaterloo.ca*

The sandpile model was introduced in 1987 [1], [2] to study self-organized criticality. It is a discrete event dynamical system always considered on a fixed graph with certain toppling rules for the stabilization of the configurations of the graph. Such a model leaves room for the variability of both the graph and the stabilization rules. In this work, we consider the well-known Abelian sandpile model (ASM) on finite graphs of certain families and the non-Abelian model on directed rooted trees defined in [3].

The interest of the study is the structure of the semigroup and group of recurrent configurations of the sandpile, the neutral element and the generators of this group, as well as idempotents, and possible decompositions of the semigroups. In ASM we have a semigroup acting on itself and can consider the recurrent group of sandpile that is the minimal ideal of the commutative monoid. So, for example, the initial study for the Abelian sandpile shows the cyclicity of the recurrent group of a circle graph with one sink vertex and the dependence of the general form of the generator and the neutral element on the size of the graph. In the case of the semigroup being aperiodic as in the case of a non-Abelian sandpile semigroup on a directed rooted tree, we can study the aperiodic complexity [4] of the semigroup and constructively show the emulation of the sandpile semigroup by the wreath product of irreducible semigroups.

References

[1] Bak, P., Tang, C. & Wiesenfeld, K. Self-organized criticality. *Physical review A* 38, 364 (1988).

[2] Bak, P., Tang, C. & Wiesenfeld, K. Self-organized criticality: An explanation of the 1/f noise. *Physical review letters* 59, 381 (1987).

[3] Ayyer, A., Schilling, A., Steinberg, B. & Thiery, N. M. Directed nonabelian sandpile models on trees. *Communications in Mathematical Physics* 335, 1065-1098 (2015).

[4] Nehaniv, C. L. Complexity of finite aperiodic semigroups and star-free languages in *Semigroups, Automata and Languages* (eds Jorge Almeida, G. M. S. G. & Silva, P. V.) 195-209 (World Scientific Press, Singapore, 1996).

The VI International AMMCS
Interdisciplinary Conference
Waterloo, Ontario, Canada

Order Symmetry: A New Fairness Criterion for Assignment Mechanisms

Rupert Freeman[1], Mark C. Wilson[2], Geoffrey Pritchard[3]

[1] *University of Virginia*
[2] *University of Massachusetts Amherst*
[3] *University of Auckland, New Zealand*

We introduce a new criterion, *order symmetry*, for assignment mechanisms that match n objects to n agents with ordinal preferences over the objects. An assignment mechanism is order-symmetric with respect to some probability measure over preference profiles if every agent is equally likely to receive their favorite object, every agent is equally likely to receive their second favorite, and so on. When associated with a sufficiently symmetric probability measure, order symmetry is a relaxation of anonymity that, crucially, can be satisfied by discrete assignment mechanisms. Furthermore, it can be achieved without sacrificing other desirable axiomatic properties satisfied by existing mechanisms. In particular, we show that it can be achieved in conjunction with strategyproofness and universal efficiency via the Top Trading Cycles mechanism (but not Serial Dictatorship). The practical utility of order symmetry is substantiated by simulations on Impartial Culture and Mallows-distributed preferences for four common assignment mechanisms. Our formalization clarifies the difference between TTC and RSD, which have been treated as completely equivalent by many authors over the last 25 years.

The VI International AMMCS
Interdisciplinary Conference
Waterloo, Ontario, Canada

Ensemble Monte Carlo Penalty Finite Element Method for Navier-Stokes Equations with Random Forcing and Initial Conditions

R. Fang[1], W. Layton[2]

[1] *University of Pittsburgh, Pittsburgh, Pennsylvania, USA, ruf10@pitt.edu*

[2] *University of Pittsburgh, Pittsburgh, Pennsylvania, USA, wjl@pitt.edu*

We present a novel approach combining the ensemble Monte Carlo technique with a penalty method to efficiently solve the time-dependent incompressible Navier-Stokes equations (NSE) with random forcing and initial conditions.

Our algorithm solves a linear system with a shared coefficient matrix and multiple right-hand sides, which reduces CPU time and memory usage. By relaxing the incompressibility condition, this algorithm uncouples the velocity and pressure, reducing the computational complexity that enables the use of larger ensemble sizes. Larger ensemble sizes are essential for modeling the uncertainty and variability of flows, particularly for turbulent flows.

We first apply this algorithm to deterministic NSE and derive an optimal error estimate of the numerical velocity using the finite element method with temporal and spatial discretization. Then, we extend it to the NSE with random forcing and initial conditions, which captures the uncertainty and variability in fluid flow.

Theoretical analysis demonstrates the accuracy of our approach. This approach shows promising results in improving flow predictions and has the potential to enhance the efficiency and accuracy of fluid simulations. We are currently conducting numerical experiments to validate the accuracy and performance of our method.

On Optimization of Conservation laws with space discontinuous flux

F.Ancona[1]

[1] *University of Padova, Italy, ancona@math.unipd.it*

We shall discuss optimization problems for conservation laws with space discontinuous flux or evolving at a junction. Such problems are investigated in the context of inflow controls acting at the discontinuity interface or of distribution controls acting at the junction. The analysis and characterization of the corresponding attainable profiles at a fixed time for these problems yields the existence of optimal solutions. Applications to traffic flow and petroleum reservoir models will be addressed.

References

[1] F. Ancona, A. Cesaroni, G. M. Coclite, M. Garavello, *On the optimization of conservation law models at a junction with inflow and flow distribution controls*, SIAM J. Control Optimization **56**(5), pp. 3370-3403 (2018).

[2] F. Ancona, A. Cesaroni, G. M. Coclite, M. Garavello, *On optimization of traffic flow performance for conservation laws on network*, Minimax Theory Appl. **6**(2), pp. 205-226 (2021).

[3] F. Ancona, M.T. Chiri, *Attainable profiles for conservation laws with flux function spatially discontinuous at a single point*, ESAIM: COCV **26**(124), pp. 1-33 (2020).

[4] F. Ancona, L.Talamini, *Backward-forward characterization of attainable set for conservation laws with spatially discontinuous flux*, in preparation (2023).

The VI International AMMCS
Interdisciplinary Conference
Waterloo, Ontario, Canada

Advances in Tabulating Carmichael Numbers

A. Shallue[1], J. Webster[2]

[1] *Illinois Wesleyan University, Bloomington, IL, ashallue@iwu.edu*
[2] *Butler University, Indianapolis, IN, jewebste@butler.edu*

A Carmichael number is a squarefree, composite, integer n that is a Fermat pseudoprime to the base a for every a relatively prime to n. Carmichael numbers have long been of theoretical and practical interest. On the one hand, they exhibit divisibility properties that are of mathematical interest. On the other hand, a table of Carmichael numbers is useful for primality testing.

The presenter will report on new work that gives algorithmic improvements to the problem of tabulating Carmichael numbers, the first such improvements since the work of Pinch [1]. These improvements are expected to culminate in world record tabulations.

References

[1] B. Pinch, *The Carmichael numbers up to* 10^{15}, Math. Comp. **61**(203), 381-391 (1993).

The VI International AMMCS
Interdisciplinary Conference
Waterloo, Ontario, Canada

What can theta functions tell us about abelian threefolds?

C. Vincent[1]

[1] *University of Vermont, Burlington, USA christelle.vincent@uvm.edu*

In this talk we will summarize our work of the last six years on the construction of CM Jacobians of dimension 3 over $\mathbb{C}$, done jointly with Sorina Ionica, Pinar Kılıçer, Kristin Lauter, Elisa Lorenzo Garcìa, Maike Massierer, and Adelina Mânzăţeanu. We begin with a period matrix for a complex abelian threefold which we have constructed to have complex multiplication by a sextic field, to be simple, and to admit a principal polarization. From these objects we can compute the *theta constants* associated to the threefold, which are the values taken by some theta functions when evaluated at a period matrix of the threefold. Over the years we have succeeded in wresting a lot of very cool information from these constants!

The VI International AMMCS
Interdisciplinary Conference
Waterloo, Ontario, Canada

Algebraic Structure and Complexity of Games

Z. Gao[1], C. L. Nehaniv[2], A. Egri-Nagy[3]

[1] *University of Waterloo, Waterloo, z72gao@uwaterloo.ca*
[2] *University of Waterloo, Waterloo, cnehaniv@uwaterloo.ca*
[3] *Akita International University, Akita, Japan, egri-nagy@aiu.ac.jp*

In this study, we explore the algebraic structure of two-player games and verify their complexity. Assuming that a game has discrete and finite action and observation space, we define its complexity to be the minimal Krohn-Rhodes complexity among the best-play automata. This definition was first introduced by Rhodes, who also made several conjectures on the complexity of Tic Tac Toe, Nim, Hex, and Go [1]. Therefore, our main objective is to find suitable state-space formulations for these games, construct their best-play automata, decompose and analyze their complexity. Wherever applicable, we also aim to make connections to classical game theory. For example, Sprague-Grundy theorem states that all impartial games have equivalent nimbers [2]. We shall compare nimbers and their resulting winning strategies with our assorted impartial game complexity findings.

We apply the following methodology. Firstly, we perform a full minimax tree search to obtain the optimal sets of strategies each player could use. Secondly, we nondeterministically choose an optimal strategy for one of the players and construct a optimal-play automaton. Thirdly, we apply tools such as SgpDec to decompose this transformation semigroup and check its complexity [3]. At the present moment, we have decomposed several simple games. For example, a sample machine for Tic Tac Toe is shown in Fig. 1 below. In this construction, each state is a board position in opponent's view, and each arrow with label (0-8) represents a possible move from the opponent. The arrow leads to a new state where our player made an optimal response to the opponent's move already. A duplicate therefore illegal move will go to a garbage state permanently. We found two natural subgroups acting on valid game states, which implies a Krohn-Rhodes complexity at most 2.

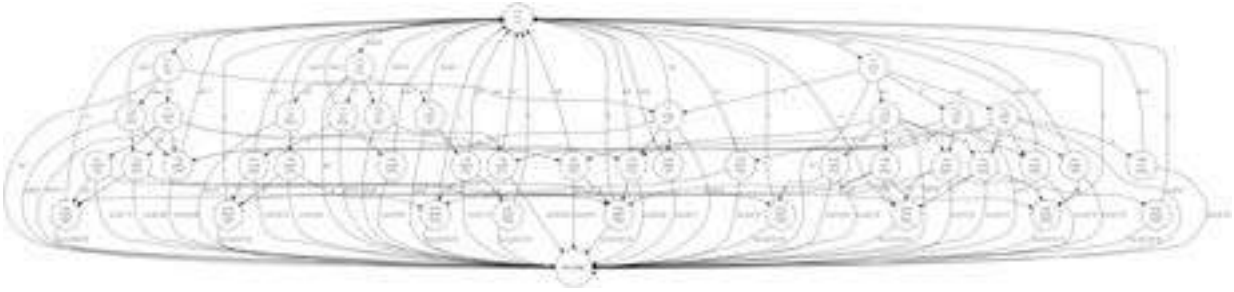

Figure 1: One construction of optimal gameplay machine for Tic Tac Toe.

This study is significant because it provides an abstract algebraic view on finite discrete games. We construct hierarchical coordinate systems to navigate their optimal gameplay loops and study their complexities. Overall, our research serves to bridge the gap between algebraic automata theory and classical game theory.

References

[1] J. Rhodes, *Complexity of Games*, in *Applications of Automata Theory and Algebra*, World Scientific, pp. 241-256 (2009).
[2] A. N. Siegel, *Combinatorial Game Theory*, American Mathematical Society, Providence, RI, pp. 180-181 (2013).
[3] A. Egri-Nagy, J. D. Mitchell and C. L. Nehaniv, *SgpDec: Cascade (De)Compositions of Finite Transformation Semigroups and Permutation Groups*, in *Mathematical Software ICMS 2014*, ed. H. Hong and C. Yap, Springer Berlin Heidelberg, pp. 75-82 (2014).

A Pressure-Based Model of IV Fluid Therapy Induced Volume Kinetics in Cats

Sarah Abel[1], Xiu Ting Yiew[2], Shane Bateman[3], Allan R. Willms[4]

[1] *Department of Mathematics & Statistics, University of Guelph, Canada, sabel01@uoguelph.ca*
[2] *Department of Clinical Studies, Ontario Veterinary College, University of Guelph, Canada, xyiew@uoguelph.ca*
[3] *Department of Clinical Studies, Ontario Veterinary College, University of Guelph, Canada, sbateman@uoguelph.ca*
[4] *Department of Mathematics & Statistics, University of Guelph, Canada, awillms@uoguelph.ca*

Medical health care for pets is becoming more common. For this reason, veterinary researchers are interested in the kinetics of intravenous (IV) fluid therapy and how it affects the movement of fluids within animals. Clinical researchers have in the past used a heuristic linear ordinary differential equation (ODE) model, designed initially for humans, that attempts to mimic these kinetics [1, 2]. However, this model is, at best, only loosely based on the physical and biological realities of the phenomena. We have developed a nonlinear ODE model for these volume kinetics that is based on pressure, both hydrostatic and osmotic, as the driving force in volume changes in the plasma and the interstitial space. Our model is of the same order of complexity as the linear model, having the same number of free parameters. To assess the model we have compared our new model's and the linear model's abilites to fit experimental data from cats. These experiments involved measuring hemoglobin, hematocrit, red blood cell count, blood pressure, urine excretion, and other physiological properties in cats undergoing IV fluid therapy every 5 to 15 minutes for 3 hours. These data were used to determine blood plasma volume and urine volume over time. Although the data are somewhat noisy and both models are relatively gross caricatures of the complicated biological and physical processes involved, the comparison indicates that our model better captures the kinetics of these volume spaces, especially when blood pressure data are included in the models.

References

[1] L. Ståhle , A. Nilsson and R. G. Hahn, *Modelling the volume of expandable body fluid spaces during I.V. fluid therapy*, British Journal of Anaesthesia, **78**, pp. 138-143 (1997).

[2] R. G. Hahn, D. Drobin and J. Zdolsek, *Distribution of crystalloid fluid changes with the rate of infusion: A population-based study*, Acta Anaesthesiologica Scandinavica, **60**, pp. 569–578 (2016), doi: 10.1111/aas.12686.

The VI International AMMCS
Interdisciplinary Conference
Waterloo, Ontario, Canada

Diverse myelination patterns impact action potential conduction timing

A. Talidou[1,2], J. Lefebvre[1,2,3]

[1] *University of Ottawa, Canada, {Afroditi.Talidou, Jeremie.Lefebvre}@uottawa.ca*
[2] *Krembil Brain Institute, Canada*
[3] *University of Toronto, Canada*

The white matter (WM) consists mostly of myelinated axons that support coordination of neural signals between different brain regions. The conduction of action potentials (APs) along WM is sensitive to myelin, a lipid-rich material wrapping around axons in a spiral fashion, formed by glial cells called oligodendrocytes. Myelin notably influences the time it takes for APs to traverse towards their post-synaptic targets (known as conduction delay). How do changes of myelin sheath length and location along individual axons influence conduction timing? Previous studies aiming to answer this question are based on the simplified assumption that myelin sheaths are periodically located along axons and are thus very symmetric. However, periodic myelin patterns are far from reality. Experimental results in mice show distinct myelin patterns [1]. In our work we estimate conduction delays along axons of diverse myelination, namely the myelin sheaths have different longitudinal lengths and are randomly distributed along axons.

We build a comprehensive mathematical model based on the cable theory [2]:

$$\frac{\partial u}{\partial t} = k\frac{\partial^2 u}{\partial x^2}\,, \tag{1}$$

$$\frac{\partial u}{\partial t} = k\frac{\partial^2 u}{\partial x^2} + I(u)\,, \tag{2}$$

$$u_-(\alpha,t) = u_+(\alpha,t) \quad \text{and} \quad \frac{\partial u_-}{\partial x}(\alpha,t) = \frac{\partial u_+}{\partial x}(\alpha,t)\,, \tag{3}$$

where $k \in R$, $x \in [x_{min}, x_{max}]$ and $t > 0$. The solution of Eq. 1 is the AP within a myelinated segment. Eq. 2 describes the dynamics at an unmyelinated segment. The highly nonlinear term $I(u)$ is the sum of the ionic currents. At the interface (α) between a myelinated and an unmyelinated segment we apply continuity conditions (see Eq. 3). By adding appropriate initial and boundary conditions we solve the system numerically using advanced techniques. Given the complexity of the nonlinear system some mathematical analysis is provided whenever possible.

We found that low levels of myelination incur high variability of conduction timing whereas higher levels of myelination are more robust to lengthwise geometric changes of myelin sheaths. By increasing the lengths of individual axons we found that conduction time varies with axon length – AP conduction delays are variable on longer axons.

References

[1] G. S. Tomassy et al., *Distinct Profiles of Myelin Distribution Along Single Axons of Pyramidal Neurons in the Neocortex*, Science, Vol 344, Issue 6181, pp. 319-324 (2014).

[2] G. Ashida, W. Nogueira, *Spike-Conducting Integrate-and-Fire Model*, eNeuro, **4** 5 (2018).

Evaluating and Improving Flow Models for Low Permeability Media

S. Schrader[1], L. Davis[2]

[1] *Montana Technological University, Butte, USA sschrader@mtech.edu*
[2] *Montana State University, Bozeman, USA lisa.davis@montana.edu*

The governing equations for fluid flow in porous media are often based on Darcy's Law (1), which relates the flow rate of a fluid to the permeability of the media k, the viscosity of the fluid μ, and the pressure gradient causing the flow. The numerical models resulting from these equations have wide applications but encounter significant challenges when the permeability is low.

$$q = -\frac{kA}{\mu}\frac{dp}{dx} \tag{1}$$

The objective of this work is to improve the numerical modeling of low permeability flow by first investigating the effects of the low permeability on the performance of numerical models and then using an empirically derived model to replace Darcy's Law in the development of the numerical model and comparing the results. A PDE has been developed for time dependent flow of slightly compressible fluid (liquid with a significant amount of dissolved gas) by combining Darcy's Law with Conservation of Mass and a fluid model based on a small and constant fluid compressibility. The governing equation has the form given below.

$$\frac{\partial^2 p}{\partial x^2} = \varphi(c_t)\frac{\mu}{k}\frac{\partial p}{\partial t} \tag{2}$$

For the numerical study, dimensionless parameters are found using the Buckingham PI theorem to provide a dimensionless PDE. This equation is discretized and solved, providing a tool to monitor how numerical performance changes with lower permeability. Fuquan [1] classifies low permeability reservoirs as those with a permeability less than 0.05 darcies, and [1] states that flow in such reservoirs does not follow Darcy's Law. In these cases an alternative to Darcy's Law is needed in order to successfully model flow of incompressible fluids in steady state conditions. Alternative models have been developed based on empirical data, including a threshold pressure gradient model (3) developed by Huang [2].

$$v = \left\{ \begin{array}{ll} 0 & \frac{dp}{dx} < G \\ \frac{-k}{\mu}\left(\frac{dp}{dx} - G\right) & \frac{dp}{dx} \geq G \end{array} \right\} \tag{3}$$

To improve the modeling of the time dependent case for slightly compressible fluids, the threshold pressure gradient model has also been combined with Conservation of Mass and the slightly compressible fluid model to develop a PDE designed for transient flow. Numerical simulations allow us to compare the numerical performance with those of the model based on Darcy's Law. This comparison allows us to determine if this approach gives better numerical performance. The validity of the results of the new model will be further investigated by the construction of a laboratory apparatus designed to provide the same type of boundary condition control and pressure measurements predicted by the numerical model. This new way of modeling low permeability flow can have a significant impact for the goal of developing full field scale simulation tools for subsurface modeling.

References

[1] S. Fuquan et al, , *Single and two-phase flow model in low-permeability reservoir*, Petroleum. **2**, 1, pp. 183*190 (2019).
[2] Y. Huang et al, *An overview on nonlinear porous flow in low permeability porous media*, in *Theoretial and Applied Mechanics Letters* Vol 3, No 2 (2013).

The VI International AMMCS
Interdisciplinary Conference
Waterloo, Ontario, Canada

Hyperelliptic curves in abelian surfaces

E. Gazaki[1], J. Love[2]

[1] *University of Virginia, Charlottesville, USA, eg4va@virginia.edu*
[2] *Centre de recherches mathématiques / McGill University, Montreal, Canada, jon.love@mcgill.ca*

We describe a method to produce a large collection of pairwise non-isomorphic hyperelliptic curves that all map birationally into a product of elliptic curves, and discuss applications to rational equivalences in Chow groups and rational curves in Kummer surfaces.

Algebraic Applications in Investigation of Musical Symmetry

O. Ibragimova[1], C. L. Nehaniv[1]

[1] *University of Waterloo, Waterloo, Canada, oibragim@uwaterloo.ca*

This study explores the intersection of mathematics and music theory by investigating the algebraic structures of discrete dynamical systems in the context of musical symmetry. Building on a body of literature that demonstrates the applications of mathematics in music theory, including Michiel Schuijer's "Analyzing Atonal Music Pitch-Class Set Theory and Its Contexts" [1], which presents a pitch-class set theory application in musicology, and Robert W. Peck's application of the wreath product to concepts in music theory [2], this study formalizes notes, melodies, and operations over them in algebraic terms, presenting a dynamical system that models the space of melodies and operations over them. The obtained dynamical system is analyzed in detail, including finding equations for symmetric melodies and providing solutions for them. Concrete examples of symmetric melodies for each symmetry case are provided. The methodology involves defining domains of notes and melodies as sets and presenting possible dynamical systems in terms of transformation groups and semigroups. The study demonstrates the potential for mathematical approaches to uncover new insights in the arts by utilizing dynamical systems. The findings contribute to the growing body of research on the application of algebra to music theory, offering new avenues for analyzing musical works. The significance of this study lies in its ability to combine diverse fields, showcasing the importance of interdisciplinary research in unlocking new perspectives in the arts. It is hoped that this study will inspire further exploration of the intersection between mathematics and music theory.

References

[1] Schuijer, Michiel. *Analyzing atonal music: Pitch-class set theory and its contexts*. University Rochester Press, 2008.
[2] Peck, Robert W. *"Wreath products in transformational music theory."* Perspectives of New Music 47.1 (2009)

A Numerical Study of Time Filtered Schemes for Hyperbolic Equations

L. Davis[1], C. Drapaca[2], F. Pahlevani[3]

[1] *Montana State University, Bozeman, USA, lisa.davis@montana.edu*
[2] *Penn State University, State College, USA, csd12@psu.edu*
[3] *Penn State University, Abington College, Abington, USA, fxp10@psu.edu*

The focus of this presentation is the development and analysis of a time filtering process for a linear hyperbolic equation motivated by the modeling of the transcription of ribosomal RNA in bacteria (see Refs. [1, 2]). Recently the time filter has been combined with fully implicit schemes for nonlinear problems in order to increase accuracy with minimal modifications to existing code (see Ref. [3]). In this talk, we demonstrate the numerical study of adding a time filter to first and second order schemes for hyperbolic problems. A new explicit implementation is presented, and increased accuracy of the filtered upwind scheme is observed for test problems. The typical treatments for explicit schemes for hyperbolic problems require calculations for CFL conditions in order for the filtered schemes to remain stable. A stability condition for the new algorithm is derived. Numerical computations illustrate stability and convergence as well as dissipation and dispersion of the filtered schemes.

References

[1] L. Davis, F. Pahlevani and T. Susai Rajan, *An Accurate and Stable Filtered Explicit Scheme for Biopolymerization Processes in the Presence of Perturbations*, Applied and Computational Math. **10**, 6, pp. 121-137 (2021).
[2] K. Boatman, L. Davis, F. Pahlevani and T. Susai Rajan, *Numerical Analysis of a Time Filtered Scheme for a Linear Hyperbolic Equation Inspired by DNA Transcription Modeling*, Journal of Computational and Applied Math. **429** (2023).
[3] A. Guzel and W. Layton, *Time filters increase accuracy of the fully implicit method*, BIT Numerical Math. 58, pp. 301-315 (2018).

Decay rates for the damped wave equation with time dependent damping

P. Kleinhenz[1],

[1] *Michigan State University, East Lansing, USA kleinh29@msu.edu*

Given a Riemannian manifold (M,g) and a nonnegative function $W \in C^0(M)$, the initial value problem for the damped wave equation is

$$(\partial_t^2 - \Delta_g + W\partial_t)u = 0, \quad (u, \partial_t u)|_{t=0} = (u_0, u_1) \in H^1(M) \times L^2(M). \tag{1}$$

It describes the evolution of a vibrating system in the presence of a damping force, W.

The quantity of particular interest is the energy

$$E(u,t) = \frac{1}{2}\int_M |\nabla u|^2 + |\partial_t u|^2 dx. \tag{2}$$

This energy is non-increasing, so it is of interest to find a rate $r(t) \to 0$ as $t \to \infty$, such that

$$E(u,t) \leq r(t)E(u,0), \tag{3}$$

for all solutions with initial data in $H^1(M) \times L^2(M)$. It was shown in [1, 2] that (3) holds with $r(t) = Ce^{-ct}$, if and only if, the damping satisfies the Geometric Control Condition (GCC). The GCC is the existence of some $L > 0$ such that every geodesic of length at least L intersects $\{W > 0\}$.

It is natural to consider the case where the damping W depends on time as well. In [3] it was shown that if W is time periodic and satisfies the finite time Geometric Control Condition (ftGCC), then (3) holds with $r(t) = Ce^{-ct}$. The ftGCC is the existence of some $T > 0$ such that every geodesic in $M \times [0,\infty)$ starting from $t = 0$ intersects $\{W > 0\}$ by time T.

I will discuss a generalization of these results to full time dependence. Let $\phi_t(x,\xi)$ be the geodesic in M starting at $(x,\xi) \in S^*M$. The time dependent Geometric Control Condition (tGCC) is the existence of some $\overline{C} > 0, T_0 > 0$, such that for all $(x,\xi) \in S^*M, t_0 \in [0,\infty)$ and $T > T_0$

$$\frac{1}{T}\int_0^T W(\phi_t(x,\xi), t + t_0)dt \geq \overline{C}. \tag{4}$$

If the tGCC holds, then exponential decay occurs in (3). This notion of long time averages of the damping comes from [4], where it was shown this is equivalent to the GCC when W does not depend on time. When W is time periodic this is equivalent to the finite time GCC of [3]. The proof of exponential energy decay relies on a careful application of propagation of singularities, where the escape function is explicitly constructed to ensure the uniformity of constants.

References

[1] J. Rauch and M. Taylor *Exponential Decay of Solutions to Hyperbolic Equations in Bounded Domains*, Indiana Univ. Math. J., **24**, 1, pp.79-86 (1975).

[2] J. Ralston, *Solutions of the wave equation with localized energy*, Communications on Pure and Applied Mathematics, **22**, 6, pp.807-823 (1969).

[3] J. Le Rousseau, G. Lebeau, P. Terpolili, E. Trélat, *Geometric control condition for the wave equation with a time-dependent observation domain*, Analysis & PDE, **10**, 4, pp.983-1015, 2017.

[4] G. Lebeau, *Equation des Ondes Amorties* in *Algebraic and Geometric Methods in Mathematical Physics: Proceedings of the Kaciveli Summer School, Crimea, Ukraine, 1993*, Springer Netherlands, pp.73-109 (1996).

Complex oscillatory patterns in a predator-prey model featuring three timescales

Susmita Sadhu

Georgia College & State University, Milledgeville, USA, susmita.sadhu@gcsu.edu

We consider a two-trophic ecosystem that models the interaction between a specialist predator (one that relies exclusively on a single prey species), a generalist predator (one that takes advantage of alternative food sources in addition to consuming the focal prey species), and their common prey featuring three-timescales. Assuming that the prey operates on a faster timescale, while the specialist and generalist predators operate on slow and superslow timescales respectively, we portray the model in the framework of singular perturbed system of equations. Treating the predation efficiency of the generalist predator as the primary varying parameter and the proportion of its diet formed by the prey species under study as the secondary parameter, the system exhibits a host of rich and interesting dynamics, such as relaxation oscillations, mixed-mode oscillations, subcritical elliptic bursting, torus canards, and mixed-type torus canards. Grouping the timescales into two classes and using the timescale separation between classes, we perform two-timescale analyses to gain insight about the dynamics. Using the geometric properties and singular flows in combination with bifurcation analysis, we classify the oscillatory dynamics and describe the transitions from one type of dynamics to the other.

References

[1] S. Sadhu, *Complex oscillatory patterns in a three-timescale model of a generalist predator and a specialist predator competing for a common prey*, Discrete Continuous Dynamical Systems B **28**, 5, pp. 3014-3051 (2023).

Relaxation of heavy hole spins in wurtzite semiconductor quantum dots

S. Prabhaakar[1], R. Melnik[2]

[1] *Northwest Missouri State University, Maryville, MO, USA, sanjay@nwmissouri.edu*
[2] *Wilfrid Laurier University, Waterloo, Canada, rmelnik@wlu.ca*

Based on stain dependent 8-band *k.p* method, we investigate the phonon mediated spin flip rate in wurtzite GaN Quantum Dots (QDs). In an unstrained QDs, our study shows that the crossing between heavy holes and light holes with opposite spin states takes place with the accessible values of the magnetic fields. As a result, we find the cusp-like structure in the spin flip rate near the crossing point. However, in strained QDs with piezo-electromechanical effects, the relaxation rate for heavy holes is a monotonous function of the magnetic fields. Also, the spin relaxation rate for electrons in the conduction band in both unstrained and strained (with piezo-electromechanical effects) QDs are a monotonous function of the magnetic fields. In particular, piezo-electromechanical effects enhance the phonon mediated spin-flip rate by two orders of magnitude at low magnetic fields. We also analyze the individual contribution of longitudinal, transverse acoustic phonon and phonon due to longitudinal acoustic deformations potentials in the spin transition rates.

References

[1] S. Prabhakar, R. Melnik, LL Bonilla, *Coupled Multiphysics, barrier localization, and critical radius effects in embedded nanowire superlattices*, J. Appl. Phys. **113**, 244306 (2013).
[2] S. Prabhakar, R Melnik, LL Bonilla, *Electrical control of phonon-mediated spin relaxation rate in semiconductor quantum dots: Rashba versus Dresselhaus spin-orbit coupling*, Phys. Rev. B 87,235202 (2013).

Machine-Learning-based Spatial Route Planning in Polar Regions

C. Robertson[1]

[1] *GSTS, Dartmouth, Nova Scotia, colin.robertson@gsts.ca*

Increasing shipping activity in northern regions is anticipated with warming climate, as the number of navigable days increases with declines in sea ice thickness and concentration [1]. An increasingly dynamic sea ice regime raises interesting questions for spatial modelling of optimal shipping routes, which must incorporate a wide variety of factors representing antecedent, current, and forecasted conditions. Geospatial routing in real-world applications typically rely on grid-based approaches to represent the landscape as a friction surface, and movement over this landscape as cost minimization problem. Given the wide geographical area and overall sparsity of ground-truth data in arctic regions, multi-resolution approaches hold some potential. Discrete global grid systems have emerged as a candidate data model for geospatial data integration with multi-resolution properties determined by the system parameter known as aperture. In this paper we explore the unique characteristics of applying DGGS data model to spatial route planning in arctic domain with an emphasis on multi-resolution fusion and route planning. A machine-learning model for spatial route prediction in arctic environment based on the XGBoost modelling framework [2] is introduced and evaluated against vessel trip data. Finally, we discuss implications of route planning models in an applied software deployment context, highlighting aspects of data acquisition, runtime, and model evaluation and retraining. Dynamic spatial route planning algorithms are needed for operational planning of vessel trips and for managing increased vessel traffic density and associated impacts to communities.

References

[1] Min, C. et al. *Toward Quantifying the Increasing Accessibility of the Arctic Northeast Pas-sage in the Past Four Decades*. Adv. Atmos. Sci. (2023).

[2] Chen, T. & Guestrin, C. *XGBoost: A Scalable Tree Boosting System*. in Proceedings of the 22nd ACM SIGKDD International Conference on Knowledge Discovery and Data Mining 785–794 (2016).

Energy-conserved numerical methods for Electromagnetic Propagations in Nonlinear Metamaterials and with Stochastic Noises

Dong Liang[1]

[1] *Department of Mathematics and Statistics, York University, Toronto, M3J 1P3, Canada, dliang@yorku.ca*

Due to unusual physical properties that cannot be found in natural materials, metamaterials have many important applications such as in aerospace application, aircraft radar and radio frequency, microwave and wireless interconnect, nanolithography and medical imaging, cloaking device, and so on. Modeling interaction of electromagnetic waves within nonlinear dispersive media and with stochastic affection is very important. In this talk, we will present our study of energy law of electromagnetic propagations in metamaterials with stochastic noise and nonlinearity and our development of energy-conserved numerical methods for metamaterial electromagnetic computations. Because of the local solution behavior and geometrical and media feature, designing local mesh refinements is crucial to improve the resolution capacity of solution within metamaterials the computation is required to improve the resolution capacity and efficiency of solution. However, in the presence of local mesh refinements, the sudden change of the mesh sizes inevitably produces spurious reflections in the electromagnetic fields. We will also present the energy-conserved local mesh-refined S-FDTD schemes for solving electromagnetic propagations in metamaterials.

Biophysical Modelling of the Mammalian Circadian Clock Suggests Mechanisms for Altered Behaviour of PER2::LUC Mice

A.R. Stinchcombe[1], M.R. Ralph[2]

[1] *Department of Mathematics, University of Toronto, Toronto, Ontario, Canada, stinch@math.toronto.edu*

[2] *Department of Psychology, University of Toronto, Toronto, Ontario, Canada, martin.ralph@utoronto.ca*

A ubiquitous tool in circadian biology is the PER2::LUC mouse, a genetically modified animal with cells that fluoresce along with their internal 24 hour clock. The period 2 (PER2) protein is a core protein in the transcription-translation feedback loop that underlies the circadian clock and its concentration within cells is a direct indication of the time of day. Recently there has been mounting evidence that this genetic modification alters the clock and its response to light [1]. In particular, the intrinsic period in constant darkness is longer in the PER2::LUC mouse than the wildtype mouse and the PER2::LUC mouse has dissociated rhythms in constant light. Is is imperative to understand the cause of these differences, which we address using a detailed simulation [2, 3]. The site of the master clock is the suprachiasmatic nucleus consisting of 20,000 electrically and chemically coupled neurons. The molecular clock is a transcription-translation feedback loop within each neuron that is modelled by a system of 180 ordinary differential equations. On a faster timescale, the electrical activity of these neurons is driven by voltage-gated ion channels, internal calcium dynamics, and synaptic currents, which are described by a ten-variable ordinary differential equation. I will discuss some of the details of our model, as well as the numerical challenges associated with solving this large and multi-scale differential equation. The proposed mechanisms for the altered behaviour of the PER2::LUC mouse arising from the simulation will be compared against wheel-running and open-field activity, structural imaging of the PER2 protein, and genetic sequencing.

References

[1] M.R. Ralph, S. Shi, C.H. Johnson, P. Houdek, T. C. Shrestha, P. Crosby, J.S. O'Neill, M. Sládek, Adam R. Stinchcombe, and Alena Sumová, *Targeted modification of the Per2 clock gene alters circadian function in mPer2 luciferase (mPer2 Luc) mice* PLOS Comput. Biol. **17**, 5, e1008987 (2021).

[2] D. DeWoskin, W. Geng, A.R. Stinchcombe, and D.B. Forger, *It is not the parts, but how they interact that determines the behaviour of circadian rhythms across scales and organisms* Interface Focus **4**, 3, 20130076 (2014).

[3] D. DeWoskin, J. Myung, M.D. Belle, H.D. Piggins, T. Takumi, and D.B. Forger, *Distinct roles for GABA across multiple timescales in mammalian circadian timekeeping.* Proc. Natl. Acad. Sci. U.S.A. **112**, 29, E3911-E3919 (2015).

The VI International AMMCS
Interdisciplinary Conference
Waterloo, Ontario, Canada

Delegate Apportionment Methods: the Quota Condition, Bias, and Thresholds

Michael A. Jones[1], David McCune[2], Jennifer M. Wilson[3]

[1] *Mathematical Reviews, American Mathematical Society, Ann Arbor, MI, USA Amaj@ams.org*
[2] *William Jewell College, Liberty, MO, USA mccuned@william.jewell.edu*
[3] *Eugene Lange College, The New School, New York, NY, USA wilsonj@newschool.edu*

The US presidential primaries are a series of state elections held every four years to determine the Democratic Party and Republican Party candidates for president. Each state holds a primary (or caucus) in which voters select their preference for one of their party's presidential candidates. The popular votes at the district and at the state level are converted into delegates using an apportionment method. If a candidate wins a majority of the delegates during the primaries, then that candidate becomes the party's nominee for president. If no candidate wins a majority, then the nominee is determined at the convention.

The seven quota-based apportionment methods used in the primaries from 2008 to 2020 were introduced and described mathematically in [2]. In this talk, the methods are recalled and then analyzed. We determine which delegate apportionment methods satisfy lower or upper quota. For methods that do not satisfy the quota condition, we evaluate how badly quota can be broken under these methods and for which candidates. We also give estimates for how frequently quota is broken by using simulations and data from previous primaries.

We consider two approaches to measure bias. The first is based on a pairwise comparison of apportionment methods that Balinski and Young [1] use to compare stationary divisor methods. Using this approach, not all of the seven methods are comparable to one another, as some methods advantage stronger candidates and other methods disadvantage weaker candidates. The second approach is based on the idea of seat bias, which was first introduced in [5] to analyze bias in apportioning representatives to the US House of Representatives. A state's seat bias is the expected deviation of its apportionment from its quota. Adapting this notion to delegate allocation, we investigate and compare the delegate bias for different candidates under each apportionment method.

Finally, we compare the delegate threshold values of each apportionment method. Delegate thresholds, which are generalizations of the threshold of inclusion and threshold of exclusion, introduced in [4], indicate the minimum and maximum percentage of the vote that candidates receive to obtain a fixed number of delegates.

The content of this talk appears in [3, Ch. 5].

References

[1] M.L. Balinski and H.P. Young, *Fair representation: Meeting the ideal of one man, one vote*, 2nd ed., Brookings Institution Press (2001).

[2] M.A. Jones, D. McCune and J.M. Wilson, *New quota-based apportionment methods: the allocation of delegates in the Republican presidential primary*, Math. Social Sci., **108**, pp. 122–137 (2020).

[3] M.A. Jones, D. McCune and J.M. Wilson, *Delegate apportionment in the US presidential primaries: A mathematical analysis*, Studies in Choice and Welfare, Springer, Cham (2023).

[4] S. Rokkan, *Elections: electoral systems*, Macmillan Company (1968).

[5] K. Schuster, F. Pukelsheim, M. Drton, and N.R. Draper, *Seat biases of apportionment methods for proportional representation*, Electoral Studies, **22**, 4, pp. 651–676 (2003).

The VI International AMMCS
Interdisciplinary Conference
Waterloo, Ontario, Canada

tost.II: A temporal operator-splitting template library in deal.II

K.R. Green[1], S. Dominguez-Rivera[2], R.J. Spiteri[1]

[1] *University of Saskatchewan, Saskatoon, Canada, kevin.green, raymond.spiteri@usask.ca*

[2] *Siemens EDA, Saskatoon, Canada, sebastian.rivera@siemens.com*

Operator-splitting methods are a popular divide-and-conquer method for solving ordinary differential equations, most notably those derived from a method-of-lines discretization of a partial differential equation involving multiple physical processes or multiple scales. The main idea is to express the right-hand side of the differential equation as a sum of different parts and integrate the parts separately. Sometimes the parts are referred to as *fractions*, leading to the terminology *fractional-step methods* [5, 6].

The objective of operator splitting is to reduce a given problem into sub-problems that are somehow easier to handle. This could be because the entire problem is too large to handle monolithically, i.e., with one integration method, or because there exist specialized methods to deal with one or more of the parts; e.g., a part may be linear or known to be stiff. In other words, operator splitting is done in the name of feasibility (obtaining a solution at all) or efficiency (obtaining a solution in less time).

In my view, operator splitting is a necessary evil and should not be entered into lightly. In practice it seems, however, that this is exactly what is done! Implementations of operator splitting are commonly done on an *ad hoc* basis. Little theoretical attention is paid to choice of operators, order of operators, choice of splitting methods, or choice of sub-integrators. This has led to gaps in methodology and observations that are not well understood. For example, although it is known that real-valued operator splitting methods of order greater than two require negative time steps in each operator [4], it is still possible to obtain stable solutions [2, 3] in the presence of diffusion.

The purpose of this work is to create software for the systematic study of operator-splitting methods. The software is called tost.II and is built on the well-known deal.II finite element library [1] to leverage the latter's powerful spatial discretization capabilities. The temporal operator splitting algorithm implemented by tost.II exposes the operators, the order in which they are applied, the operator splitting method coefficients (including complex-valued ones), and the (arbitrary) sub-integrators to direct user input.

The tost.II package is available at https://github.com/uofs-simlab/tostii.

References

[1] D. Arndt, W. Bangerth, M. Feder, M. Fehling, R. GassmÃ¶ller, T. Heister, L. Heltai, M. Kronbichler, M. Maier, P. Munch, J.-P. Pelteret, S. Sticko, B. Turcksin, and D. Wells, *The deal.II library, version 9.4*, J. N. Math., 30(3):231–246 (2022).

[2] J. Cervi and R. J. Spiteri, *High-order operator splitting for the bidomain and monodomain models*, SIAM J. Sci. Comput., 40(2):A769–A786 (2018).

[3] J. Cervi and R. J. Spiteri, *A comparison of fourth-order operator splitting methods for cardiac simulations*, Appl. Numer. Math., 145:227–235 (2019).

[4] G. Goldman, T.J. Kaper, *Nth-order operator splitting schemes and nonreversible systems*, SIAM J. Numer. Anal. 33(1):349–367 (1996).

[5] G. Marchuk, *On the theory of the splitting-up method*, in: Numerical Solution of Partial Differential Equations-II, Academic Press, pp.469–500 (1971).

[6] R.J. Spiteri and S. Wei, *Fractional-step Runge–Kutta methods: Representation and Linear Stability Analysis*, J. Comp. Phys., 111900 (2023).

[7] N.N. Yanenko, *The method of fractional steps*, in: The Solution of Problems of Mathematical Physics in Several Variables, Springer-Verlag, New York-Heidelberg, translated from the Russian by T. Cheron. English translation edited by M. Holt (1971).

The VI International AMMCS
Interdisciplinary Conference
Waterloo, Ontario, Canada

Boundary error control for numerical solution of BSDEs by the convolution method

X. Gao[1], C. Hyndman[1],

[1] *Department of Mathematics and Statistics, Concordia University, Montréal, Canada*
cody.hyndman@concordia.ca

We first review the convolution approach for the numerical solution of backward stochastic differential equations (BSDEs) introduced in [1]. We then propose a method for improving the boundary errors obtained when valuing options. We we modify the damping and shifting schemes used in [1], which transforms the target function into a bounded periodic function so that Fourier transforms can be applied successfully. Adaptive shifting reduces boundary error significantly. We present numerical results for our implementation and provide a detailed error analysis showing the improved accuracy and convergence of the modified convolution method.

References

[1] C. Hyndman and P. Oyono Ngou, *A convolution method for numerical solution of backward stochastic differential equations*, Methodol. Comput. Appl. Probab. **17**, 1, pp. 1-29, (2017).

Inferring Bacterial Conjugation Events with Integer Programming

N. Kendal-Freedman[1], B. Ingalls[1]

[1] *University of Waterloo, Waterloo, Canada, nmkendal@uwaterloo.ca*

Microbial genetic engineering, the modification of microbes to express novel genes, has applications in fields including health, agriculture, bio-manufacturing, and environmental remediation [3]. In some cases, the goal is to modify the behaviour of an environmental population, which requires modified genetic elements to spread from the engineered organisms to other members of the population. One mechanism we can use is bacterial conjugation, the process by which bacteria transfer genetic information stored on extra-chromosomal plasmids to adjacent cells.

Although bacterial conjugation has been studied extensively, there are a range of challenges involved in developing mathematical models that capture interactions among single cells [1]. One challenge is that the process is highly stochastic and requires individuals to be considered separately, making it unsuitable for traditional differential equation models. Agent-based modelling has become an important tool in such cases; these models can be used to investigate population dynamics within large groups of autonomous individuals, including those with high degrees of stochasticity [4].

Our group is conducting experiments in which *E. coli* cells grow and interact in the 2D focal plane of a microscope. Time-lapse imaging allows us to capture the dynamics of cell growth and motion. By tagging cells with florescent proteins, we can identify the genetic state of each cell and observe the transfer of plasmids via changes in florescence signatures. However, there is a delay (on the order of tens of minutes) between gene transfer from conjugation events and the appearance of a fluorescence signal.

In the context of epidemiology, Fajardo *et al.* consider an infection network where only some cases of an illness are known [2]. They demonstrate how an integer program can be used to infer the progression of the illness through the population, including a set of all infected individuals and by whom they were infected. From our data, we construct contact networks and lineage trees that allow us to formulate our problem similarly to Fajardo *et al.* Our contact network is a graph with a vertex for each cell in each time-point snapshot. The edge set consists of 'horizontal' edges representing physical contacts at each snapshot, along with 'vertical' edges representing the evolution of a lineage over time.

We formulate an integer program to find a directed Steiner tree on this graph, with the fluorescing bacteria as the Steiner nodes. Further, we impose additional biologically motivated constraints; for instance, we require that every 'infected' bacterium passes on the plasmid to its daughter cells. We then optimize for the most likely set of transmissions, where we consider factors such as the latency period between receiving and expressing the plasmid and the duration of each contact. Validating our model on our experimental data allows us to use these results for calibration of an agent-based model for bacterial conjugation.

References

[1] A. Yip, J. Smith-Roberge, S. Haghayegh, M. Aucoin, and B. Ingalls. *Calibrating spatiotemporal models of microbial communities to microscopy data: A review*, PLoS Comput. Biol. **18**, 10 (2013).

[2] D. Fajardo and L. Gardner, *Inferring contagion patterns in social contact networks with limited infection data*, Netw. Spat. Econ. **13**, 4, pp. 399-426 (2013).

[3] F. Padilla-Vaca, F. Anaya-VelÃ¡zquez, and B. Franco, *Synthetic biology: Novel approaches for microbiology*, Int. Microbiol. **18**, 2, pp. 71-84 (2015).

[4] J. Leveau *et al.*, *The individual microbe: single-cell analysis and agent-based modelling*, Front. Microbiol. **9**, 2825 (2018).

Chemical Rate Laws and Mean First Assembly times for aggregating systems

P. Kunwar[1], K. Rohlf[2]

[1] *Toronto Metropolitan University (formerly Ryerson University), Canada, pradeep.kunwar@torontomu.ca*
[2] *Toronto Metropolitan University (formerly Ryerson University), Canada, krohlf@torontomu.ca*

The Becker Döring model (BD) is extended, and considered as a system of chemical reactions. The extended Becker Döring model (EBDM) can be used to better describe the aggregation and fragmentation mechanisms in the self-assembly of molecules. The chemical system corresponding to the EBDM can be expressed as

$$C_r + C_s \underset{k^-_{r,s}}{\overset{k^+_{r,s}}{\rightleftharpoons}} C_{r+s}, \tag{1}$$

where C_r are the concentrations of a cluster of size r, and $r = 1, 2, 3 \ldots$ is the aggregation number representative of a cluster being made up of r base units of size 1. The forward and backward reaction rates are $k^+_{r,s}$, and $k^-_{r,s}$ respectively, and are based on an r^{th}-sized cluster either aggregating with another cluster forming a larger-sized cluster, or being created through fragmentation from a larger cluster.

The general master equation for EBDM in a finite-sized setting is developed, for which there is a largest cluster of size N that can be formed. A set of chemical reactions is proposed for an approximate mechanism relevant for simulations using Reactive multiparticle collision dynamics (RMPC). For constant rates of reactions with $N = 10$ and $s = 5$, the time evolution of clusters is found using stochastic SSA and RMPC simulations, and compared with the finite Smoluchowski equation, the traditional ODEs for (1), as well as an approximate ODE system for RMPC that we have developed. Additionally, the Becker Döring model dynamics are tested statistically when $N = 4$, for the effect of diffusion on the concentration profiles in our RMPC system. We conclude that there are changes in the concentrations when changing the RMPC diffusion parameter $(k_B T/m)$, but agreement with the corresponding system of ODEs is maintained.

Finally, different reaction rates are considered for $N = 3$ (constant $k^+_{r,s} = p$, product $k^+_{r,s} = prs$, sum $k^+_{r,s} = p(r+s)$) for aggregation and fragmentation, and changes in the mean first assembly time — the average time at which a largest cluster first forms in the system from a monomer-only initial condition — are discussed. Theoretical mean first assembly times (MFAT), theoretical mean first assembly times for approximate RMPC dynamics, simulation-based MFATs using SSA, and simulation-based MFATs using RMPC are compared. The significance and implications of these results will be discussed.

References

[1] K. Rohlf, S. Fraser, R. Kapral, *Reactive multiparticle collision dynamic*,Cumputer Physics Communications 197 (2008) 132-139.
[2] D.T. Gillespie, *Exact stochastic simulation of coupled chemical reactions*, J. Phys. Chem. **81**, pp. 2340-2361 (1977).
[3] D.J. Higham *Modeling and Simulating Chemical Reactions*, SIAM Review **50**, No.2, pp. 347-368 (2008).
[4] J.A.D. Wattist, and J.R. King, *Asymptotic solutions of the Becker-Döring equations*, J. Phys A: Math Gen. **31**, pp. 7169-7189 (1998).
[5] R. Yvinec, M.R. D'Orsogna and T. Chou, *First passage times in homogeneous nucleation and self-assembly*, J. Phys. Chem. **137**, 244107, (2012).
[6] L.J.S Allen, *An introduction to Mathematical Biology*, Pearson Education Inc. U.S.A.(2007).
[7] A.Sayyidmousavi ,K. Rohlf, *Reactive multi-particle collision dynamics with reactive boundary conditions*, physical biology (2018).
[8] A. Yvinec,M.R.D'Orsogna,T. Chou *First passage time in homogeneous nucleation and self-assembly*, journal of chemical physics 137,244107 (2012).

Statistically Augmented Finite Element Models to Study Knee Biomechanics

A.L. Lerner[1], E. Leatherman[2], B. Steineman[3], J. Leadem[1], M. Montes de Oca[1], S. Letendre[3], S. Maher[3]
[1] *University of Rochester, Rochester, New York, USA, amy.lerner@rochester.edu*
[2] *Kenyon College, Gambier, Ohio, USA, leatherman1@kenyon.edu*
[3] *Hospital for Special Surgery, New York, NY, USA, mahers@hss.edu*

The human knee is a complex structure that is prone to injury, which can lead to osteoarthritis resulting in disability. Biomechanical studies often use finite element (FE) modeling to develop understanding of the risk for progression of disease. However, models must address uncertainties in inputs and variations between individuals. In this work, we study treatments for injuries to the meniscus, a fibro-cartilagenous structure that provides cushioning and stability in the knee. One of the most common surgical procedures is the partial meniscectomy. In most individuals, this treatment is successful in reducing pain, but in others, rapid progression to osteoarthritis occurs [1]. Our goal is to identify characteristics of the patient or injury that lead to successful outcomes. In this presentation we will describe development of validated FE models, sensitivity to model inputs and describe a predictive statistical model based on knee geometry, tissue properties and injury characteristics.

We have developed five FE models based on four cadaveric knees and one volunteer. Model geometries were based on magnetic resonance imaging to allow segmentation of cartilage, meniscus and bone surfaces. Using a custom loading apparatus, knees were loaded in the MR scanner to identify the bony motions between unloaded and loaded states [2]. FE models were generated for analysis with Abaqus software. Cartilage was assumed to be isotropic linear elastic, while menisci were modeled as transversely isotropic, and meniscal attachments were nonlinear springs. Each model geometry was run with 70 material property combinations based on a maximin space filling algorithm [3]. This efficient design explored the design space across a range of inputs, while allowing identification of complex relationships between input parameters. We characterized anatomic variations with 20 parameters of the bones and menisci. Small and large partial meniscectomies were simulated in each model to explore the impact of the size and location of the injury and treatment.

Validations of models show very good agreement with sensors measuring contact pressures. Our results indicate that the role of the meniscus is most dependent on anatomic variations and size of the meniscectomy, with widely ranging material properties contributing minimally to the % load carried by the meniscus. Initial predictive models based on geometric features, material properties and size of meniscectomy were highly successful in predicting load distributions in the treated knee.

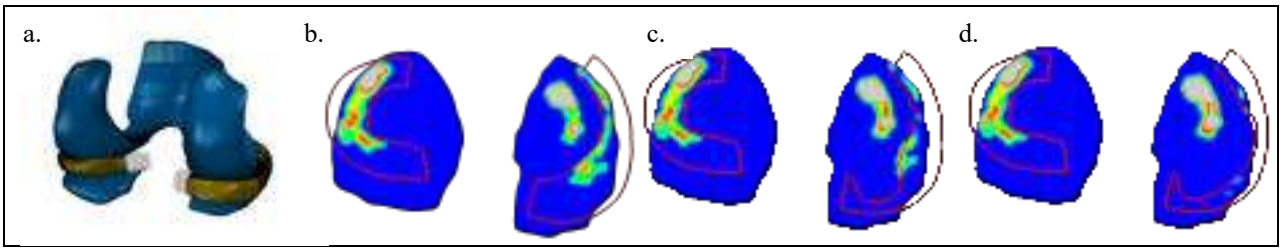

Figure 1: a.) Image-based finite element model of the human knee, including cartilage and meniscus. b.) Contour plots indicating distribution of contact pressure in the intact knee, c.) with small meniscectomy and d) large meniscectomy.

References

[1] B. Feeley and B. Lau, *Biomechanics and Clinical Outcomes of Partial Meniscectomy*, JAAOS, 26(24): (2018)
[2] H. Wang, M. Koff et al, *An MRI-compatible loading device to assess knee joint cartilage deformation*, J. Biomech (2015)
[3] T. Santner, B. Williams, W. Notz, *The Design and Analysis of Computer Experiments*, 2nd Ed, Springer-Verlag, NY, NY (2018)

The VI International AMMCS
Interdisciplinary Conference
Waterloo, Ontario, Canada

Optimized Distortion and Proportional Fairness in Voting

S. Ebadian[1], A. Kahng[1], D. Peters[1,2], N. Shah[1]

[1] *University of Toronto, Canada, {soroush,nisarg}@cs.toronto.edu, ansonkahng@gmail.com*

[2] *CNRS, LAMSADE, Université Paris Dauphine–PSL, France, dominik@lamsade.fr*

A voting rule decides on a probability distribution over a set of m alternatives, based on rankings of those alternatives provided by agents. We assume that agents have cardinal utility functions over the alternatives, but voting rules have access to only the rankings induced by these utilities. We evaluate how well voting rules do on measures of social welfare and of proportional fairness, computed based on the hidden utility functions.

In particular, we study the *distortion* of voting rules, which is a worst-case measure. It is an approximation ratio comparing the utilitarian social welfare of the optimum outcome to the social welfare produced by the outcome selected by the voting rule, in the worst case over possible input profiles and utility functions that are consistent with the input. The previous literature has studied distortion with unit-sum utility functions (which are normalized to sum to 1), and left a small asymptotic gap in the best possible distortion. Using tools from the theory of fair multi-winner elections, we propose the first voting rule which achieves the optimal distortion $\Theta(\sqrt{m})$ for unit-sum utilities. Our voting rule also achieves optimum $\Theta(\sqrt{m})$ distortion for a larger class of utilities, including unit-range and approval (0/1) utilities.

We then take a similar worst-case approach to a quantitative measure of the fairness of a voting rule, called *proportional fairness*. Informally, it measures whether the influence of cohesive groups of agents on the voting outcome is proportional to the group size. We show that there is a voting rule which, without knowledge of the utilities, can achieve an $O(\log m)$-approximation to proportional fairness, which is the best possible approximation. As a consequence of its proportional fairness, we show that this voting rule achieves $O(\log m)$ distortion with respect to the Nash welfare, and selects a distribution that is approximately stable by being an $O(\log m)$-approximation to the core, making it interesting for applications in participatory budgeting.

Twists of the Burkhardt Quartic Threefold

Nils Bruin[1], Eugene Filatov

[1] *Simon Fraser University, Burnaby BC, Canada. nbruin@sfu.ca*

The moduli space of principally polarized abelian surfaces with full 3-level structure admits a birational quartic model in $\mathbf{P}^4$, called the Burkhardt quartic threefold. Its geometry is well-studied and characterized by its large number of isolated singular points and its large automorphism group.

Over non-algebraically-closed fields it admits many twists. Some of those, but not all, parametrize different 3-level structures on abelian surfaces. We identify an explicit representative of an element in the Brauer group that measures whether a given twist parametrizes abelian surfaces. The ones that do not, still parametrize Kummer quartic surfaces.

Even more surprisingly, the Brauer element is of period dividing 2, but may be of index 4. We give an example of such a quartic surface over a bivariate function field. We even get to conclude that this surface has only one rational point.

In this talk we will give a description of the beautiful underlying classical algebraic geometry as well as the way the representative of the Brauer element can be obtained, and how one can use it to prove the absence of rational points.

References

[1] N. Bruin and E. Filatov, *Twists of the Burkhardt quartic threefold*, Res. number theory **8**, 73 (2022).

Deep Reinforcement Learning of Viscous Incompressible Flow

K.M.S. Park[1], A.R. Stinchcombe[1]

[1] *Department of Mathematics, University of Toronto, Toronto, Ontario, Canada, minseong.park@mail.utoronto.ca, stinch@math.toronto.edu*

Many applications of partial differential equations are either high dimensional or involve domains with irregular boundaries. In both cases, traditional grided methods face considerable challenges constructing and storing grids. We present a grid-free and highly parallelizable Monte Carlo method for quasilinear elliptic and parabolic equations based on their connection with Brownian motion [1, 2]. Additionally, we represent the solution using a deep neural network trained using reinforcement learning and a loss derived from a martingale of the stochastic process. We demonstrate our numerical method on the incompressible Navier-Stokes equations [3]. The output of the deep neural network is the vector potential for the flow, which allows us to avoid computing the pressure while nonetheless maintaining incompressibility. Problem parameters, like the fluid viscosity, are inputs to the neural network allowing us to solve families of problems concurrently. Borrowing ideas from domain decomposition methods, regular parts of the domain are solved with finite difference or integral equation methods and provide training data for the neural network. Our high-performance PyTorch implementation will be exhibited on several challenging fluid flow problems.

References

[1] J. Han, , M. Nica, and A.R. Stinchcombe, *A derivative-free method for solving elliptic partial differential equations with deep neural networks* J. Comput. Phys. **419** 109672 (2020).

[2] C. Martin, H. Zhang, J. Costacurta, M. Nica, and A.R. Stinchcombe *Solving elliptic equations with Brownian motion: bias reduction and temporal difference learning* Methodol. Comput. Appl. Probab. **24**, 3, 1603-1626 (2022).

[3] K.M.S. Park and A.R. Stinchcombe, *Deep reinforcement learning of viscous incompressible flow*, J. Comput. Phys. **467** 111455 (2022).

The VI International AMMCS
Interdisciplinary Conference
Waterloo, Ontario, Canada

Supersingular Isogeny Graphs and Orientations

S. Arpin[1], M. Chen[2], K. E. Lauter[3], R. Scheidler[4], K. E. Stange[5], H. T. N. Tran[6]

[1] *Mathematics Institute, Universiteit Leiden, Leiden, The Netherlands, Sarah.Arpin@colorado.edu*
[2] *University of Birmingham, Birmingham, UK, m.chen.1@bham.ac.uk*
[3] *Facebook AI Research, Meta, Seattle, WA, USA, klauter@fb.com*
[4] *University of Calgary, Calgary, Alberta, Canada, rscheidl@ucalgary.ca*
[5] *University of Colorado Boulder, Boulder, CO, USA kstange@math.colorado.edu*
[6] *Concordia University of Edmonton, Edmonton, Alberta, Canada, hatran1104@gmail.com*

A supersingular isogeny graph is a graph whose vertices are supersingular elliptic curves over $\overline{\mathbb{F}}_p$ (where p is typically a large prime in our context), and whose edges represent isogenies of degree ℓ (typically a small prime). Hard problems concerning pathfinding in supersingular isogeny graphs form a basis for post-quantum isogeny-based cryptography. In this talk, I will describe the structure of isogeny graphs of CM curves, and of oriented supersingular curves, and their relationship to the structure of supersingular isogeny graphs. In particular, the endomorphism ring of a supersingular elliptic curve is an order in a quaternion algebra. Embeddings of imaginary quadratic orders into this quaternion order are called *orientations*. Explicit knowledge of this endomorphism ring leads to well-known pathfinding algorithms. In joint work, we develop classical and quantum algorithms for path-finding under the assumption that *only one* endomorphism from this order is known (equivalently, one orientation). In related work, we demonstrate a bijection between the cycles in a fixed isogeny graph and the cycles in the union of all CM graphs which cover it. As a result, we count the cycles in the isogeny graph in terms of certain class numbers of imaginary quadratic orders.

The VI International AMMCS
Interdisciplinary Conference
Waterloo, Ontario, Canada

Analysis of a Model for Ribosome Abundance Regulation Mechanisms in Prokaryotes

J. Shea[1], L. Davis[1], B. Quaye[2], T. Gedeon[1]

[1] *Montana State University, Bozeman, Montana, USA, {lisa.davis}@montana.edu*

[2] *Department of Economics, Washington University, St. Louis, Missouri, USA*

We construct a model of the feedback mechanisms that regulate abundance of ribosomes in *E.coli*, a prototypical prokaryotic organism. The translation process contains an important feedback loop: ribosomes are made up of proteins, which need to be translated by ribosomes. The goal of the work is to model the main feedback loops that control abundance of ribosomes in response to external conditions. The model accounts for the concentrations of the free ribosomes R, ribosomal RNA (rRNA) denoted by r, and proteins p, which are translated from mRNA m using ribosomes R. We include direct negative feedback loops where ribosomal proteins, when in excess, slow down their own translation. The effect of the signaling molecule ppGpp is also included as a negative feedback mechanism, along with the effect of the abundance of building blocks for mRNA and rRNA synthesis. The model consists of a system of six differential equations parameterized by 23 parameters. Our analysis shows that for all values of parameters, the model system has either one equilibrium S, or two equilibria S and P in the biologically feasible region $\mathbb{R}^{6+}$.

Equilibrium S represents the *stationary* state of the system where there are no free ribosomes, no free ribosomal proteins, and both the rRNA and mRNA concentrations remain at base level. In a broader context of allocation of cellular resources, this corresponds to a state of the cell where all existing ribosomes are engaged in translation. This is consistent with a stationary growth phase. The state P represents the *proliferative* state of the system where ribosomal proteins and ribosomes are being produced at a rate that produces ribosomes that are not needed for ribosomal protein translation. Hence, these *extra* ribosomes can be allocated to enzymes and transport complexes that allow cellular growth. A stability analysis shows that P emerges from S by a transcritical bifurcation and, when P exists, it is asymptotically stable. When only the equilibrium S exists in $\mathbb{R}^{6+}$, it is also asymptotically stable. The key determinant of the transition between the stationary regime and the proliferative regime is the state of the feedback loop between ribosomes and ribosomal proteins. The proliferative equilibrium P exists, if and only if the production rate of ribosomal proteins exceeds a threshold value that is comprised of two terms, one of which describes the demand for these proteins through production of ribosome rRNA scaffold and the other describes the assembly rate of these proteins.

In the ODE model, transcription and translation are considered to be instantaneous; however, a more biologically reasonable assumption is that free ribosomes and mRNA are sequestered in a compartment accounting for the time required for translation for example. Fundamentally the transcription and translation can be characterized by a molecular motor elongating along a DNA or mRNA strand in order to transfer genetic information to a nascent copy. The newest phase of the work seeks to model these processes using a prototypical compartment model. Each compartment model takes the form of a hyperbolic conservation law where the biological parameters inform the model construction. These compartments account for the time and spatially dependent processes required to produce rRNA as well as the interactions between ribosomes and mRNA required to produce the ribosomal proteins. Each of these elements is essential for ribosome assembly. Numerical results are presented to compare the results of the original ODE model with the new combined system of ODEs and PDEs. In particular, we characterize the equilibria of the combined system and compare it to that of the original ODE system model.

The VI International AMMCS
Interdisciplinary Conference
Waterloo, Ontario, Canada

p-Norm Approval Voting

H. Nathan[1], K. Shultis[2], J. Sorrells[3], M. Orrison[4]

[1] *New York University, New York, USA, nathanhari@gmail.com*
[2] *Gonzaga University, Spokane, USA, shultis@gonzaga.edu*
[3] *Converse University, Spartanburg, USA, jessica.sorrells@converse.edu*
[4] *Harvey Mudd College, Claremont, USA, orrison@hmc.edu*

Approval voting is a well-studied voting procedure [1]. The procedure is relatively simple: Given a set of candidates, each voter chooses a subset of the candidates, and the candidate chosen the most is then declared the winner. Approval voting can also be described in terms of distributing points, where each voter gives 1 or 0 points to each candidate, and the candidate who receives the largest total number of points is the winner.

Viewing approval voting in terms of distributing points can be helpful when thinking about variations of approval voting. For example, with satisfaction approval voting [2], a voter who chooses a k-element subset of candidates (where $k \geq 1$) will give each candidate in the subset $\frac{1}{k}$ points. As with approval voting, the candidate who receives the largest total number of points is declared the winner.

Interestingly, approval voting and satisfaction approval voting can be viewed as the extreme ends of a one-parameter family of voting procedures we are calling *p-norm approval voting* procedures. In this talk, we will present some of the many properties we have discovered about this seemingly simple family of voting procedures.

To begin to explain, suppose there are n candidates $c_1, \ldots, c_n$. If a voter chooses a subset S of these candidates, then we can encode this choice as a 0-1 vector $\mathbf{x} = [x_1, \ldots, x_n]$ where $x_j = 1$ if $c_j \in S$, and $x_j = 0$ if $c_j \notin S$. For example, if $n = 5$ and the voter chooses $\{c_2, c_5\}$, then the associated vector is $\mathbf{x} = [0,1,0,0,1]$.

Let $p \geq 1$ be a real number. The p-norm of a vector $\mathbf{x} = [x_1, \ldots, x_n]$ is

$$\|\mathbf{x}\|_p = \left(\sum_{j=1}^{n} |x_j|^p \right)^{1/p}.$$

The limit of $\|\mathbf{x}\|_p$ as p approaches infinity then gives rise to the infinity norm $\|\mathbf{x}\|_\infty = \max\{|x_1|, \ldots, |x_n|\}$. For example, if $\mathbf{x} = [0,1,0,0,1]$, then $\|\mathbf{x}\|_1 = 2$, $\|\mathbf{x}\|_2 = \sqrt{2}$, and $\|\mathbf{x}\|_\infty = 1$.

For each $p \in [1, \infty]$, we can now create a voting procedure where if $\mathbf{x} = [x_1, \ldots, x_n]$ is the 0-1 vector associated with a voter's choice of candidates (as described above), and $\mathbf{x}$ is nonzero, then that voter will give $1/\|\mathbf{x}\|_p$ points to each candidate in the set chosen by the voter. We recover approval voting when $p = \infty$, and we recover satisfaction approval voting when $p = 1$. When $p = 2$, we get a voting procedure we are calling *quadratic approval voting*, which is a simplified version of quadratic voting [3], and which in turn was the original motivation for our work.

References

[1] S. Brams and P. Fishburn, *Approval Voting*, 2nd ed., Springer, New York, USA (2007).

[2] S. Brams and M. Kilgour, *Satisfaction approval voting*, in *Mathematical and Computational Modeling, Pure Appl. Math.*, Wiley, Hoboken, USA, pp. 275-298 (2015).

[3] S. Lalley and E.G. Weyl, *Quadratic Voting: How Mechanism Design Can Radicalize Democracy*, AEA Papers and Proceedings **108**, pp. 33-37 (2018).

The VI International AMMCS
Interdisciplinary Conference
Waterloo, Ontario, Canada

Algebraic structure of computation with a focus on causality

Utkarsh Bajaj[1]

[1] *University of Waterloo, ubajaj@uwaterloo.ca*

We investigate the algebraic structure of a computational process by studying its causal structure –the description of how different events in the computation affect each other. Specifically, given a computation, we can algorithmically produce a *causal set* [1], which is (almost) a partially ordered set. Then, we can use tools from Lorentzian geometry to analyze these causal sets and get a description of the dynamics the computation might be attempting to describe.

First, we compile different computational systems (DFAs, Turing machines, and a functional programming language) into *hypergraph rewriting system* [2], from which we can canonically produce causal sets for the original causal set. We see that the resultant causal sets encode the dimension of the computation i.e. the level of concurrency. If we get large antichains in the causal set, that translates into there being more concurrent events, which in physics, translates to higher energy-momentum flux [1].

We also extend this formalism to algebraic decompositions of computational processes, which are the focus of Krohn-Rhodes theory. Using tools from algebraic topology and commutative algebra, we define what it means to "glue" certain computations together, and study what the resulting causal set looks like. We also investigate the relation to Scott topology in computer science and Zariski topology, and discuss some applications of algebraic geometry to our research.

References

[1] Jonathan Gorard. *Some Relativistic and Gravitational Properties of the Wolfram Model.*
[2] Stephen Wolfram. *Technical Introduction to the Wolfram Physics Project.*

Superposition of two excitation types for gonadotropin-releasing hormone neuron forms two types of exocytosis

M. Chugunova[1], S. A. Campbell

[1] *University of Waterloo, Canada, mchuguno@uwaterloo.ca*

Gonadotropin-releasing hormone (GnRH) neurons work as a trigger of the reproductive axis in mammals. These neurons exhibit two types of exocytosis: a surge and a pulsatile one [1]. Traditionally, changes in the neuron dynamics are connected and explained by changes in parameters of the action potential, transmitted by a neuron's membrane. However, in the case of GnRH neurons, the experimental data demonstrates that the switch in the type of the hormone release is connected rather with the location of the GnRH neuron activation. Action potential initiated in the proximity of soma is necessary for the surge of GnRH. The second type, the pulsatile release of GnRH, is driven by the synaptic activities on the distal part of the neurons [2].

Both types of the exocytosis initiation target the intracellular calcium dynamics. The increase in calcium ions due to the electrical spikes near soma is short-lived. On the other hand, the increase in calcium ions in the distal parts of the GnRH lasts for tens of minutes.

We have built the mathematical and computational models of the electrical and chemical dynamics in GnRH neurons. The model, in silico, reveals the connection between the action potential, neuropeptides, and calcium ion dynamics. Moreover, our model confirms the functionality of the bundling between multiple GnRH neurons.

References

[1] R. Nelson and L. Kriegsfeld, *An introduction to behavioral endocrinology*, Oxford University Press (2022).
[2] L. Wand et al, Different dendritic domains of the GnRH neuron underlie the pulse and surge modes of GnRH secretion in female mice, eLife; 9: e53945, pp. 1-19 (2020).

The VI International AMMCS
Interdisciplinary Conference
Waterloo, Ontario, Canada

Unconditional Computation of Fundamental Units in Number Fields

R. Yee[1], M. Jacobson[2], H. Tran[4]

[1] *University of Calgary, Canada, randy.yee1@ucalgary.ca*
[2] *University of Calgary, Canada, jacobs@ucalgary.ca*
[4] *Concordia University of Edmonton, Canada, ha.tran@concordia.ab.ca*

In the current literature, the most-well known algorithm for computing a system of fundamental units in a number field without relying on any unproven assumptions or heuristics is due to Buchmann [1] and has an expected run time of$O(\Delta_K^{1/4+\varepsilon})$. If one is willing to assume the GRH, then the index-calculus method [2] will compute the logarithm lattice corresponding to the unit group in subexponential time with respect to the logarithm of the discriminant. In this case, the complexity and correctness of the method are both dependent on the GRH.

Generalizing the work of de Haan et al. [3] for real quadratic number fields, we present a hybrid algorithm which combines techniques of [1] with an alternate method due to Pohst and Zassenhaus [4] which, given a full rank sublattice as input, computes the basis of the logarithm lattice for a number field in asymptotically fewer operations than current unconditional methods in the literature.

References

[1] J. A. Buchmann, *Zur Komplexität der Berechnung von Einheiten und Klassenzahl Algebraischer Zahlkörper*, Habilitationsschrift (1987).

[2] J.A. Buchmann, *A subexponential algorithm for the determination of class groups and regulators of algebraic number fields*, in *Séminaire de Théorie des Nombres, Paris 1988–1989, volume 91 of Progr. Math.*, Boston, MA, pp.27-41 (1990).

[3] R. de Haan, M. J. Jacobson, Jr., and H. C. Williams. *A fast, rigorous technique for computing the regulator of a real quadratic field*. Math. Comp., 76(260):2139â2160 (electronic), (2007)

[4] M. Pohst and H. Zassenhaus. *Algorithmic Number Theory*, volume 30 of Encyclopedia of Mathematics and its Applications. Cambridge University Press (1997).

The VI International AMMCS
Interdisciplinary Conference
Waterloo, Ontario, Canada

Computing Class Groups of Quartic Number Fields

D. Marquis[1]

[1] *University of Calgary, Canada, david.marquis@ucalgary.ca*

Computing the class group and unit group of a number field is a fundamental problem in number theory. In practice the fastest algorithms for doing this in quadratic fields use an approach called self-initialization. This algorithm works by sieving a carefully chosen sequence of norm forms of ideals. Despite its success, it has never been adapted to fields of higher degree. In this talk we discuss adapting this algorithm to fields of fixed degree and ongoing work on its implementation. Although fields of degree two and three are the subject of ongoing research, quartic fields have not received significant attention. We describe how our implementation can be applied most efficiently to such fields.

Sparse Random Feature Models and Applications in Signal Processing and Epidemiologic Data

G. Tran[1]
[1] *University of Waterloo, Canada, giang.tran@uwaterloo.ca*

Random feature methods have been successful in various machine learning tasks, are easy to compute, and come with theoretical accuracy bounds. They serve as an alternative approach to standard neural networks since they can represent similar function spaces without a costly training phase. However, for accuracy, random feature methods require more measurements than trainable parameters, limiting their use for data-scarce applications or problems in scientific machine learning. In this talk, we will introduce the sparse random feature expansion to obtain parsimonious random feature models. Specifically, we leverage ideas from compressive sensing to generate random feature expansions with theoretical guarantees even in the data-scarce setting. We also present a sparse random mode decomposition to extract intrinsic modes from challenging time-series data and propose a new method to predict the infectious using sparse random feature models and time-delay equations. Comparisons show that our proposed approaches perform better or are comparable to other state-of-the-art or popular methods. Applications of our methods on identifying important variables in high-dimensional settings as well as on decomposing music pieces, visualizing black-hole mergers, and epidemiologic forecasting will be addressed. The talk is based on several joint work with R. Ward (UT Austin), H. Schaeffer (UCLA), L. Ho (Dal), E. Saha (UWaterloo), and N. Richardson (UBC).

Optimization and Math Modelling in COVID19 Data Analysis

Anthony Kearsley[1],

[1] *Applied and Computational Mathematics Division, NIST, Maryland, USA, Anthony.Kearsley@nist.gov*

Data analysis is becoming increasingly dependent on mathematical models to understand and analyze real-world phenomenon. Mathematical models employ variables and equations that establish relationships between variables with the goal of describing a real-world phenomenon but subtle aspects of the partnership between mathematical modeling and data analysis are often overlooked. In this talk we examine the task of extracting meaningful information from experiments with an eye towards potential to bias, or even corruption of drawn conclusions. We present a real-world example involving COVID-19 detection and the role baseline subtraction and thresholding plays in the analysis of polymerase chain-reaction (PCR) measurements, the mainstay tool for early detection of many viruses. We compare standard empirical (e.g. linear) data analysis models against an alternative that employs a simple but non-standard mathematical model. Time permitting the task of mathematical classification as it pertains to SARS-CoV-2 antibody testing will be presented and how a modeling-based approaches rooted in conditional probability and optimal-decision theory can improve classification accuracy. We will attempt to highlight the importance of embedding applied mathematics in settings where they can bring more rigor and concentration to tasks such as data analysis.

Keywords: Data Analysis, Baseline Subtraction, Mathematical Models.

Machine Learning for Molecular Sensing in the Lab and in Nature

J.N. Wei[1]

[1] *Google Deepmind* weijennifer@google.com

I will present two applications of machine learning for molecular sensing: mass spectrometry and olfaction.

Mass spectrometry is a method that chemists use to identify unknown molecules. Spectra from unknown samples are compared against existing libraries of mass spectra; highly matching spectra are considered candidates for the identity of the molecule. I will discuss some work in using machine learning models to predict mass spectra[1], which can be used to expand the coverage of mass spectral libraries and thus, our ability to identify unknown compounds.

The second project will discuss machine learning applications to a more natural form of molecular sensing: olfaction. I will discuss some recent work by my team in modeling olfaction in humans and in mosquitos [2,3]. Further, I will discuss how we use our model of mosquito olfaction to identify potent mosquito repellent candidates.

References

[1] Wei, J.N., Belanger, D., Adams, R.P. and Sculley, D., 2019. Rapid prediction of electron–ionization mass spectrometry using neural networks. ACS central science, 5(4), pp.700-708.
[2] Lee, B.K., Mayhew, E.J., Sanchez-Lengeling, B., Wei, J.N., Qian, W.W., Little, K., Andres, M., Nguyen, B.B., Moloy, T., Parker, J.K., Gerkin, R.C., Mainland, J.D., Wiltschko, A.B.,2022. A Principal Odor Map Unifies Diverse Tasks in Human Olfactory Perception. bioRxiv https://doi.org/10.1101/2022.09.01.504602.
[3] Wei, J.N., Vlot, M., Sanchez-Lengeling, B., Lee, B.K., Berning, L., Vos, M.W., Henderson, R.W., Qian, W.W., Ando, D.M., Groetsch, K.M., Gerkin, R.C., Wiltschko, A.B., and Dechering, K.D. 2022.. A deep learning and digital archaeology approach for mosquito repellent discovery. bioRxiv. https://doi.org/10.1101/2022.09.01.50460.

The VI International AMMCS
Interdisciplinary Conference
Waterloo, Ontario, Canada

Sensitivity analysis of climate-economic models

Matheus R Grasselli[1]

[1] *McMaster University, Canada, grassel@mcmaster.ca*

Assessing the economic impacts of climate change, as well as the effects of economic activity on the climate, requires the use of complex models with high computational costs and a very large number of parameters. In this talk, I will apply global sensitivity analysis techniques from statistics (such as Sobol indices) and machine learning (such as random forests) to representative climate-economic models in order to identify and rank the most important parameters and quantify their effect on select output variables. This will then be followed by both backtesting and exploration of forward scenarios under these models, taking parameter uncertainty into account. In particular, I will describe the effect of uncertainty on the expected result of policiers such as carbon taxes, green financing, and green investment.

Switching spinless and spinful topological phases of quantum matter by modulating gauge fluxes

Y. X. Zhao[1,2], Z. D. Wang[2],

[1] *Nanjing University, Nanjing, China*
[2] *The University of Hong Kong, Hong Kong, China*

It is known that spinless and spin-1/2 systems have distinct topological phases of quantum matter. For instance, in the tenfold topological classification table for the Altland-Zirnbauer symmetry classes, they belong to class AI and AII, respectively, in terms of time-reversal symmetry, with completely different topological classifications. Their distinction in symmetry and topology extends to the regime of crystalline topological phases. This distinction intrinsically hinders the realizability of spinful topological phases by spinless systems and vice versa. Here, we provide a systematical method to surpass this intrinsic boundary: switch spinless and spinful topological phases by modulating gauge fluxes [1, 4]. We first reveal that for a given lattice the different symmetry algebras of spinless and spin-1/2 systems correspond to different projective representations of the same symmetry group. Considering gauge fluxes, each symmetry group is projectively represented. Hence, we shall explore the possibility of switching the projective representations for spinless and spin-1/2 systems by modulating gauge fluxes, and thereby further realizing the topological phases of one by the other. Moreover, the systematical method will be applied to both Hermitian and non-Hermitian symmetry classes and topological phases [2, 3]. Besides the apparent fundamental importance, our work can significantly enable the realizability of electronic topological phases with spin-orbital coupling by various spinless artificial crystals.

References

[1] Z. Y. Chen, Z. Zhang, S. A. Yang, Y. X. Zhao*, *Classification of time-reversal-invariant crystals with gauge structures*, Nat. Comm. **14**, 743 (2023).

[2] Z. Y. Chen, S. A. Yang, Y. X. Zhao*, *Brillouin Klein bottle from artificial gauge fields*, Nat. Comm. **13**, 2215 (2022).

[3] L. B. Shao, Q. Liu, R. Xiao, S. A. Yang, Y. X. Zhao*, *The gauge-field extended $k \cdot p$ method and novel topological phases*, Phys. Rev. Lett. **127**, 076401 (2021).

[4] Z. Y. Chen, S. A. Yang, Y. X. Zhao*, *Switching spinless and spinful topological phases with projective PT symmetry*, Phys. Rev. Lett. **126**, 196402 (2021).

Reactive Multiparticle Collision Dynamics (RMPC) as stochastic simulations of reaction-diffusion systems

K. Rohlf[1]

[1] *Toronto Metropolitan University, Canada, krohlf@torontomu.ca*

Particle-based numerical methods have gained much popularity over the last few decades, and now provide computationally feasible alternatives to traditional discretization methods for reaction-diffusion systems. Stochastic effects can easily be incorporated, and exploration beyond the macroscopic PDE model are possible, leading to solutions that are not possible within the PDE paradigm. Multiparticle Collision Dynamics (MPC) has been shown to be capable of providing particle-based alternatives for traditional fluid flow problems [1, 2, 3, 4], and with addition of reactions (Reactive Multiparticle Collision Dynamics, RMPC) can provide numerical solutions for reaction-diffusion systems subject to different boundary conditions [5, 6, 7, 8, 9, 10, 11]. Within MPC/RMPC, the diffusion can be controlled in one of three ways: (i) varying the collision angle in the multiparticle collision rule [5, 6], (ii) varying the equilibrium temperature related k_BT/m parameter value [5], or (iii) using a probability-to-free-stream approach [5]. In cases where the concentration of a chemical species falls below a critical threshold locally, the local diffusivity of that chemical species can change, leading to non-constant diffusivities for that chemical species throughout the spatial domain and in time [9]. This can be corrected by using a density-dependent collision angle [5, 6], or by adding a sufficient number of bath particles [7]. The last choice (iii) is the most computationally efficient option, allowing for a large enough range in diffusivities between chemical species to allow Turing pattern formation [5].

An overview of RMPC dynamics will be presented, followed by diffusion coefficient expressions in the form of Green-Kubo equations. The different RMPC diffusion-control mechanisms will be discussed and assessed in the context of their ability to provide a stochastic simulation option comparable to partial-differential equation solutions for reaction-diffusion systems.

References

[1] A. Malevanets and R. Kapral, *Mesoscopic model for solvent dynamics*, J. Chem. Phys., **110**, pp. 8605-8613 (1999).

[2] S. Rabba and K. Rohlf, *Pressure curves for compressible flows with slip through asymmetric local constrictions*, IJANS **3**, pp. 21-40 (2018).

[3] L. Regmi and K. Rohlf, *Weakly compressible flow through a cylinder with pressure-dependent viscosity and Navier-slip at the wall*, Eur. J. Mech B/Fluids **60**, pp. 13-23 (2016).

[4] S. Bedkihal, J.C. Kumaradas and K. Rohlf, *Steady flow through a constricted cylinder by multiparticle collision dynamics*, Biomech. Model. Mechanobiol. **12**, pp. 929-939 (2013).

[5] A. Sayyidmousavi and K. Rohlf, *Stochastic simulations of the Schnakenberg model with spatial inhomogeneities using Reactive Multiparticle Collision Dynamics*, AIMS Math. **4**, pp. 1805-1823 (2019).

[6] A. Sayyidmousavi and K. Rohlf, *Reactive multi-particle collision dynamics with reactive boundary conditions*, Phys. Biol. **15**, pp. 045007-1–12 (2018).

[7] D. Barrows and K. Rohlf, *Optimal bath particle density selection for reactive multiparticle collision dynamics*, CAIMS 2021 Annual Meeting (2021).

[8] K. Rohlf, S. Fraser and R. Kapral, *Reactive multiparticle collision dynamics*, Comput. Phys. Commun. **179**, pp. 132-139 (2008).

[9] R. Strehl and K. Rohlf, *Multiparticle collision dynamics for diffusion-influenced signaling pathways*, Phys. Biol. **13**, pp 046004 (2016).

[10] K. Tucci and R. Kapral, *Mesoscopic model for diffusion influenced reaction dynamics*, J. Chem. Phys. **120**, pp. 8262-8270 (2004).

[11] K. Tucci and R. Kapral, *Mesoscopic multiparticle collision dynamics of reaction-diffusion fronts*, J. Chem. Phys. B **109**, pp, 21300-21304 (2005).

The VI International AMMCS
Interdisciplinary Conference
Waterloo, Ontario, Canada

A Tire Side Slip Model with Dynamic Friction Distribution over the Contact Patch

Shengxuan Zhao[1], Xianchao Zhang[2], Nan Xu[1]

[1] *State Key Laboratory of Automotive Simulation and Control, Jinlin University, Changchun, jilin, China, zhaosx22@mails.jlu.edu.cn, xu.nan0612@gmail.com*
[2] *FAW Volkswagen Co., Ltd. Qingdao Branch, qingdao, shandong, China, xianchao.zhang@faw-vw.com*

The tire forces and moments come mainly from the shear stress and sliding friction at the tread-road interface. The friction coefficient isn't uniform over the contact patch because of the pressure and velocity distribution. However, most of the existing tire models don't consider the influence of friction coefficient distribution. This paper aims to present a tire model considering friction distribution over the contact patch, and it can be applied to steady-state and non-steady-state conditions.

A discrete analytical tire model is proposed firstly in this paper considering compliance of carcass, then the velocity distribution is discussed. Finally, rubber friction model considering velocity and pressure distribution is introduced. The model appropriately expresses the high-speed tire mechanical characteristics through simulation.

Non-Fourier Bioheat Transfer Analysis of Interstitial Laser Ablation for Treating Brain Tumors

S. Singh[1], L. Bianchi[2], S. Korganbayev[2], P. Namakshenas[2], R. Melnik[3], P. Saccomandi[2]

[1] *University of Prince Edward Island, Charlottetown, Canada, sunsingh@upei.ca*
[2] *Politecnico di Milano, Milan, Italy, paola.saccomandi@polimi.it*
[3] *Wilfrid Laurier University, Waterloo, Canada, rmelnik@wlu.ca*

Interstitial laser ablation has emerged as a promising alternative treatment modality for treating difficult-to-access brain tumors [1]. During these therapies, a very thin flexible optical laser fiber (0.2-0.8 mm in diameter) is inserted within the target site to transport the near-infrared wavelength laser light. The interaction of light irradiated from the laser fiber tip results in the photothermal heating of biological tissue. This irreversible damage attained due to the heating of biological tissue is significantly dependent on several critical factors, viz., laser wavelength, laser power, treatment time, and thermal and optical properties of the tissue [2]. Computational modelling and simulation serve as a powerful tool for the prediction of heat propagation induced due to light-tissue interactions within the biological tissues during such therapies. In the present study, a finite-element-based model has been developed for predicting the temperature distribution and ablation (damage) volumes in the brain tissue subjected to interstitial laser ablation.

The main governing equations of this coupled model related to laser-tissue interactions are Beer Lambert's law and the bioheat transfer equation. Notably, the numerical predictions related to heat transport and ablation volume attained during laser therapy are tremendously dependent on the thermal properties of the biological tissues considered in the model [3, 4]. Thus, to enhance the accuracy of numerical prediction, we will utilize the temperature-dependent thermal properties of the *ex vivo* brain tissue quantified experimentally. Further, to improve the prediction accuracy, the lagging behavior associated with the finite speed of thermal signals propagation within biological tissue, i.e., non-Fourier effects, is also incorporated [5]. The fidelity and integrity of the developed model have been evaluated by comparing the computational results with those obtained with experimental studies conducted on the *ex vivo* brain tissue in terms of spatiotemporal temperature profile attained using fiber Bragg grating (FBG) sensors. The water vaporization effects have also been incorporated in the model to account for the abrupt decline in thermal conductivity of the biological tissue beyond the boiling point temperature of 100 ^{o}C. Parametric studies have been conducted to quantify the effect of laser fiber diameter, input power, treatment time, laser wavelength, and thermal relaxation times on the efficacy of interstitial laser ablation of the brain. The new findings and associated quantifications reported in this study could significantly assist clinical practitioners in the treatment planning stage of interstitial laser ablation of the brain by providing the optimal thermal dosage required to successfully ablate the tumor.

References

[1] A.M. Mohammadi and J.L. Schroeder, *Laser interstitial thermal therapy in treatment of brain tumors–the NeuroBlate System*, Expert Rev. Med. Devices 11, 2, pp. 109-119 (2014).
[2] A. Mohammadi, L. Leonardo Bianchi, S. Korganbayev, M.D. Landro and P. Saccomandi, *Thermomechanical modeling of laser ablation therapy of tumors: Sensitivity analysis and optimization of influential variables*, IEEE. Trans. Biomed. Eng. 69, 1, pp. 302-313 (2021).
[3] S. Singh and R. Melnik, *Thermal ablation of biological tissues in disease treatment: A review of computational models and future directions*, Electromagn. Biol. Med. 39, 2, pp. 49-88 (2020).
[4] L. Bianchi, F. Cavarzan, L. Ciampitti, M. Cremonesi, F. Grilli and P. Saccomandi, *Thermophysical and mechanical properties of biological tissues as a function of temperature: A systematic literature review*, Int. J. Hyperthermia 39, 1, pp. 297-340 (2022).
[5] S. Singh and R. Melnik, *Coupled thermo-electro-mechanical models for thermal ablation of biological tissues and heat relaxation time effects*, Phys. Med. Biol. 64, 24, pp. 245008 (2019).

Numerical Modeling and Simulation of Acupuncture-like Physical Therapy to Promote Healthy Aging

S. Singh[1], A. Escobar[2], Z. Wang[2], Z. Zhang[3], C. Ramful[3], C. Xu[2]

[1] *Faculty of Sustainable Design Engineering, University of Prince Edward Island, Charlottetown, Canada, sunsingh@upei.ca*
[2] *Department of Engineering Physics, McMaster University, Hamilton, Canada, cqxu@mcmaster.ca*
[3] *Advanced Electronics and Photonics Research Center, National Research Council Canada, Ottawa, Canada, zhiyi.zhang@nrc-cnrc.gc.ca*

Aging is an inevitable law of life, and it's no secret that Canada's population is also aging. Canadians aged 65 and older account for 19 % of the total population and are more prone to pain conditions [1]. Acupuncture is one of North America's fastest-growing complementary and alternative medicine therapies that has received significant attention in treating many diseases, such as musculoskeletal pain, gastrointestinal disorders, stroke, gynecological diseases, and neurological disorders [2, 3, 4]. A recent study [5] by the University of California researchers highlighted that long-term, regular traditional acupuncture may be considered as a possible treatment modality for old-age people with multiple chronic conditions. Other highlighted health benefits to older people were reduced polypharmacy, physical and mental health improvements, increased social contact, and thus an overall increase in quality of life. Moving along this line, the proposed study aims to develop an acupuncture-like but completely non-invasive therapy to provide thermal stimulus to the tissue utilizing a near-infrared Light-Emitting Diode (LED) for providing various types of pain relief in old-age people. In the present study, the effectiveness of this technique has been evaluated utilizing a computational modeling framework, highlighting the temperature rise attained within the skin tissue. Notably, a 3D multilayer computational domain of skin comprising of the epidermis, dermis, and subcutaneous tissue has been considered that is irradiated by near-infrared LED. The optical, thermal, and bio-physical properties of skin tissue considered in the present study have been acquired from the recent literature. The spatiotemporal temperature distribution has been obtained by solving the Pennes bioheat transfer equation coupled with the Beer-Lambert law. The irradiation profile of the LED light has been experimentally characterized and imposed at the boundary of the skin surface for predicting temperature rise as a function of depth for different values of LED power and irradiation time. The experimental validation of the developed model has been done by comparing the numerical model predictions with those obtained by experimental tests conducted on Agar gel under the same environmental conditions. The findings reported in the present study would be utilized for developing a miniature device that could be easily mounted on textile-based wearable products (e.g., glove, head/arm/wrist/chest band, knee/neck pad, socks). Such a device would be beneficial in providing on-demand physical stimulus at home without needing periodic clinic visits to prevent and treat age-related diseases without medications, hence, promoting healthy aging.

References

[1] M. Hartt, S. Biglieri, M.W. Rosenberg and S. Nelson, *Aging people, aging places: Experiences, opportunities, and challenges of growing older in Canada*, Policy Press (2021).
[2] S. Austin, Z. Ramamonjiarivelo, H. Qu and G. Ellis-Griffith, *Acupuncture use in the United States: who, where, why, and at what price*?, Health Marketing Quarterly 32, 2, pp. 113-128 (2015).
[3] M.H. Jun, Y.M. Kim and J.U. Kim, *Modern acupuncture-like stimulation methods: a literature review*, Integrative Medicine Research 4, 4, pp. 195-219 (2015).
[4] J. Zhu, J. Li, L. Yang and S. Liu, *Acupuncture, from the ancient to the current*, The Anatomical Record 304, 11, pp. 2365-2371 (2021).
[5] R. Pagones, J.L. Lee and S. Hurst, *Long-term acupuncture therapy for low-income older adults with multimorbidity: A qualitative study of patient perceptions*, The Journal of Alternative and Complementary Medicine 24, 2, pp. 161-167 (2018).

Global Stability, Instability, and Periodicity in Some Differential Delay Physiological Models

Anatoli F. Ivanov[1]

[1] *Pennsylvania State University, United States, aivanov@psu.edu*

We study the dynamics in simple form differential equations with delay which serve as mathematical models of physiological processes in human body. Such equations appear in several instances, in particular, - as a pluripotential stem cell model [1] and as a delay model of megakaryopoiesis [2].

Both models are studied with unified approaches recently developed in papers [3, 4]. Sufficient conditions are derived when the unique positive equilibrium is globally asymptotically stable. It is shown that when the equilibrium is linearly unstable the corresponding differential delay equation admits a periodic solution slowly oscillating about it. The theoretical results are demonstrated in particular models with the nonlinearities and parameters used in actual applications.

References

[1] M.C. Mackey, *Unified hypothesis of the origin of aplastic anaemia and periodic hematopoiesis.* Blood **51**, pp. 941-956 (1978).

[2] L. Boullu, M. Adimy, F. Crauste, and L. Pujo-Menjouet, *Oscillation and asymptotic convergence for a delay differential equation modeling platelet production.* Discrete and Continuous Dynamical Systems, Ser. B **24**, no. 6, pp. 2417-2442 (2019).

[3] A.F. Ivanov, *Global asymptotic stability in a differential delay equation modeling megakaryopoiesis.* Functional Differential Equations **28**, nos. 3-4, pp. 103-116 (2021).

[4] A.F. Ivanov and B. Lani-Wayda, *Periodic solutions in a differential delay equation modelling megakaryopoiesis.* Proceedings of ISAAC-2021, Springer-Verlag, 2023, 12 pp. (to appear)

Robust continuation method for tracing solution curves with critical points

S. Léger[1]

[1] *Université de Moncton, Moncton, Canada, sophie.leger@umoncton.ca*

The finite element simulation of very large deformation of hyperelastic material is still a challenging problem [1, 2]. The problems are generally driven by a loading parameter, and it is often observed that for some values of this parameter, the solution varies extremely rapidly due to geometric and/or material non linearities, often leading to the break down of the solution process. To improve the solution process, numerical continuation methods are often used and have proved to be a very powerful tool [3, 4]. However, these methods can still lead to undesired results. In particular, near severe limit points and cusps, the solution process frequently encounters one of the following situations: divergence of the algorithm, a change in direction which makes the algorithm backtrack on a part of the solution curve that has already been obtained and omitting important regions of the solution curve by converging to a point that is much farther than the one anticipated. Detecting these situations is not an easy task when solving practical problems since the shape of the solution curve is not known in advance. This talk will therefore present an improved Moore-Penrose continuation method that will include two key aspects to solve difficult problems: detection of problematic regions during the solution process and additional steps to deal with them. The proposed approach can either be used as a basic continuation method or simply activated when difficulties occur. Numerical examples will be presented to show the efficiency of the new approach.

References

[1] S. Léger, A. Fortin, C. Tibirna and M. Fortin, *An updated Lagrangian method with error estimation and adaptive remeshing for very large deformation elasticity problems*, Int. J. Numer. Meth. eng. **100**, 13, pp. 1006-1030 (2014).

[2] S. Léger and A. Pepin, *An updated Lagrangian method with error estimation and adaptive remeshing for very large deformation elasticity problems: the three-dimensional case*, Comput. Meth. Appl. Mech. Eng. **309**, pp. 1-18 (2016).

[3] S. Léger, J. Deteix and A. Fortin, *A Moore-Penrose continuation method based on a Schur complement approach for nonlinear finite element bifurcation problems*, Comput. Struct. **152**, pp. 173-184 (2015).

[4] S. Léger, J. Haché and S. Traoré, *Improved algorithm for the detection of bifurcation points in nonlinear finite element problems*, Comput. Struct. **191**, pp. 1-11 (2017).

[5] S. Léger, P. Larocque and D. LeBlanc, *Improved Moore-Penrose continuation algorithm for the computation of problems with critical points*, Comput. Struct. **281** (2023).

Modeling and Analysis of Mass-Spring systems with Friction – Detachment Waves

Meir Shillor

Oakland University, Michigan, USA, shillor@oakland.edu

The talk describes our recent mathematical model for the dynamics of a two mass-spring-damper system with friction, and has two parts. The main part describes a mathematical study of the way detachment or slip waves, when the system transits from stick to slip motion, propagate in discrete and (future work) continuous systems. The introduction of friction changes the problem into a system of differential set-valued inclusions, which are mathematically interesting, but rather complex. Together with the analysis, we depict simulation results which provide insight into the process of the initiation of sliding.

The second short part, describes the use of such a 'simple' system as an example of a very general existence and uniqueness theorem for systems described by set-valued pseudomonotone operators, Kuttler and Shillor, [2] and K.T. Andrews et al. [3]. These results were used to establish the existence of weak or variational solutions of rather complex dynamical systems with contact and friction, as well as adhesion, damage, and thermal effects.

We follow closely [1].

References

[1] M. Shillor and K.L. Kuttler, *Detachment waves in frictional contact: I – A two-mass system,* Nonlinear Analysis: Real World Applications **73**, 103907 (2023).

[2] K.L Kuttler and M. Shillor, *Set-valued pseudomonotone maps and degenerate evolution inclusions,* Comm. Contemp. Math. **1** 1, pp. 87-123 (1999).

[3] K.T. Andrews, K. L. Kuttler, J. Li and M. Shillor, *Measurable solutions for elliptic inclusions and quasistatic problems,* Special issue of *Mathematical Analysis with Applications to Mechanics, Computers and Mathematics with Applications,* M. Barboteu, R. Brouzet, W. Han, S. Migorski and M. Shillor, (Eds), (2018), https://doi.org/10.1016/j.camwa.2018.09.025

Speed limits for two-qubit gates with weakly anharmonic qubits

S. Ashhab[1], F. Yoshihara[1,2], T. Fuse[1], N. Yamamoto[3], A. Lupascu[4], K. Semba[1,5]

[1] *National Institute of Information and Communications Technology, Koganei, Tokyo, Japan*
[2] *Department of Physics, Tokyo University of Science, Shinjuku, Tokyo, Japan*
[3] *Quantum Computing Center and Department of Applied Physics and Physico-Informatics , Keio University, Yokohama, Kanagawa, Japan*
[4] *Institute for Quantum Computing, Department of Physics and Astronomy, and Waterloo Institute for Nanotechnology, University of Waterloo, Waterloo, Ontario, Canada*
[5] *Institute for Photon Science and Technology, The University of Tokyo, Bunkyo-ku, Tokyo, Japan*

We consider the implementation of two-qubit gates when the physical systems used to realize the qubits possess additional quantum states in the accessible energy range [1]. We use optimal control theory to determine the maximum achievable gate speed for two-qubit gates in the qubit subspace of the many-level Hilbert space, and we analyze the effect of the additional quantum states on the gate speed. We identify two competing mechanisms. On one hand, higher energy levels are generally more strongly coupled to each other. Under suitable conditions, this stronger coupling can be utilized to make two-qubit gates significantly faster than the reference value based on simple qubits. On the other hand, a weak anharmonicity constrains the speed at which the system can be adequately controlled: faster operations require stronger control fields, which leads to faster decoherence and uncontrolled leakage outside the qubit space. In order to account for this constraint, we modify the pulse optimization algorithm to avoid pulses that lead to appreciable population of the higher levels. Then we find that the presence of the higher levels can lead to a significant reduction in the gate speed. We compare the optimal-control gate speeds with those obtained using the cross-resonance/selective-darkening protocol. We find that the latter, with some optimization, can be used to achieve relatively fast CNOT gates. These results can help the search for optimized gate implementations and provide guidelines for desirable conditions on anharmonicity to enable the utilization of the higher levels in realistic systems.

This work was supported by MEXT Quantum Leap Flagship Program Grant No. JPMXS0120319794 and by Japan Science and Technology Agency Core Research for Evolutionary Science and Technology Grant No. JPMJCR1775. A.L. acknowledges support from the National Sciences and Engineering Council of Canada.

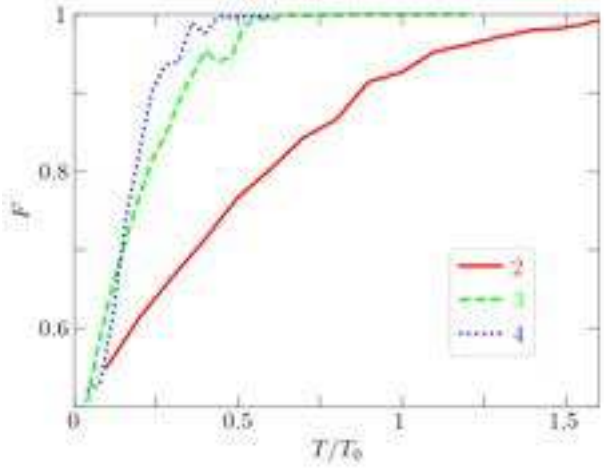

Figure 1: Two-qubit CNOT gate fidelity as a function of pulse time for numerically optimized pulses. The minimum gate time is identified as the pulse time at which the fidelity exceeds a preset threshold, e.g. 99.9%. The different lines correspond to different models of the qubits in which each qubit is replaced by a multi-level system with 2, 3 or 4 energy levels. The more the levels, the faster the CNOT gate.

References

[1] S. Ashhab et al., Phys. Rev. A **105**, 042614 (2022).

The VI International AMMCS
Interdisciplinary Conference
Waterloo, Ontario, Canada

Interplay between Amyloid-beta and Calcium Dynamics in Alzheimer's Disease: A Physics-Informed Bayesian Approach

Hina Shaheen[1], Roderick Melnik[2], Sundeep Singh[3]

[1] *MS2Discovery Interdisciplinary Research Institute, Wilfrid Laurier University, Waterloo, ON, Canada, shah8322@mylaurier.ca*
[2] *MS2Discovery Interdisciplinary Research Institute, Wilfrid Laurier University, Waterloo, Canada, rmelnik@wlu.ca*
[3] *Faculty of Sustainable Design Engineering, University of Prince Edward Island, Charlottetown, Canada, sunsingh@upei.ca*

Alzheimer's disease (AD) is a devastating neurodegenerative condition affecting millions worldwide. One of the leading indicators of AD is the abnormal buildup of extracellular amyloid-β ($A\beta$) in senile plaques, which leads to calcium (Ca^{+2}) dyshomeostasis [1, 2]. Despite numerous research endeavours, the molecular mechanisms driving $A\beta$ deposition and Ca^{+2} dysregulation in AD remain unclear. However, recent studies suggest a positive feedback loop between $A\beta$ and Ca^{+2} levels, where $A\beta$ interferes with neuronal Ca^{+2} levels, which then affect the formation of $A\beta$ [3].

Notably, the buildup of intraneuronal $A\beta$ accumulation is related to synaptic impairments, neuronal loss, and cognitive failure in AD patients. To gain a better understanding of the interplay between $A\beta$ and Ca^{+2} levels in AD, a novel stochastic model has been developed. This model utilizes a physics-based Bayesian approach to analyze the positive feedback loop between $A\beta$ and Ca^{+2}, using data from the Alzheimer's Disease Neuroimaging Initiative (ADNI). We analyzed the data for $A\beta$ concentration and fitted it to the developed stochastic model using the approximate Bayesian computation (ABC) technique. ABC is a data-driven strategy that utilizes a number of low-cost numerical simulations [4]. By investigating the interplay between $A\beta$ and Ca^{+2} levels at different phases of disease development, the model has shown that disrupting $A\beta$ metabolism or intracellular Ca^{+2} homeostasis leads to a relative growth rate in both Ca^{+2} and $A\beta$, which corresponds to the development of AD.

These findings suggest that targeting the Ca^{+2} balance or the balance between $A\beta$ and Ca^{+2} through chelation therapy may help reduce the symptoms associated with AD and pave the way for new research possibilities in AD treatment. Moreover, by considering the probabilistic nature of AD, the stochastic model offers a reliable framework for modelling the disease. Therefore, the model can provide more precise predictions about the disease's progression and potential outcomes with regular patient visits and observational data. Ultimately, this research may lead to new treatment options that alleviate the symptoms of AD.

References

[1] S. Moonen, M.J. Koper, E. Van Schoor, J.M. Schaeverbeke, R. Vandenberghe, C.A. von Arnim, T. Tousseyn, B. De Strooper, and D.R Thal, *Pyroptosis in Alzheimer's disease: Cell type-specific activation in microglia, astrocytes and neurons*, Acta Neuropathologica 145, 2, pp. 175-195 (2023).

[2] T. Gomez-Isla, and M.P. Frosch, *Lesions without symptoms: understanding resilience to Alzheimer disease neuropathological changes*, Nature Reviews Neurology 18, 6, pp. 323-332 (2022).

[3] Y. Zhang, and W. Wang, *Mathematical analysis for stochastic model of Alzheimer's disease*, Communications in Nonlinear Science and Numerical Simulation 89, pp. 105347 (2020).

[4] Beaumont, M.A, *Approximate Bayesian Computation*, Annual Review of Statistics and its Application 6, pp. 379-403 (2019).

Balancing statistical power and accuracy through multi-objective optimization of rhythm detection experiments

T. Silverthorne[1,2,3], M. Carlucci[2,3], A. Petronis[2,3], A. Stinchcombe[1]

[1] *Department of Mathematics, University of Toronto, Toronto, Canada*
[2] *The Krembil Family Epigenetics Laboratory, The Campbell Family Mental Health Research Institute, Centre for Addiction and Mental Health, Toronto, Canada*
[3] *Institute of Biotechnology, Life Sciences Center, Vilnius University, Vilnius, Lithuania*

Mathematical models are useful for exploring the structure and function of biological oscillators. Especially in systems where oscillations are under-explored, model development may be limited by the availability of high-quality experimental data. Obtaining high-quality data can be challenging due to the presence of multiple oscillation timescales, ethical constraints on sampling frequency and amount, as well as financial constraints on the total number of samples collected for downstream processing. Given these challenges and constraints, it is imperative to optimize the remaining degrees of freedom, such as the distribution of measurements.

In this talk, we treat the scheduling of measurements in a rhythm detection experiment as a multi-objective optimization problem. We seek measurement distributions that are capable of accurately characterizing oscillations (low bias and variance of amplitude and phase estimators), while maintaining adequate statistical power for reliable oscillation detection. In order to lessen the computational burden of power optimization, we apply a recently developed technique of hypervolume scalarization [1] in our optimization method. We use simulation studies along with easily-computable power heuristics [2] to measure the robustness of our designs to uncertainties in parameter values so that they may be applied in realistic experimental settings.

Our optimization protocol has applications in testing the theory of chrono-epigenetics [3]. Epigenetics is the study of chemical modifications to DNA. Methylation level (an epigenetic modification) predictably changes with age [4] and also oscillates on shorter timescales, such as hours and days in regions of the DNA with some of the most significant regulatory roles [5, 6, 7]. These findings led to the chrono-epigenetic hypothesis, which proposes that important epigenetic changes associated with aging, development, and disease are controlled by deterministic oscillations [3]. At the moment there is no consensus as to why biologically meaningful DNA regions are enriched for methylation oscillations [8]. We anticipate that the use of optimal sampling strategies will improve the feasibility of experimental tests of this theory.

References

[1] R. Zhang and D. Golovin, *Random hypervolume scalarizations for provable multi-objective black box optimization*, ICML, pp. 11096-11105 (2020).
[2] I. Kim, S. Balakrishnan and L. Wasserman, *Minimax optimality of permutation tests*. Ann. Stat., pp. 225-251 (2020).
[3] E.S. Oh and A. Petronis. *Origins of human disease: the chrono-epigenetic perspective*. Nat. Rev. Genet., pp. 533-546 (2021).
[4] S. Horvath and K. Raj. *DNA methylation-based biomarkers and the epigenetic clock theory of ageing*, Nat. Rev. Genet., pp. 371-384 (2018).
[5] S. Rulands, et al. *Genome-scale oscillations in DNA methylation during exit from pluripotency*, Cell Syst., pp. 63-76 (2018).
[6] G. Oh, et al. *Cytosine modifications exhibit circadian oscillations that are involved in epigenetic diversity and aging* Nat. Commun., (2018).
[7] G. Oh, et al. *Circadian oscillations of cytosine modification in humans contribute to epigenetic variability, aging, and complex disease* Genome Biol., pp. 1-14 (2019).
[8] A. Parry, et al. *Active turnover of DNA methylation during cell fate decisions* Nat. Rev. Genet. 22.1, pp. 59-66 (2021).

Semi-Analytical Solutions for SIHR Rumor Spreading Model in Social Networks

S. Chakouvari[1], R. Fallahpour[2], H. Askari[3]

[1] *University of Guilan, Iran, s.falah@gmail.com*
[2] *University of Toronto, Toronto, Canada, rosa.fp68@gmail.com*
[3] *University of Waterloo, Waterloo, Canada, h2askari@uwaterloo.ca*

In social networks, the spreading of rumors and epidemics exhibit notable distinctions, particularly when accounting for the reciprocal influence of forgetting and remembering mechanisms. Simultaneously, due to the nonlinearity and intricate elements inherent in these models, attaining an analytical or semi-analytical solution poses a formidable challenge. This article seeks to address this challenge by focusing on the development of semi-analytical solutions for a novel rumor spreading model known as the Susceptible-Infected-Hibernator-Removed (SIHR) model [1], mathematically described as below:

$$\frac{dI(t)}{dt} = -(\lambda + \beta)\bar{k}I(t)S(t)$$
$$\frac{dS(t)}{dt} = \lambda\bar{k}I(t)S(t) - \alpha\bar{k}S(t)(S(t) + H(t) + R(t)) - \delta S(t) + \xi H(t) + \eta\bar{k}S(t)H(t)$$
$$\frac{dH(t)}{dt} = \delta S(t) - \xi H(t) - \eta\bar{k}S(t)H(t)$$
$$\frac{dR(t)}{dt} = \beta\bar{k}I(t)S(t) + \alpha\bar{k}S(t)(S(t) + H(t) + R(t))$$

To analytically solve the above nonlinear differential equation, two advanced techniques, namely the Laplace Adomian Decomposition Method (LADM) and the Differential Transformation Method (DTM), are employed [2]. By leveraging these methods, the aim is to derive efficient and accurate solutions for the SIHR model, thereby contributing to a deeper understanding of rumor dynamics in social networks.

References

[1] L. Zhao, J. Wang, Y. Chen, Q. Wang, J. Cheng, H. Cui, *SIHR rumor spreading model in social networks.* Phys. A: Stat. Mech. Appl. **391**, 7, pp.2444-2453 (2012).
[2] E. Esmailzadeh, D. Younesian, H. Askari, *Analytical methods in nonlinear oscillations.* Netherlands: Springer (2018).

The VI International AMMCS
Interdisciplinary Conference
Waterloo, Ontario, Canada

Cutsets and EF1 Fair Division of Graphs

J. Chen[1], W.S. Zwicker [2]

[1] *TU Wien, Austria, jiehua.chen@tuwien.ac.at*
[2] *Murat Sertel Center for Advanced Economic Studies, Bilgi University, Istanbul, Turkey; Union College, Schenectady, NY, USA zwickerw@union.edu*

In fair division of a connected graph $G = (V,E)$, each of n agents receives a share of G's vertex set V. These shares partition V, with each share required to induce a connected subgraph. Each agent uses her assigned valuation function to determine the non-negative numerical value of her share, and these values determine whether the allocation is fair in some specified sense. We show that *graph cutsets*, introduced here, constitute obstacles to divisions that are fair in the EF1 (envy free up to one item) sense. If G guarantees connected EF1 allocations for n agents with valuations that are *CA* (common and additive), then G contains no *cutset of gap* ≥ 2 for n agents. If G guarantees connected EF1 allocations for n agents with valuations in the broader *CM* (common and monotone) class, then G contains no *generalized* cutset of gap ≥ 2 for n agents. These results rule out the existence of connected EF1 allocations in a variety of situations. They generalize one direction of the characterization, in Biló et al [1], of graphs that guarantee connected EF1 allocations for $n = 2$ agents as those containing no *trident* (regardless of whether valuations are *CA* or *CM*), and suggest that the CA vs CM distinction may be consequential for EF1 graph division when there are more than 2 agents. Additionally, we provide an example of a (non-traceable) graph on eight vertices that has no cutsets of gap ≥ 2 at all, yet fails to guarantee connected EF1 allocations for three agents with *CA* preferences.

References

[1] V. Bilò, I. Caragiannis, M. Flammini, A. Igarashi, G. Monaco, D. Peters, C. Vinci, and W.S. Zwicker, *Almost envy-free allocations with connected bundles*, Games and Economic Behavior **131**, pp. 197-221 (2022).

The VI International AMMCS
Interdisciplinary Conference
Waterloo, Ontario, Canada

A Multiscale model of protein allostery: Side chain concerted motions initiated by Brownian kicks

F. J. Burkowski[1]

[1] *University of Waterloo, fjburkowski@uwaterloo.ca*

Allosteric regulation in proteins has been studied for more than 55 years but the fundamental mechanisms of allosteric signalling and the time scales of their propagations remain elusive (see Refs. [1,2,3]). In this talk I avoid coarse grained models and offer a more detailed description of allostery that emphasizes the role of side chain atoms with one degree of freedom (DoF1: positioned by knowing the Chi 1 angle when the backbone is assumed to be fixed). The resulting near neighbor residue graph shows clear small world network properties with highly connected regions just below the binding site, illustrated in Figure 1 as a cluster of hydrophobic residues represented by yellow nodes. Meanwhile, lattice-like structures float over beta sheets and serve to connect the binding site nodes with other regions of the protein. Interactions are due to concerted (cooperative) motions involving changes in dihedral angles within the side chains. In this study, molecular dynamics simulations provided statistics recording the interactions between neighboring atom pairs (DoFn – DoFm interactions, where n and m designate the number of Chi angles).

Brownian motion has been studied for well over a century and the usual emphasis has been on the path taken by the large particle within a solvent bath (see Ref. [4]). Instead, I focus on the collision event itself: Prior to the collision we have the particle surrounded by molecules moving in a chaotic milieu (high dimensional specification of this motion).

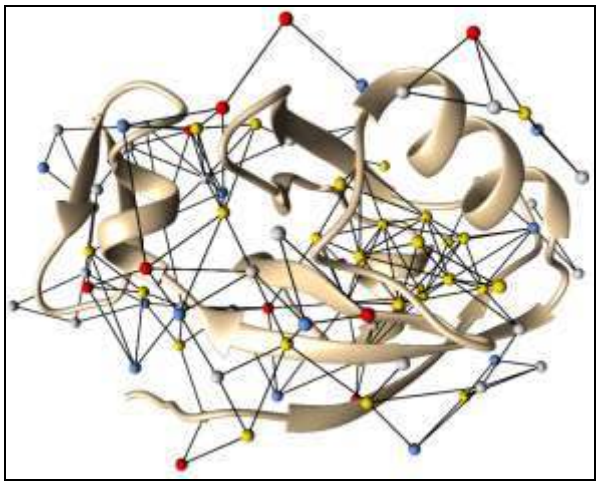

Figure 1: The residue network for the PDZ3 domain

When the rare but certain collision event occurs, the particle moves in a linear jump (low dimensional specification of that motion). Immediately after the collision, there is a deceleration of the particle due to dissipative collisions with the solvent molecules. I consider this multiple time scale event as the most elementary expression of "order out of chaos".

I contend that an analogous type of phenomenon occurs along pathways that start at the protein-water interface and end at the more concentrated hydrophobic core. Signal transmission tends to be directional and I will argue that when the model is applied to the PDZ3 domain, the resulting descriptions are consistent with the functional behaviour of a scaffold protein.

References

[1] G.M. Verkhivker, et al. *Allosteric Regulation at the Crossroads of New Technologies: Multiscale Modeling, Networks, and Machine Learning*, Front. Mol. Biosci. **7**, pp. 136-136 (2020).
[2] A. Kolinski, *Multiscale Approaches to Protein Modeling*, Springer Verlag, (2011).
[3] O. Bozovic, J. Ruf, C. Zanobini, et al. *The Speed of Allosteric Signaling Within a Single-Domain Protein*, J. Phys. Chem. Lett. **12**, 17, pp. 4262-4267 (2021).
[4] A. Genthon, *The concept of velocity in the history of Brownian motion*, EPJ H **45**, pp. 49–105 (2020).

Mathematical Analysis of Avian Influenza

S. Chakouvari[1], R. Fallahpour[2], H. Askari[3]

[1] *University of Guilan, Iran, s.falah@gmail.com*
[2] *University of Toronto, Toronto, Canada, rosa.fp68@gmail.com*
[3] *University of Waterloo, Waterloo, Canada, h2askari@uwaterloo.ca*

This article presents the development of two sets of semi-analytical solutions for a mathematical model that elucidates the transmission of avian influenza from birds to humans. The model under consideration emphasizes the potential occurrence of two types of avian influenza outbreaks if preventive measures are not taken by humans. Additionally, it emphasizes that simply maintaining a low overall number of infected humans is inadequate to ensure alleviation from the disease. The mathematical description of the analyzed model is provided below [1]:

$$\frac{dX(t)}{dt} = c - bX(t) - \omega X(t)Y(t)$$
$$\frac{dY(t)}{dt} = \omega X(t)Y(t) - (b+m)Y(t)$$
$$\frac{dS(t)}{dt} = \lambda - \mu S(t) - (\beta_1 Y(t) + \beta_2 H(t))S(t)$$
$$\frac{dB(t)}{dt} = \beta_1 S(t)Y(t) - (\mu + d + \varepsilon)B(t)$$
$$\frac{dH(t)}{dt} = \beta_2 S(t)H(t) + \varepsilon B(t) - (\mu + \alpha + \gamma)H(t)$$
$$\frac{dR(t)}{dt} = \gamma H(t) - \mu R(t)$$

To obtain efficient and accurate solutions for the avian influenza model, we employ two advanced techniques: the Laplace Adomian Decomposition Method (LADM) and the Differential Transformation Method (DTM) [2]. These methods are utilized to solve the coupled nonlinear differential equation mentioned above. By leveraging the capabilities of LADM and DTM, we aim to derive precise solutions for the avian influenza model.

References

[1] S. Iwami, Y. Takeuchi, X. Liu, *Avian–human influenza epidemic model*. Math. Biosci. **207**,pp. 1-25 (2007).
[2] E. Esmailzadeh, D. Younesian, H. Askari, *Analytical methods in nonlinear oscillations.* Netherlands: Springer (2018).

Between 1 and (1/e): History and Methods of an Oscillation Criterion for First-Order Delay Differential Equations

J.I. Stavroulakis[1]

[1] *Ariel University, Israel, john.ioannis.stavroulakis@gmail.com*

We investigate the oscillation of the first-order delay differential equation

$$x'(t) + p(t)x(\tau(t)) = 0, t \geq t_0 \in \mathbb{R}, \tag{1}$$

where $p: \mathbb{R} \to [0, +\infty)$, $\tau: \mathbb{R} \to \mathbb{R}$, $\tau(t) \leq t$, $\lim_{t\to\infty} \tau(t) = \infty$. We trace the evolution of the relevant literature, from the seminal results of

$$\liminf_{t\to\infty} \int_{\tau(t)}^{t} p(s)ds > \frac{1}{e}, \tag{2}$$

and

$$\limsup_{t\to\infty} \int_{\tau(t)}^{t} p(s)ds > 1, \tag{3}$$

to the recent, sharp, condition

$$\limsup_{t\to\infty} \int_{\tau(t)}^{t} p(s)ds > \kappa(\liminf_{t\to\infty} \int_{\tau(t)}^{t} p(s)ds), \tag{4}$$

where $\kappa : [0, \frac{1}{e}] \to [\frac{1}{e}, 1]$ is strictly decreasing, continuous. We focus on the ideas and methods applied to oscillation, both such as they were perceived at the time, and in the broader perspective of the overall advancements and improvements upon the criteria.

References

[1] R. Bellman and K.L. Cooke, Differential Difference Equations, Academic Press, New York, 1963.

[2] Y.I. Domshlak and A.I. Aliev, *On oscillatory properties of the first order differential equations with one or two retarded arguments*, Hiroshima Math. J., **18**, pp. 31-46, (1988).

[3] L.H. Erbe and B.G. Zhang, *Oscillation tests for delay equations*, The Rocky Mountain Journal of Mathematics , **29**, pp. 197-207, (1999).

[4] J.K. Hale, Theory of Functional Differential Equations, Springer-Verlag, New York, 1977.

[5] J. Jaroš and I.P. Stavroulakis, *Oscillation for first order linear differential equations with deviating arguments*, Differential Integral Equations, **1**, pp. 305-314, (1988).

[6] R.G. Koplatadze and T.A. Chanturija, *On oscillatory and monotonic solutions of first order differential equations with deviating arguments*, Differential'nye Uravnenija, **18**, pp. 1463-1465, (1982).(in Russian)

[7] M.K. Kwong, *Oscillation of first order delay equations*, J. Math. Anal. Appl., **156**, pp. 274-286, (1991).

[8] B.R. Hunt and J.A. Yorke, *When all solutions of* $x'(t) = -\sum q_i(t)x(t - T_i(t))$ *oscillate*, J. Differential Equ., **53**, pp. 139-145, (1984).

[9] G. Ladas, V. Lakshmikantham, and L.S. Papadakis, *Oscillations of higherorder retarded differential equations generated by the retarded arguments*, in Delay and functional differential equations and their applications, Academic Press, New York, 1972.

[10] A.D. Myshkis, *Linear Differential Equations with Delayed Argument*, Moscow, Nauka, 1972 (in Russian).

[11] M. Pituk, I.P. Stavroulakis, and J.I. Stavroulakis, *Explicit values of the oscillation bounds for linear delay differential equations with monotone argument*, Communications in Contemporary Mathematics, **25**, 3, 2150087, (2021).

[12] M. Pituk and J.I. Stavroulakis, *The first positive root of the fundamental solution is an optimal oscillation bound for linear delay differential equations*, J. Math. Anal. Appl., **507**, 1, 125789, (2022).

[13] J.S. Yu, Z.C. Wang, B.G. Zhang, and X.Z. Qian, *Oscillations of differential equations with deviating arguments*, Panamer. Math. J., **2**, pp. 59-78, (1992).

The VI International AMMCS
Interdisciplinary Conference
Waterloo, Ontario, Canada

On Totally Real PCF Parameters

C. Noytaptim[1], C.Petsche[2]

[1] *Oregon State University, USA, chatchai.noytaptim@gmail.com*
[2] *Oregon State University, USA, petschec@math.oregonstate.edu*

In this talk, we classify all post-critically finite unicritical polynomials defined over a maximal totally real extension of rational numbers. We use tools from complex potential theory and number theory. This is joint work with Clay Petsche.

References

[1] C. Noytaptim and C. Petsche. *Totally real algebraic integers in short intervals, Jacobi polynomials, and unicritical families in arithmetic dynamics*. Preprint, `https://arxiv.org/pdf/2211.07086.pdf`.

Two-person fair division with additive cardinal valuations

D. Marc Kilgour[1], Rudolf Vetschera[2],

[1] *Department of Mathematics, Wilfrid Laurier University, Waterloo, ON N2L3C5, CANADA. mkilgour@wlu.ca@ku.dk*
[2] *Department of Business Decisions and Analytics, University of Vienna, A-1090 Vienna, AUSTRIA. rudolf.vetschera@univie.ac.at*

Whether independent participants can share a resource fairly is an important and easily understood social choice problem. Is it possible to assign each agent a satisfactory proportion, or is it impossible to reconcile their conflicting interests? Among the criteria that have been proposed for a good allocation are utilitarianism and maximinality. Another criterion is envy-freeness. One agent envies another if the first would prefer the other?s assignment to its own; in an envy-free allocation, no agent envies any other.

We assume a finite set of indivisible items, over which each of two players has known preferences. Preferences are measured on a cardinal scale and are additive in that each player?s utility for any bundle of items is the sum of its utilities for the specific items in the bundle.

Even in the two-player case, it is possible that no envy-free allocation exists. We focus on the existence of envy-freeness and its relation with other desirable properties of allocations including efficiency, in the senses of Pareto and lexicographic optimality, maximum utility sum, and maximum Nash product. Are envy-freeness, and the related property called EFx, related to the utility of the worse-off player? We study these relationships both formally and using a comprehensive simulation, obtaining some analytic proofs as well as assessments of the frequency of some useful relationships.

Our approach is to assume that both players? utilities are chosen at random, independently, according to a distribution defined by Lebesgue measure. The only constraints are that each player?s utilities are non-negative and sum to 1. We identify certain properties of allocation problems that can potentially simplify the task of fair allocation, demonstrate their existence and relationship, and use them in simulations.

The VI International AMMCS
Interdisciplinary Conference
Waterloo, Ontario, Canada

Self-similar Heat Transfer in a Turbulent Particle-laden Free Flow

H. R Zandi Pour[1], M. Iovieno[1],

[1] *Politecnico di Torino, Dipartimento di Ingegneria Meccanica e Aerospaziale, Torino, Italy, hamid.zandipour@polito.it*

The inherently multiscale nature of fluid turbulence plays a major role in most natural and engineered systems, so that understanding and modeling turbulence at different scales is crucial for many applications, ranging from improving aerodynamic performance to optimizing industrial processes. When particles are suspended in a fluid, their interactions with the turbulent flow structures result in modified flow patterns, altered energy transfer mechanisms, and the emergence of new scales, making the understanding and modeling of particle-laden turbulent flows a challenging and active area of research. Present study focuses on analyzing the fluid-particle thermal interaction in a particle-laden turbulent flow, which recently has received attention [1, 2, 3], and for which experiments cannot provide a detailed picture. Specifically, we investigate a basic archetypal non-isothermal flow configuration, where an initial temperature step between two isothermal regions is advected by a turbulent, isotropic solenoidal velocity field. In this scenario, the flow is seeded with a set of identical inertial particles smaller than the Kolmogorov length scale. Utilizing the formalism introduced by Pousanrari and Mani [2] to represent particle dynamics, we demonstrate that the advection by the turbulent velocity field produces a self-similar evolution of both fluid and particle statistics for any particle inertia. Remarkably, when rescaled with a single length scale deduced from the mean temperature, all temperature and velocity-temperature moments collapse. This length scale shows a $t^{1/2}$ diffusive growth. The outcome of such analysis with a set of Direct Numerical Simulations (DNS) at moderate Reynolds number, carried out by using the Eulerian-Lagrangian point particle model, valid for small heavy sub-Kolmogorov particles, in both one-way coupling and two-way thermal coupling regimes. We considered a wide range of particle Stokes numbers, from 0.1 to 3, and a Taylor microscale Reynolds number up to 124. The thermal Stokes number to Stokes number ratio, which depends only on the ratio between the particle specific heat and fluid specific heat, is kept constant and equal to 4.43, which is representative of water droplets in air. The simulations allow to confirm self-similarity up to third order moments and the $t^{1/2}$ scaling, as in [4]. Moreover, the DNS data allow to complement the self-similar analysis by providing quantitative values for the phenomenological coefficients of the unclosed terms in Pouransari and Mani approach. The implications on turbulent modelling will be discussed. Overall, our analysis allows to quantify the role of particle inertia and thermal inertia on the ability of turbulence to transport heat, and to highlight the effect of the modulation of the carrier flow temperature fluctuations by particle thermal feedback.

References

[1] M. Carbone and A. Bragg, *Multiscale fluid-particle thermal interaction in isotropic turbulence*, J. Fluid Mech. **881**, pp. 679-721 (2019).

[2] H. Pouransari and A. Mani, *Particle-to-fluid heat transfer in particle-laden turbulence*, Physical Review Fluids **7**,(2018).

[3] I. Saito and T. Watanabe, *Modulation of fluid temperature fluctuations by particles in turbulence*, J. Fluid Mech. **931**,(2022).

[4] H. Zandi Pour and M. Iovieno, *Heat transfer in a non-isothermal collisionless turbulent particle-laden flow*, Fluids **345**,(2022).

The VI International AMMCS
Interdisciplinary Conference
Waterloo, Ontario, Canada

Comparing Algorithms for Fair Allocation of Indivisible Items with Limited Information

F. Ziaei[1], D. M. Kilgour[2]

[1] *Wilfrid Laurier University, Waterloo, Canada, ziae0890@mylaurier.ca*
[2] *Wilfrid Laurier University, Waterloo, Canada, mkilgour@wlu.ca*

In studies of collective decision-making, the problem of allocating indivisible items fairly and efficiently is now recognized as the most difficult. Here, various algorithms for finding allocations are assessed on their ability to achieve the desirable properties of envy-freeness, Pareto-optimality, maximin, maximum Borda sum, and Borda maximin. Two players with additive preferences allocate an even number of indivisible items when their only information is the other's strict preference ordering. Algorithms under study include both naive and sophisticated versions of sequential selection, bottom-up sequential selection (or sequential rejection), balanced alternation, bottom-up balanced alternation, and fallback bargaining. The results suggest that fallback bargaining, the only simultaneous algorithm, satisfies most fairness and efficiency criteria but has some distinctive drawbacks.

References

[1] F. Ziaei and D. M. Kilgour, *Comparing Algorithms for Fair Division of Indivisible Items* in *22th International Proceedings of Group Decision and Negotiation* GDN, 51-62(2022).

[2] D. M. Kilgour and R. Vetschera, *Two-player fair division of indivisible items: Comparison of algorithms*, in *European Journal of Operational Research* 271(2), 620-631 (2018).

[3] C. Klamler, *The Notion of Fair Division in Negotiations. Handbook of Group Decision and Negotiation* (2021).

The VI International AMMCS
Interdisciplinary Conference
Waterloo, Ontario, Canada

Comparison of extended Kalman filter and recurrent neural networks for state estimation

Avneet Kaur[1], Kirsten Morris[2]

[1] *University of Waterloo, Canada, a93kaur@uwaterloo.ca*
[2] *University of Waterloo, Canada, kmorris@uwaterloo.ca*

State estimation of a dynamical system refers to estimating the state of a system given a noisy model, measurements and some information about the initial state. While Kalman filtering[1] is optimal for estimation of linear systems with Gaussian noises, calculation of optimal estimators for high order non-linear systems of ordinary differential equations is challenging. A common method is to linearize the system at each step and use a Kalman filter on the linearization; this is known as an Extended Kalman Filter (EKF). However, this approach is not optimal and is not always stable. We focus on establishing a pathway to explore optimal methods for state estimation of high-order systems by using neural nets. We train a recurrent neural network(RNN) to estimate the state of a system. An RNN seems the obvious choice of neural net due to its structure[2] and the presence of approximation theory [3]. These results imply that an optimal estimator can be implemented as an RNN to arbitrary accuracy.

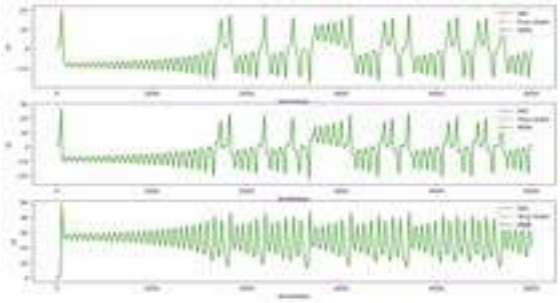

(a) Estimated states vs true states

↓Property/Method →	RNN	EKF
MSE	0.2346	0.4180
Execution time(in sec)	0.24	54.46

(b) MSE and execution time

Figure 1: State trajectory, mean squared error and execution time comparison for Lorenz system. Note that time $t = 0.01\times$timesteps and varies from 1 to 50 seconds. All data considered had additive white Gaussian noises.

An EKF is compared to the RNN for several examples of discretized systems of differential equations, including the Lorenz equations. Details of training the RNN are briefly described. Our results show that execution time and mean square error are both significantly reduced (Table 1b). Figures will be presented that show, except for the initial time-steps, matching of estimated state to the true state (Fig. 1a) . It is explained how the linearization error is reduced when an RNN is used and the consequences of this for the estimation error.

Future work will be further testing on higher-order systems and also showing convergence and stability of the RNN.

References

[1] R. Kalman, *A new approach to linear filtering and prediction problems* (1960).
[2] Ian Goodfellow, Yoshua Bengio, and Aaron Courville, *Deep Learning* The MIT Press, Cambridge, Massachusetts (2016)
[3] A. M. Schäfer and H. G. Zimmermann, *Recurrent neural networks are universal approximators* in *Artificial Neural Networks-ICANN 2006* Part I 16, pp. 632-640 (2006)

The VI International AMMCS
Interdisciplinary Conference
Waterloo, Ontario, Canada

An extension of May's Theorem to three alternatives: axiomatizing Minimax voting

W. H. Holliday[1], E. Pacuit[2]

[1] *University of California, Berkeley, weshholliday@berkeley.edu*
[2] *University of Maryland, epacuit@umd.edu*

Voting on two alternatives appears unproblematic in comparison to voting on three. For two alternatives, May's Theorem [6] and its descendants uniquely characterize majority voting. For three alternatives, one faces the problem of majority cycles and the related Arrow Impossibility Theorem [1]. Nonetheless, we have shown that by adding some desirable axioms to May's axioms, we can uniquely determine how to vote on three alternatives. In particular, we add two axioms stating that the voting method should be immune to *spoiler effects* and avoid what is known as the *strong no show paradox* [2, 7].

We say that a preferential voting method suffers from a spoiler effect in an election if a candidate A would have won without a candidate B in the election, and a majority of voters prefer A to B, but with B included in the election, neither A nor B wins [3]. We say that a preferential voting method suffers from a strong no show paradox in an election if a candidate A would have won without some coalition of voters in the election, and A is the favorite candidate of each voter in the coalition, but with the coalition of voters included in the election, A loses [7].

Our main theorem states that any preferential voting method satisfying our enlarged set of axioms, which includes some weak homogeneity and invariance axioms, agrees with *Minimax* voting [9, 5] in all three-alternative elections, except perhaps in some improbable knife-edged elections in which ties may arise and be broken in different ways. A number of sophisticated Condorcet voting methods [10, 8, 3, 4] agree with Minimax in (at least non-knife-edged) three-alternative elections, so our result provides support for this common solution to the problem of voting on three alternatives.

References

[1] K.J. Arrow, *Social Choice and Individual Values*, 2nd ed., John Wiley & Sons, Inc., New York (1963).

[2] P.C. Fishburn and S.J. Brams, *Paradoxes of Preferential Voting*, Mathematics Magazine **56**, 4, pp. 207-214 (1983). DOI: 10.2307/2689808.

[3] W.H. Holliday and E. Pacuit, *Split Cycle: A new Condorcet-consistent voting method independent of clones and immune to spoilers*, Public Choice, Forthcoming. Available at `https://arxiv.org/abs/2004.02350`.

[4] W.H. Holliday and E. Pacuit, *Stable Voting*, Constitutional Political Economy, Forthcoming. DOI: 10.1007/s10602-022-09383-9.

[5] G.H. Kramer, *A dynamical model of political equilibrium*, Journal of Economic Theory **16**, 2, pp. 310-334 (1977). DOI: 10.1016/0022-0531(77)90011-4.

[6] K.O. May, *A Set of Independent Necessary and Sufficient Conditions for Simple Majority Decision*, Econometrica **20**, 4, pp. 680-684 (1952).

[7] J. Pérez, *The Strong No Show Paradoxes are a common flaw in Condorcet voting correspondences*, Social Choice and Welfare **18**, 3, pp. 601-616 (2001). DOI: 10.1007/s003550000079.

[8] M. Schulze, *A new monotonic, clone-independent, reversal symmetric, and condorcet-consistent single-winner election method*, Social Choice and Welfare **36**, pp. 267-303 (2011). DOI: 10.1007/s00355-010-0475-4.

[9] P.B. Simpson, *On Defining Areas of Voter Choice: Professor Tullock on Stable Voting*, The Quarterly Journal of Economics **83**, 3, pp. 478-490 (1969). DOI: 10.2307/1880533.

[10] T.N. Tideman, *Independence of Clones as a Criterion for Voting Rules*, Social Choice and Welfare **4**, pp. 185-206 (1987). DOI: 10.1007/bf00433944.

New variance related dynamics in the Wilson-Cowan model

N. Doyon[1,2], V. Pinchaud[3], P. Desrosiers[1,2]

[1] *Laval University, Quebec, Canada,*
[2] *CIMMUL, Quebec, Canada,*
[3] *McGill, Montreal, Canada*

Wilson-Cowan equations have been used for decades to describe neural populations [1]. In this formalism. individual neurons are in one of three states: Active, Sensitive or Refractory. Transitions between states occur in a stochastic manner. Let $A(t), S(t), R(t)$ stand for the proportion of neurons in each state at time t. Their expected values evolve according to

$$\frac{dE[A]}{dt} = E[-\beta A + \alpha SF(A)], \quad \frac{dE[S]}{dt} = E[R - \alpha SF(A)], \quad \frac{dE[R]}{dt} = E[-R + A]. \tag{1}$$

Here, $F(A) = \sigma((wA-\theta)/s)$ with σ being the sigmoid function is a bounded activation function. The parameters $(\alpha, \beta, \gamma, w, \theta, s)$ specify the model. In the meanfield approximation, expectations are dropped and (1) becomes a system of odrdinary differential equations (ODEs). However, the meanfield approximation may fail to capture the behaviour of the underlying stochastic atomistic model.

Equation (1) is not closed since the right hand side is not a function of $E[A], E[S]$ and $E[R]$. A task of interest is to approximate (1) by a close ODE system that captures the behaviour of the underlying stochastic system. The moment closure method is a natural approach in which one develops the right-hand side with a Taylor expansion. However, this can lead the solutions making no physiological sense (i.e. with proportions outside to $[0,1]$ range). As an alternative, we here apply the method of size expansion developed by Gast et al. [2]. We show the importance of taking variances and covariances into account when building an ODE system approximating (1) [3]. We compare the quality of various approximations using the ground truth obtained from solving the master equation.

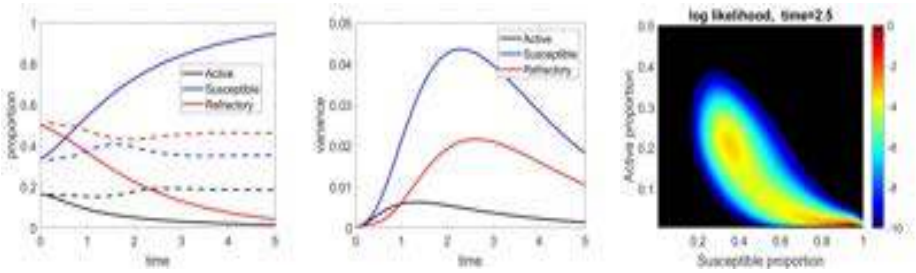

Figure 1: **Left**: True (full lines) and meanfield (dash lines) solutions. **Center**: Time courses of variances. **Right**: State distribution at $t = 2.5$ from the master equation. This illustrates the insufficiency of the meanfield approach ($\alpha = 1.4, \beta = 2.5, \gamma = 1, w = 5.5, \theta = .75, s = .1$).

References

[1] JD Cowan, J Neuman and W van Drongelen , *Wilson-Cowan Equations for Neocortical Dynamics*, The Journal of Mathematical Neuroscience, Vol 6.1 (2016).

[2] N Gast, L Bortolussi, and M Tribastone, *Size expansions of mean field approximation: Transient and steady-state analysis*, Performance Evaluation, Vol 129, pp. 60-80 (2019).

[3] V Painchaud, P Desrosiers and N Doyon, *The determining role of covariances in large networks of stochastic neurons*, arXiv:2212.09705 (2022).

Some Further Results on Ordinal Bayesian Incentive Compatible Probabilistic Voting Rules

M. Karmokar[1], D. Majumdar[2], S. Roy[3]

[1] *Indian Statistical Institute, Kolkata, India.* {*madhuparnakarmokar@yahoo.in*}

[2] *Concordia University, Montreal Canada.* {*dipjyoti.majumdar@concordia.ca*}

[3] *Indian Statistical institute, Kolkata, India.* {*souvik.2004@gmail.com*}

1 Extended Abstract

Ordinal Bayesian Incentive Compatibility (OBIC) is a natural weakening of dominant strategy incentive compatibility or strategyproofness in models of strategic voting. Introduced in d'Aspremont and Peleg (1988), OBIC has been studied extensively in deterministic voting models (see for example, Mishra (2016)). The present paper explores the consequences of OBIC in a probabilistic voting model. A probabilistic or random voting rule selects, for every profile of voter preferences, a lottery over the alternatives. A random voting rule is thus represented by a *random social choice function (RSCF)* that associates with every profile of voter preferences a lottery over alternatives. A random social choice function is OBIC if the interim expected outcome probability distribution from reporting truthfully first order stochastically dominates any interim outcome probability distribution induced by misreporting. The interim expected outcome probability is computed with reference to the voter's *prior beliefs* about the (possible) preferences of the other voters and is based on the assumption that the other voters follow the truth-telling strategy.

Allowing for randomization is often conceived as a means to resolve conflicts in collective decision making. For voting problems however, the celebrated result by Gibbard (1977) demonstrates that over the universal domain, the only random social choice functions that are strategyproof and satisfy *unanimity* are *random dictatorships*.

The notion of OBIC as a incentive requirement clearly depends on the priors. Our results are two-fold. First, we consider a class of priors which can be described as a small generalization of the uniform priors. We demonstrate that the randomized version of the plurality rule is OBIC over a large class of domains, if and only if the prior belongs to the class we consider.

Second, we study OBIC with a *generic* class of priors. For *deterministic* social choice

functions Majumdar and Sen (2004) demonstrate the equivalence of strategyproofness and OBIC for a large class of priors. The class of is generic in the set of independently distributed common prior in a topological sense. We pursue this line of research for random social choice functions. It is well known, (see for example Majumdar and Roy (2021)) that generic priors as defined in Majumdar and Sen (2004) or Mishra (2016) do not precipitate equivalence of strategyproofness and OBIC for random social choice functions. The reason such a condition works in those papers is that for each profile of preferences a deterministic social choice function selects a *degenerate* lottery over alternatives. We consider random social choice functions where for each profile, the probability weight on each alternative belongs to a finite set X.We then consider OBIC with respect to priors that are "generic" with respect to the elements in the set X in a specific sense. We call this condition on priors Condition-G^*. Condition-G^* that we identify depends crucially on the set X. Our main result is that any RSCF whose range is restricted to the set X, is OBIC with respect to a prior satisfying Condition-G^* if and only if it is a random dictatorship. Our second result identifies condition that precipitate equivalence between strategyproofness and OBIC for RSCFs.

References

d'Aspremont, C. and B. Peleg (1988): "Ordinal Bayesian Incentive Compatible Representation of Committees," *Social Choice and Welfare*, 5, 261–280.

Gibbard, A. (1977): "Manipulation of Schemes that mix Voting with Chance," *Econometrica*, 46, 665–681.

Majumdar, D. and S. Roy (2021): "Ordinally bayesian Incentive Compatible Probabilistic Voting Rules," *Mathematicxal Social Sciences*, 114, 11–27.

Majumdar, D. and A. Sen (2004): "Ordinal Bayesian Incentive Compatible Voting Rules," *Econometrica*, 72, 523–540.

Mishra, D. (2016): "Ordinal Bayesian Incentive Compatibility in Restricted Domains," *Journal of Economic Theory*, 163, 925–954.

The VI International AMMCS
Interdisciplinary Conference
Waterloo, Ontario, Canada

Some Stability Results on Impulsive Systems with Time Delay

Xinzhi Liu[1]

[1] *University of Waterloo, Waterloo, Canada, xzliu@uwaterloo.ca*

The theory of impulsive systems is attracting an increased interest of many researchers around the globe since it provides a general framework for mathematical modeling of many real world phenomena. Some typical physical systems that exhibit impulsive behavior include impact mechanics, thruster-based maneuver of a spacecraft, interest rate adjustment in financial market, and drug administration in cancer therapy. This talk discusses the stability problems of impulsive systems with time delay. A few approaches are presented and several stability criteria are established. Moreover, some examples are given to illustrate effectiveness of the theoretical results.

The VI International AMMCS
Interdisciplinary Conference
Waterloo, Ontario, Canada
June 9, 2023

Unsupervised methods for quantification of nanostructure order

M.P. Tino[1], N.M. Abukhdeir[1,2],

[1] *Department of Chemical Engineering, University of Waterloo, Waterloo, Canada*
[2] *Department of Physics and Astronomy, University of Waterloo, Waterloo, Canada*
nmabukhdeir@uwaterloo.ca

Although reliable and robust image characterization techniques exist for nanomaterials [5], post-processing of these images to quantify structure/property relationships is an underdeveloped research area [1]. Quantification of nanostructure order is made difficult by the presence of complex spatially-varying pattern symmetries on the nanoscale [1]. Moreover, recent research has utilized nanomaterial defects for improved or novel material functionality [6], referred to as *defect structure engineering* [3]. For self-assembled materials, the importance of defects on the resulting ordered nanostructures is critical for their use in devices and other technological applications [8]. Thus the development of computational methods to automate the identification and classification of nanomaterial defects is key for further progress in both research and technological applications.

Recent work using *polar shapelets*, a family of orthogonal basis functions with rotational symmetry properties [4], has been used to identify local pattern order [2]. These existing shapelet-based methods rely on user input [2], where incorrect input can lead to less accurate order quantification, including poor resolution of pattern defects. The goal of this research project is to enhance the current *supervised* method to be both unsupervised and more computationally efficient. Both of these objectives are achieved through the use of clustering analysis [7].

Previous work used a subset of shapelets to capture at most hexagonal order [2]. However, results in this work use higher-order shapelets via a *reduced response basis* resulting from clustering analysis. This reduced basis is used to automate the classification of defect regions, which involve order response with degenerate phase, versus defect-free regions of the pattern. This reduces computational complexity while increasing defect identification resolution. This significant result is used to develop efficient unsupervised shapelet methods for quantification of nanostructure order.

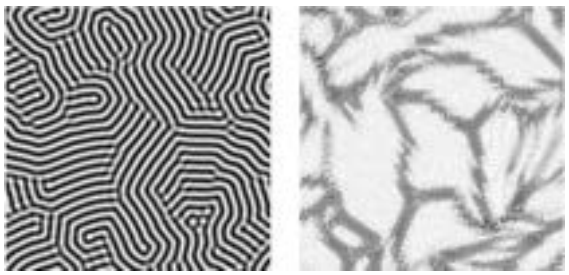

Figure 1: Simulated self-assembly stripe nanostructures (left). The result of applying the *unsupervised* shapelet-based method to automatically identify grain boundary defects (right).

References

[1] N. M. Abukhdeir. Computational characterization of ordered nanostructured surfaces. *Materials Research Express*, 3(8):082001, 2016.

[2] T. J. Akdeniz, D. J. Lizotte, and N. M. Abukhdeir. A generalized shapelet-based method for analysis of nanostructured surface imaging. *Nanotechnology*, 30(7):075703, 2018.

[3] J. Gubicza. *Defect structure and properties of nanomaterials*. Woodhead Publishing, 2017.

[4] R. Massey and A. Refregier. Polar shapelets. *Monthly Notices of the Royal Astronomical Society*, 363(1):197–210, 2005.

[5] S. Mourdikoudis, R. M. Pallares, and N. T. Thanh. Characterization techniques for nanoparticles: comparison and complementarity upon studying nanoparticle properties. *Nanoscale*, 10(27):12871–12934, 2018.

[6] D. Rhodes, S. H. Chae, R. Ribeiro-Palau, and J. Hone. Disorder in van der waals heterostructures of 2d materials. *Nature materials*, 18(6):541–549, 2019.

[7] J. Wu. *Advances in K-means clustering: a data mining thinking*. Springer Science & Business Media, 2012.

[8] W. Li, M Müller. Defects in the self-assembly of block copolymers and their relevance for directed self-assembly. *Annual review of chemical and biomolecular engineering*, 6:187–216, 2015.

The VI International AMMCS
Interdisciplinary Conference
Waterloo, Ontario, Canada

Strictly Uniform Exponential Decay of the Mixed-FEM Discretization for the Wave Equation.

Luis A. Mora, Kirsten Morris, David C. del Rey Fernández

Department of Applied Mathematics, University of Waterloo, Canada, {lmora,kmorris,ddelreyfernandez}@uwaterloo.ca

Generally, partial differential equations (PDEs) need to be approximated in order to design controllers and estimators. One issue with some numerical methods is that spurious high-frequency eigenvalues can occur. While not significant in simulation, they negatively affect controller design, disturbing the stability margin. A uniform stability margin, or more generally uniform stabilizability, is a necessary condition for controller and estimator convergence. In this work, we use a stain–momentum formulation of the wave equation with boundary dissipation, i.e., considering the material parameters ρ and τ, the boundary dissipation β, and defining $q(x,t) = -\frac{\partial w(x,t)}{\partial x}$ and $p(x,t) = \rho \frac{\partial w(x,t)}{\partial t}$ where $w(x,t)$ is the wave deflection, we obtain the following system:

$$\frac{\partial}{\partial t}\begin{bmatrix} q(x,t) \\ p(x,t) \end{bmatrix} = \begin{bmatrix} 0 & -1 \\ -1 & 0 \end{bmatrix} \frac{\partial}{\partial x}\begin{bmatrix} \tau q(x,t) \\ p(x,t)/\rho \end{bmatrix}, \quad \forall x \in [a,b] \tag{1}$$

$$\text{subject to } p(a,t) = 0 \quad \text{and} \quad -\tau q(b,t) + \beta \frac{p(b,t)}{\rho} = 0. \tag{2}$$

with total energy given by $E(t) = \frac{1}{2}\int_a^b \tau q^2(x,t) + \frac{p^2(x,t)}{\rho} dx$. As shown in [1], using the multiplier approach [2, Ch.7] we define an auxiliary Lyapunov functional $V(t) = E(t) + \varepsilon \int_a^b p(x,t)m(x)q(x,t)dx$, where $m(x) = x - a$ is a multiplier function and $\varepsilon \geq 0$, allowing us to obtain bounds for the exponential decay rate and amplitude, expressed in terms of the physical parameters. We extend this approach for the approximated model analysis, setting the conditions for the construction of the discrete Lyapunov function. Proving that, from the multiplier approach point of view, a first-order mixed finite-element method (MFEM) yields strictly uniformly exponentially stable approximations, i.e., the discrete energy exponential decay rate and amplitude obtained are equal to the continuous system one's. The scheme uses linear splines as basis functions and piecewise constant splines for test functions, as shown in Figure 1. Numerically, the decay rate appears to match the exact decay rate of the original partial differential equation.

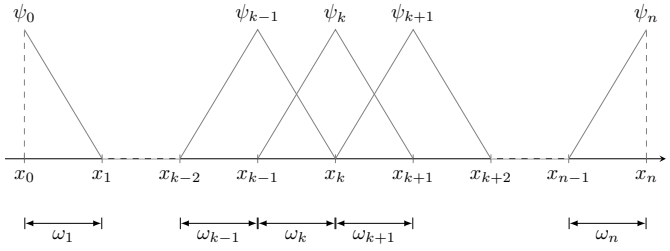

Figure 1: Basis ψ_k and test functions w_k used for the Mixed-FEM approximation.

References

[1] L. A. Mora and K. Morris, *Exponential Decay Rate of Port-Hamiltonian Systems with One Side Boundary Damping* in The 25th International Symposium on Mathematical Theory of Networks and Systems, MTNS 2022, pp. 1001–1006.

[2] M. Tucsnak and G. Weiss, *Observation and Control for Operator Semigroups*. Basel: Birkhäuser Basel, 2009.

Stabilization of a Parabolic-Elliptic System via Backstepping

Ala' Alalabi[1] and Kirsten Morris[1]

[1] *Department of Applied Mathematics, University of Waterloo,*
aalalabi@uwaterloo.ca, kmorris@uwaterloo.ca

The aim is stabilization of the following class of parabolic-elliptic systems

$$w_t(x,t) = w_{xx}(x,t) - \rho w(x,t) + \alpha v(x,t), \tag{1}$$

$$0 = v_{xx}(x,t) - \gamma v(x,t) + \beta w(x,t), \tag{2}$$

$$w_x(0,t) = 0, \quad w_x(1,t) = u(t), \quad v_x(0,t) = 0, \quad v_x(1,t) = 0, \tag{3}$$

where $x \in [0,1]$ and $t \geq 0$. The parameters ρ, α, β, γ are real, with α, β both nonzero. Also $\gamma \neq -(n\pi)^2$ so the operator $\gamma I - \partial_{xx}$ is invertible which ensures the well-posedness of (1)-(3) [1]. Such systems appear in the mathematical modelling of lithium-ion cells [2]. In the case when the parabolic equation is stable, it would be expected that the coupling between the equations would either enhance the convergence rate or at least keep it unchanged. However, it was shown in [3] that a linear parabolic-elliptic system can be unstable for some parameters. The control problem of such systems was considered in [4] where two control inputs were required. We design one boundary control using a backstepping approach. Explicit calculation of the eigenfunctions is not required. We use a backstepping transformation previously used for parabolic equations [4] which does not rely on reduction to a single equation. The result is an explicit expression for a boundary control that stabilizes the coupled system; or more generally, improves the decay rate in the situation when the original system is stable. The result is illustrated with simulations. Figure 1 presents the parabolic state $w(x,t)$ before and after control.

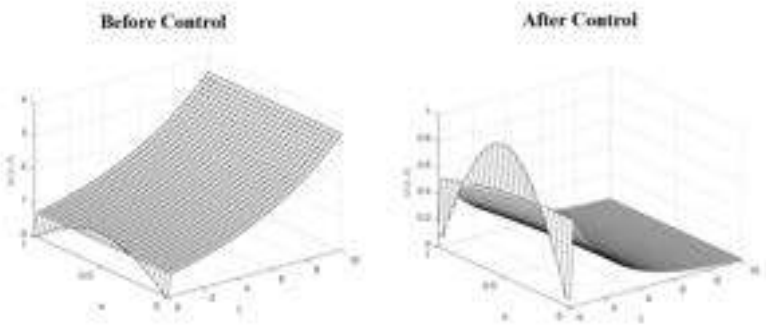

Figure 1: A 3D landscape of the dynamics of the parabolic state of system (1)-(3) before and after applying the control

References

[1] B. Jacob and K. Morris, *On solvability of dissipative partial differential-algebraic equations*. IEEE Control Systems Letters, 6, pp.3188-3193 (2022).

[2] J. Wu, J. Xu, and H. Zou, *On the well-posedness of a mathematical model for lithium-ion battery systems*. Methods and Applications of Analysis, 13(3), pp.275-298 (2006).

[3] H. Parada, E. Cerpa, and K. Morris, *Feedback control of an unstable parabolic-elliptic system with input delay*, preprint, (2022).

[4] M. Krstic and A. Smyshlyaev, *Boundary control of PDEs: A course on backstepping designs*. Society for Industrial and Applied Mathematics (2008).

An Analysis of Statistical Machine Learning Performance in Bankruptcy Prediction

Wayne Shen[1], Cristina Stoica[2], Xu Wang[3]

[1] *Wilfrid Laurier University, Waterloo, Canada, shen2670@mylaurier.ca*
[2] *Wilfrid Laurier University, Waterloo, Canada, cstoica@wlu.ca*
[3] *Wilfrid Laurier University, Waterloo, Canada, xwang@ wlu.ca*

Bankruptcy risk is the probability of a company failing to repay its debt obligation. Though, with the ever-developing data analysis techniques and methodologies, statistical models can efficiently capture and analyze the pattern and extract information or variances of the entire dataset for better decision-making than ordinary procedures and formulas. Thus, this data-driven project will apply statistical machine learning algorithms to address the imbalance of the dataset and discover the optimal prediction of the bankruptcy of the companies in Taiwan from 1999 to 2019[4].

In this analysis, we apply Random Undersampling, Random Oversampling, and Synthetic Minority Oversampling Technique (SMOTE)[5] to the training set and compare their performance with four different statistical machine learning methods to estimate the bankruptcy of 6819 companies. The statistical machine learning algorithms include Logistic Regression, K-Nearest Neighbors, Random Forest, and Support Vector Machine. Furthermore, this project will also discuss the chosen tuning parameters and interpret the symbolization behind each recorded metric. For our study, we will be the most interested in comparing sensitivity and specificity across different techniques and methods instead of only comparing the accuracy that holds trivial meaning.

Although all sampling techniques provided similar results in most machine learning methods, our results showed that applying the Random Undersampling technique and Random Forest method on the dataset has the best result in sensitivity and specificity with a minimal difference illustrated by the low standard deviation of ten distinct trial simulations. The dataset was collected from the University of California Irvine Repository of Machine Learning Databases, and the simulation of this analysis was completed in R.

References

[1] B. Keller and I. Reiten, *Cluster-titled algebras are Gorenstein and stably Calabi-Yau,* Adv. Math. **211**, 1, pp. 123-151 (2007).
[2] S. Washito and K. Karabashi, *Use This Template*, in *Proceedings of the 5th International Conference on Photon Interaction* (ICPI-2012), San Francisco, USA, ed. A. Chen, pp. 22-24 (2012).
[3] A.B. Smith, *Describing the style for the AMMCS-CAIMS-2015 book of abstracts*, in C.D. Science (ed.), General Book of Wisdom, 2nd ed., University of Queensland, pp. 23-42 (2014).
[4] Liang D, Tsai CF. (2020). *Taiwanese Bankruptcy Prediction Data Set*. UCI Repository of Machine Learning Databases. https://archive.ics.uci.edu/ml/datasets/Taiwanese+Bankruptcy+Prediction
[5] Dongyuan Wu. (2022). *SMOTE_NC: Synthetic Minority Oversampling Technique-Nominal Continuous.* R Package Documentation. https://rdrr.io/github/dongyuanwu/RSBID/man/SMOTE_NC.html

The VI International AMMCS
Interdisciplinary Conference
Waterloo, Ontario, Canada
June 15, 2023

Modeling quantum photonic neural networks with experimental imperfections

J. Ewaniuk[1], J. Carolan[2], B. J. Shastri[3], N. Rotenberg[4]

[1] *Centre for Nanophotonics, Queen's University, Kingston, Canada, jacob.ewaniuk@queensu.ca*
[2] *Wolfson Institute for Biomedical Research, University College London, London, United Kingdom, jacquescarolan@gmail.com*
[3] *Centre for Nanophotonics, Queen's University, Kingston, Canada, bhavin.shastri@queensu.ca; Vector Institute, Toronto, Canada*
[4] *Centre for Nanophotonics, Queen's University, Kingston, Canada, nir.rotenberg@queensu.ca*

Quantum photonic neural networks (QPNNs) are reconfigurable photonic circuits inspired by machine learning that can be taught to process quantum photonic states deterministically. They have been proposed to realize key components of emerging quantum technologies [1], act as a platform for quantum computation and simulation [2], and even speed up conventional machine learning tasks [3]. Here, we build on the early proposals [2, 3] and show how to construct a model of imperfect QPNNs, which we then use to benchmark their performance. We first consider the effect of standard nanophotonic imperfections on the network, specifically considering photon loss and imperfect routing. As shown in Fig. 1, a randomly selected amount of loss and directional coupler splitting ratio variation is assigned to each component throughout the network from distributions chosen to match recent experimental results. We further incorporate weak optical nonlinearities by specifying an effective nonlinear phase shift less than the ideal π. With these imperfections, we construct a network transfer function and demonstrate how it is used to train the QPNN, where its fidelity (the chance it produces the correct output state for any given input) is optimized by varying the programmable phase shifters in each Mach-Zehnder interferometer (MZI) throughout the network. This process relies on advanced numerical modeling and runtime-sensitive operations to describe how an imperfect QPNN affects incoming photons. In our analysis, we find that the QPNN *learns* to correct imbalances across its components and maximize the effect of the weak nonlinearities available. We then extend this result to unravel an intricate relationship between the network's imperfections and its size, providing a guide to the optimal design of QPNNs for near-term experimental applications. Overall, our work paves the way for using QPNNs as a fundamental building block of quantum technologies.

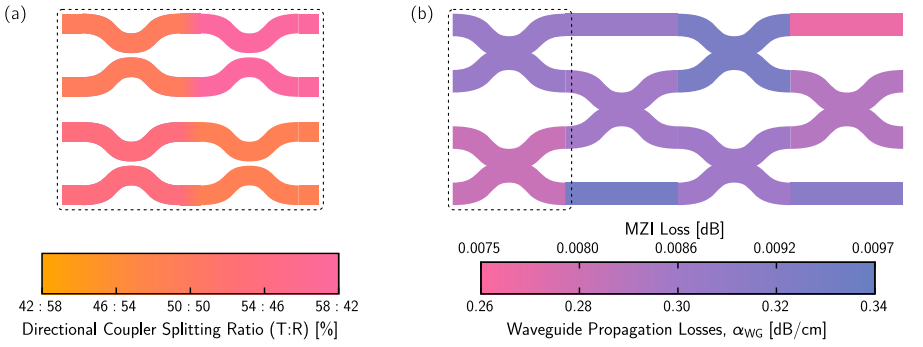

Figure 1: Imperfection distribution in a QPNN. (a) Directional coupler splitting ratios and (b) photon losses assigned to individual network components.

References

[1] J. Ewaniuk *et al.*, *Imperfect Quantum Photonic Neural Networks*, Adv Quantum Technol. **6**, 2200125 (2023).
[2] G. R. Steinbrecher *et al.*, *Quantum optical neural networks*, npj Quantum Inf. **5**, 60 (2019).
[3] R. Parthasarathy and R. T. Bhowmik, *Quantum Optical Convolutional Neural Network: A Novel Image Recognition Framework for Quantum Computing*, IEEE Access **9**, 103337 (2021).

Modelling the influence of campaign contributions and advertising on Presidential elections

Maria Gallego[1]

[1] *Department of Economics, Wilfrid Laurier University, 75 University Avenue West, Waterloo, Ontario, Canada, N2l 3C5. Gallego at mgallego@wlu.ca.*

We use a theoretical stochastic valence framework to examine how candidates in a presidential election choose their multidimensional policy positions and advertising campaigns. We develop a stochastic electoral model of a presidential election where candidates use the contributions received from special interest groups (SIGs) to run their electoral campaigns.

Prior to the election, candidates announce their policy platforms and advertising (ad) campaigns and use the contributions of SIGs to generate a SIG policy and ad campaign valence that enhance their electoral prospects.

Voters' preferences depend on candidates' policies relative to their ideal policy and on candidates' ad campaign messages relative to their ideal message frequency, their campaign tolerance level and are also influenced by the endogenously determined SIG policy and ad campaign valences. Voters' non-campaign evaluation of candidates, voters' mean valence, and their private idiosyncratic valence also influence their choices.

Voters choose the party that gives them highest utility. Since parties do not observe voter's idiosyncratic valence but know it is drawn from a type I extreme value distribution, parties know that the probability that each voter votes for any party has a conditional logit specification. Using these probabilities, parties choose their policy positions to maximize their expected vote share – the average across voters of their voting probabilities, taking into account the expected policy positions of the other parties.

In equilibrium, candidates' critical campaigns depend the effect candidates weighted electoral mean (*the electoral pull*) and on the marginal effect that the SIG valences (*the SIG pull*) have on voters' choices. In local Nash equilibrium (LNE), candidates' campaigns *balance* the electoral and SIG pulls. Candidates' campaigns constitute a strong (weak) LNE of the election if the expected vote shares of all candidates are greater than the sufficient (necessary) pivotal vote shares which happens only when there are enough voters voting for each candidate with high enough probability. If the expected vote share of at least one candidate is lower than its necessary pivotal vote share, then the critical campaigns are not a LNE of the election.

The VI International AMMCS Interdisciplinary Conference Waterloo, Ontario, Canada

The Impact of Brexit in the 2015 UK General Election

Maria Gallego[1] and Man Wai Mak[1]

[1] *Department of Economics, Wilfrid Laurier University, 75 University Avenue West, Waterloo, Ontario, Canada, N2l 3C5. Gallego at mgallego@wlu.ca; Mak @ makx9440@mylaurier.ca*

We use the framework of multidimensional voting valence model to examine the effects of the prospect of a Brexit referendum on the 2015 UK general election. That is, we study whether the possibility of an EU membership referendum promised by the UK Conservative Prime Minster at the beginning of the electoral campaign affected voters decisions in the 2015 UK general election.

Theoretical model: Voters have preferences over a multidimensional policy space and vote for the party that gives them highest utility with their ideal policies distributed in the policy space. Voters' utilities have a policy and an exogenous valance. The policy components in voters' utilities are modelled using separable additive negative quadratic terms to capture the fact that the farther a party is from the voter's ideal point in any dimension the lower the utility the voter derives from that party. The valence has two components, the known mean valence common to all voters, and an idiosyncratic valence. Voters choose the party that gives them highest utility. Since parties do not observe voter's idiosyncratic valence but know it is drawn from a type I extreme value distribution, parties can estimate the probability that each voter votes for any party using a conditional logit specification. Using these probabilities, parties choose their policy positions to maximize their expected vote share –the average across voters of their voting probabilities, taking into account the expected policy positions of the other parties. In the Nash equilibrium parties locate at the mean of voters' preferences in each dimension.

Empirical Strategy: We use this theoretical framework to study the effect that a future Brexit referendum had on the 2015 British general election. We estimate conditional logit models using data from the British Election Study to examine the impact of voters' opinions towards a future Brexit referendum and political proximity to different parties on the probability of voting for each of the five major parties (Conservatives, Labour, Liberal Democrats, UK Independence Party and Scottish National Party) after controlling for voters' sociodemographic characteristics.

We use conditional logit models to estimate the impact that voters' opinions on leaving the EU, on immigration and on future unemployment prospects had on the probability of voting for each party after controlling for voters' sociodemographic characteristics, voters' distance from parties' ideology and policy positions. The results show that when the average voter would vote to stay in the EU in a future referendum and prefers higher immigration levels, s/he is respectively 10%, 7.6% and 2.38% *more* likely to vote respectively for the Labour, Liberal Democrats and Scottish National Party and is 6.7% and 10.6% *less* likely to vote Conservative and United Kingdom Independence Party than when voting to leave the EU. We estimate the distances of parties' policy and ideology positions to that of voters and find that the probability that the mean voter votes for any party decreases by 1% to 3.4% in the policy space and by 0.9% to 4.6% in the ideology dimension the farther a party is from the mean voter.

The VI International AMMCS
Interdisciplinary Conference
Waterloo, Ontario, Canada
14-18 August 2023

Non-ergodicity of the Kusnezov–Bulgac–Bauer thermostatted harmonic oscillator

L. Butler[1]

[1] *University of Manitoba, Winnipeg, Canada, leo.butler@umanitoba.ca*

Molecular dynamics is largely devoted to the computation of *statistical*-mechanical properties of matter using *classical*-mechanical models. A classical problem is to simulate these properties when the number of particles (N), volume (V) and temperature (T) are held constant. This models the properties of a closed, microscopic system (M) in contact with a heat bath at a fixed temperature T.

Nosé, and Hoover, proposed a simple model which augments the Hamiltonian equations of system M with a single state variable [6, 2]. This time-varying pseudo-friction mediates the exchange of energy between the system M with total energy $H(q,p)$ and heat bath. The equations of motion are:

$$\begin{aligned} \dot{q} &= H_p, \quad \dot{p} = -H_q - \varepsilon\zeta p, \\ &\qquad \dot{\zeta} = \varepsilon\,(p\cdot H_p - T)\,, \end{aligned} \tag{1}$$

where q is the vector of configurations of M, p is the conjugate momentum vector and ζ is the pseudo-friction. The coefficient ε is a proxy for the speed of heat flow, and $p\cdot H_p$ is the instantaneous temperature of the system M.

Researchers have recognized the shortcomings of this *thermostat*: even for the harmonic oscillator, the system has positive-measure sets of invariant KAM tori when ε is sufficiently small [7, 4, 1].

Kusnezov, Bulgac and Bauer (KBB) introduced an extension which utilizes two state variables and $2m+2$ arbitrary functions to parameterize friction-like terms [3]. Their equations are

$$\begin{aligned} \dot{q} &= H_p - h_2(\xi)F(q,p), \quad \dot{p} = -H_q - h_1(\zeta)G(q,p), \\ \dot{\xi} &= F\cdot H_q - T\bar{F}_q, \qquad \dot{\zeta} = G\cdot H_p - T\bar{G}_p, \end{aligned} \tag{2}$$

Ergodicity of these equations imply that the Birkhoff averages of functions $f(q,p)$ converge almost everywhere to the space average. The KBB thermostat is a popular alternative to the Nosé–Hoover thermostat. Apparently, it samples from the extended canonical ensemble much better than Nosé–Hoover [5].

We apply the authors' "preferred couplings" [3, eqn. 35] to a 1-dimensional harmonic oscillator. By means of averaging theory and rigorous numerics, we prove that the four-dimensional extended phase space of (eqn. 2) possesses an abundance of invariant 3-dimensional KAM tori when the temperature $T \cong 1$.

References

[1] L. T. Butler, J Math Phys, 61 (2020), p. 082702.
[2] W. G. Hoover, Phys. Rev. A., 31 (1985), pp. 1695–1697.
[3] D. Kusnezov, A. Bulgac, and W. Bauer, Ann. Physics, 204 (1990), pp. 155–185.
[4] F. Legoll, M. Luskin, and R. Moeckel, Arch. Ration. Mech. Anal., 184 (2007), pp. 449–463;
Nonlinearity, 22 (2009), pp. 1673–1694.
[5] D. Mentrup and J. Schnack, Physica A: Statistical Mechanics and its Applications, 297 (2001), pp. 337 – 347;
Physica A: Statistical Mechanics and its Applications, 326 (2003), pp. 370 – 383.
[6] S. Nosé, J. Chem. Phys., 81 (1984), pp. 511–519;
Molecular Physics, 52 (1984), pp. 255–268;
Molecular Physics, 57 (1986), pp. 187–191.
[7] H. A. Posch, W. G. Hoover, and F. J. Vesely,Phys. Rev. A (3), 33 (1986), pp. 4253–4265.

The VI International AMMCS
Interdisciplinary Conference
Waterloo, Ontario, Canada

From Interval-Valued Neurons to Convex-Set-Valued Neurons

B. Boreland[1], H. Kunze[2], K. Levere[3]

[1] *Deloitte*
[2] *University of Guelph, Guelph, Canada hkunze@uoguelph.ca*
[3] *University of Guelph, Guelph, Canada klevere@uoguelph.ca*

In recent years, the concept of an interval-valued neuron has appeared in the literature. Interval valued neurons are used to process interval-valued data, with typical applications examples being the mushroom dataset (www.mykoweb.com/CAF) or the electricity market. When the information that is available features uncertainty, variability, or inaccuracy, representing the data as being interval-valued can be useful. While the resulting neural network can be implemented by representing the interval-valued neuron in terms of the center and (positive) radius of the interval, a recent suggestion is to instead represent the neuron by the two interval endpoints and add a term to the cost function that penalizes endpoints crossing. After discussing this design, we will introduce the notion of a convex-set-valued neuron, focusing in particular on the implementation of polygon-valued neurons and the resulting neural network. Some examples will be presented, and a motivating potential application will be discussed.

A Numerical Study of the Dynamics of Particles at Fluid Interface

S. Alavi[1], C. Denniston[2]

[1] *Western University, London, Canada, salavi8@uwo.ca*
[2] *Western University, London, Canada, cdennist@uwo.ca*

The special dynamics of interfacial particles has received increasing attention both in fundamental studies and technological applications in the past few years. Colloidal particles residing at a fluid interface are abundantly found in industrial materials and biological systems [1, 2]. In order to have a better understanding of the unique physical properties of particles at the interface, extensive attention should be paid to the surface interaction between the particle and the fluid. In this research, a computational method is employed to study the wetting properties of spherical particles at a liquid-gas interface. Different wetting boundary conditions will be tested to analyze the adsorption of the particle onto the interface. The simulations will be performed using a modified version of the lb/fluid package in LAMMPS, which is an implementation of Lattice Boltzmann method for simulating fluid mechanics. These results can provide us with enough insights to study interfacial particles with more complex conditions.

References

[1] S. Dasgupta, T. Auth and G. Gompper, *Nano- and microparticles at fluid and biological interfaces*, Journal of Physics: Condensed Matter **29**, 373003, pp. 41 (2017).

[2] Bernard P. Binks, *Colloidal Particles at a Range of FluidâFluid Interfaces*, Langmuir **33**, 28, pp. 6947â6963 (2017).

A Poisson Tweedie Framework for Joint Mean and Dispersion Regression Modeling

S. Chen[1], Z. Wang[2], D. Soave[2]

[1] *Wilfrid Laurier University, Waterloo, Canada, chen8470@mylaurier.ca*
[2] *Wilfrid Laurier University, Waterloo, Canada*

Researchers have long been interested in analyzing variance heterogeneity and related tests to understand the effects of covariates on variance. One area of particular interest is in studying variance in gene expression, which is closely linked to biological processes. While traditional statistical distributions such as Poisson and Negative Binomial have been used to model count data, they have limitations in capturing the complexity of real-world count data applications due to their mean and variance relationship. To solve this problem, we propose using the Poisson-Tweedie distribution, which has a flexible shape and dispersion that can accommodate overdispersed data. The Poisson-Tweedie distribution includes the Poisson, Negative Binomial, and Poisson Inverse Gaussian distributions as special cases. We have implemented a Poisson-Tweedie mean and dispersion regression framework using maximum likelihood methods and examined its numerical properties via simulation. We have also demonstrated its application through a differential gene expression analysis involving cancer tumour samples.

The VI International AMMCS
Interdisciplinary Conference
Waterloo, Ontario, Canada

Ensemble-Based Deep Learning Approach for Road Updates Extraction from High-Resolution Satellite Imagery

S. S. Sehra[1], S. K. Sehra[2], J. Singh[3], D. Becker[4], S. M. Bedawi[5]

[1] *Wilfrid Laurier University, Waterloo, Canada, ssehra@wlu.ca*
[2] *Wilfrid Laurier University, Waterloo, Canada, sksehra@wlu.ca*
[3] *Chitkara University, Punjab, India, jaiteg.singh@chitkara.edu.in*
[4] *Wilfrid Laurier University, Waterloo, Canada, dbecker@wlu.ca*
[5] *Carlton University, Ottawa, Canada, safaabedawi@cunet.carleton.ca*

Most road networks are known but may not be updated to include newly constructed roads, especially in rural and underserved areas across the world. Extraction of new roads allow for automated updating of local maps and/or contributions to crowd-sourced maps such as OpenStreetMap. The increasing availability of satellite and aerial imagery has led to a growing interest in methods for updating road networks without manual input. In this work, we expand upon existing methods using an ensemble of deep learning techniques applied to high-resolution satellite imagery to further improve results and organize the data analysis into a re-usable computational pipeline.

Our model has three component: pre-processing the satellite data, building a pool of deep learning models to extract the road network; and post-processing the model outputs to extract updates in a road network for a given bounding box.

The pre-processing component involves acquisition of high-resolution satellite images from SpaceNet, Sentinel-2, and PlanetScope (a proprietary satellite data provider) and annotation with ground truth labels for road and non-road pixels. Data augmentation (geometric transformation and pixel transformation) is performed to provide the large amount of training data required for deep learning models as small datasets can cause models to overfit the data, resulting in low accuracy on out-of-sample data.

The second component involves training a diverse set of deep learning models suitable for image segmentation tasks, each model in the ensemble having different architectures and/or hyper-parameter variations for diversity. We then train each model separately using the training dataset, optimizing them with appropriate loss functions and evaluation metrics while utilizing data augmentation techniques to enhance the diversity of training data. Once trained, the predictions of individual models are combined to create an ensemble prediction, which is also evaluated and adjusted to ensure satisfactory results on a validation set.

In the final component, we apply the final ensemble model to a testing dataset, which was not used during the model training component. We post-process the predictions with techniques like topological and morphological operations to refine the road extraction results and perform comparison of resulted road network with existing road network from OpenStreetMap to extract the updates. This provides updates to the road maps like OpenStreetMap without introducing errors in parts of the map that remain up-to-date. The proposed approach has been evaluated empirically with several state-of-the-art road extraction methods and demonstrated the effectiveness of the approach.

The VI International AMMCS
Interdisciplinary Conference
Waterloo, Ontario, Canada

Temperature Profile in Thin Nanowires

R. Meyer[1], G. W. Gibson[2], A. N. Robillard[3]

[1] *Laurentian University, Sudbury, Canada, rmeyer@cs.laurentian.ca*
[2] *Laurentian University, Sudbury, Canada, gw_gibson@laurentian.ca*
[3] *Laurentian University, Sudbury, Canada, an_robillard@laurentian.ca*

In this work, we use non-equilibrium molecular dynamics simulations and phonon Monte Carlo simulations to study the temperature profile of silicon nanowires placed between two heat baths with different temperatures. Both simulation methods predict the temperature gradient to be steeper in the vicinity of the heat baths than in the centre of the system. This contradicts Fourierś law which predicts a constant gradient throughout the system. However, the simulation results can be understood with the help of a simple radiator model or similar solutions of the Boltzmann transport equation which both predict a discontinuous temperature jumps at the interfaces between the heat baths and the nanowire. We show that the radiator model is able to explain the reduction of the temperature gradient in the centre of the system compared to the macroscopic Fourier model. This indicates that the steep gradients observed in the simulations are continuous manifestations of the discrete temperature jumps found with the analytical methods.

Climate Change Modelling and Forecasting with Fourier Autoregressive Moving Average Processes

A. I. Taiwo[1], T. O. Olatayo[2], F. E. Ayo[3], A. Titilola[4]

[1] *Olabisi Onabanjo University, Nigeria taiwo.abass@oouagoiwoye.edu.ng*
[2], *Olabisi Onabanjo University Nigeria bisi.olatayo@oouagoiwoye.edu.ng*
[3] *Olabisi Onabanjo University Nigeria bisi.olatayo@oouagoiwoye.edu.ng*
[4] *Olabisi Onabanjo University Nigeria adewale.titilola6565@gmail.com*

Modelling and forecasting climatic variables have been done using models which did not properly capture the cyclical variation present in these series [1, 2, 3]. This study aims to propose a Fourier autoregressive moving average model (FARMA) in which Fourier terms with the ability to handle cyclical movement were added to the model based on the work of [4]. The model is given as

$$y_{k\omega+v} = \varphi_0 + \sum_{i=1}^{p(v)} \left[\varphi_i(v)\, cos2\pi k/_{\omega} + \varphi_i^{*}\, sin2\pi k/_{\omega}\right] y_{k\omega+v-i} + \varepsilon_{k\omega+v} + \sum_{i=1}^{q(v)} \left[\vartheta_i(v)\, cos2\pi k/_{\omega} + \vartheta_i^{*}\, sin2\pi k/_{\omega}\right] \varepsilon_{k\omega+v-i} \quad (1)$$

where $v$the period index$(v = 1, 2, \ldots, \omega)$, k is the year index$(k = 0 \pm 1, \pm 2, \ldots)$, $\varphi_i(v)$ and$\vartheta_i(v)$ the Fourier autoregressive and moving average coefficients, ω is the number of seasons. The model stages: identification, estimation, diagnostic and forecasting with its evaluation metrics were also constructed.

From the implementation of the model, the Nigerian monthly rainfall series from 1994 to 2022 was considered. The identification stage yielded FARMA(1,1), (1,2), (2,1) and (2,2) models based on Periodic Autocorrelation and Partial Autocorrelation functions. The coefficients were estimated using the Discrete Fourier transform method. FARMA(1,1) models were taken as the optimal model with regard to the lowest values of Periodic Akaike and Bayesian Information criteria. The Periodic Residual Autocorrelation Function was used to determine that the residual of the fitted models was white noise.

The time-ahead forecast displayed a continuous rising cyclical movement from January 2023 to December 2030 with small values of Periodic Root Mean Square, Mean Absolute, and Mean Absolute Percentage Errors, whereas the in-sample forecast showed a close reflection of the original monthly rainfall series.

The often used Box and Jenkins univariate models forecast and its evaluation metrics considered did not exhibit a better cyclical movement when contrasted with the FARMA models.

The proposed model becomes a significant tool that ascertains rainfall continuously rising cyclical movement contributes to climate change in Nigeria. This further indicated that there may be rapid climate change in years ahead and the Government at all levels needs to put in place plans to curtail its effects**.**

References

[1] R. Mahmood, S. Jia S. and W. Zhu, *Analysis of climate variability, trends, and prediction in the most active parts of the Lake Chad basin, Africa,* Sci. Rep. **9**, 6317, pp. 1-18 (2019).
[2] A. Karim, A.O. Kube and B.I. Ibn Saeed, *Modeling of Monthly Meteorological Time Series*, J. Stat. and Econ. Meth. 9, 4, pp. 117-136 (2020).
[3] Y. Wang, M. Gueye, S.J. Greybush, H. Greatrex, A.J. Whalen, P. Ssentongo, F. Zhang, G.S. Jenkins and S.J. Schiff, *Verification of operational numerical weather prediction model forecasts of precipitation using satellite rainfall estimates over Africa*, Metro Appl. **30**, 1, pp. (2023).
[4] A.I. Taiwo, T.O. Olatayo and S.A. Agboluaje, *Time Series Model Building with Fourier Autoregressive Model, South Afri. Stat. J.* **54**, 2, pp. 243-254 (2020).

The VI International AMMCS
Interdisciplinary Conference
Waterloo, Ontario, Canada

State Complexity Relations in Evolved Players of the Iterated Prisoner's Dilemma

Jing Lu[1], Chrystopher L. Nehaniv[2]

[1] *University of Waterloo, Waterloo, Canada, j289lu@uwaterloo.ca*
[2] *University of Waterloo, Waterloo, Canada, chrystopher.nehaniv@uwaterloo.ca*

The relationship between the complexity and physical aspects of an organism has been difficult to study on the typical timescale of evolution in biological systems. By evolving digital organisms modelled as finite state machines, which can be generated much faster, we can investigate how these factors might interact [1]. The iterated prisoners' dilemma serves as a good model of how populations might evolve cooperative strategies – even when a rational actor would always choose to betray others [2].

We examine the complexity of players in evolved populations of finite automata that play iterated prisoners' dilemma, using rigorous mathematical measures from algebraic automata theory (Krohn-Rhodes complexity). In particular, we test Rhodes' hypothesis that evolved organisms will have complexity close to their number of possible states [3].

To mimic biological evolution, the players must have some measure of fitness which determines their likelihood of reproducing and passing on their traits to the next generation. For this simulation, the fitness comes from the summed score of a player's games against all other members of the population. A penalty based on the player's number of states may also be applied. It simulates the cost of having more complex biological features – for example, additional energy consumption. See Eq. (1).

$$PlayerFitness = (\frac{PlayerScore - Penalty}{100})^2. \tag{1}$$

Players selected for reproduction undergo crossover and mutation to create a new member of the next generation. After 100 generations, we examine trends in fitness, cooperative moves, and the upper bound of Krohn-Rhodes complexity calculated using holonomy decomposition in GAP [4].

Three evolving population groups were compared. A control group where the fitness was always set to 1 regardless of performance, one without a penalty, and one with an exponential penalty.

We found that when the fitness calculation is related to performance, i.e., evolutionary pressure is present, complexity is close to the number of states of a player. This is in line with Rhodes' hypothesis [3]. Additionally, not only do the groups with evolutionary pressure differ from the one without, the group with an exponential penalty function also differs significantly from the one without penalty.

References

[1] L. J. Fogel, A. Owens, and M. J. Walsh, *Artificial Intelligence through Simulated Evolution*, John Wiley & Sons, New York (1966).
[2] J. Golbeck, *Evolving Strategies for the Prisoner's Dilemma*, PhD thesis, University of Maryland (2002).
[3] J. Rhodes, *Applications of Automata Theory and Algebra: Via the Mathematical Theory of Complexity to Biology, Physics, Psychology, Philosophy, and Games*, edited by C. L Nehaniv, foreword by M. W. Hirsch, World Scientific, Singapore (2010).
[4] A. Egri-Nagy, J. Mitchell, and C. L. Nehaniv, *SgpDec: Cascade (de)compositions of finite transformation semigroups and permutation groups*, in *Mathematical Software ICMS 2014: 4th International Congress, Seoul, South Korea, August 5-9, 2014*, pages 75-82. Springer Berlin Heidelberg. (2015).

The VI International AMMCS
Interdisciplinary Conference
Waterloo, Ontario, Canada

Quasi-synchronization of fractional-order multiplex networks with parameter mismatch via intermittent control

Yao Xu[1], Xinzhi Liu[2], Wenxue Li[3]

[1] *Department of Mathematics, Harbin Institute of Technology (Weihai), Weihai 264209, China, yaoxu0125@163.com*
[2] *Department of Applied Mathematics, Faculty of Mathematics, University of Waterloo, Waterloo, Canada, xzliu@uwaterloo.ca*
[3] *Department of Mathematics, Harbin Institute of Technology (Weihai), Weihai 264209, China, wenxue810823@163.com*

In this paper, the quasi-synchronization issue of fractional-order multiplex networks with parameter mismatch is considered by intermittent control. To better describe the complexity, ambiguity, and network topology in the actual world, parameter mismatch, intra-layer and inter-layer structures are both introduced into the mathematical model of fractional-order multiplex networks. By the graph theory and the Lyapunov method, under intermittent control, some sufficient conditions of quasi-synchronization are shown, and the allowable error bound is estimated. Finally, theoretical results are applied to power systems, and some numerical simulations are presented, which demonstrates the effectiveness of our results.

A Bayesian framework for the concurrent estimation of time-varying and time-invariant parameters in stochastic compartmental models

B. Robinson[1], P. Bisaillon[1], J.D. Edwards[2], T. Kendzerska[3], A. Sarkar[1]

[1] *Carleton University, Ottawa, ON, Canada, {brandon.robinson,philippe.bisaillon,abhijit.sarkar}@carleton.ca*
[2] *University of Ottawa and University of Ottawa Heart Institute, Ottawa, Ontario, Canada, jedwards@ottawaheart.ca*
[3] *University of Ottawa and The Ottawa Hospital Research Institute, Ottawa, Ontario, Canada, tkendzerska@toh.ca*

We present a framework for parameter estimation in dynamical systems consisting of both of time-varying and time-invariant parameters. Traditional approaches to such problems involves appending the set of parameters to the system state and jointly estimating the elements of this augmented state using nonlinear filters. In a conventional setting, the time-varying parameters are driven by noise to induce artificial perturbation. A downside of this approach is the increased nonlinearity and the artificial dynamics that are introduced while estimating parameters in this manner. To alleviate these undesirable effects, we leverage Markov chain Monte Carlo (MCMC) methods to estimate the set of time-invariant parameters in our system, while relying on a nested state estimation procedure for the concurrent estimation of the system state and the time-varying parameters. Critically, the use of MCMC for the estimation of time-invariant system parameters also permits the joint estimation of the noise strength that optimally drives the dynamics of the time-varying parameters.

We demonstrate the performance of the algorithm for simple compartmental models having a combination of time-varying and time-invariant parameters. Consider the SIR model, a system of three coupled ordinary differential equations,

$$\frac{dS}{dt} = -\beta SI, \qquad \frac{dI}{dt} = \beta SI - \gamma I, \qquad \frac{dR}{dt} = \gamma I, \tag{1}$$

where S, I, and R are models states which categorize the population as either *susceptible*, *infectious*, or *recovered*. The parameter β reflects the number of disease transmitting interactions occur per unit time, which may intuitively vary in time given seasonal trends, lockdowns or other non-pharmaceutical intervention measures. The parameter γ is the reciprocal of the average time to recovery, hence it is more likely to remain constant.

In this example, the state vector is augmented to include the time-varying parameter β, such that it is estimated within the nonlinear filtering framework. Static parameters are concurrently estimated using MCMC.

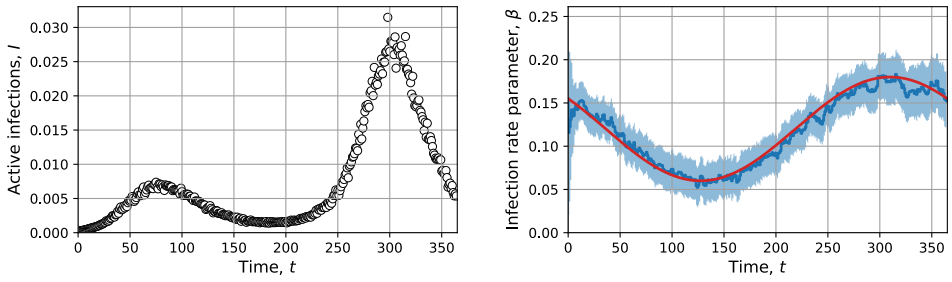

Figure 1: Left: synthetic data for two waves of infections (I compartment). Right: comparison of the true (red) and estimated (blue) values of the time-varying infection rate parameter (β).

Mathematical Models of Exercise-Induced Metabolic Alterations in Men and Women

S. Abo[1], A. T. Layton[2]

[1] *Department of Applied Mathematics, University of Waterloo, Waterloo, Canada, sabo@uwaterloo.ca*
[2] *Department of Applied Mathematics, Cheriton School of Computer Science, Department of Biology, and School of Pharmacy, University of Waterloo, Waterloo, Ontario, Canada, anita.layton@uwaterloo.ca*

During aerobic exercise, women oxidize significantly more lipids and less carbohydrates than men. This sexual dimorphism in substrate metabolism has been attributed, in part, to the observed differences in epinephrine and glucagon levels between men and women during exercise [1, 2]. To identify the underpinning candidate physiological mechanisms for these sex differences, we developed a sex-specific multi-scale mathematical model that relates cellular metabolism in the organs to whole-body responses during exercise. We conducted simulations to test the hypothesis that sex differences in the exercise-induced changes to epinephrine and glucagon would result in the sexual dimorphism of hepatic metabolic flux rates via the glucagon-to-insulin ratio (GIR). Indeed, model simulations indicate that the shift towards lipid metabolism in the female model is primarily driven by the liver. The female model liver exhibits resistance to GIR-mediated glycogenolysis, which helps preserve hepatic glycogen stores. This decreases arterial glucose levels and promotes the oxidation of free fatty acids. Furthermore, in the female model, skeletal muscle relies on plasma free fatty acids as the primary fuel source, rather than intramyocellular lipids, whereas the opposite holds true for the male model.

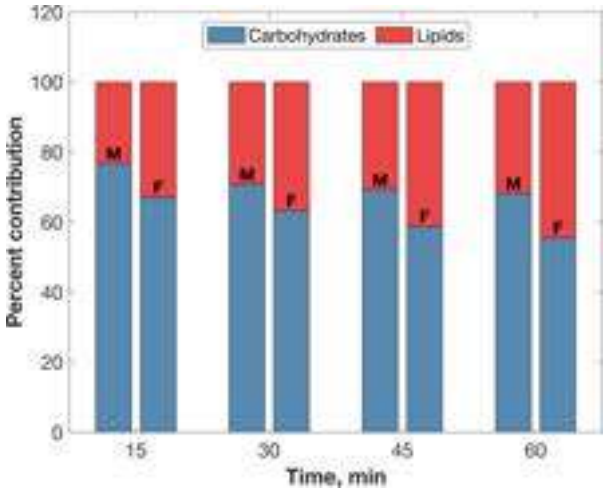

Figure 1: Relative contribution of fuel sources to whole-body ATP production. Percent contribution values are instantaneous values at 15, 30, 45 and 60 min, respectively. Moderate intensity exercise at 60% VO_2max (150W). **M**: male model; **F**: female model.

References

[1] S. L. Carter, C. Rennie, and M. A. Tarnopolsky, *Substrate utilization during endurance exercise in men and women after endurance training*, Am. J. Physiol. Endocrinol. Metab. **280**, 6, pp. E898-E907 (2001).

[2] B. Ahrén, *Autonomic regulation of islet hormone secretion–implications for health and disease*, Diabetologia **43**, pp. 393-410 (2000).

Efficient Method to Estimate Second-order Sensitivities for Stochastic Discrete Biochemical Systems

F. Jabeen[1], S. Ilie [2]

Toronto Metropolitan University, Toronto, Canada,
[1]*fauzia.jabeen@torontomu.ca*
[2]*silvana@torontomu.ca*

The understanding of highly complex biochemical systems requires advanced mathematical models and simulation strategies. When dealing with well-stirred biochemical networks that involve some reacting species in small molecular counts, the Chemical Master Equation, a stochastic discrete model, is commonly employed to capture the random fluctuations specific to these systems. Sensitivity analysis is a powerful tool to study the system's behaviour. It quantifies the change in the model's output due to small variations in its parameters. In this regard, second-order sensitivities are quite valuable for identifying extrema in expected outcomes. We propose an effective and accurate method to estimate second-order sensitivities for the Chemical Master Equation. This method relies on a tau-leaping technique and finite-difference schemes. We illustrate the benefits of the proposed sensitivity estimator by testing it on various models of interest.

References

[1] Gillespie, D.T., *Exact Stochastic Simulation of Coupled Chemical Reactions*, J. Chem. Phys. , **81**, pp. 2340-2361 (1977).

[2] Gillespie, D.T., *Approximate Accelerated Stochastic Simulation of Chemically Reacting Systems*, J. Chem. Phys. , **115**, pp. 1716-1733 (2001).

[3] Varma, A., Morbidelli, M. and Wu, H. , *Parametric Sensitivity in Chemical Systems*, Cambridge University Press, Cambridge (1999).

[4] M. Morshed, B. Ingalls and S. Ilie, *An efficient finite-difference strategy for sensitivity analysis ofstochastic models of biochemical systems*, Bio. Systems, **151**, pp. 43-52 (2017).

[5] D.F. Anderson, *An Efficient Finite Difference Method for Parameter Sensitivities of Continuous Time Markov Chains*, SIAM. J.Numer. Anal. **50**, 5, pp. 2237-2258 (2012).

The VI International AMMCS
Interdisciplinary Conference
Waterloo, Ontario, Canada

A Ramsey-Like Conjecture for Dividing a Circle

Walter Stromquist[1]

[1] *Bryn Mawr College, Bryn Mawr, PA, USA, mail@walterstromquist.com*

Start with 31 points evenly spaced on a circle, each arbitrarily colored blue or red. Is it always possible to find 5 of these points, all of the same color, that divide the circle into arcs proportional to $1, 2, 4, 8, 16$ (in some order)?

The answer is yes, as can be verified by checking every possible coloring. The question was inspired by a problem proposed by Robert Tauraso in the American Mathematical Monthly [1]. The 31-point result leads to a nice solution to that problem. But the more interesting question is whether the result generalizes.

> **Conjecture.** Let $k \geq 1$. Given $2^k - 1$ points, evenly spaced on a circle and each arbitrarily colored blue or red, it is possible to select k of the points, all of the same color, that divide the circle into arcs proportional to $1, 2, 4, \ldots, 2^{k-1}$ (in some order).

The conjecture is trivially true when $k = 1$ and $k = 2$, and is easy to prove when $k = 3$ or $k = 4$. Computer proofs exist when $k \leq = 7$. Does the conjecture hold in general?

Some curiosities occur. We cannot require that the arc lengths occur in any particular cyclic order. It is possible that there are "winners" (successful selections of k points) of both colors. It is also possible that the only winners are of the minority color. If $k \geq 3$ then for any coloring, the number of winners is even. The minimum number of winners (over all colorings) is 2 (for 7 points), 4 (for 15 points), and 10 (for 31 points).

János Pach reports [2] that the conjecture would be false if any other finite sequence were substituted for the initial powers of 2. It was his group who used a SAT solver to verify the conjecture when $k = 7$.

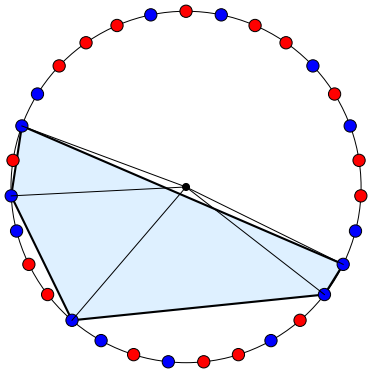

In this example, the selected points are shown as vertices of a pentagon. The arc lengths appear in the order $1, 16, 2, 4, 8$.

Ramsey Theory has not found much application in fair division problems. The best-known Ramsey theorems guarantee the existence of certain complete graphs, or certain arithmetic progressions. Neither of these is of much use to us. But this conjecture asserts the existence of a partition of a circle into prescribed parts. Our subject is all about partitioning things into prescribed parts. If the conjecture is true, how long will it take to find applications to practical fair division problems?

References

[1] R. Tauraso, *Problem 12251,* Amer. Math. Monthly **128**, 5, p. 467 (May, 2021).

[2] G. Damásdi, N. Frankl, J. Pach, D. Pálvölgyi, *Monochromatic Configurations on a Circle*, in preparation.

The VI International AMMCS
Interdisciplinary Conference
Waterloo, Ontario, Canada

Spatio-Temporal Point Processes: A Novel Approach to Modeling Real Estate Transaction Dynamics

I. Fraser[1], Y. Liu[1], X. Wang[1]

[1] *Wilfrid Laurier University, Waterloo, Canada, natural-sciences@wlu.ca*

In this research, we delve into the application of Spatio-Temporal Point Processes (STPPs) for modeling the distribution and occurrence of residential real estate transactions. Real estate markets have critical economic implications, and our novel Self-Exciting Spatio-Temporal Point Process (SESTPP) approach offers a new lens through which to understand the potentially intricate dynamics of real estate markets.

The motivation behind this work is the demonstrated ability of SESTPPs across various disciplines ranging from seismology to criminology [1] to model events that increase the probability of observing future events. Given the potential for one real estate transaction to stimulate others nearby, the self-exciting assumption finds relevance in this research direction.

Key questions this research aims to answer include the insights gained by STPP and SETPP models applied to real estate transactions, the existence and characteristics of clustering phenomena, the presence of self-exciting behavior, and the efficacy of a proposed model in predicting future transaction distribution and identifying potential areas for investment or development.

Notable challenges in this study are model design and selecting appropriate parameter estimation techniques for the intensity function, which lacks a standard practice for real estate transaction data. Balancing the weighting between spatially continuous and temporally discrete components and acknowledging housing market dynamics within the model parameters are additional hurdles. Furthermore, an appropriate model for the background rate of real estate transactions (including seasonal effects and heterogeneity due to measured covariates) must be considered.

The proposed research offers a repeatable procedure for the analysis, model fitting, and model diagnostics of real estate transaction data as a SESTPP, uncovering the underlying mechanisms that result in observed transaction patterns. Moreover, this work contributes by developing a novel SESTPP model designed for the unique characteristics of real estate transaction data. This study is expected to advance academic understanding of STPPs' application to bigdata while providing a reference that can inform decisions relating to real estate investment strategies, market analysis, and policymaking.

References

[1] Alex Reinhart. "A Review of Self-Exciting Spatio-Temporal Point Processes and Their Applications." Statist. Sci. 33 (3) 299 - 318, August 2018. https://doi.org/10.1214/17-STS629

The VI International AMMCS
Interdisciplinary Conference
Waterloo, Ontario, Canada

Neural Difference Equations

H. Kunze[1], D. La Torre[2]

[1] *University of Guelph, Guelph, Canada hkunze@uoguelph.ca*
[2] *SKEMA Business School, Sophia Antipolis, France davide.latorre@skema.edu*

A first-order difference equation takes the general form $x_{n+1} = f(x_n)$, for $n = 0, 1, 2, ldots$, where x_0 is the initial value. When x_n represents an observation value at time n, one can seek to solve the inverse problem of recovering and estimation of f given the time series $\{x_n\}_{n=0}^{N}$. In the setting of a particular application, there is often some expectation of the functional form of f, so the inverse problem becomes one of parameter estimation.

We instead consider the problem of producing as the right-hand side of the difference equation a neural network, say f_{NN}, which can be thought of as a "black box," $f_{NN} : \mathbb{R} \to \mathbb{R}$, that somehow predicts the next value given preceding value.

We illustrate the problem by using the public COVID case dataset for Canada, with x_n being the number of new cases (as reported in the dataset) on day n of such reporting. In the talk, we seek to represent f_{NN} as a multi-layer perceptron neural network and explore the impact of different architecture choices on the model results.

The VI International AMMCS
Interdisciplinary Conference
Waterloo, Ontario, Canada

Exploring the use of gradients in the Structural Similarity image quality measure

Amelia Kunze and Edward R. Vrscay

University of Waterloo, Waterloo, Ontario, Canada, {agkunze,ervrscay}@uwaterloo.ca

The L^2-based mean square error (MSE) and its variations continue to be the most widely employed metrics in image processing. It is well known, however, that these L^2-based measures perform poorly in terms of measuring the **visual quality** of images since the L^2 metric, by definition, cannot capture spatial relationships. This motivated the introduction and development of the so-called Structural Similarity image quality measure (SSIM) [4] which, along with its variations, continues to be one of the most effective measures of visual quality. The SSIM index measures the difference/similarity between two images by combining three components of the human visual system (HVS) – luminance, contrast and structure. The structure term of SSIM, perhaps the most discerning component, measures the **correlation** between two images (or image blocks) **x** and **y**.

The work reported here is a portion of a larger investigation of the use of **image gradients** in image processing, especially in the context of image quality measures [2]. We start with the observation that L^2 distances between image gradients are able to discern visual quality better than MSE. This naturally leads to an investigation of "gradient-based SSIM" measures, to be referred to as "gradSSIM." In this talk, we consider the simplest form of the gradSSIM, in which the usual SSIM is multiplied by an additional term which measures the correlation between **image gradients** $\nabla\mathbf{x}$ and $\nabla\mathbf{y}$. There is, of course, the question of how to define the correlation between two N-vectors, the components of which are (gradient) vectors. One can easily define some rather simple-minded schemes which work on each of the components of the gradient vectors and then combine the results to produce with a scalar. But perhaps the most "rigorous" method is Hotelling's **canonical correlation method** (CCA) [1]. As will be reported, our simple-minded methods yield results that differ very little, if at all, from CCA. Our gradSSIM measure works well in the case of the "Einstein images" [3], further penalizing the poorest images while preserving a relative ordering consistent with that of SSIM. In an effort to determine if these more punitive scores are "better" than those of SSIM, we examined gradSSIM over a larger range of image distortions as provided in the LIVE image database at `https://live.ece.utexas.edu/research/Quality/subjective.htm`.

In the literature, the usual way of characterizing the effectiveness of an image quality measure is to plot, for each distorted image in the database, its computed image quality e.g., SSIM, vs. its "DMOS" value, i.e., its subjective quality rating relative to its corresponding reference image. (DMOS=0 implies no visible difference.) Using this framework, we found that our gradSSIM performs much better than SSIM for visually poor (mid-to-high DMOS) images. During this research, however, we found it necessary to examine the roles of the so-called "stability constants" employed in the SSIM. It turns out that SSIM is very sensitive to changes in the stability constants, with little or no discussion of these effects in the literature. As such, our report will also explore the effect of changes in the stability constants on both SSIM and gradSSIM.

References

[1] H. Hotelling, *Relations Between Two Sets of Variates*, Biometrika **28**, 3-4, pp. 321-377 (1936).

[2] A. Kunze, *An investigation of the use of gradients in imaging, including best approximation and the Structural Similarity image quality measure*, M.Math. Thesis, Department of Applied Mathematics, University of Waterloo (2023).

[3] Z. Wang, A. Bovik and H.R. Sheikh, *Structural Similarity Based Image Quality Assessment*, Chapter 7 in *Digital Video Image Quality and Perceptual Coding*, H.R. Wu and K.R. Rao, Eds., Marcel Dekker Series in Sig. Proc. and Comm., Nov. 2005.

[4] Z. Wang, A. Bovik, H. Sheikh and E. Simoncelli, *Image quality assessment: from error visibility to structural similarity*, IEEE Transactions on Image Processing **13**, 4, pp. 600-212 (2004).

The VI International AMMCS
Interdisciplinary Conference
Waterloo, Ontario, Canada

Design and Optimization of InP Grating for Efficient Light Coupling in Quantum Photonic Circuits

K. Shadkami[1], O. Mahboub[2,3], N. Rotenberg[4]

[1] *Centre for Nanophotonics, Queen's University, Kingston, Canada, k.shadkami@queensu.ca*
[2] *Centre for Nanophotonics, Queen's University, Kingston, Canada, o.mahboub@queensu.ca*
[3] *STA, National School of Applied Sciences, Abdelmalek Essaadi University, Tetouan, Morocco, Omahboub@uae.ac.ma*
[4] *Centre for Nanophotonics, Queen's University, Kingston, Canada, nir.rotenberg@queensu.ca*

Efficient coupling of light in and out of integrated photonic circuits is crucial for achieving high-performance quantum devices. Many techniques were employed to achieve this coupling and one of the more promising methods is the use of grating couplers [1]. This study presents the design and optimization of such gratings in InP and at telecom wavelengths using finite element method (FEM, COMSOL Multiphysics) [2]. To do so, we first use 2D models, followed by full 3D simulations as we trade off between speed and accuracy.

We first use a 2D model to optimize the grating parameters with a series of rapid scans. These parameters include the periodicity of the grating (Λ), waveguide height (h), grating etch depth (ed), and number of gratings (n). The aim is to achieve optimal light coupling efficiency at a desired wavelength and coupling angle, here 1550 nm and 10°, respectively, across a 3dB spectral bandwidth of at least 170nm. Figure 1 shows a typical geometry, with a zoom in on the grating region and with the boundary layers clearly. Note that an InP substrate, which reflects downwards coupled light is also included, and in this stage the distance from the grating to substrate was also optimized.

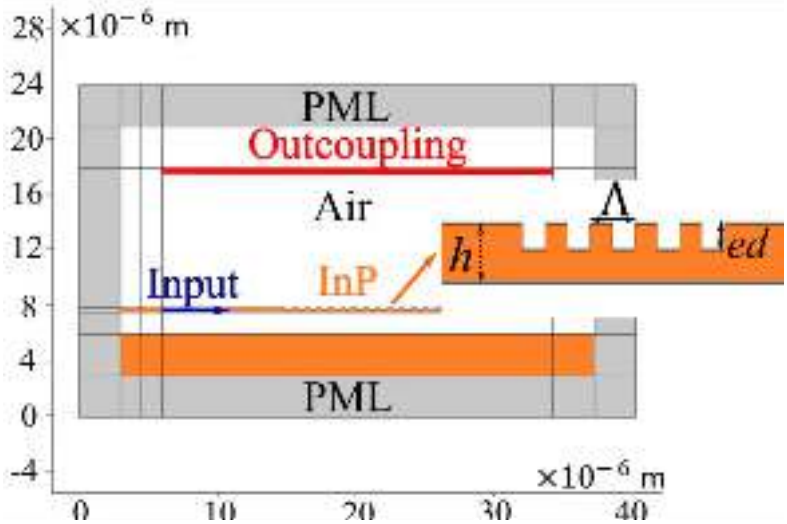

Figure 1: 2D view of the simulation domain of the grating coupler, including an inset which shows the design parameters.

Once an optimal geometry is identified, we switch to a full, three-dimensional model to ensure the accuracy of our device. Here, we use circular gratings which efficiently funnel the light in and out of the waveguide [1]. The circular grating geometry introduces additional design complexity as additional grating parameters, such as radius and grating periodicity, effect the coupling efficiency.

Our results demonstrate that the optimized 2D and 3D grating designs achieved significantly enhanced light coupling efficiency. The findings provide valuable insights into the design principles and optimization strategies for efficient light coupling in InP circuits. The proposed designs have the potential to advance the performance of integrated photonic devices, facilitating their integration into various applications, such as optical communication systems and quantum photonics.

References

[1] Zhou, X., Kulkova, I., Lund-Hansen, T., Hansen, S.L., Lodahl, P. and Midolo, L., 2018. High-efficiency shallow-etched grating on GaAs membranes for quantum photonic applications. *Applied Physics Letters*, *113*(25), p.25110

[2] D.Taillaert, F. V. Laere, M. Ayre, W. Bogaerts, D. V. Thourhout, P. Bienstman, and R. Baets, "Grating couplers for coupling between optical fibers and nanophotonic waveguides," Japanese Journal of Applied Physics, vol. 45, no. 8R, p. 6071, 2006.

Effect of Thermo-electromechanical Coupling on the Performance of Lead-free Piezoelectric Materials

Akshayveer[1], R. Melnik[1]

[1] *MS2Discovery Interdisciplinary Research Institute, Wilfrid Laurier University, Waterloo, Ontario N2L 3C5, Canada, {aakshayveer, rmelnik}@wlu.ca*

Lead-free piezocomposites provide an environmentally beneficial approach for detecting and harvesting energy from mechanical stimuli, and it is critical to build realistic models that can represent the basic physical processes behind their performance. The influence of temperature is largely neglected in current piezoelectric designs, which are based on electromechanical coupling only. The performance of many lead-free piezoelectric materials degrades with increasing temperature because it diminishes the propensity of domain switching and phase coexistence [1]. Here, we provide a more precise modelling paradigm to assess how temperature affects the functionality of the piezoelectric material. In this paper, $Bi_{0.5}Na_{0.5}TiO_3$ (BNT) piezoelectric inclusions of a definite shape are positioned over a PDMS matrix at predefined locations as shown in Fig. 1. The volume fraction of BNT inclusions is kept fixed and the piezoelectric response of the system with thermo-electromechanical model is compared with conventional electromechanical model. The thermo-electromechanical model is expected to predict the performance of piezoelectric material more accurately and it will also help us in finding the right operating temperature for BNT-type of materials. Aside from this goal, the research will help us develop solutions to make it perform at greater temperatures and expand the application sector for this sort of piezoelectric material.

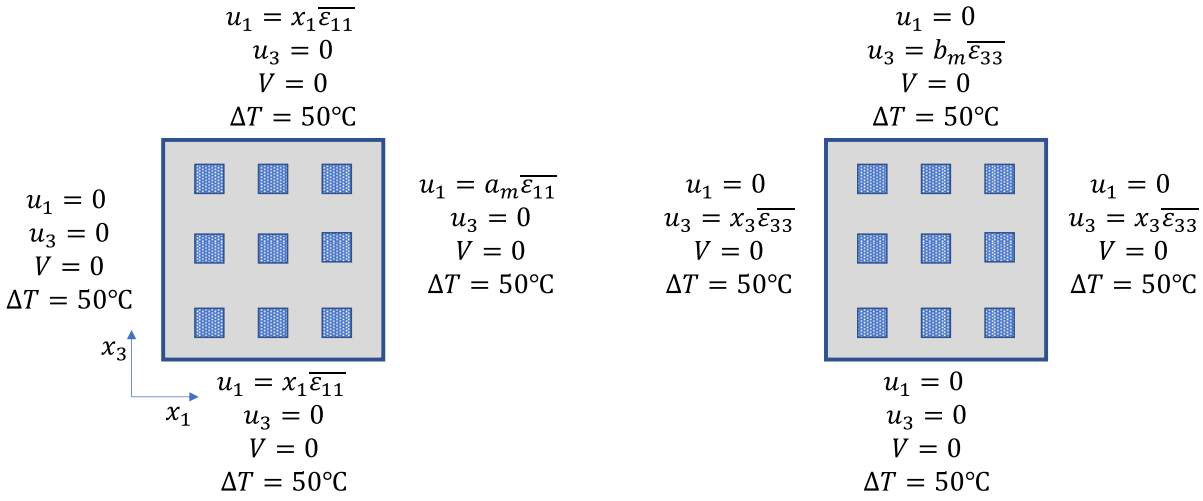

Figure 1: Schematic diagram of BNT inclusions on PDMS matrix with different boundary conditions.

References

[1] J. Yin, Y. Wang, Y. Zhang, B. Wu, and J. Wu, *Thermal depolarization regulation by oxides selection in lead-free BNT/oxides piezoelectric composites*, Acta Mater. **158**, 269–277 (2018).

The VI International AMMCS
Interdisciplinary Conference
Waterloo, Ontario, Canada
16 juin 2023

Modeling Variable Compliance to Non-Pharmaceutical Interventions in Controlling Outbreaks

J. Bélair

Département de mathématiques et de statistique et Centre de recherches mathématiques, Université de Montréal
Centre for Disease Modeling, York University

Management of the COVID-19 pandemic required the deployment of non pharmaceutical interventions (NPIs) [social isolation, physical distancing, mask-wearing, hand-washing], and administration of repeated doses of vaccine as they became available. We are interested in the consequences, for the dynamics of the disease, of variable adherence to the NPIs, and the motivation generating the lack thereof, so we investigate a model for the change in attitude *post*-infection. A basic SEIRS model is expanded by **a.** introducing a structure in the infectious class, to reflect the variable severity of symptoms and the presence of asymptomatic cases; and **b.** considering the population divided into two classes according to their degree of adherence to the NPIs. Analysis of the ensuing model is guided by epidemiological observations in Québec. Time permitting, a recent analysis of a simpler model for compliance *pre*-infection will be presented.

Retirement Risks with Glide Paths

Agassi Iu[1]

[1] *Wilfrid Laurier University, Waterloo, Canada, iuxx9590@mylaurier.ca*

Retirement planning has been an ongoing issue for everyday Canadians. There are concerns of not being able to meet retirement goals with inadequate saving habits, and fear of being exposed to market downfall. The goal of our project is to investigate asset allocation strategies that protect investor from downside risks in financial markets. We construct a simple portfolio setting with two assets of different risk characteristics: an equity and bond index. The value of the equity $\{E_t\}_{t\geq 0}$ and bond indices $\{B_t\}_{t\geq 0}$ are assumed to be modelled by geometric Brownian motion. A glide path is the proportion of equity assets in a portfolio at time t, expressed by the function $p_t \equiv p(t)$ in (1).

$$p_t = \frac{E_t}{E_t + B_t} \tag{1}$$

A conventional glide path has higher equity proportion in the portfolio at the beginning of accumulation period, and gradually decreases the equity proportion until maturity. This aims to protect investors from poor market returns and potentially lose all of the savings near retirement. It can be shown glide paths that employ constant proportion strategies as (2) can outperform the respective time-deterministic glide paths with regards to reducing volatility of terminal wealth [1].

$$\tilde{p} = \frac{1}{t}\int_0^t p_s ds \tag{2}$$

However, this proposition is counter intuitive to the downside risk protection at maturity with relatively high weights in equity near retirement in (2). We use Brownian bridges to explore the extreme probabilities of downside risks near retirement. This study plans to answer the questions: if we condition on poor market performance on the last several years prior to retirement, how does such condition affect the overall performance of portfolio and probability of reaching retirement goals? What are the portfolio allocation strategies that provides better protection under specific market scenarios? And what are the risk characteristics of the proposed glide paths?

References

[1] P. Forsyth and K.R. Vetzal, *Optimal Asset Allocation for Retirement Saving: Deterministic vs. Time Consistent Adaptive Strategies*, Applied Mathematical Finance. **26**, 1, pp. 1-37 (2018).

Effect of Environmental Fluctuations on Patterns in an Ecosystem

Swadesh Pal[1], Roderick Melnik[1]

[1] *M3AI Laboratory, MS2Discovery Interdisciplinary Research Institute,*
Wilfrid Laurier University, Waterloo, ON, Canada N2L 3C5, {spal, rmelnik}@wlu.ca

Various types of regular and irregular patterns are found in semiarid vegetation, and they depend on the landscape, e.g., stationary irregular mosaic-type patterns on flat ground, alternate vegetation stripes with patches on hillside areas, etc [1]. It is known that there is a regular interaction between the vegetation and the living species in that habitat because some animals adapt to live in a semiarid ecosystem and depend on plants as their food source. Most of the previous studies have been concerned with either the vegetation patterns incorporating the interaction between vegetation and groundwater or two or more species' interactions, e.g., predator-prey. We construct a coupled mathematical model to bridge a link between the vegetation and living species that depend on this vegetation. There are many environmental factors that affect the resulting patterns. For instance, low rainfall in a semiarid ecosystem affects the depending species, and the living species population can go to extinction due to insufficient food resources. This is due to multiple stable states present in the system. Like low rainfall, different environmental fluctuations may cause catastrophic shifts in an ecosystem [2]. We further explain how these external fluctuations can shift from one stable state to another stable state or to a new state which was not present in the absence of noise [3].

References

[1] C. A. Klausmeier, *Regular and Irregular Patterns in Semiarid Vegetation*, Science **284**, 5421, pp. 1826-1828 (1999).

[2] M. Scheffer et al., *Early-warning signals for critical transitions*, Nature **461**, 7260, pp. 53-59 (2009).

[3] K. Higgins et al., *Stochastic Dynamics and Deterministic Skeletons: Population Behavior of Dungeness Crab*, Science **276**, pp. 1431-1435 (1997).

The VI International AMMCS
Interdisciplinary Conference
Waterloo, Ontario, Canada

Countering Partisan Gerrymandering with Multimember Electoral Districts

D. Cooper[1]

[1] *Morehouse College, Atlanta, USA, duane.cooper@morehouse.edu*

In recent years, the mathematical community has given considerable attention and energy to matters of districting, especially in the United States. Much of this work has addressed the effects of gerrymandering on representation in legislatures, most of which are composed from single-member electoral districts.

This work presents results showing how multimember electoral districts, in conjunction with supporting election methods — cumulative voting and others — can blunt the most extreme misrepresentation that can occur in gerrymandered single-member districts. The analysis is primarily combinatorial. The results showing decreased misrepresentation for two-parties are generalized over district size and population size. Some classic examples are used to illustrate the results, and the specific instance of current congressional districting in the state of Ohio is examined.

We conclude by considering how these results analyzing fair representation to parties can be extended to examine fair representation for individual citizens.

Leveraging cellphone-derived mobility networks in spatiotemporal infectious disease models

Justin J. Slater[1], Patrick E. Brown[2], Jeffrey S. Rosenthal[2], Jorge Mateu[3]

[1] *Department of Mathematics and Statistics, University of Guelph, Canada, @jslate04@uoguelph.ca*
[2] *Department of Statistical Sciences, University of Toronto, Canada*
[3] *Department of Mathematics, University Jaume I of Castellon*

In spatial/spatiotemporal models for COVID-19, spatial proximity is used as a proxy for mobility. This is because regions that are near each other are likely to have many people moving between them, leading to similar Covid-19 risk. But what if we *knew* the amount of mobility between regions? Would this improve spatiotemporal models for COVID-19?

In this work, we develop a spatiotemporal modelling framework that leverages cellphone-derived mobility networks to model COVID-19 case counts in 245 subregions of Castilla-Leon, an autonomous community in Spain. We first show that mobility better captures the spatial dependence in COVID-19 case counts than spatial proximity. We do so by extending the classic Besag, York, and Mollié modelling framework to include a mobility structured random effect. We show that this random effect captures the majority of variation in COVID-19 case counts, but advise users to still include a measure of proximity as this is still an important model feature.

We then develop a mechanistic spatiotemporal infectious disease model, where contact rates between susceptible and infectious people is a function of mobility. We show that, with some simplifications, this model reduces to an 'endemic-epidemic' model with an additional network autoregressive term that is based on mobility. We found that the mobility term was the strongest predictor of cases overall (see 1), but the strength varied spatially. We use this model to estimate important epidemiological quantities such as reproductive numbers and travel risk, accounting for uncertainty in our esimates. We argue that mobility data is likely a key component in infection disease surveillance.

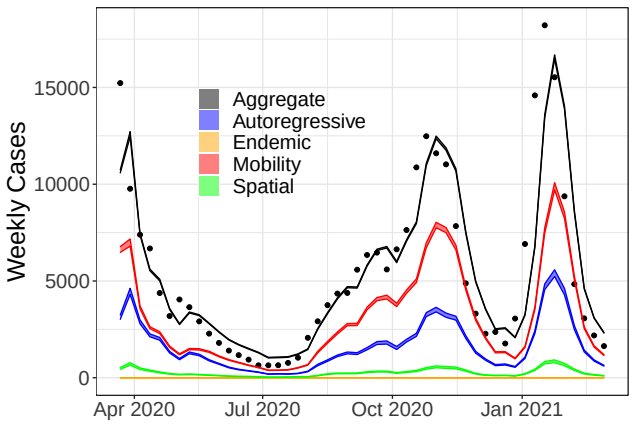

Figure 1: Model results aggregated over Castilla-Leon in the first year of the pandemic. Case counts associated with mobility (red) are estimated to be higher than those from other sources.

The Influence of Coupled Electromechanical Effects on the Behavior of Active Biological Materials

Akepogu Venkateshwarlu[1], Roderick Melnik[1]

[1]*M3AI Laboratory, MS2Discovery Interdisciplinary Research Institute,*
Wilfrid Laurier University, Waterloo, Ontario, N2L3C5, Canada, {avenkateshwarlu,rmelnik}@wlu.ca

Active matter extracts energy from its surroundings through microscopic components, like biological cells, and converts it into mechanical work [1,2]. The biological cell (BC) is comprised of various organelles, such as mitochondria, microtubules, and the nucleus. BCs exhibit complex behavior when they are exposed to external mechanical loads [3,4]. In the present study, a coupled electromechanical model of a biological cell has been developed to further investigate the complex behavior of biological cells subjected to the piezoelectric and flexoelectric effects of its constituent organelles under external forces. A more precise modeling approach based on the finite element method has been presented to capture the non-local flexoelectric effect alongside the linear piezoelectric effect. Investigations on the impact of changes in applied forces on the intrinsic piezoelectric and flexoelectric contributions to the electroelastic response have been conducted systematically while also considering coupling coefficient alterations. Furthermore, it has been found that the mechanical degradation of the organelles enhances the piezoelectric and flexoelectric responses related to electromechanical coupling. Comparisons have been made between the contributions of the flexoelectric and piezoelectric effects. The insights obtained from the present study provide a better understanding of the mechanics of biological cells that are difficult to explain through experiments, which is crucial in developing novel advanced medical treatments based on tissue engineering, regenerative, and personalized medicine.

References

[1] O. Hallatschek, S. S. Datta, K. Drescher, J. Dunkel, J. Elgeti, B. Waclaw and N. S. Wingreen, *Proliferating active matter*, Nat. Rev. Phys (2023).

[2] D. Needleman and Z. Dogic, *Active matter at the interface between materials science and cell biology*, Nat. Rev. Mater, **2**, pp. 17048 (2017).

[3] M. Dogterom and G. H. Koenderink, *Actin-microtubule crosstalk in cell biology*, Nat. Rev. Mol. Cell Biol **20**, pp. 38-54 (2019).

[4] S. Singh, J. A. Krishnaswamy and R. Melnik, *Biological cells and coupled electro-mechanical effects: The role of organelles, microtubules, and nonlocal contributions*, J. Mech. Behav. Biomed. Mater **110**, pp. 103859 (2020).

Integrating Emotion-specific Factors into the Dynamics of Bio-social and Ecological Systems: An Example of Predator-Prey Models Accounting for Psychological Effects

S. Saha[1] and R. Melnik[1]

[1] *M3AI Laboratory, MS2Discovery Interdisciplinary Research Institute and Department of Mathematics, Wilfrid Laurier University, {ssaha, rmelnik}@wlu.ca*

Most mathematical models in biological, social, and ecological sciences developed up to date ignore the influence of psychological factors. Take, for example, a class of models that describe the dynamics of predators and preys. Substantial progress has been made in this area and additional effects have now been incorporated in such models. This includes but is not limited to such important considerations as the Allee effect, the influence of dispersal-induced resilience to environmental fluctuations, and others (see, e.g., [1] and references therein). Yet, surprisingly, very little has been done in analyzing the influence of emotions on the dynamics of the underlying bio-social and ecological systems such as predators and preys. At the same time, it has been known for a long time that, based on brain reactions, the psychophysiology of emotional arousals would play a crucial role in the dynamics. The resulting dynamics can be substantially augmented in response to the anticipation of potentially aversive as well as highly pleasant outcomes. In this contribution, we start with the analysis of fear effects where the impact on and functional response to dynamic interactions of the system have already been analyzed in the literature, including refuge, and harvesting (see, e.g., [2,3] and references therein). From such simpler mechanistic models, we move to the development of a model where we attempt to account for the fact that the source of such psychological effects, and in particular the reaction to them, is in the brain, which then is expressed through emotions that augment the dynamics of predator and prey. We demonstrate the significance of these effects on the dynamics and propose some possible mechanisms of control. Finally, we discuss an extension of our analysis to nonlocal models and emphasize the importance of non-equilibrium phenomena in some of the above considerations.

References

[1] R. Crespo-Miguel, J. Jarillo, and F. J. Cao-Garcia, *Dispersal-induced resilience to stochastic environmental fluctuations in populations with Allee effect*, Phys. Rev. E **105**, 014413 (2022).
[2] H. K. Qi and X. Z. Meng, *Threshold behavior of a stochastic predator-prey system with prey refuge and fear effect*, App. Math. Lett. **113**, 106846 (2021).
[3] D. Hua and X. B. Liu, *Dynamical analysis in a piecewise smooth predator-prey model with predator harvesting*, Int. J. Biomath. 16, 6, 2250118 (2023).

The VI International AMMCS
Interdisciplinary Conference
Waterloo, Ontario, Canada

Quantifying Dependence Between Spatio-Temporal Point Processes and their Mark Distributions with Application to Wildland Fires

D.G. Becker[1], D.G. Woolford[2], C.B. Dean[3]

[1] *Wilfrid Laurier University, Waterloo, Canada, dbecker@wlu.ca*
[2] *The University of Western Ontario, London, Ontario*
[3] *The University of Waterloo, Waterloo, Ontario*

If a model predicts that there will be more fires than average in a given region, we might expect those fires to also be larger than average; we expect some sort of dependence between ignition and size. In this work, we fit models that account for this dependence and further inform this intuition. In particular, we estimate the ignition rate as a log-Gaussian Cox process, which has a spatial random effect that is split into a spatial process effect and a shared effect (both effects being spatial Gaussian processes) The shared portion of the random effect also appears in the model for fire sizes, which is a Survival model that accounts for the rounded nature of the data.

Our models are fit to recorded fire sizes in British Columbia from 1953 to 2003, which are rounded to the nearest 0.1 hectares with a preference for rounding to the nearest acre (before 1975) or hectare (after 1975). We find that the quantities tend to be independent in the southern, populated regions of British Columbia but dependent in the northern regions which are less populated and thus fires are not fought as aggressively. For lightning-caused fires, we find that the distance to roadways is a significant covariate in lightning ignitions, but this covariate decreased over time (possibly indicating that detection has improved and we are now more likely to notice fires further from the road).

Predictions from spatial models must be evaluated carefully, and standard cross-validation schemes are not appropriate. We discuss extensions to this work that assess the predictive capabilities of the model using Bayesian prediction diagnostics as well as cross-validation schemes for joint spatial models. These extensions incorporate the shared random effects structure of the work and suggest residual diagnostic tests.

The VI International AMMCS
Interdisciplinary Conference
Waterloo, Ontario, Canada

Privacy-Preserving Cryptocurrency Transactions in a Regulated Decentralized Environment (PPCT-RDE)

Issameldeen Elfadul [1]

[1] *School of Computer Science and Engineering, University of Electronic Science and Technology of China, Chengdu, Sichuan, China.*

Abstract. Decentralized Payment Systems (DPS), commonly referred to as cryptocurrencies, are wildly successful and extensively adopted Blockchain applications. However, the strong anonymity and security provided by these systems can pose a threat to the country's safety because they can be exploited for illegal activities without the ability to trace or prevent such transactions.
In this article, we introduce Privacy-Preserving Cryptocurrency Transactions in a Regulated Decentralized Environment (PPCT-RDE), which seeks to ensure compliance with government regulations and oversight while maintaining transaction secrecy and participant identity security.
Utilization of the RSA accumulator in conjunction with the Schnorr protocol is the key element of the proposed solution. This mixture permits meeting government regulations and facilitates revocation in the event of a violation. In addition, to ensure transaction privacy and anonymity, the used strategy combines ring signatures, stealth addresses, and Pedersen commitments. The suggested protocol (PPCT-RDE) satisfies the fundamental security requirements outlined in the literature and achieves complete anonymity. Furthermore, despite achieving complete anonymity, the performance analysis proves the feasibility and effectiveness of our proposed protocol.

Keywords: Privacy-preserving, Cryptocurrency transactions, Regulated.

The VI International AMMCS
Interdisciplinary Conference
Waterloo, Ontario, Canada

Computational Considerations for Implementation of the Collage Method for ODE Inverse Problems

N.A. Boettger[1], K.M. Levere[2]

[1] *University of Guelph, Guelph, Canada nboettge@uoguelph.ca* [2] *University of Guelph, Guelph, Canada klevere@uoguelph.ca*

For decades, mathematical modelling has been used to better understand the world around us. The process of mathematical modelling often necessitates the use of parameter estimation techniques to inform aspects of models that are difficult or impossible to measure. The goal of many inverse problems is to minimize the approximation error; the distance, with respect to an appropriate metric, between a given solution and the solution obtained using recovered parameters. While historical methods such as Tikhonov regularization (see [7]) and iterative schemes have been shown to accurately solve a wide variety of parameter estimation problems, they are often computationally expensive to implement. In the realm of parameter estimation for ordinary differential equations (ODEs), the more recently proposed collage-coding framework for parameter estimation has recognized significant gains in computational expense as well as accuracy [6]. This alternative approach to solving an inverse problem bounds the approximation error above by a new distance (called the collage distance) that is, in practice, easier to minimize. The collage method has been extended to a wide variety of problems, including delay, fractional, and random DEs, variational problems, and partial differential equations [2, 3, 4, 5].

The collage method for solving inverse problems has been well established theoretically. With roots in fractal image compression, the Collage Theorem that establishes the collage distance is a simple consequence of the well-known Banach's Fixed Point Theorem [7]. However, in practice, a number of computational considerations arise during implementation that depend on the complexity of the problem at hand. In this paper, we review the theoretical underpinnings of the collage-coding method for solving inverse problems for ODEs. We then present a comprehensive investigation of computational challenges and choices that may be faced during implementation. Examples showcasing the results of this investigation are presented and discussed.

References

[1] M.F. Barnsley, V. Ervin, D. Hardin, and J. Lancaste, *Solution of an inverse problem for fractals and other sets*, Proc. Natl. Acad. Sci, **83** pp. 1975-1977, (1985).

[2] H.E. Kunze, and E.R. Vrscay, *Solving Inverse Problems for Ordinary Differential Equations Using the Picard Contraction Mapping*, Inverse Problems, **15**, pp. 745-770, (1999).

[3] H.E. Kunze, D. La Torre, K.M. Levere, and E.R. Vrscay, *Solving Inverse Problems for Deterministic and Random Delay Integral Equations Using the Collage Method*, International Journal of Mathematics & Statistics (IJMS), **11(1)**, (2012).

[4] H.E. Kunze, D. La Torre, K.M. Levere, and M. Ruiz Galán, Inverse Problems via the "Generalized Collage Theorem" for Vector-Valued Lax-Milgram-Based Variational Problems

[5] H. Kunze, D. La Torre, and E.R. Vrscay, *A generalized collage method based upon the Lax-Milgram functional for solving boundary value inverse problems*, Nonlinear Analysis: Theory, Methods & Applications, **71(12)**, pp. 1337-1343, (2009).

[6] K.M. Levere, B. Boreland, and J. Dewhurst, *A Computational Comparison of Three Methods for Solving a 1D Boundary Value Inverse Problem*, Springer Proceedings in Mathematics & Statistics, Waterloo, 2021.

[7] A. Tikhonov and V. Arsenin. *Solutions of Ill-posed Problems*. V.H. Winston & Sons, Washington, 1977.

The VI International AMMCS
Interdisciplinary Conference
Waterloo, Ontario, Canada

Modelling Tools for Mine Water and Environmental Management

Harry Gaebler[1], Alireza Ghane[2], Jige (Gene) Shen[3]

[1] *Ecometrix Incorporated, Mining Services – Applied Mathematician & Environmental Modeller, hgaebler@ecometrix.ca*
[2] *Ecometrix Incorporated, Mining Services – Hydrodynamics & Water Quality Modeller, aghane@ecometrix.ca*
[3] *Ecometrix Incorporated, Canadian Health Physicist & Programmer, jshen@ecometrix.ca*

The mining industry plays a vital role in the global economy, but its operations often impact surrounding ecosystems, particularly water bodies. To minimize environmental risks and ensure sustainable mining practices, the use of mathematical models has gained significant prominence. Of particular interest to the mining industry is the creation of surface water models, not only to track the movement of water across a site, but also to assess changes in water quality and help identify the need for treatment prior to discharging water off site.

Due to the continual need for these surface water models, Ecometrix has established a unique development team focused on creating mining specific comprehensive models that encompassing various environmental aspects of mine sites, including surface water and groundwater modeling, hydrodynamics modelling, plume delineation, waste rock pile and tailing area analysis. These models are able to predict crucial factors such as runoff and seepage volumes and accurately forecasts the movements of flushed constituents from waste rock piles and tailing areas to the surrounding environment. Specific modules have been designed to calculate acid generation within mine sites and determine lime consumption for treatment purposes. By providing essential information for both management and regulatory purposes, this model enables effective decision-making and ensures compliance with environmental standards.

To enhance the model's capabilities, further developments are on-going including the addition of a more detailed 2D seepage module, a 2D hydrodynamic module for pit lakes and a 2D geochemical module to accurately calculate the transient flow and transport of chemical species within the waste rock piles. These advancements will enhance the model's accuracy and comprehensiveness, enabling more precise analysis and mitigation strategies for environmental impacts associated with mining activities.

This presentation focuses on the use of these various mathematical models, with an application to mining.

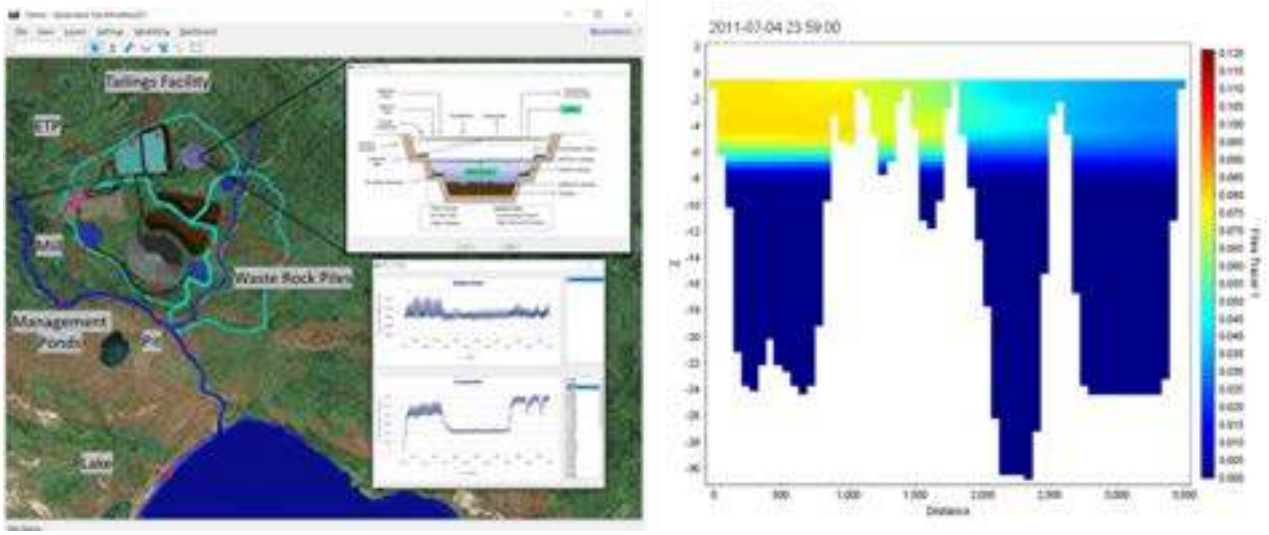

Figure 1: Example of Site Models and Outputs

The VI International AMMCS
Interdisciplinary Conference
Waterloo, Ontario, Canada

Telling Oil Temperature for Frying from Audio and Video Signals based on Multimodal Learning

M. Veremchuk[1], Z. Pan[1], K.A Scott[1]

[1] *University of Waterloo, Canada, {mrveremc, zhao.pan, ka3scott}@uwaterloo.ca*

Accurate oil temperature control plays a vital role in achieving optimal cooking outcomes. One may wonder how a chef tells the oil temperature prior to the invention of modern cooking thermometers. The ”chopstick test” had been widely used: by dipping the tip of chopsticks or small pieces of food into hot oil, bubbles, and associated noise were created. An experienced chief can tell the oil temperature by watching the bubble morphology and/or hearing the acoustic signals from the tests. However, it is not clear how a human cook utilizes visual and auditory perception or its fusion to detect the temperate and which perception channel is more effective. We collected video and audio data in a controlled kitchen environment using smartphone sensors, with wet chopsticks acting as a controlled stimulus for bubble generation, and a thermometer for labeling and ground truth. We built and trained end-to-end neural networks mapping the video and audio signals separately to the temperature, and multimodal learning models that fuse the perception of the unstructured audio and video data. The data processing with a neural network is much faster than with a thermometer because it takes a few seconds for the device to stabilize the temperature. We discovered a notable performance advantage of the audio modality over the video modality. However, the optimal prediction was achieved through multimodal learning. This study not only demonstrates the potential of multimodal machine learning techniques for fusing unstructured data but implies that high-frequency low-dimension signals (e.g., audio) can be more effective than higher-dimensional data (e.g., video) for specific applications such as learning the ”chopstick test”, which could be used in real-time applications.

Modeling the compaction of bacterial chromosomes by biomolecular crowding and the cross-linking protein H-NS

B.-Y. Ha[1] and Y. Jung[2]

[1] *University of Waterloo, Waterloo, Ontario, Canada*
[2] *Korea Institute of Science and Technology Information, Daejeon, Korea*

The way chromosomes are spatially organized influences their biological functions. Cells orchestrate the action of various molecules toward organizing their chromosomes: chromosome-associated proteins and the surrounding "free" molecules often referred to as crowders. Chain molecules like chromosomes can be entropically condensed in a crowded medium. A number of recent experiments showed that the presence of the protein H-NS enhances the entropic compaction of bacterial chromosomes by crowders [1, 2]. Using a coarse-grained computational model, we discuss the physical effects on bacterial chromosomes H-NS and crowders bring about. In this discussion, a H-NS dimer is modeled as a mobile binder with two binding sites, which can bind to a chromosome-like polymer with a characteristic binding energy. Using the model, we will clarify the relative role of biomolecular crowding and H-NS in condensing a bacterial chromosome, offering quantitative insights into recent chromosome experiments [1, 2]. In particular, they shed light on the nature and degree of crowder and H-NS synergetics: while the presence of crowders enhances H-NS binding to a bacterial chromosome, the presence of H-NS makes crowding effects more efficient, suggesting two-way synergetics in condensing the chromosome.

References

[1] A. S. Wegner, K. Wintraecken, R. Spurio, C. L. Woldringh, R. de Vries, and T. Odijk, *Compaction of isolated Escherichia coli nucleoids: Polymer and H-NS protein synergetics*, J. Struct. Biol. **194**, 129-137 (2016).

[2] T. M. Cristofalo et al, *Cooperative effects on the compaction of DNA fragments by the nucleoid protein H-NS and the crowding agent PEG probed by Magnetic Tweezers*, Biochim. Biophys. Acta (BBA) - General Subjects **1864**, 129725 (2020).

The VI International AMMCS
Interdisciplinary Conference
Waterloo, Ontario, Canada

Patterns of Substitution in Discrete Choice

S. Horan[1], A. Adam[2]

[1] *University of Montreal, Canada, sean.horan@umontreal.ca*
[2] *Princeton University, USA, arthur.adam@umontreal.ca*

We use the "discard model" of Luce [1] and Marley [2] to study the effect of adding (or removing) one product on the probability of choosing the remaining products. Since the discard model does not require the Regularity axiom, it accommodates a rich variety of substitution patterns (including complementarity, attraction, choice overload, and compromise) that are directly ruled out by other models of discrete choice.

We first provide an axiomatic characterization to identify the model's testable implications. We then provide a "qualitative" characterization model à la Samuelson [3], identifying the kinds of directional changes in choice probabilities that can invariably be explained by the model and, conversely, the directional changes can never be explained by the model. Next, we show that behaviour consistent with the model exhibits many of the same features as the Slutsky matrix from classical demand theory. Finally, we establish microfoundations, showing that the "perturbed utility model" (Refs. [4, 5, 6]) delivers discrete choice behavior that is consistent with the model.

References

[1] R.D. Luce, *Response Latencies and Probabilities*, in K.J. Arrow, S. Karlin, P. Suppes (eds.), Mathematical Methods in the Social Sciences, Stanford University Press, pp. 297-311 (1960).

[2] A.A.J. Marley, *The Relation between the Discard and Regularity Conditions for Choice Probabilities*, J Math Psych, **2(2)** pp. 242-253 (1965).

[3] P.A. Samuelson, Foundations of Economic Analysis, Harvard University Press (1947).

[4] D. L. McFadden and M. Fosgerau, *A Theory of the Perturbed Consumer with General Budgets*, Technical report, National Bureau of Economic Research (2012).

[5] D. Fudenberg, R. Iijima, and T. Strzalecki, *Stochastic Choice and Revealed Perturbed Utility*, Ecma, **83(6)** pp. 2371-2409 (2015).

[6] R. Allen and J. Rehbeck, *Identification with Additively Separable Heterogeneity*, Ecma, **87(3)** pp. 1021-1054 (2019).

The VI International AMMCS
Interdisciplinary Conference
Waterloo, Ontario, Canada

Asymptotic expansion of the scattering amplitude using local approximations of the Dirichlet to Neumann operator

Yassine Boubendir

Mathematical Science department, NJIT, USA. boubendi@njit.edu

A high-frequency expansion to simulate the scattering amplitude in the exterior of a convex obstacle has been developed by A. Majda. It is based on (1) approximating the normal derivative of the total field by its Kirchhoff approximation, and (2) utilization of the stationary phase method for the analytical evaluation of the integral representation of the scattering amplitude. In this talk, we describe a new methodology in designing these kinds of expansions. It uses Bayliss-Turkel type local approximations to the Dirichlet-to-Neumann operator. We will describe this local approximation as well as the derivation of the new expansion. Some preliminary results will be presented to validate the new high-frequency approximation to the scattering amplitude.

Joint with: Fatih Ecevit and Souaad Lazergui

The VI International AMMCS
Interdisciplinary Conference
Waterloo, Ontario, Canada

Dynamic Optimization of Covered Call Strategies Under Alternative Models

M. Perryman[1], G. Campolieti[2]

[1] *Wilfrid Laurier University, Waterloo, Canada, perr2360@mylaurier.ca*
[2] *Wilfrid Laurier University, Waterloo, Canada, gcampolieti@wlu.ca*

The basis of a covered call portfolio consists of selling call options while simultaneously holding the underlying asset. This paper presents a dynamic risk-return optimization framework to select quantities of call options with various strikes and maturities to sell in a covered call strategy on a single asset and then scaled to a portfolio of stocks or ETFs. We discuss some of the pitfalls of current strategies being used in the industry by asset managers from Canada and the United States, which opens up the need for improvements and strategy validation. Tractable formulations of expected return and variance for covered call portfolios are formulated using the Geometric Brownian Motion (GBM) [1] framework. We derive the Call Risk Premiums first introduced by Figelman (2008) [3] of the options to find the optimal overwriting ratios for a portfolio that maximizes expected return and develop an alternative portfolio for sufficiently risk-averse investors. We find that there are alternative ways of minimizing downside risk while being able to capture greater upside by maximizing the Call Risk Premium rather than selling strictly at-the-money (ATM) call options. We also explore static and dynamic partial overwriting strategies on our dynamic fully-overwritten portfolios and back-test our results between 2015 and 2021. We find that our proposed strategies outperform the Cboe S&P 500 BuyWrite Index (BXM) [2] and the SPDR S&P 500 ETF Trust (SPY) on a risk-adjusted basis during the time frame, simultaneously selling call options at different strike prices for all risk measures often optimal, and lower partial overwriting ratios for strategies which sell closer to the money are more advantages.

References

[1] Giuseppe Campolieti and Roman N. Makarov. *Financial Mathematics: A Comprehensive Treatment*. CRC Press, Taylor Francis Group, 2014.

[2] Chicago Board Options Exchange. *Index Dashboard: Cboe S&P 500 BuyWrite Index*. Cboe `https://www.cboe.com/us/indices/dashboard/bxm/`. 2021.

[3] Ilya Figelman. "Expected Return and Risk of Covered Call Strategies". In: *Journal of Portfolio Management* 34 (4 2008), pp. 81–97. URL: `https://www.proquest.com/scholarly-journals/expected-return-risk-covered-call-strategies/docview/56773620/se-2?accountid=15090`.

The VI International AMMCS
Interdisciplinary Conference
Waterloo, Ontario, Canada

PETSC-PIC: A Structure Preserving Full Geometry Toolkit for Kinetic Particle-in-Cell Plasma Simulation

J. Pusztay[1], D. Finn[2], M. Knepley[3], M. Adams[4]

[123] *University at Buffalo, Buffalo, USA, josephpu@buffalo.edu*
[4] *Lawrence Berkeley National Laboratory, Berkeley, USA*

The notion of structure preservation has existed for years in regards to the symplectic structure and preservation thereof within the context of numerical plasma simulation. More recently is the notion of metriplectic structure presented by Morrison [1], and for the Landau collision integral by [2]. This casts the Vlasov system in terms of two primary brackets. The Poisson bracket may be evolved symplectically with any choice of structure preserving method by discretizing the electrostatic potential via Finite Elements, and a choice of symplectic integration method. The second Metric bracket represents collisional action between the individual particles amongst the species and between species.

Recent work on conservative discretizations of the Landau collision integral were performed by Adams et al [3], and were implemented in PETSc for exascale use in the Finite Element basis representation. More recently, however, the appropriate Maxwellian steady state and moment preservation of a particle basis representation were proven by Carillo et al [4] with energy conservation in the time discretization granted by Hirvijoki[5]. To aid in rapid prototyping and development of kinetic plasma codes, we have developed a suite of tools in the PETSc library to evolve such conservative systems with the full Vlasov-Poisson-Landau system being possible in a full geometry particle basis. Poisson solves are discretized via H1 or H(div) finite elements with the RT element on tensor cells and the option of BDM on simplices. Time evolution is handled via symplectic methods including Symplectic Euler, Stormer-Verlet, 3rd and 4th order split symplectic methods, as well as Implicit Midpoint and Discrete Gradients. Collisional dynamics are handled via the particle discretization of the Landau collision integral put forth by Carillo et al [4], Hirvijoki [5] and verified by [6]. Unification of these two brackets are performed via a Strang splitting between the operators to evolve each bracket separately. Verification tests of each bracket are presented, with a study of Landau damping by Finn et al. [7] and two stream instability verifying the Poisson solver, and multi species isotropization results in comparison to the rates presented in the NRL plasma formulary as the primary verification of the particle basis Landau collision integral.

References

[1] P. Morrison, *A paradigm for joined Hamiltonian and dissipative systems*, in *Physica D: Nonlinear Phenomena* (1986), vol. 18, pp. 410-419

[2] E. Hirvijoki and M. Kraus and J. Burby, *Metriplectic particle-in-cell integrators for the Landau collision operator* in Arxiv (2018), eprint 1802.05263

[3] M. Adams and D. Brennan and M. Knepley and P. Wang, *Exascale Landau collision operator in the CUDA programming model applied to thermal quench plasmas*, in 2022 IEEE International Parallel and Distributed Processing Symposium (IPDPS)

[4] J. Carrillo and J. Hu and L. Wang and J. Wu, *A particle method for the homogeneous Landau equation*, in Journal of Computational Physics: X (2020), vol. 7, pp. 100066

[5] E. Hirvijoki, *Structure-preserving marker-particle discretizations of Coulomb collisions for particle-in-cell codes* in Plasma Physics and Controlled Fusion (2021), vol 63, pp 044003

[6] F. Zonta and J. Pusztay and E. Hirvijoki, *Multispecies structure-preserving particle discretization of the Landau collision operator* in Physics of Plasmas (2022), vol. 29, pp. 123906

[7] D. Finn and M. Knepley and J. Pusztay and M. Adams *A Numerical Study of Landau Damping with PETSc-PIC* on ArXiv (2023), eprint 2303.12620

Modeling Sex-Differences in Alzheimer's Disease

C.S. Drapaca[1]

[1] *Pennsylvania State University, University Park, USA, csd12@psu.edu*

Alzheimer's disease (AD) is a degenerative disease characterized by an abnormal extracellular accumulation of amyloid-β ($A\beta$) plaques and formation of tau-containing neurofibrillary tangles inside neurons that lead to progressive memory loss and cognitive decline [1]. An increasing number of clinical studies have shown that postmenopausal females are at a higher risk of getting AD than males, and AD in females evolves faster than in aged-matched males with AD. AD has no cure presently. Mathematical models can provide valuable insights into the AD onset and progression, and help with the development of therapies. Most models of AD existing in the literature do not account for sex differences. This talk will present a novel mathematical model of AD that uses variable-order fractional temporal derivatives to describe the temporal evolutions of relevant cells' populations and $A\beta$ fibrils [2]. The variable fractional order models fading memory due to neuroprotection loss caused by AD progression with age. Different expressions of the variable fractional order are used for the two sexes and a sharper decreasing memory corresponds to the female's neuroprotection decay caused by the fast estrogen decrease experienced by postmenopausal females. A correction to the expressions of the variable fractional orders given in [2] will be presented that reinforces the findings in the paper. Numerical simulations will be presented that show the population of surviving neurons decreased more in postmenopausal female patients than in males at the same stage of the disease. The results also suggest that if a treatment (that may include estrogen replacement therapy) is applied to female patients, then the loss of neurons slows down at later times, since preserving model's long memory (represented by fractional order values closer to 0) corresponds to conserving neuroprotection. Also, the sooner a treatment starts the better the outcome is.

References

[1] R.A. Nebel, N.T. Aggarwal, L.L. Barnes, A. Gallagher, J.M. Goldstein, K. Kantarci, M.P. Mallampalli, E.C. Mormino, L. Scott, W.H. Yu, P.M. Maki and M.M. Mielke, *Understanding the impact of sex and gender in Alzheimer's disease: A call to action*, Alzheimers Dement. **1**4(9), pp. 1171-1183, (2018). doi: 10.1016/j.jalz.2018.04.008.

[2] C.S. Drapaca, *Mathematical Investigation of Sex Differences in Alzheimer's Disease*, Fractal Fract. **6**, 457 (2022). https://doi.org/10.3390/fractalfract6080457

Simulation of Hubbard Model in Realistic Voltage-Controlled Quantum Dot Devices

Z.D. Merino[12], B. Khromets[12], J. Baugh[123]

[1] *Institute for Quantum Computing, University of Waterloo, Waterloo, Ontario, Canada N2L 3G1*
[2] *Department of Physics and Astronomy, University of Waterloo, Waterloo, Ontario, Canada N2L 3G1*
[3] *Department of Chemistry, University of Waterloo, Waterloo, Ontario, Canada N2L 3G1*

Quantum dot spin qubits have emerged as a promising platform for quantum information processing, necessitating scalable quantum control schemes to achieve high-fidelity unitary gate operations. However, the small footprint of quantum dots (tens of nanometers) that enhances qubit density also poses challenges, such as cross talk between gate electrodes. The evolution of the quantum state is governed by electrical signals that control the effective parameters of the system Hamiltonian. In this study, we address these challenges and facilitate the exploration of control schemes and semiconductor architectures based on laterally defined quantum dots [1]. To this end, we present Hubbard model simulations performed using Quantum Dots in Python (QuDiPy), our open-source software package. These simulations calculate relevant effective parameters, construct a system Hamiltonian, and subsequently diagonalize it to determine the many-body energy spectra for any gate geometry. The simulations conducted using QuDiPy, with a specific focus on arrays of 2-3 quantum dots, play a crucial role in tackling current experimental challenges in spin qubit devices. They enable the identification of voltage ranges that maintain desired charge configurations during qubit manipulation and facilitate the mapping of electrical cross talk between gates. As a result, the QuDiPy simulator shows promise as a valuable tool for developing scalable spin qubit devices.

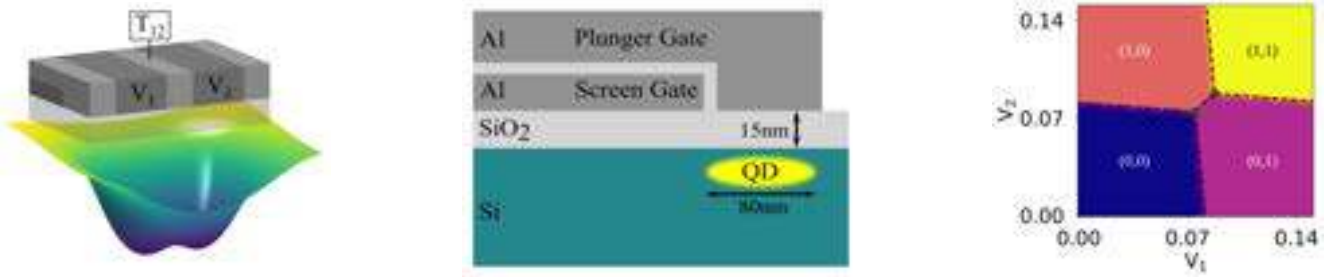

(a) (b) (c)

Figure 1: (a) Electric potenital and (b) material cross section for a realistic double quantum dot device. (c) QuDiPy simulated charge stability diagram for a double quantum dot that identifies charge transitions and triple points [2].

References

[1] B. Buonacorsi, Z. Cai, E. B. Ramirez, K. S. Willick, S. M. Walker, J. Li, B. D. Shaw, X. Xu, S. C. Benjamin, and J. Baugh, *Network architecture for a topological quantum computer in silicon*, Quantum Science and Technology, 4 (2019), p. 025003.

[2] S. D. Sarma, X. Wang, and S. Yang, *Hubbard model description of silicon spin qubits: Charge stability diagram and tunnel coupling in si double quantum dots*, Physical Review B, 83 (2011).

The VI International AMMCS
Interdisciplinary Conference
Waterloo, Ontario, Canada

Anomaly Detection of Time-series Data with Gaussian Process with Application to Wind Turbine Blade

A. Omar[1], N. Dabiran[2], M. Khalil[3], A. Sarkar[4]

[1] *Carleton University, Ottawa, ON, Canada, {asmaomar}@cmail.carleton.ca*
[2] *Carleton University, Ottawa, ON, Canada, {nastarandabiran}@cmail.carleton.ca*
[3] *Sandi National Laboratories, P.O. Box 969 MS 9051, Livermore, CA 94551-9051, United States, {mkhalil}@sandia.gov*
[4] *Carleton University, Ottawa, ON, Canada, {abhijit.sarkar}@carleton.ca*

Anomaly detection is a widely-discussed subject within the field of machine learning (ML), especially concerning condition monitoring of structural systems. It involves analyzing and processing time-series measurements to identify instances of abnormal conditions. Anomaly detection is commonly performed through statistical methods or ML techniques. In this research, we leverage the insights from a well-known data-informed ML algorithm known as *Gaussian process* (GP),

$$\mathbf{f}(\mathbf{x}) \backsim GP(m(\mathbf{x}), k(\mathbf{x}, \mathbf{x}')), \tag{1}$$

in which the priors $\mathbf{f}$ are modeled with GP having the mean $m(\mathbf{x})$ and the covariance kernel $k(\mathbf{x}, \mathbf{x}')$ (see Refs. [1]) and the posteriors obtained by conditioning with the observation. Our objective is to detect abnormal conditions in a time-series dataset. In this regard, a baseline model is constructed exclusively based on normal conditions. Through the training process of the baseline model, we learn the model hyperparameters (θ). This baseline model is then utilized to compute the evidence function, which is also known as the anomaly score indicator, to identify the anomalous dataset. Consequently, for an unseen time-series dataset $\mathbf{x}^*$ and $\mathbf{y}^*$, the anomaly score indicator (see Refs. [2]),

$$\log \mathrm{p}(\mathbf{y}^*|\mathbf{x}^*, \theta) = \log \int \mathrm{p}(\mathbf{y}^*|\mathbf{f}, \mathbf{x}^*)\mathrm{p}(\mathbf{f}|\mathbf{x}^*, \theta) d\mathbf{f}, \tag{2}$$

informs to which level the new dataset aligns with the baseline model. This study shows the effectiveness of the anomaly score indicator in identifying anomalous conditions in scenarios where visual detection is deemed possible and impossible. Moreover, the implementation of ML-II in estimating the baseline model's hyperparameters is compared with MAP-II and hierarchical Bayes (utilizing MCMC) for anomaly detection purposes. To highlight the benefits of this model, we apply the algorithm to a set of synthetic data of a wind turbine blade, including healthy and damaged datasets. This result demonstrates that ML-II successfully detects abnormal conditions when visual detection is possible, while MAP-II and hierarchical Bayes excel in scenarios where visual detection is not feasible.

References

[1] K. Murphy, *Probabilistic Machine Learning: An introduction*, MIT Press. (2012).

[2] N. Twomey, H. Chen, T. Diethe, and P. Flach, *An application of hierarchical Gaussian processes to the detection of anomalies in star light curve*, Neurocomputing. 342, pp. 152-163 (2019).

The VI International AMMCS
Interdisciplinary Conference
Waterloo, Ontario, Canada

Sparse Bayesian Neural Networks: Tackling Overfitting, Uncertainty Quantification and Computational Challenges

N. Dabiran[1], B. Robinson[2], R. Sandhu[3], M. Khalil[4], A. Sarkar[4]

[1] *Carleton University, Ottawa, ON, Canada, {nastarandabiran}@cmail.carleton.ca*
[2] *Carleton University, Ottawa, ON, Canada, {brandonrobinson}@cmail.carleton.ca*
[3] *Computational Science Center, National Renewable Energy Laboratory, Golden, CO, United States, {rimple_sandhu}@outlook.com*
[4] *Sandia National Laboratories, P.O. Box 969 MS 9051, Livermore, CA 94551-9051, United States, {mkhalil}@sandia.gov*
[5] *Carleton University, Ottawa, ON, Canada, {abhijit.sarkar}@carleton.ca*

The widespread adoption of neural networks (NNs) across many sectors has triggered a revolutionary transformation within the realm of machine learning. NNs are predominantly developed within the frequentist statistical framework. However, there has been a notable surge of interest in their Bayesian statistical formulations in recent years. The frequentist NNs lack the capability to provide uncertainties in the predictions, and hence their robustness can not be adequately assessed particularly when data are noisy and sparse. Conversely, the Bayesian neural networks (BNNs) naturally offer predictive uncertainty by applying Bayes' theorem. However, their computational requirements pose significant challenges. Moreover, both frequentist NN and BNN suffer from overfitting issues, which render their predictions unwieldy away from the available data space. To address both these problems simultaneously, we leverage insights from a hierarchical Bayesian setting in which prior, conditional on hyperparameter, is used to construct a BNN by applying a semi-analytical framework known as nonlinear sparse Bayesian learning (NSBL) (see Refs. [1]). This methodology leads to the following expression of the parameter posterior

$$\mathrm{p}(\boldsymbol{\phi} \mid \mathscr{D}, \boldsymbol{\alpha}) = \frac{\mathrm{p}(\mathscr{D} \mid \boldsymbol{\phi})\mathrm{p}(\boldsymbol{\phi} \mid \boldsymbol{\alpha})}{\mathrm{p}(\mathscr{D} \mid \boldsymbol{\alpha})} \tag{1}$$

where $\boldsymbol{\phi}$, $\mathscr{D}$ and $\boldsymbol{\alpha}$ are the parameter, data and hyperparameter vectors respectively. The parameter prior $\mathrm{p}(\boldsymbol{\phi})$ and hyperparameter probability density function (pdf) $\mathrm{p}(\boldsymbol{\alpha})$ are assumed to be Gaussian and Gamma distributions respectively. We call our network *sparse Bayesian neural network* (SBNN) which encourages the automatic pruning of redundant parameters based on the concept of automatic relevance determination (ARD). This network possesses the ability to utilize a hybrid prior (see Refs. [2]), which enables the incorporation of ARD priors and informative priors in a combined manner. This setup provides a favorable choice for incorporating *a priori* knowledge of underlying system physics into the models. Additionally, a Gaussian mixture model approximation of the posterior distribution as a function of the hyperparameters $\boldsymbol{\alpha}$ is proposed. This allows for the semi-analytical calculation of Bayesian entities, thereby alleviating computational burden in the evidence optimization process required for identifying the optimal sparse NN that reduces overfitting. The superiority of the proposed SBNN algorithm is illustrated through a regression problem. The results are compared for BNNs obtained using standard Bayesian inference, hierarchical Bayesian inference, and the sparse BNN equipped with the proposed algorithm.

References

[1] R Sandhu, M Khalil, C Pettit, D Poirel, A Sarkar, *Nonlinear sparse Bayesian learning for physics-based models*, Journal of Computational Physics, 426, pp. 109728 (2021).

[2] R Sandhu, C Pettit, M Khalil, D Poirel, A Sarkar, *Bayesian model selection using automatic relevance determination for nonlinear dynamical systems*, Computer Methods in Applied Mechanics and Engineering, Elsevier, 320, 237-260 (2017).

Modified Pennes Bioheat Equation with Heterogeneous Blood Perfusion

M. Singh[1]

[1] *Department of Mechanical Engineering, University of Maryland Baltimore County, Baltimore, Maryland, USA, msingh6@umbc.edu*

The classical Fourier's law-based Pennes bioheat equation [1], is one of the widely used continuum modelling approaches used to predict temperature distribution within the biological tissue. It describes the heat conduction within the biological tissue and the heat transfer due to blood perfusion and metabolism. It assumes homogeneous (isotropic) blood perfusion to represent the whole biological tissue domain.

To account for heterogeneous blood perfusion, modifications to the traditional Pennes bioheat equation are proposed in this work. One approach to incorporate heterogeneous blood perfusion in the Pennes bioheat equation is to introduce a spatially varying perfusion coefficient $\omega_b(x,y,z)$ or blood perfusion distribution function extracted from medical imaging. This coefficient represents the local blood perfusion rate at each spatial location or point (x,y,z) within the tissue and can vary across different regions of the tissue. The heterogeneity in blood perfusion can arise from several factors such as variations in blood vessel density, vessel diameter, or vessel functionality across different regions of the tissue. By incorporating the spatially varying perfusion parameter into the Pennes bioheat transfer equation (Eq. 1), the model can account for the non-uniform distribution of blood flow and may provide more accurate temperature predictions within the tissue.

$$\rho c \frac{\partial T}{\partial t} = \nabla \cdot (k \nabla T) + \omega_b(x,y,z) \rho_b c_b (T_b - T) + Q'''_{met} \tag{1}$$

where ρ is density, c is specific heat, k is thermal conductivity, T is the temperature at any spatial location and at any instant of time, t is time, ω_b is the local blood perfusion rate, and T_b is the arterial blood temperature (~ 37°C). Q_{met}''' is the volumetric heat generation rate due to metabolism and ∇ is the gradient operator.

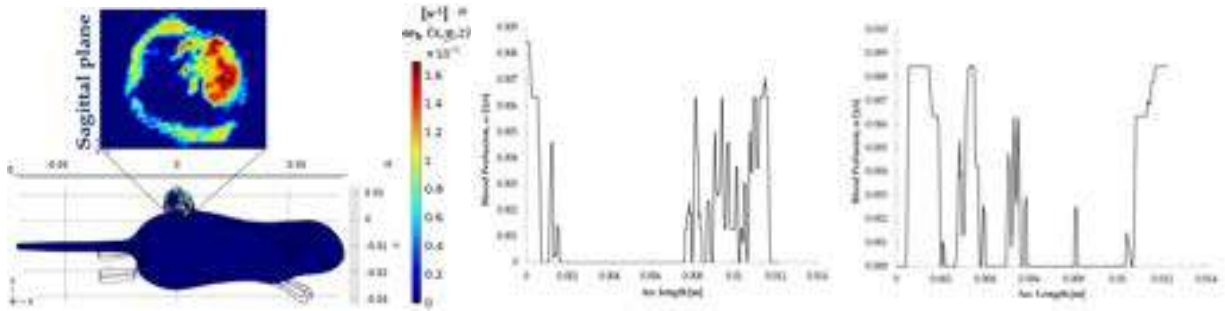

Figure 1: Resulting perfusion at each tumour tissue location (red is high, blue is low).

By incorporating heterogeneous blood perfusion in mathematical models, the temperature predictions can be more accurate, accounting for the non-uniform delivery of heat and cooling effects associated with varying blood perfusion rates. For example, tumours often exhibit variations in blood flow due to irregular vasculature and other physiological factors. This is particularly important in thermal therapies such as hyperthermia or thermal ablation, where precise temperature control is crucial for treatment effectiveness and avoiding excessive thermal damage to surrounding healthy tissue. It provides a means to account for variations in blood flow and perfusion patterns, which can have important implications for understanding the treatment response, optimizing thermal therapies, and predicting temperature distributions in heterogeneous tissues.

References

[1] H.H. Pennes, *Analysis of tissue and arterial blood temperature in the resting forearm*, J. Appl. Physiol. **1**, pp. 93-122 (1948).

The VI International AMMCS
Interdisciplinary Conference
Waterloo, Ontario, Canada

The effects of nonlinearity on the dynamics of a flexible spinning blade undergoing pitching

D. Clarabut[1], B.Robinson[2], D.Poirel[3], A.Sarkar[4]

[1] *Carleton University, Department of Civil and Environmental Engineering, Ottawa, Ontario, Canada, davidclarabut@cmail.carleton.ca*
[2] *Carleton University, Department of Civil and Environmental Engineering, Ottawa, Ontario, Canada, brandonrobinson@cmail.carleton.ca*
[3] *Royal Military College of Canada, Department of Mechanical and Aerospace Engineering, Kingston, Ontario, Canada, poirel-d@rmc.ca*
[4] *Carleton University, Department of Civil and Environmental Engineering, Ottawa, Ontario, Canada, abhijit.sarkar@carleton.ca*

This research aims to study the nonlinear structural dynamics of a system inspired by wind turbine and helicopter rotor blades. This setup consists of a flexible blade subjected to bending, rigid body pitch rotation, and spinning about the rotor axis. The structural equations of motion are derived from first principles, yielding a coupled system of partial differential equation (PDE) and ordinary differential equation (ODE). A PDE describes the bending of the cantilever blade, and the ODE describes the rigid body motion in pitch, and the spinning rotor motion is a prescribed function of time. The coupled bending and pitch motion leads to several nonlinear terms in the system dynamics. Furthermore, the imposed spinning motion introduces additional nonlinear terms that depend on the rotor velocity and acceleration.

The differential equation for the pitch motion contains an inertial nonlinearity, which is atypical in structural dynamics problems. The numerical solution of this coupled ODE and PDE system is based on implicit methods. We proceed by discretizing the PDE describing bending motion using the Galerkin's method leading to a system of nonlinear coupled ODEs. Subsequently, we discretize the ODEs in time using Houbolt's method, obtaining a system of nonlinear algebraic equations which are solved iteratively as a root-finding problem using Newton's method. A finite difference discretization is adopted to verify the solution obtained by the spatial discretization using the Galerkin method. Simulation results are presented to understand the influence of various nonlinear terms on the observed nonlinear dynamics.

The VI International AMMCS
Interdisciplinary Conference
Waterloo, Ontario, Canada

Bayesian Inference of Geo-spatial COVID-19 Spread using Scalable Solvers

Sudhi Sharma[1], Brandon Robinson[1], Victorita Dolean[2], Pierre Jolivet[3], Rimple Sandhu[5], Mohammed Khalil[6], Jodi D. Edwards[7,8], Tetyana Kendzerska[8,9,10], Abhijit Sarkar[1]

[1] *Civil and Environmental Engineering, Carleton University, Canada,*
[2] *Department of Mathematics and Statistics, University of Strathclyde, UK,*
[3]*Labaratoire J.A. Dieudonné, CNRS, Université Côte d'Azur, France,*
[4] *Sorbonne University, CNRS, LIP6, Paris, France,*
[5] *National Renewable Energy Laboratory, USA,*
[6] *Sandia National Laboratories, USA,*
[7] *School of Epidemiology and Public Health, University of Ottawa and University of Ottawa Heart Institute, Canada*
[8] *ICES, Ottawa, Canada*
[9] *The Ottawa Hospital Research Institute, Canada*
[10] *Department of Medicine, Division of Respirology, University of Ottawa, Canada*

The spatio-temporal spread of COVID-19 infections is modelled using a partial differential equation-based compartmental model having susceptible-exposed-infected-recovered and deceased (SEIRD) compartments. These coupled nonlinear PDEs contain many parameters (such as infection rate, diffusion coefficients etc.) which are uncertain. A Bayesian inference methodology called Nonlinear Sparse Bayesian Learning (NSBL) is leveraged to estimate the parameters effectively alleviating overfitting and reducing the uncertainty [1]. The overwhelming computational burden for repeated forward solutions of a high-resolution PDE model required for the Bayesian inference is handled using parallel scalable domain decomposition-based solvers. An overlapping restricted additive Schwarz solver for the fine grid and algebraic multigrid for the coarse solution allow multiple levels of error reduction providing excellent scalabilities [2]. Numerical illustrations of the methodology involve the second wave of infection of COVID-19 in Southern Ontario, using data collected by public health units between September 1, 2020, and February 28, 2021. The proposed combination of NSBL and domain decomposition-based solvers permits the construction of reliable predictive models [3] considering uncertainty.

References

[1] Sandhu, R., Khalil, M., Pettit, C., Poirel, D. and Sarkar, A., *Nonlinear sparse Bayesian learning for physics-based models.*, Journal of Computational Physics, 426, p.109728.

[2] S. Sharma, V. Dolean, P. Jolivet, B. Robinson, J. D. Edwards, T. Kendzerska, A. Sarkar, *Scalable computational algorithms for geo-spatial covid-19 spread in high performance computing*, arXiv preprint arXiv:2208.01839 (2022).

[3] B. Robinson, J. D. Edwards, T. Kendzerska, C. L. Pettit, D. Poirel, J. M. Daly, M. Ammi, M. Khalil, P. J. Taillon, R. Sandhu, S. Mills, S. Mulpuru, T. Walker, V. Percival, V. Dolean, A. Sarkar, *Comprehensive compartmental model and calibration algorithm for the study of clinical implications of the population-level spread of covid-19: a study protocol* BMJ Open 12 (3) (2022).

Domain Decomposition-based Scalable Solvers for Time Dependent and Nonlinear Stochastic Systems

Sudhi Sharma[1], Pierre Jolivet[2], Victorita Dolean[3], Abhijit Sarkar[1]

[1] *Civil and Environmental Engineering, Carleton University,*
[2] *Sorbonne UniversitÃ©, CNRS, LIP6, Paris 75252, France,*
[3] *Department of Mathematics and Statistics, University of Strathclyde,*

Computational models for natural and engineering systems inherently possess uncertainties in the form of model parameters, assumptions in the mathematical models and the noise in calibration data. Sampling-based approaches to handle these uncertainties become overwhelmingly expensive for large scale models with high resolution discretizations in space/time. Uncertainties in model parameters for time dependent and nonlinear partial differential equation (PDE) models are handled using a sampling-free approach with domain decomposition (DD)-based solvers. The sampling-free stochastic Galerkin method transforms the PDE with random model parameters into a large system of coupled linear or nonlinear PDEs. The increase in number of random parameters in the model increases the computational requirements necessitating a scalable solver.

An acoustic wave propagation model with a random field representation of wave speed is handled using a non-overlapping DD method. The symmetric and positive-definite coefficient matrix of the system is solved using a conjugate-gradient based iterative method and associated Neumann-Neumann vertex-based preconditioner for acoustic wave propagation problem in two dimensions. However, the complex spatial coupling and the coupling among the stochastic expansion coefficients can affect the scalabilities of the solver in three dimensions. Hence, a wirebasket-based preconditioner is utilized to enrich the coarse grid allowing better global error propagation and improved scalability for an elastic wave propagation model in three dimensions. For nonlinear stochastic PDEs, the coefficient matrix of the associated linearized algebraic system is non-symmetric which requires the use of generalized minimum residual (GMRES) method based iterative solvers. A multilevel Schwarz preconditioner combining DD and algebraic multigrid method is proposed for efficient error reduction for large scale models [1]. Finally, the solvers are also tested on a nonlinear time dependent model of geo-spatial spread of COVID-19 with random diffusion coefficients.

References

[1] S. Sharma, V. Dolean, P. Jolivet, B. Robinson, J. D. Edwards, T. Kendzerska, A. Sarkar, *Scalable computational algorithms for geo-spatial covid-19 spread in high performance computing*, arXiv preprint arXiv:2208.01839 (2022).

Investigations on the Impact of Loss Function Normalization Methods in Physics Informed Neural Networks for Infectious Disease Modeling

M. Pantano[1], B. Robinson[1], J.D. Edwards[2], T. Kendzerska[3], A. Sarkar[1]

[1] *Carleton University, Ottawa, ON, Canada, {michael.pantano,brandon.robinson,abhijit.sarkar}@carleton.ca*
[2] *University of Ottawa and University of Ottawa Heart Institute, Ottawa, Ontario, Canada, jedwards@ottawaheart.ca*
[3] *University of Ottawa and The Ottawa Hospital Research Institute, Ottawa, Ontario, Canada, tkendzerska@toh.ca*

We present investigations and findings of several loss function normalization methods for a physics informed neural network (PINN) tailored for infectious disease modeling. The loss in PINNs typically consist of a standard network loss based on the misfit between model outputs and observations, in addition to a contribution from the residuals of governing differential equations underpinning the system mechanics. In the context of compartmental models, Shaier et al. have proposed a variant of the PINN model they named Disease Informed Neural Network (DINN) [1]. Consider the SIRD model, a system of four coupled ordinary differential equations:

$$\frac{dS}{dt} = -(\beta/N)SI, \tag{1}$$

$$\frac{dI}{dt} = (\beta/N)SI - \gamma I - \mu I, \tag{2}$$

$$\frac{dR}{dt} = \gamma I, \tag{3}$$

$$\frac{dD}{dt} = \mu I, \tag{4}$$

where S, I, R, and D are models states which categorize the population as either *susceptible*, *infectious*, *recovered*, or *dead*. The parameter β reflects the transmission rate. The parameter γ is the recovery rate. The parameter μ is the death rate of infected individuals. The neural network outputs the model states at discrete instances of time. The DINN framework also permits the estimation of unknown model parameters. The disease dynamics are enforced through the DINN by ensuring that the model outputs minimize the residual of Eqs. (1-4).

For numerical experiments, we consider synthetic data generated using static values of parameters β, γ, and μ. The use of synthetic data wherein the true parameter values are known, allows us to test the robustness of the network and different loss function approaches. We assess how the performance of the DINN compares with standard parameter estimation methods when data are sparse, noisy, and incomplete. The investigations include normalizing the loss functions passively via normalizing the data and residuals prior to training [1], normalizing via weighted loss [2], and Pareto scaling optimization. An important reason for investigating different loss functions for the DINN is the proposed dual goal of a DINN for disease spread prediction, and compartmental model parameter estimation. Understanding the role that network and residual loss has on the capacity to accomplish the two goals may be conducted through tests on the two core components of the loss function and its normalization.

References

[1] S. Shaier, M. Raissi, and P. Seshaiyer. *Data-Driven Approaches for Predicting Spread of Infectious Diseases Through DINNs: Disease Informed Neural Networks*. Letters in Biomathematics 9 (1), 71-105. (2022).

[2] S. Han, L. Stelz, H. Stoeker, L. Wang, K. Zhou. *Approaching epidemiological dynamics of COVID-19 with physics-informed neural networks*. (2023)

Heterogeneous Blood Perfusion Redistribution for Magnetic Nanoparticle Assisted Thermal Ablation: A Coupled Complex System Under Imaging Guidance

M. Singh[1]

[1] *Department of Mechanical Engineering, University of Maryland Baltimore County, Baltimore, Maryland, USA, msingh6@umbc.edu*

Heterogeneity of tumour is a typical trademark of tumour vascular development. Inaccurate temperature predictions may lead to inadequate heating or cooling of target regions, potentially reducing treatment effectiveness or causing unintended damage to surrounding healthy tissues. This study incorporates heterogeneous blood perfusion at each tumour voxel location, thereby relaxing the assumption of uniform blood perfusion. Dynamic variations in blood perfusion at each spatial location is studied for vascular-stasis [1] and thermal-damage [2] based perfusion algorithms for a magnetic nanoparticle assisted thermal ablation (refer fig. 1). After introspection of spatial-temporal perfusion maps, the thermal damage propagation is different. In our coupled model, magnetic nanoparticles migrate from the regions of higher concentration to the regions of lower concentration due to enhancement in interstitial space from 20% to 80%. No computational studies have been published so far to assimilate these aspects for three-dimensional heterogeneous perfusion in a quantitative manner. Incorporating three-dimensional perfusion to measure the heat transfer characteristics of the biological tissues is exemplary. We infer that quantitative perfusion metrics informed computational models may play an important role in optimizing the treatment efficacy of thermal therapies.

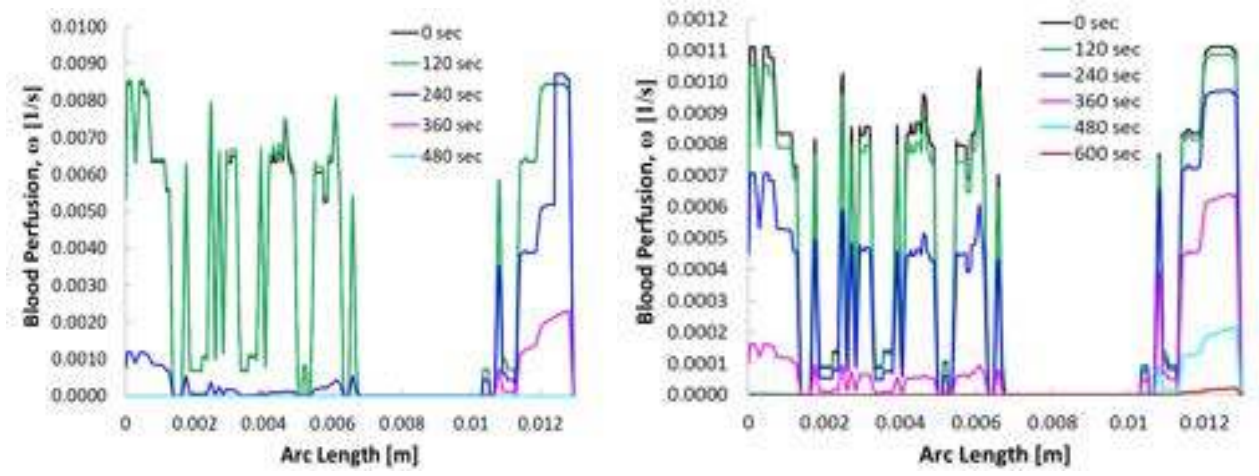

Figure 1: Blood perfusion redistribution as a function of tumor spatial location for two perfusion algorithms (Anisotropic blood perfusion as a function of (a) vascular stasis and as a function of (b) thermal damage).

References

[1] M. Singh, *Incorporating Vascular-stasis Based Blood Perfusion to evaluate the Thermal Signatures of cell-death using Modified Arrhenius Equation with Regeneration of Living Tissues during Nanoparticle-assisted Thermal Therapy*, Int. Comm. Heat and Mass Transf. **135**, pp. 106046 (2022).

[2] M. Singh, *Biological Heat and Mass Transport Mechanisms Behind Nanoparticles Migration Revealed under MicroCT Image Guidance, Int. J. Therm. Sci.* **184**, pp. 107996 (2023).

Benchmarking computational PD models: A comparative study

S. Swapnasrita[1,2], J. C. de Vries[2], C. Öberg[3], K. G. F. Gerritsen[2], A. Carlier[1]

[1] *MERLN Institute for Regenerative Medicine, Maastricht University , the Netherlands*
[2] *Department of Nephrology and Hypertension, University Medical Center Utrecht, the Netherlands*
[3] *Department of Clinical Sciences Lund, Division of Nephrology, SkÃ¥ne University Hospital, Lund University, Lund, Sweden*

In silico models of peritoneal dialysis (PD) are useful tools to study and improve treatment outcomes and make the treatment more patient-specific. They can help in deciphering the underlying mechanisms according to the transport status of a patient. Several mathematical models of have been developed in the past decades, but what is lacking is a direct comparison of the models to estimate their accuracy with respect to predicting (pre-)clinical data. Benchmarking is also important to identify which PD models can be easily made patient specific.

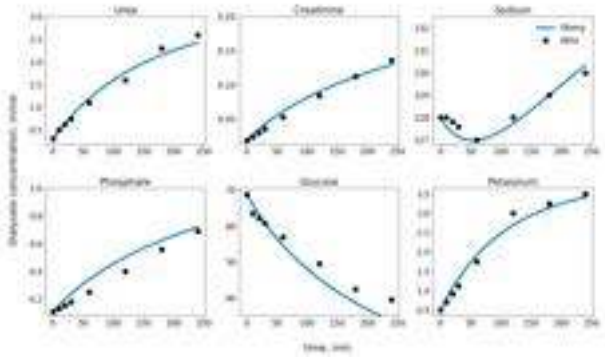

Figure 1: The predicted dialysate concentration of different solutes by Öberg model.

Two mechanistic models (Graff [1], Öberg [2]) and two analytical models used in clinical practice and research (Garred [3], Waniewski [4]) were chosen. The four models, in combination, encompass various mechanisms that are essential to PD (diffusion, convection, lymphatics). The dataset consisted of data from multiple static dwells (n = 16) in uremic pigs. Each model was trained by fitting the dialysate solute concentrations (in a subset of the dwells) to predict the mass transfer area coefficient (MTAC) of each solute. With fitted MTAC, we predicted the dialysate solute concentrations in the remaining dwells. The model by Öberg appears to be the optimal model in terms of low error in solute concentration predictions, applicability of the model to multiple datasets (with different initial dialysate concentration), physiological MTAC values and reasonable ultrafiltration values in pigs. Applying the model to the data obtained in the uremic pig experiments showed a good predictive accuracy of the Öberg model (Fig. 1). Notably, the Öberg model accurately predicted the effects of sodium sieving, whereas other models did not. This model is also modular and has been applied to automated PD and continuous flow PD.
In summary, the modified Öberg model provided an accurate prediction of solute concentrations throughout a static dwell in uremic pigs. In the future, we aim to extend this model to human data.

References

[1] J. Graff et al., ASAIO J. **40**, 4, pp.1005-1011 (1994).
[2] C. Öberg and G. Martuseviciene, Perit. Dial. Int, **39**, 3, pp. 236-242 (2019).
[3] LJ. Garred et al., ASAIO J. **6**, 3, pp. 131-137 (1983).
[4] J. Waniewski, J. Mem. Sci. **274**, 1-2, pp. 24-37 (2006).

The VI International AMMCS
Interdisciplinary Conference
Waterloo, Ontario, Canada

Open Source Workflows for Mass Spectrometry Analysis

D. Patel[1], R. Dargan[1], S. Forbes[1,2] and W.S. Burr[3]

[1] *Department of Chemistry, Biochemistry and Physics, UQTR, Canada*
darshil.patel, rushali.dargan@uqtr.ca
[2] *Department of Chemistry and Biochemistry, University of Windsor, Canada*
shari.forbes@windsor.ca
[3] *Department of Mathematics, Trent University, Canada, wesleyburr@trentu.ca*

It is very common for workflows connected to mass spectrometry to be entirely contained to closed-source software provided by instrumentation manufacturers, e.g., LECO instruments are designed to work with the *ChromaTOF* [1] mass spectrometry data system, and the *StatCompare* suite of statistical tools. These tools have many advantages: they are professionally designed, with modern graphical interfaces; they are tested and known to process the data types produced by the instrument; and they are standard. They also have disadvantages: the algorithms are not publicly exposed; the process is limited to the implementation; and occasionally new instruments are released which are not supported by the current version of the software suites.

In this talk we will discuss the development of two open source tools: the `subMaldi` package [4] for single dimension mass spectrometry data; and `gcgcWork` [2, 3] for the reproduction of a somewhat standard GCxGC workflow and pipeline, similar to key components provided by *ChromaTOF*. Both are created for the R programming environment, and available on GitHub. We will discuss the issues with implementation, especially with respect to data size and format, and lay out the challenges ahead for producing higher quality, user-friendly software for common chemical analyses. In both cases, the packages were developed to aid in the analysis of forensic science data sets: `subMaldi` for dried bloodstain chemical analysis; and `gcgcWork` for VOC analysis from human body decomposition.

References

[1] LECO, (2023) *An Introduction to LECO's Comprehensive Two-Dimensional Gas Chromatography (GCxGC) with ChromaTOF Software*. Available from: `https://bit.ly/chromaTOF`

[2] R. Dargan, (2022) *Comparing the Decomposition Odour Between Cadavers and Human Remains being used as Cadaver Detection Dog Training Aids* (PhD thesis, UQTR, Quebec, Canada).

[3] D. Patel, (2023) *Identifying the transition from ante-mortem odour to post-mortem odour* (PhD thesis, UQTR, Quebec, Canada).

[4] Yeh, K., Castel, S., Stock, N. L., Stotesbury, T., & Burr, W. (2021). subMALDI: an open framework R package for processing irregularly-spaced mass spectrometry data. Journal of Open Source Software, 6(65), 2694.

The VI International AMMCS
Interdisciplinary Conference
Waterloo, Ontario, Canada

Modelling Terror Attack Data Cluster Phenomena with Self-Exciting Point Process and Forecasting Future Terror Events with Statistical Learning Methods

Siyi Wang[1]. Xu Wang[2], Chenlong Li[3]

[1] *McMaster University, Hamilton, Ontario, Canada*
[2] *Wilfrid Laurier University, Waterloo, Ontario, Canada, xwang@wlu.ca*
[3] *Taiyuan University of Technology, China*

Rampant terrorism poses a serious threat to the national security of many countries worldwide, particularly due to separatism and extreme nationalism. This paper focuses on the development and application of a temporal self-exciting point process model to the terror data of three countries: the US, Turkey, and the Philippines. To account for occurrences with the same time-stamp, the paper introduces the order mark and reward term in parameter selection. The reward term considers the triggering effect between events in the same time-stamp but different order. Additionally, the paper provides comparisons between the self-exciting models generated by day-based and month-based arrival times. Another highlight of the paper is the development of a model to predict the number of terror events using a combination of simulation and machine learning, specifically the random forest method, to achieve better predictions. *This research offers an insightful approach to discover terror event patterns, and forecast future occurrence of terror events, which may have practical application towards national security strategies.*

Financial News Headlines Sentiment Analysis Enhances Stock Market Prediction

W. Fan[1] , R. Makarov[2], X. Wang[3]

[1] *Wilfrid Laurier University, Waterloo, Canada, fanx5821@mylaurier.ca*
[2] *Wilfrid Laurier University, Waterloo, Canada, rmakarov@wlu.ca*
[3] *Wilfrid Laurier University, Waterloo, Canada, xwang@wlu.ca*

Financial news headlines are informative in predicting the stock market movement and providing valuable insights to investors. The information, such as the sentiment of news headlines and specific keywords, can often be extracted for data analysis and model fitting.Our study aims to analyze the impact of financial news headlines related to Apple (AAPL) from January 1st, 2012, to May 31st, 2019, on Apple's stock return and develop a profitable trading strategy. Our analysis consists of data preparation, machine learning model training and evaluation. Our data preparation method involves preprocessing techniques to clean, tokenize, and extract features from the headlines. In detail, we perform sentiment analysis on the headlines using FinBERT[1], a state-of-the-art financial-oriented BERT model, which provides three categories of sentiment scores, positive, negative and neutral. The three scores are used as sentiment features.

To explore the relationship between headlines and stock prices, we build a range of multi-class classification models, including Logistic Regression, Decision Tree, Random Forest, and Neural Networks. We also apply cross-validation to evaluate the models. These models allow for a comprehensive analysis of how features of headlines influence stock price movements. Moreover, We utilize dedicated performance metrics[2], which provide an overall assessment of the models in a trading environment. Furthermore, the study constructs trading strategies, which utilize vanilla call and put options, based on the predictions made by the models. We believe that our study has the potential in understanding the relationship between financial news headlines and the stock market. By gaining insights into this relationship, investors can effectively optimize their trading strategies and make informed decisions.

References

[1] D. Araci, *Finbert: Financial sentiment analysis with pre-trained language models,* CoRR, vol. abs/1908.10063. (2019).

[2] J. He, *Application of Sentiment Analysis in Stock Market Predictio,*. Wilfrid Laurier University. Theses and Dissertations (Comprehensive). 2544. (2023).

Portfolio Management and Option Pricing under a Multi-Asset Jump-Diffusion Model with Systemic Risk

R.N. Makarov[1]

[1] *Wilfrid Laurier University, Waterloo, Canada, rmakarov@wlu.ca*

We study a multi-asset jump-diffusion pricing model, combining a systemic-risk asset with several conditionally-independent ordinary assets. Our approach allows for analyzing and modelling a portfolio that integrates high-activity security, such as an Exchange Trading Fund (ETF) tracking a major market index (e.g., S&P500), and several low-activity securities not frequently traded on financial markets. The number of securities can be increased without losing the tractability of the model. We propose a Laplace-transform-based approach to computing Value-at-Risk (VaR) and Expected Shortfall (ES) of portfolio returns. Additionally, European-style basket options written on the extreme and average stock prices or returns can be evaluated semi-analytically. One of the main features of the proposed model is the possibility of estimating parameters for each asset price process individually. We present the conditional maximum likelihood method for fitting asset price processes to empirical data. Alternatively, the least-square method calibrates the model to option values. The number of parameters grows linearly in the number of assets compared to the quadratic growth through the correlation matrix, which is typical for many other multi-asset models. We discuss the properties of the proposed model, the estimation of its parameters using conditional and standard MLE methods, a least-squares technique, the valuation of VaR and ES metrics, and pricing European-style basket options. We develop semi-analytic pricing formulae for VaR, ES, and call and put options on a geometric or arithmetic average value and a maximum or minimum price. Computational results are compared with Monte Carlo estimates.

References

[1] Y. Chen and R.N. Makarov, *Modelling asynchronous assets with jump-diffusion processes*, in *Recent Advances in Mathematical and Statistical Methods* (AMMCS-2017), Springer Proceedings in Mathematics & Statistics. Springer, (2017).

[2] R. Xu and R.N. Makarov, *High-frequency statistical modelling for jump-diffusion multi-asset price processes with a systemic component*, in *Recent Developments in Mathematical, Statistical and Computational Sciences* (AMMCS-2019), Springer Proceedings in Mathematics & Statistics, pp. 747-757. Springer (2021).

Using the High Dimensional Consensus Mass Spectral similarity algorithm for improved identification of isomers

Deborah F. McGlynn[1], Jason Eveleth[1], Nirina Rabe Andriamaharavo[2], Anthony J. Kearsley[1]

[1] *1Applied and Computational Mathematics Division, National Institute of Standards and Technology, Gaithersburg, Maryland 20899, United States*

[2] *2Mass Spectrometry Data Center, National Institute of Standards and Technology, Gaithersburg, Maryland 20899, United States*

The most widely utilized methods to positively identify the mass spectra of an analyte often struggle when faced with isomers or similarly structured compounds. Additionally, for identification of compounds with many isomers, both the mass spectrum and retention index are often needed. Ultimately, final compound identification is at the discretion of the researcher. Given the potential for incorrect characterization, development of improved methods for identification of unknown analytes with similar spectra is an active research area. Recently, a new method called high-dimensional consensus (HDC) mass spectral (HDCMS) for similarity scoring was developed and applied to fentanyl analogs. In lieu of more traditional similarity measures it builds a measure of dissimilarity based on a constructed probability distribution associated with collections of replicate spectra. The method is a promising approach for differentiating spectra of isomers. In this poster we present results for applying HDC to distinguish several monoterpenes that are not differentiable by current methods, even with the use of retention index. To measure the efficacy of the HDC algorithm, we apply the technique to 15 replicates of 9 monoterpenes (C10H16) with retention indices that differ by less than 30 and spectral similarity match factors that are greater than 900. Match factors were determined by calculating the cosine similarity between 20 monoterpene library spectra from the NIST20 library. The replicate spectra used in the HDC algorithm were taken by Gas Chromatography-Mass Spectrometry (GC-MS) using the same instrument parameters. With replicate terpene measurements we calculate the mean, variance, and standard deviation of the mass-to-charge ratio (m/z) and intensity of each collection of replicates in order to build a probability density approximation. The findings from this compound identification numerical experiment are compared to results produced by existing and widely used match methods such as cosine similarity or modified cosine similarity.

The VI International AMMCS
Interdisciplinary Conference
Waterloo, Ontario, Canada

Model invariants and functional regularization

H. Stein[1,2]

[1] *Two Sigma, New York, NY, USA Harvey.Stein@twosigma.com*
[2] *Columbia University, New York, NY, USA hjstein@columbia.edu*

When modeling data, we would like to know that our models are extracting facts about the data itself, and not about something arbitrary, like the order of the factors used in the modeling. Formally speaking, this means we want the model to be invariant with respect to certain transformations.

Here we look at different models and the nature of their invariants. We find that regression, MLE and Bayesian estimation all are invariant with respect to linear transformations, whereas regularized regressions have a far more limited set of invariants. As a result, regularized regressions produce results that are less about the data itself and more about how it is parameterized.

To correct this, we propose an alternative expression of regularization which we call functional regularization. Ridge regression and lasso are special cases of functional regularization, as is Bayesian estimation. But functional regularization preserves model invariance, whereas ridge and lasso do not. It is also more flexible, easier to understand, and can even be applied to non-parametric models.

Last Passage Time in Option Pricing: Spectral Expansions for Solvable Diffusions

G. Campolieti[1], Y. Sui[2]

[1] *Wilfrid Laurier University, Waterloo, Canada, gcampolieti@wlu.ca*

[2] *Wilfrid Laurier University, Waterloo, Canada, suix3850@mylaurier.ca*

This paper contributes to the understanding and practical utilization of last passage time in derivative markets and Excursion Theory. In the context of derivative markets, the practical relevance of last passage time is demonstrated through the design of path-dependent step options that directly rely on its dynamics. Furthermore, we extend our analysis to include barrier options with killing. Closed-form spectral expansion pricing formulas for these last passage step options and barrier options are derived under various one-dimensional time-homogeneous diffusion models. These include Geometric Brownian Motion (GBM), the Constant Elasticity of Variance (CEV) model, and other solvable nonlinear state-dependent volatility models. The accuracy and effectiveness of our theoretical results are validated through numerical computations, providing further support for their practical applicability.

Furthermore, the paper explores the application of last passage time in excursion theory for solvable diffusions. It investigates the density of $D_l(T)$, which represents the probability density of the excursion process straddling time t, as well as the joint density with last passage time. Additionally, the density under the scenario of killing is derived. The efficient and accurate numerical calculations of our spectral expansion formulas outperform Monte Carlo simulations.

References

[1] G. Campolieti, *Solvable Diffusions in Financial Mathematics*, Working book (2023).

[2] G. Campolieti and Y. , *Closed-form Formulae for marginal and joint distributions involving last passage times for Families of Solvable Diffusions*,Working paper (2023).

Energy losses and transition radiation in particle/anisotropic 2D-material interaction

K. Akbari[1], Z. Miskovic[2]

[1] *Department of Applied Mathematics, University of Waterloo, and Department of Physics, Queen's University, Canada*
kakbari@uwaterloo.ca
[2] *Department of Applied Mathematics and Waterloo Institute for Nanotechnology, University of Waterloo, Canada*
zmiskovic@uwaterloo.ca

Interactions of graphene and other two-dimensional (2D) materials with externally moving charged particles have been studied in recent years in the context of Electron Energy Loss Spectroscopy in Scanning Transmission Electron Microscope, which has become a very popular experimental technique for exploring the excitation of plasmons in graphene over a broad range of frequencies. On the other hand, the technological need for a stable and tunable source of terahertz (THz) radiation has prompted several recent studies of the electromagnetic radiation from graphene, induced by its interaction with fast electron beams.

We have recently developed a fully relativistic theory of energy losses for a fast charged particle traversing single-layer graphene [1, 3, 7] and multi-layer graphene (MLG) [2, 4, 5] . It was shown that the total energy loss of the external particle consists of two components: the energy absorbed by graphene layers in the form of electronic excitations (Ohmic losses), which include the excitation of Dirac plasmon polaritons (DPP), and the energy that is emitted in the far field as transition radiation (TR). We have also studied the effects of varying the charged particle energy and angle of incidence [1, 3, 7], as well as the effects of hybridization between the DPPs in different graphene layers within MLG structures [3]-[5], in both the Ohmic energy loss distributions and in the angular spectra of TR.

In recent work, we have applied our methodology to phosphorene, a single layer of black phosphorus, which exhibits strongly anisotropic optical properties. Describing this anisotropy by a 2D conductivity tensor, we have explored the possibility of directional excitation of the hyperbolic plasmon polaritons in phosphorene, which may arise in the infrared frequency range, by using incident charged particles under oblique angles of incidence upon phosphorene [6].

References

[1] Z. Miskovic *et al.*, Phys. Rev. B **94**, 125414 (2016).
[2] K. Akbari *et al.*, ACS Photonics **4**, 1980 (2017).
[3] K. Akbari *et al.*, Phys. Rev. B **98**, 195410 (2018).
[4] K. Akbari *et al.*, Surf. Sci. **446**, 191 (2018).
[5] K. Akbari *et al.*, Nanotechnology **29**, 225201 (2018).
[6] K. Akbari *et al.*, Nanoscale **14**, 5079-5093 (2022).
[7] K. Akbari *et al.*, Phys. Rev. B **105**, 045408 (2022).

Behaviour quantification vis-a-vis adoption of public policy - lessons from nonpharmaceutical measures during COVID-19 in Ontario

Sarah Smook[1], Lia Humphrey[2], David Lyver[3], Rhiannon Loster[4], Z. Mohammadi[5], M. G. Cojocaru[6]

[1] *University of Guelph, Canada, ssmook@uoguelph.ca*
[2] *University of Guelph, Canada, humphrel@uoguelph.ca*
[3] *University of Guelph, Canada, dlyver@uoguelph.ca*
[4] *University of Guelph, Canada, rloster@uoguelph.ca*
[5] *University of Guelph, Canada, zmohammadi@uoguelph.ca*
[6] *University of Guelph, Canada, mcojocar@uoguelph.ca*

In this work, we provide a granular view of factors affecting COVID-19 disease transmission across the province of Ontario, Canada in 2020. Using a generalized multi-linear regression process, we determine the perceived risk of infection and personal discomfort of complying with non-pharmaceutical interventions (NPIs) to Ontarians across 34 public health units. With the use of game theory, we model a decision making, time-dependent, process by which we estimate how average individuals in each PH region decide to minimize their risk of infection, as well as their discomfort to adhering to measures. This model gives an estimate on NPI (mask use, mobility reductions, etc.) adoption rate across Ontario from March to December 2020. Using an SEIRL compartmental model for ON, we highlight how decisions fed into the transmission process, and viceversa. Finally, we explore the model versatility (i.e., application to other parts of the world, not just ON) as well as its applicability to scenario testing (i.e., to differing potential emerging infections).

Non-pharmaceutical interventions; game theory and decision making models; Nash equilibrium; behavioural epidemiology; infectious disease.

References

[1] Cojocaru, M. G., Bauch, C. T., and Johnston, M. D. Dynamics of vaccination strategies via projected dynamical systems. Bulletin of Mathematical Biology 69, 5 (2007), 1453 – 1476.

[2] Division, P. A. Compliance with Mask. Tech. rep., 2020.

[3] d'Onofrio, A., Manfredi, P., and Poletti, P. The impact of vaccine side effects on the natural history of immunization programmes: an imitation-game approach. Journal of theoretical biology 273, 1 (2011), 63-71.

[4] Ferguson, N. Capturing human behaviour. Nature 446, 7137 (2007).

[5] Ferrante, G., Baldissera, S., Moghadam, P. F., Carrozzi, G., Trinito, M. O., and Salmaso, S. Surveillance of perceptions, knowledge, attitudes and behaviors of the Italian adult population (18 - 69 years) during the 2009â2010 a/h1n1 influenza pandemic. European journal of epidemiology 26, 3 (2011), 211 -219

Investigating the Impact of Novel Transmission-Blocking Anti-malarial Drugs: A Mathematical Modeling Approach

, W. A. Woldegerima[1], 2, J. Banasiak[2], R. Ouifki[3]

[1] *York University, Toronto, Canada, wassefaw@yorku.ca*
[2] *University of Pretoria, Pretoria, South Africa, jacek.banasiak@up.ac.za*
[3] *University of Pretoria, Pretoria, South Africa, ouifkir@gmail.com*

For almost a century, several prevention and treatment strategies has been employed at both the population and cellular levels, in an effort to control/eliminate malaria. Nonetheless, malaria remains a major global health problem. Emergence of resistance to antimalarial drugs and insecticides; some mosquitoes bite outdoors; most antimalarial drugs are not active against sexual stage are some of teh common challeges, [2]. Moreover, most available drugs kill malaria as it gets established in the liver or after it has infected red blood cells, but cannot tackle it once the parasite is released from the cells as gametocytes, which is when it is transmissible to other people via mosquito bites.

Recently, promising clinical advances have been made in developing novel antimalarial drugs that block parasite transmission, cure the disease, and have prophylactic effects, called transmission-blocking drugs (TBDs) [3, 4, 5]. Our main aim is to explore the potential effects of such TBDs on malaria transmission in the effort to control and eliminate the disease using mathematical models to ascertain how the presence of TBDs can mitigate the transmission of malaria parasites on both asymptomatic and symptomatic carriers in a defined hotspot of malaria. Our special focus was on the effects of the treatment coverage and the efficacy of TBDs along with the protective effect and waning effect of TBDs. For this, we propose and analyze a mathematical model for malaria transmission dynamics that extends the SEIRS-SEI type model to include a class of humans undergoing treatment with TBDs and a class of those protected because of successful treatment. The mathematical and epidemiological implications of TBDs are assessed using different approaches.

Furthermore, we fit the model to malaria data using the library "lmfit? in Python and use the validated model to explore the model's predictions under various scenarios. Results from our analysis show that the effect of treatment coverage rate on reducing reproduction number depends on other key parameters such as the efficacy of the drug. The projections of the validated model show the benefits of using TBDs in malaria control in preventing new cases and reducing mortality. In particular, we find that treating 35% of the population of Sub-Saharan Africa with a 95% efficacious TBD from 2021 will result in approximately 82% reduction on the number of malaria deaths by 2035.

References

[1] W. A. Woldegerima, R. Ouifki, and J. Banasiak. *Mathematical analysis of the impact of transmission-blocking drugs on the population dynamics of malaria*, Applied Mathematics and Computation, **126005**, 400 (2021).

[2] W.H.O, *World Malaria Report 2021*, World Helath Organization `https://www.who.int/teams/global-malaria-programme/reports/world-malaria-report-2021`.

[3] K. A. Andrews, D. Wesche, J. McCarthy, J. J. Mo ?hrle, J. Tarning, ⋯, and T. Grasela, *Model-informed drug development for malaria therapeutics*. Annual review of pharmacology and toxicology, **58**, pp. 567?582 (2018).

[4] L. -M. Birkholtz, T. L. Coetzer, D. Mancama, D. Leroy, and P. Alano, *Discovering new transmission-blocking antimalarial compounds: challenges and opportunities*, Trends in parasitology, **32(9)**, pp.669?681 (2016).

[5] J. Reader, M. E van der Watt, ⋯, and L. -M. Birkholtz, *Targeted antimalarials discovered from the open-source MMV Pandemic Response Box*, Nature communications, **12(1)**, pp. 1-15 (2021).

The VI International AMMCS
Interdisciplinary Conference
Waterloo, Ontario, Canada

Machine Learning Models to Classify and Predict Subclinical Atherosclerosesis

D. A. Adigun [1], W. A. Woldegerima [2], A. U.I. Sirisena[3]

[1] *African Institute for Mathematical Sciences (AIMS), Limbe, Cameroon deborah.adigun@aims-cameroon.org*
[2] *Department of Mathematics and Statistics, York University, Toronto, Canada, wassefaw@yorku.ca*
[3] *Jos University Teaching Hospital, Nigeria, shallom2k3@yahoo.com*

Atherosclerosis is one of the primary causes of cardiovascular disease (CVD). Its early stage is subclinical atherosclerosis (SCA) which is determined by the measurement of the carotid intima-imedia thickness (CIMT). In this study, we used CIMT measurements with a threshold of 0.078 cm to divide the patient data into two classes. The data contained 6 variables and 221 observations. We used supervised machine learning (ML) techniques to perform a classification task with alternative ML algorithms that included Logistic Regression (LR), Support Vector Machine (SVM), Decision Tree (DT), and Random Forest (RF) . While working on our project, we noticed a disparity in the sizes of our class. For this reason, we oversampled, that is, balancing the class and gave both results of the imbalanced data and balanced data. The performance of each ML algorithm applied was also evaluated using different performance metrics. Finally, we discovered that the SVM algorithm is the optimal classifier for SCA. This prediction algorithm can help Clinicians quickly identify patients in the early stage of atherosclerosis and administer timely treatment and in turn aid in reducing the increase in cardiovascular disorders.

The VI International AMMCS
Interdisciplinary Conference
Waterloo, Ontario, Canada
DATE

Modeling the cytotoxicity of Romidepsin reveals the ineffectiveness of this drug in the "shock and kill" strategy

Qi Deng[1], Ting Guo[2], Zhipeng Qiu[3], Yuming Chen[4]

[1] *Nanjing University of Science and Technology, China,*
& Wilfrid Laurier University, Canada, dddengqiaaa@163.com
[2] *Changzhou University, China, gtnjust@163.com*
[3] *Nanjing University of Science and Technology, China, smoller_1@163.com*
[4] *Wilfrid Laurier University, Canada, ychen@wlu.ca*

The "shock and kill" strategy is being widely explored to purge Human Immunodeficiency Virus (HIV) latent reservoirs. Romidepsin, a kind of latency-reversing agents (LRAs), has been shown to induce HIV RNA transcription. However, several clinical trials testing this drug have resulted in limited effect in reducing the HIV latent reservoirs. To understand the mechanisms underlying such limited effect, we develop a multi-scale model that incorporates pharmacokinetics and considers the toxicity of romidepsin to T cells in this paper. By fitting the model to the viral load data from plasma of six patients received romidepsin, we find that the model with T cell toxicity of romidepsin can well explain the clinical data. The dynamics of latently infected cells during romidepsin administration are explored using the best-fit parameter values. The results show that latently infected cells decrease very slowly and remain very stable overall in 4 of the 6 participants under the assumption of T cell toxicity of romidepsin. This implies that the ineffectiveness of romidepsin on latent reservoirs can be explained by its toxicity to T cells. In the remaining 2 participants, however, latently infected cells are quite stable without T cell toxicity of LRAs. It is found that the estimated activation rate of latently infected cells by romidepsin and the estimated elimination rate of romidepsin on immune cells for these two patients are very different from those for the other four patients. Thus we speculate that the heterogeneous response to romidepsin across participants may also be a determining factor of the effectiveness of romidepsin. These results may have significant implications in the search for the control of the infection.

The VI International AMMCS
Interdisciplinary Conference
Waterloo, Ontario, Canada

A mathematical model between keystone species: bears, salmon, and vegetation

Christopher Middlebrook and Xiaoying Wang

Trent University, Peterborough, Canada

A keystone species is one on which other species in the ecosystem largely depend and consequently if removed there are drastic effects on the ecosystem. Bears, salmon, and vegetation are unique in an ecosystem because all three are keystone species dependent on one another. We propose a stoichiometric model to study the aforementioned ecosystem where bears consume salmon and vegetation. The results show that the bear population may coexist with salmon and vegetation populations at a steady state or oscillate periodically. Moreover, a small vegetation growth rate drives the vegetation population to extinction whereas salmon coexist with bears but the populations oscillate periodically. On the other hand, the salmon population goes to extinction but the vegetation coexists with bears at a steady state when the vegetation growth rate is large.

Deciphering the stochastic spatiotemporal dynamics of calcium transients using the flux-balance model

A. Quint[1], S. Komarova[2], A. Khadra[3]

[1] *McGill University, Montreal, Canada,* anthony.quint@mail.mcgill.ca
[2] *McGill University, Montreal, Canada,* svetlana.komarova@mcgill.ca
[3] *McGill University, Montreal, Canada,* anmar.khadra@mcgill.ca

Calcium plays fundamental role in dictating subcellular signaling and cell fate in biological systems. It does so through the formation of calcium signals that are regulated by channels and pumps expressed on the membrane of the cell and on the membrane of storage compartments within the cell such as the endoplasmic reticulum (ER). Depending on the cell type, these signals exhibit distinct and very interesting stochastic spatiotemporal dynamics ranging in behaviour from being oscillatory with very complex profiles [1], to being purely transient embedding key features [2, 3]. One can use the calcium flux-balance model [4] to explain how these signals are generated, and apply slow-fast analysis [5] to decipher their underlying dynamics. In this talk, I will outline our recent work using this approach to explain the calcium profiles seen in two cell types: oligodendrocytes and osteoblasts.

References

[1] O. Lawrence, N. Desjardins, X. Jiang, K. Sareen, J.Q. Zheng and A. Khadra, *Characterizing Spontaneous Ca^{2+} Local Transients in OPCs Using Computational Modeling*, Biophys. J. **121**, 23, pp. 4419-4432 (2022).
[2] N. Mikolajewicz, D. Smith, S.V. Komarova and A. Khadra, *High-Affinity P2Y2 and Low-Affinity P2X7 Receptor Interaction Modulates ATP-Mediated Calcium Signalling in Murine Osteoblasts*, PLoS Comp. Biol. **17**, e1008872 (2021).
[3] L. Mackay, N. Mikolajewicz, S.V. Komarova and A. Khadra, *Systematic Characterization of Dynamic Parameters of Intracellular Calcium Signals*, Front. Physiol. **7**, pp. 525 (2016).
[4] A. Sherman, Y.X. Li, and J.E. Keizer, *Whole—Cell Models*, *Computational Cell Biology*, New York: Springer, pp. 101-139 (2002).
[5] B. Ermentrout and D.H. Terman, *Mathematical foundations of neuroscience*, New York: Springer, pp. 331-367 (2010).

The VI International AMMCS
Interdisciplinary Conference
Waterloo, Ontario, Canada

Reconfiguration of vertex colouring and forbidden induced subgraphs

M. Belavadi[1], K. Cameron[2], O. Merkel[3]

[1] *Wilfrid Laurier University, Waterloo, Canada mbelavadi@wlu.ca*
[2] *Wilfrid Laurier University, Waterloo, Canada, kcameron@wlu.ca*
[3] *Wilfrid Laurier University, Waterloo, Canada, owenmerkel@gmail.com*

Let G be a finite simple graph with vertex-set $V(G)$ and edge-set $E(G)$. For a positive integer k, a *k-colouring* of G is a mapping $\alpha: V(G) \to \{1,2,\ldots,k\}$ such that $\alpha(u) \neq \alpha(v)$ whenever $uv \in E(G)$. We say that G is *k-colourable* if it admits a k-colouring and the *chromatic number* of G, denoted $\chi(G)$, is the smallest integer k such that G is k-colourable.

The reconfiguration graph of the k-colourings, denoted $\mathscr{R}_k(G)$, is the graph whose vertices are the k-colourings of G and two colourings are adjacent in $\mathscr{R}_k(G)$ if they differ in colour on exactly one vertex. We say that G is *k-mixing* if $\mathscr{R}_k(G)$ is connected and the *k-recolouring diameter* of G is the diameter of $\mathscr{R}_k(G)$. Given two k-colourings α and β of G, deciding whether there exists a path between the two colourings in $\mathscr{R}_k(G)$ was proved to be PSPACE-complete for all $k > 3$ [1]. The problem remains PSPACE-complete for graphs with bounded bandwidth and hence bounded treewidth [2]. In this paper, we investigate the connectivity and diameter of $\mathscr{R}_{k+1}(G)$ for a k-colourable graph G restricted by forbidden induced subgraphs. We explore the structural properties of graph classes defined by forbidden induced subgraph to study the diameter and connectivity of the reconfiguration graph. A graph G is H-free if no induced subgraph of G is isomorphic to H. Let P_n, C_n, and K_n denote the path, cycle, and complete graph on n vertices, respectively. For two vertex-disjoint graphs G and H, the *disjoint union* of G and H, denoted by $G+H$, is the graph with vertex-set $V(G) \cup V(H)$ and edge-set $E(G) \cup E(H)$.

We show that $\mathscr{R}_{k+1}(G)$ is connected for every k-colourable H-free graph G if and only if H is an induced subgraph of P_4 or $P_3 + P_1$. We also start an investigation into this problem for classes of graphs defined by two forbidden induced subgraphs. We show that if G is a k-colourable $(2K_2, C_4)$-free graph, then $\mathscr{R}_{k+1}(G)$ is connected with diameter at most $4n$. Furthermore, we show that $\mathscr{R}_{k+1}(G)$ is connected for every k-colourable (P_5, C_4)-free graph G.

A preprint is available at https://arxiv.org/abs/2206.09268.

References

[1] P. Bonsma, L. Cereceda. Finding Paths between graph colourings: PSPACE-completeness and superpolynomial distances. *Theoretical Computer Science*, 410:5215–5226, 2009.

[2] M. Wrochna. Reconfiguration in bounded bandwidth and tree-depth. *Journal of Computer and System Sciences*, 93:1–10, 2018.

Index of Authors

The AMMCS 2023 Conference
Book of Abstracts

ISBN: 978-0-9918856-4-0